ALEXANDRE GONÇALVES DE REZENDE

AVALIAÇÃO DA EXPRESSÃO GÊNICA EM CÉLULAS DE MAMÍFEROS UTILIZANDO O *SEMLIKI FOREST VIRUS*

Dissertação apresentada ao programa de pós-graduação interunidades em Biotecnologia USP / Instituto Butantan / IPT, para obtenção do título de Mestre em Biotecnologia.

São Paulo
2014

ALEXANDRE GONÇALVES DE REZENDE

AVALIAÇÃO DA EXPRESSÃO GÊNICA EM CÉLULAS DE MAMÍFEROS UTILIZANDO O *SEMLIKI FOREST VIRUS*

Dissertação apresentada ao programa de pós-graduação interunidades em Biotecnologia USP / Instituto Butantan / IPT, para obtenção do título de Mestre em Biotecnologia.

Área de concentração: Biotecnologia

Orientador: Dra. Soraia Attie Calil Jorge

Versão original

São Paulo
2014

DADOS DE CATALOGAÇÃO NA PUBLICAÇÃO (CIP)
Serviço de Biblioteca e Informação Biomédica do
Instituto de Ciências Biomédicas da Universidade de São Paulo

reprodução não autorizada pelo autor

Rezende, Alexandre Gonçalves de.
Avaliação da expressão gênica em células de mamíferos utilizando o Semliki Forest virus / Alexandre Gonçalves de Rezende. -- São Paulo, 2014.

Orientador: Profa. Dra. Soraia Attie Calil Jorge.

Dissertação (Mestrado) – Universidade de São Paulo. Instituto de Ciências Biomédicas. Programa de Pós-Graduação Interunidades em Biotecnologia USP/IPT/Instituto Butantan. Área de concentração: Biotecnologia. Linha de pesquisa: Expressão gênica utilizando vetores virais.

Versão do título para o inglês: Evaluation of gene expression in mammalian cells using the Semliki Forest virus.

1. Semliki Forest Virus (SFV) 2. Glicoproteína do vírus rábico (RVGP) 3. Expressão de proteínas recombinantes 4. Cultura de células de mamíferos I. Jorge, Profa. Dra. Soraia Attie Calil II. Universidade de São Paulo. Instituto de Ciências Biomédicas. Programa de Pós-Graduação Interunidades em Biotecnologia USP/IPT/Instituto Butantan III. Título.

ICB/SBIB026/2014

UNIVERSIDADE DE SÃO PAULO
Programa de Pós-Graduação Interunidades em Biotecnologia
Universidade de São Paulo, Instituto Butantan, Instituto de Pesquisas Tecnológicas

---

Candidato(a): Alexandre Gonçalves de Rezende.

Título da Dissertação: Avaliação da expressão gênica em células de mamíferos utilizando o Semliki Forest virus.

Orientador(a): Profa. Dra. Soraia Attie Calil Jorge.

A Comissão Julgadora dos trabalhos de Defesa da **Dissertação de Mestrado,** em sessão pública realizada a ...../...../....., considerou

( ) Aprovado(a) **( ) Reprovado(a)**

Examinador(a): Assinatura: .....
Nome: .....
Instituição: .....

Examinador(a): Assinatura: .....
Nome: .....
Instituição: .....

Presidente: Assinatura: .....
Nome: .....
Instituição: .....

COMISSÃO DE ÉTICA NO USO DE ANIMAIS
INSTITUTO BUTANTAN
Av. Dr. Vital Brazil, 1500, CEP 05503-900, São Paulo, SP, Brazil
Telefone: (55) (011) 2627-9585 - Fax: (55) (011) 2627-9505
ceuaib@butantan.gov.br

CERTIFICADO

Certificamos que o projeto intitulado "Estudo da expressão gênica em células de mamíferos utilizando o vírus Semliki Forest", **protocolo nº 905/12**, sob a responsabilidade de Soraia Attie Calil Jorge e Alexandre Gonçalves de Rezende – que envolve a criação e/ou utilização de animais pertencentes ao filo Chordata, subfilo Vertebrata (exceto o homem), para fins de pesquisa científica – está de acordo com os preceitos da Lei nº 11.794, de 8 de outubro de 2008, do Decreto 6.899, de 15 de julho de 2009 e de normas complementares, bem como está de acordo com os Princípios Éticos na Experimentação Animal adotado pelo Colégio Brasileiro de Experimentação Animal (COBEA), e foi aprovado pela COMISSÃO DE ÉTICA NO USO DE ANIMAIS DO INSTITUTO BUTANTAN (CEUAIB) em reunião de 11/4/12.

We certify that the research entitled "Study of gene expression in mammalian cells using the Semliki Forest virus", **protocol number 905/12**, under the responsibility of Soraia Attie Calil Jorge and Alexandre Gonçalves de Rezende – which involves the breeding and/or use of animals belonging to phylum Chordata, subphylum Vertebrata (except human beings), for scientific research – is in agreement with Brazilian laws for use of experimental animals and the Ethical Principles in Animal Research adopted by the Brazilian College of Animal Experimentation, and was approved by the ETHICAL COMMITTEE FOR ANIMAL RESEARCH of BUTANTAN INSTITUTE in the meeting of 4/11/12.

Vigência do Projeto: 06/2012 - 07/2013	**N° de animais/espécie**
Laboratório de Imunologia Viral	25 camundongos Balb/c (F)

São Paulo, 18 de abril de 2012

Dr. Marcelo L. Santoro
Coordenador da CEUAIB

Ao meu pai, Alberto (*in memorian*), pela correta transmissão de moralidade, e entendimento da palavra persistência **.**

AGRADECIMENTOS

A meu pai Alberto (*in memorian*), por em tão pouco tempo de convívio ter me passado os conhecimentos necessários para sempre buscar o bem, e pela sua onipresença, me guiando nos momentos mais difíceis.

A minha mãe Almira, por sempre me proporcionar condições e formas para realizar meus sonhos, e cujo sorriso no rosto é sempre a meta de qualquer projeto que inicio.

A minha companheira Kelly, por todo o amor, confiança e respeito, e pelos inúmeros momentos a mim dedicados, sempre acreditando na minha capacidade, ate mesmo quando eu duvidava. E toda sua família, que me acolheu como um filho e me apoiou incondicionalmente.

Aos meus irmãos Érica e Nuno, e meus cunhados Gil e Simone, por todo o apoio e convivência harmoniosa em família, e pelas princesinhas Sofia e Larissa, que recarregam as nossas energias e enchem de alegria a todos. E pela nova princesa que entrará em breve na família e será mais um presente.

A minha orientadora Soraia, por acreditar em meu potencial e me dar uma oportunidade ímpar. E por todo conhecimento passado que será essencial em minha vida profissional.

Ao amigo Renato, por todos os conselhos passados no desenvolvimento do trabalho.

A Ana Lia, pela parceria nos projetos e pela dedicação em realizá-los.

Aos meus amigos Marcos, Carlos Augusto, Gustavo e Leme, pessoas incríveis que conheci, e que sempre se mostraram aptos a me ajudar e transferir conhecimentos.

As minhas amigas Sandra, Thaissa, Daniela, Juliana, Polyana, Luciana, Lucia, Vera, Fernanda, Rose, Nayara e Aline, pela cooperação e troca de conhecimentos, além de proporcionarem um excelente ambiente de trabalho.

Aos meus amigos e amigas de Juruaia, por ser um refugio de todos os problemas e pela demonstração de que serão pessoas que poderei sempre confiar.

Ao Instituto Butantan, pelo acolhimento, em especial ao Laboratorio de Imunologia Viral, pela estrutura fornecida, e todos os seus funcionários pela excelência e companheirismo, propiciando o correto desenvolvimento das pesquisas.

Ao programa de pós-graduação em Biotecnologia da USP pelos serviços prestados.

A CAPES pelo apoio financeiro, sem o qual o projeto não seria possível.

E principalmente a Deus, que me mostrou o caminho certo, e foi colocando pessoas tão especiais no seu decorrer, que me acrescentaram muito, e que sem duvida, são responsáveis pelo que sou hoje.

“O êxito na vida não se mede pelo caminho que você conquistou, mas sim pelas dificuldades que superou no caminho.”

Abrahan Lincoln

RESUMO

REZENDE, A. G. **Avaliação da expressão gênica em células de mamíferos utilizando o *Semliki Forest virus***. 2014. 92 f. Dissertação (Mestrado em Biotecnologia) - Instituto de Ciências Biomédicas, Universidade de São Paulo, São Paulo, 2014.

O sistema de expressão gênica derivado do *Semliki Forest Virus* (SFV) vem sendo muito utilizado nos últimos tempos para expressão em grandes quantidades de inúmeras proteínas, quando comparado com outros sistemas. O objetivo desse estudo foi otimizar a capacidade desse vetor viral de expressar proteínas em diferentes linhagens celulares de mamíferos, utilizando como alvo, a glicoproteína do vírus rábico (RVGP). Foram avaliadas formas de obtenção do vetor SFV recombinante, através de diferentes métodos de transfecção, como eletroporação e lipofecção, utilizando um lipossomo comercial chamado Transmessenger (Qiagen, Valencia, CA., U.S.A.). Foi estabelecido, um método rápido e preciso de quantificação das partículas virais, através da técnica de qPCR, para padronizar a relação entre a quantidade de vírus recombinante a ser utilizada em um processo de infecção, visando aumentar os níveis de produção da proteína heteróloga. Diferentes proporções entre vírus e células foram utilizadas em cinco linhagens distintas: BHK-21, Huh-7, VERO, L929 e HEK-293T; sendo avaliados dois tempos de coleta da RVGP após a infecção (24 e 48 h). A proteína gerada foi avaliada através de diferentes métodos como Western Blot, Dot blot e imunofluorescência indireta (IFI), sendo a quantificação da proteína realizada através de ensaio imunoenzimático (ELISA). Esse trabalho contribui para o desenvolvimento de abordagens que utilizam o SFV como vetor de expressão, indicando as melhores metodologias e linhagens celulares, que podem ser utilizadas para aplicação na produção das mais variadas proteínas.

Palavras-chave: *Semliki Forest Virus* (SFV). Glicoproteína do vírus rábico (RVGP). Expressão de proteínas recombinantes. Cultura de células de mamíferos.

ABSTRACT

REZENDE, A. G. **Evaluation of gene expression in mammalian cells using the Semliki Forest virus**. 2014. 92 p. Masters thesis (Biotechnology) - Instituto de Ciências Biomédicas, Universidade de São Paulo, São Paulo, 2014.

The expression system based on Semliki Forest virus (SFV) is a system which has been widely used in recent times for expression of many proteins in large quantities as compared with other systems. The aim of this study was to optimize the capacity of this vector to express viral proteins in different mammalian cell lines, using as target, the rabies virus glycoprotein (RVGP). We assessed two different methods of transfection to obtain recombinant SFV vector, such as electroporation and liposome commercial Transmessenger (Qiagen, Valencia, CA., U.S.A.). It was established also a fast and accurate quantification of viral particles by qPCR technique, to improve the relation between the amount of recombinant virus to be used in a process of infection, to increase production levels of the heterologous protein. Different proportions between viruses and cells were used in five distinct lineages: BHK-21, Huh-7, Vero, L929 and HEK-293T; being evaluated two sampling times after infection of RVGP (24 e 48 h). The protein was assessed by various methods such as Western blot, Dot blot and indirect immunofluorescence (IIF), and the protein quantification performed by enzyme immunoassay (ELISA). This work contributes to the development of approaches to using the SFV expression vector indicating the best methods and cell lines that can be used for application in the production of various proteins.

Keywords: *Semliki Forest Virus* (SFV). Rabies virus glycoprotein (RVGP). Expression of recombinant proteins. Culture of mammalian cells.

LISTA DE FIGURAS

Figura 1 - Esquema do vírus rábico. 26
Figura 2 - Ciclo de vida do *Semliki Forest virus* (SFV) 30
Figura 3 - Vetores utilizados no trabalho. 38
Figura 4 - Cálculos para determinação da titulação viral. 45
Figura 5 – Eletroforese em gel de agarose (0,8%) 52
Figura 6 - Expressão de RVGP a partir da infecção com o vírus SFV-RVGP obtido por diferentes métodos de transfecção. 53
Figura 7 - Gel de agarose 1,5 % com os produtos da PCR-Nested 55
Figura 8 - Curva padrão obtida por qPCR através de diferentes pares de primers 56
Figura 9 - Expressão de RVGP (µg / 1E6 células) em células BHK-21 58
Figura 10 - Efeito citopático em células BHK-21 60
Figura 11 - Dot blotting para RVGP expressa em diferentes linhagens celulares infectadas com o vírus SFV-RVGP. 61
Figura 12 - Western blotting para RVGP expressa em diferentes linhagens celulares infectadas com o vírus SFV-RVGP. 61
Figura 13 - Imagens de IFI com células BHK-21, 24 h após a infecção com SFV-RVGP. 62
Figura 14 - Expressão de RVGP (µg / 1E7 celulas) em células Huh 7. 63
Figura 15 - Efeito citopático em células Huh 7 infectadas por SFV-RVGP. 64
Figura 16 - Imagens de IFI com células Huh-7, 48 h após a infecção com SFV-RVGP. 65
Figura 17 - Expressão de RVGP (µg / 1E7 células) em células L929. 67
Figura 18 - Efeito citopático em células L929. 68
Figura 19 - Imagens de IFI com células L929, 24 h após a infecção com SFV-RVGP. 69
Figura 20 - Expressão de RVGP (µg / 1E6 células) em células Vero, utilizando diferentes MOIs (1, 10, 15 e 50), coletada 24 e 48 h após a infecção. 70
Figura 21 - Efeito citopático em células Vero. 71
Figura 22 - Imagens de IFI com células VERO, 24 h após a infecção com SFV-RVGP. 72
Figura 23 - Expressão de RVGP (µg / 1E6 células) em células HEK-293T, utilizando diferentes MOIs (1, 10, 15 e 50), coletada 24e 48 h após a infecção. 73
Figura 24 - Efeito citopático em células HEK-293T. 74
Figura 25 - Imagens de IFI com células HEK-293T, 24 h após a infecção com SFV-RVGP. 75

Figura 26 - Expressão de RVGP (ng / 1E7 células) em células BHK-21 em suspensão, coletada 24 e 48 h após a infecção. 76

LISTA DE TABELAS

Tabela 1 - Vacinas anti-rábicas.....25
Tabela 2 - Sistemas utilizados para expressão de RVGP. 32
Tabela 3 - Características dos oligonucleotídeos 41
Tabela 4 - Composição dos géis utilizados no Western blotting.....49
Tabela 5 - Resumo dos valores de RVGP (µg / 1E6 células) obtidos em cada linhagem.....77

LISTA DE ABREVIATURAS E SIGLAS

SFV - *Semliki Forest virus*

RVGP - Glicoproteína do vírus rábico

SFV-RVGP – Sistema de expressão de RVGP, baseado no SFV

pSFV-RVGP – plasmídeo contendo o gene para as proteínas não estruturais do SFV, e da RVGP

pSFV-Helper – plasmídeo contendo as proteínas estruturais do SFV

SFV-RNA – RNA correspondente ao SFV

BHK-21 – linhagem celular derivada de *Baby hamster kidney*

BHK-21 C-13 - linhagem celular derivada de *Baby hamster kidney*, adaptada a suspensão

Huh-7 - Linhagem celular derivada de *Human Hepato Cellular Carcinoma*

HEK-293T - Linhagem celular derivada de *Human Embrionic Kidney*

Vero - Linhagem celular derivada de *Green Monkey Kidney*

L929 - Linhagem derivada do tecido aureolar subcutâneo e adiposo de camundongo

NA - Linhagem celular derivada de *Neuroblastoma*

S2 - Linhagem celular derivada de *Drosophila melanogaster*

Sf9 - Linhagem celular derivada de *Spodoptera frugiperda*

MDBK - Linhagem celular derivada de *Madin Darby Bovine Kidney*

ATCC – *American Type Culture Collection*

MOI - *Multiplicity of infection*

qPCR - Q*uantitative Polymerase Chain Reaction*

RT - *Reverse Transcription*

qRT-PCR - qPCR da *Reverse Transcription*

WHO - *World Health Organization*

MS - Ministério da Saúde

PHK - *Primary Hamster Kidney*

PHKCV - *Primary Hamster Kidney Cell Rabies Vaccine*

HDCV - *Human Diploid Cell Vaccine*

PDECV - *Duck embryo cell vaccine*

PVRV - *Purified Vero Rabies Vaccine*

RNA - Ácido Ribonucléico

RNAses - Ribonuclease

DNA - Ácido Desoxirribonucléico

cDNA - DNA complementar

ORFs - O*pen Reading Frames*

SFV-26 s - Promotor subgenômico do SFV

E2 e E1 - Proteínas do envelope viral do SFV

IFI - Imunofluorescência Indireta

SFB – Soro Fetal Bovino

DMEM - *Dulbecco's Modified Eagle Medium*

IMDM - *Iscove's Modified Dulbecco's Medium*

PBS - *Phosphate buffered saline*

PBS-EDTA - *Phosphate buffered saline*, com *ethylene-diamine-tetraacetic acid*

SDS - Dodecil Sulfato de Sódio

TBS - *Tris Buffered Saline*

TE – Tampão Tris-EDTA

LB - meio *Luria-Bertani*

nsP1, nsP2, nsP3 e nsP4 - Proteínas não estruturais do SFV

Amp - Gene de resistência à ampicilina

OriC - Origem de replicação bacteriana

Tm - Temperatura de *Melting*.

GC - Par de bases nitrogenadas, formado por Guanina e Citosina

EGTA - *Ethylene Glycol Tetraacetic Acid*

dNTPs - *Deoxyribonucleotide Triphosphates*

g - Força centrifuga relativa

ng - Nanograma

µg - Micrograma

mg - Miligramas

µl - Microlitro

ml - Mililitro

µm - Micrometro

v - Volt

Ct - *Cycle Treshold*

IgG-D1 - Imunoglobulina anti-sítio III da RVGP

IgG-D1-Po - IgG-D1 conjugada com peroxidase

BSA - Albumina de soro bovino

Tween 20 - Monolaurato de Sorbitan Etoxilado 20

IgG-D1 - Imunoglobulina policlonal contra a glicoproteína rábica

αIgG-D1 - Anti-rabbit conjugado com peroxidase

TEMED - Tetrametiletilenodiamina

FITC - *Fluorescein Isothiocyanate*

DAPI - *4'-6-Diamidino-2-phenylindole*

ELISA - *Enzyme-Linked Immunosorbent Assay*

Kb – Quilobases

kDa - Quilodalton

SUMÁRIO

1 INTRODUÇÃO 21
2 REVISÃO BIBILIOGRÁFICA 23
2.1 Doença da Raiva (World Health Organization – WHO) 23
2.2 Vírus da raiva e glicoproteína do vírus rábico (RVGP) 26
2.3 Sistemas de expressão de proteínas heterólogas 27
2.4 *Semliki Forest Virus* (SFV) 29
2.5 Quantificação viral através de qRT-PCR 32
3 OBJETIVOS 35
3.1 Objetivo geral 35
3.2 Objetivos específicos 35
4 MATERIAIS E MÉTODOS 36
4.1 Células de mamíferos utilizadas para avaliar a expressão de RVGP 36
4.1.1 Baby Hamster Kidney (BHK-21) 36
4.1.2 BHK-21 suspensão 36
4.1.3 Células de Hepatocarcinoma humano (Human Hepato Cellular Carcinoma-HuH 7) 36
4.1.4 Human Embrionic Kidney (HEK-293T) 37
4.1.5 Green Monkey Kidney (VERO) 37
4.1.6 Linhagem L929 (ATCC – CCL-1) 37
4.2 Obtenção do Semliki Forest Virus recombinante (SFV-RVGP) 37
4.2.1 Transformação bacteriana para amplificação dos vetores 38
4.2.2 Obtenção dos plasmídeos 39
4.2.3 Transcrição in vitro 39
4.2.4 Transfecção por Eletroporação 39
4.2.5 Transfecção utilizando o reagente comercial Transmessenger (Qiagen) 40
4.3 Quantificação viral 40
4.3.1 Desenho de oligonucleotídeos 40
4.3.2 Extração de RNA 41
4.3.3 Tratamento com DNase 41
4.3.4 Transcrição Reversa 42
4.3.5 PCR e Nested PCR 42

4.3.6 Obtenção dos padrões para construção da curva-padrão para qPCR 43
4.3.7 qPCR 43
4.4 Ativação do vírus SFV-RVGP 45
4.5 Infecção com o vírus SFV-RVGP 45
4.6 ELISA 46
4.6.1 Reagentes e soluções 46
4.6.2 Procedimento 47
4.7 *Western-Blot* 48
4.7.1 Reagentes e Soluções 48
4.7.2 Procedimento 49
4.8 Dot Blot 50
4.9 Imunofluorescência Indireta 51
4.9.1 Reagentes e soluções 51
4.9.2 Procedimento 51
5 RESULTADOS 52
5.1 Avaliação dos métodos de linearização e transcrição *in vitro* dos vetores 52
5.2 Avaliação dos métodos de transfecção 53
5.3 Padronização da qRT-PCR 54
5.4 Titulação viral 57
5.5 Avaliação da expressão de RVGP em diferentes linhagens celulares 58
5.5.1 BHK-21 58
5.5.2 Huh-7 62
5.5.3 L929 66
5.5.4 Vero 70
5.5.5 HEK 293T 72
6 DISCUSSÃO **78**
7 CONCLUSÕES 86
REFERÊNCIAS 87
ANEXO – TRABALHOS PUBLICADOS 94
ANEXO A – Quantitative RT-PCR for titration of replication-defective recombinant Semliki Forest virus
ANEXO B – Using Statistical Tools for Improving Bioprocesses

ANEXO C – Semliki Forest Virus as a Vector: Pros and Cons for Its Use in biopharmaceutical Production

ANEXO D – Influence of aeration–homogenization system in stirred tank bioreactors, dissolved oxygen concentration and pH control mode on BHK-21 cell growth and metabolism

ANEXO E – A multivariate calibration procedure for UV/VIS spectrometric monitoring of BHK-21 cell metabolism and growth

1 INTRODUÇÃO

A raiva é uma doença mundialmente disseminada, causando a morte de mais de 55.000 pessoas por ano, sendo que os países mais pobres são os mais afetados. A dificuldade em controlar a doença após o início de seu desenvolvimento em um indivíduo faz com que a melhor abordagem contra a raiva, seja a vacinação dos principais animais reservatórios do vírus, e também de humanos (WORLD HEALTH ORGANIZATION, 2013). Porém, os custos de produção de uma vacina anti-rábica, campanhas de vacinação e sua distribuição, ainda limitam seu acesso à maioria das pessoas que vivem em áreas potencialmente de risco.

Além da questão econômica, as vacinas atualmente disponíveis são produzidas através de diferentes abordagens em todo o mundo, ocasionando em alguns casos, efeitos colaterais relacionados à sua administração. No Brasil, a vacina anti-rábica é produzida utilizando o vírus rábico inativado, o que não as garantem como uma vacina totalmente seguras, sendo contra indicado a gestantes e pessoas imunodeprimidas (NATHANSON et al., 1995). Outro fator importante é a necessidade de condições específicas para o armazenamento e distribuição do produto a regiões mais remotas, sendo este fato mais evidenciado em países em desenvolvimento, onde o acometimento de pessoas pela doença está diretamente relacionado ao seu poder aquisitivo, ocasionando em maiores dificuldades ao acesso a tratamentos e às campanhas de vacinação (ERTL, 2009). Por esses motivos, novos métodos que possam ser utilizados para aperfeiçoar o processo de produção vacinal se mostram necessários.

Visto que em um processo de infecção pelo vírus da raiva, a glicoproteína presente no envelope do vírus rábico (RVGP), é a principal indutora de anticorpos contra o vírus em questão, um sistema que seja capaz de expressá-la corretamente, com todas as modificações pós-traducionais adequadas, pode vir a ser utilizado como ferramenta no processo de produção de uma vacina anti-rábica (GAUDIN et al., 1992).

Sistemas capazes de expressar proteínas específicas em culturas celulares surgem como candidatos em potencial. Sendo que para tal finalidade, diversas abordagens vêm sendo desenvolvidas ao longo do tempo, visando uma melhor eficiência na entrega de um gene heterólogo e, consequentemente, um maior nível de produção da proteína correspondente (ASTRAY et al., 2013; DE JESUS et al., 2011). Nesse tipo de abordagem, a utilização de cultura de células eucarióticas se faz necessária quando a proteína a ser expressa necessita de

modificações pós-traducionais, sendo o caso da RVGP (WALSH et al., 2010). Existem diversos trabalhos que demonstram a utilização desse tipo de célula para esse propósito, mostrando bons índices de produção e processamentos convenientes na proteína gerada (BALDI et al., 2007; CONCEIÇÃO et al., 2007; JORGE et al., 1995, 1996). Apesar disso, muitas vezes os sistemas de expressão estudados não suprem as expectativas, devido à relação do tempo e material consumido, com os níveis de produção da proteína de interesse, além de outros problemas como a perda, por inativação ou deleção, do gene heterólogo no genoma celular (LUNDSTROM, 2003).

Neste sentido, têm-se desenvolvido sistemas de expressão transiente, que possibilitam níveis elevados de expressão gênica, de até 4 µg / 1E6 células (LUNDSTROM, 2003; PAUL et al., 1993). É o caso dos vetores virais, que permitem a utilização de fortes promotores gênicos que são responsáveis por altos níveis de expressão do transgene, e possuem uma alta eficiência de infecção e, portanto, de introdução do gene na linhagem celular desejada (TWYMAN, 2005).

O sistema de expressão gênica derivado do *Semliki Forest Virus* (SFV) vem sendo muito utilizado nos últimos tempos, para expressar inúmeras proteínas e possui ampla capacidade de infectar diferentes linhagens celulares (LUNDSTROM, 2010). Portanto, surge como um sistema com grande potencial para avaliar a produção de RVGP em várias linhagens de culturas celulares, sendo um dos objetivos desse trabalho.

O desenvolvimento deste projeto estabeleceu uma tecnologia de produção de partículas virais recombinantes (SFV-RVGP), capazes de expressar proteínas heterólogas (RVGP) em culturas de células de mamíferos. Diversas linhagens foram infectadas pelo vetor SFV-RVGP e avaliadas quanto a produção da proteína, como BHK-21, Huh-7, Vero, HEK 293T, L929 e BHK-21 adaptadas a suspensão. Além disso, uma metodologia para realizar a quantificação das partículas virais foi estabelecida através de uma metodologia de qRT-PCR, de forma a otimizar o processo de infecção, avaliando ensaios com diferentes proporções de vírus por célula.

O trabalho em questão contribui para um melhor entendimento quanto ao sistema de expressão utilizando o SFV, e sua capacidade de expressar proteínas heterólogas em diferentes linhagens de células de mamíferos. Essa abordagem pode ser estendida para a expressão de diversas outras proteínas, com potenciais usos terapêuticos e vacinais.

2 REVISÃO BIBILIOGRÁFICA

2.1 Doença da Raiva (World Health Organization – WHO)

A raiva é uma zoonose, causada pela infecção do vírus rábico, que é pertencente à família *Rabdoviridae* e ao gênero *Lyssavirus*. A infecção em humanos, geralmente ocorre após uma mordida profunda ou arranhão de um animal infectado, sendo os cães o principal hospedeiro e transmissor da doença, que tem ainda morcegos e outros animais silvestres como importantes transmissores (TORDO et al., 1988).

O desenvolvimento da doença em humanos leva a óbito, na ausência de um tratamento pós-infecção. Esse procedimento consiste na limpeza profunda do ferimento, imunização e tratamento com imunoglobulinas, logo após o contato suspeito. Uma vez que se manifestem os sintomas, não há tratamento e a doença é quase sempre fatal. Estima-se que a cada ano mais de 15 milhões de pessoas em todo o mundo recebam vacinação pós-exposição para prevenir o desenvolvimento da doença (WHO, 2013).

O custo médio por pessoa de um tratamento anti-rábico é de US$ 40 na África e de US$ 49 na Ásia, sendo esse valor considerado muito elevado para um grande número de países em que a renda média é de US$ 1 a 2 por pessoa por dia. O gasto global com a prevenção da raiva está em torno de US$ 1 bilhão (WHO, 2013).

Não estão disponíveis testes para diagnosticar a infecção pela raiva em humanos antes do aparecimento da doença clínica e, a menos que os sinais específicos de raiva, como hidrofobia ou aerofobia estejam presentes, o diagnóstico clínico pode ser difícil. A raiva humana pode ser confirmada *intra-vitam* e *post mortem* por várias técnicas de diagnósticos destinados à detecção do vírus inteiro, ou ácidos nucléicos em tecidos infectados (cérebro, pele, urina ou saliva). Com base em recomendações da *World Health Organization (*WHO*)*, a principal ferramenta para prevenir a disseminação da doença é a profilaxia, principalmente em animais reservatórios do vírus, como cães (WHO, 2013).

A doença da raiva é disseminada mundialmente, ocorrendo em mais de 150 países e territórios, sendo que apenas alguns poucos países no mundo não registraram casos de raiva recentemente, em sua maioria ilhas e penínsulas. Segundo dados da WHO, mais de 55.000 pessoas morrem por ano por acometimento da doença, principalmente na Ásia e África, que concentram 95% dos casos de óbitos. Nos países desenvolvidos há prevalência de infecções

através de animais silvestres, e na América do Sul, no ano de 2003, pela primeira vez mais pessoas morreram de raiva devido ao contato com animais selvagens, principalmente morcegos, que por mordida de cães (WHO, 2013).

A doença da raiva constitui um problema sério de saúde pública no Brasil, pois expõe um grande número de pessoas e animais ao risco de contrair a doença, que é facilmente disseminada e quase sempre fatal, necessitando de grandes esforços por parte do governo no combate eficaz da raiva animal e humana. Desde 1973, com a criação do Programa Nacional de Prevenção da Raiva, houve uma redução de 90% nos casos de raiva canina. Segundo dados do Ministério da Saúde o número de casos reportados de cães raivosos no Brasil caiu de 635, em 2002, para 83, em 2012. O Ministério da Saúde (BRASIL, 2012) subsidia anualmente duas campanhas de vacinação contra a raiva para cães e gatos, uma nacional e outra de intensificação, nas áreas de risco. No ano passado foram vacinados mais de 23 milhões de animais durante a campanha nacional e quase 5 milhões na campanha de intensificação (BRASIL, 2012).

Entre 2002 e 2007 observou-se um aumento no número de casos de raiva detectados em morcegos hematófagos no país. Em 2004 e 2005 um surto de transmissão da doença para humanos por esses animais aconteceu nos estados do Pará e Maranhão. Os animais de produção, principalmente os bovinos, também vêm sendo atingidos pela raiva ao longo dos anos, embora o Ministério da Agricultura desenvolva, desde 1966, o Programa Nacional de Controle da Raiva dos Herbívoros, que tem na vacinação sua maior aliada. A raiva humana apresentou expressiva redução nos últimos anos, visto que em 1990, foram registrados 73 casos de raiva humana no país, enquanto que em 2012 esse número caiu para apenas cinco oficialmente registrados (BRASIL, 2012).

Estima-se que, anualmente, o Governo do Brasil gaste US$ 28 milhões na profilaxia e controle da raiva, com vacinas de uso humano e para cães, imunoglobulinas, diagnóstico laboratorial, treinamento de recursos humanos e campanhas de vacinação de cães. Como comparação, nos EUA, esse custo foi estimado em mais de US$ 300 milhões anuais, sendo a maioria destinada para a vacinação de cães (MORATO et al., 2011).

Durante o processo de desenvolvimento de uma vacina contra a doença, três gerações de vacinas anti-rábicas foram utilizadas. A primeira geração consiste na vacina a partir de vírus atenuado obtido de tecido nervoso infectado, principalmente de camundongos e ovelhas recém-nascidos, como na primeira vacina anti-rábica de Pasteur, a *Fuenzalida-Palacios*. A baixa potencialidade da mesma, requerendo várias imunizações diárias para conferir proteção,

e a associação à ocorrência de uma reação adversa grave de encefalomielite alérgica, devido à presença de neuroproteínas contaminantes, no caso da *Fuenzalida-Palacios*, culminou com o desenvolvimento das vacinas de segunda geração, baseadas em culturas celulares. Estas consistem na disseminação do vírus em ovos embrionados ou em cultura de células, e posterior inativação e concentração dos mesmos. Já as de terceira geração são as vacinas recombinantes, que tendem ser mais seguras e eficazes, mas ainda se restringem a área veterinária (WU et al.,2011).

Tabela 1 - Vacinas anti-rábicas

Vacinas	Descrição	Ano
Pasteur	Vírus vivo inativado por sucessivas passagens em cérebro de coelho	1885
Fermi and Semple	Inativação da cepa de Pasteur com fenol	1911
Fuenzalida-Palacios	Propagação viral em cérebro de camundongos	1955
Flury egg passage	Propagação viral em ovos de galinha embrionados	1960
PHKCV	Primeira vacina com vírus propagado em cultura de células (*Primary hamster kidney* – PHK)	1968
HDCV	Primeira vacina com vírus purificado, concentrado e liofilizado, propagada em células humanas diplóides	1974
PDECV	Vírus obtido pela propagação em células de embrião de pato	1984
PVRV	Vírus purificado e inativado, propagado em cultura de células VERO	1985
Purevax (Merial)	Vírus canarypox recombinante expressando a RVGP – Uso veterinário	2011

Fonte: modificado de WU X. et al., 2011; European Medicines Agency (EMA).

2.2 Vírus da raiva e glicoproteína do vírus rábico (RVGP)

O vírus rábico possui como genoma uma única fita de RNA negativo, linear e não segmentado, com aproximadamente 12 kb, sendo capaz de codificar uma nucleoproteína, uma fosfoproteína, uma RNA polimerase, uma proteína de matriz e a glicoproteína de superfície (RVGP) (**Figura 1**) (TORDO et al., 1988).

Figura 1 - Esquema do vírus rábico.

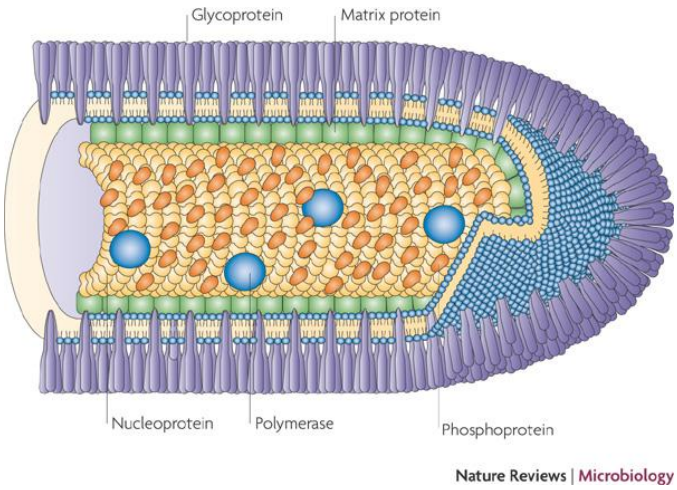

Fonte: Schnell (2010).

A RVGP, em sua forma trimérica, possui peso molecular de 140 kDa, e está presente no envelope viral como 1200 moléculas agrupadas na forma de 400 espículas triméricas, sendo responsáveis pela adesão do vírus aos receptores da célula hospedeira, e pela indução de anticorpos neutralizantes no organismo exposto ao vírus (GAUDIN et al., 1992; PERRIN et al., 1985). Ela é composta por 524 aminoácidos, sendo os 19 primeiros correspondentes ao peptídeo sinal, estando ausentes na proteína madura. Os demais se encontram organizados em três domínios: ectodomínio N-terminal glicosilado (aminoácidos de 1 a 439), um domínio hidrofóbico transmembranário (440 a 461), e o domínio hidrofílico intracitoplasmático carboxiterminal (aminoácidos de 462 a 524) (GAUDIN et al., 1999). No ectodomínio da RVGP, encontram-se 8 sítios antigênicos (I-VI, “a” e G1), dos quais, os sítios II e III, segundo estudos, demonstraram possuir a maior representação de epitopos para anticorpos neutralizantes (97%), sendo portanto, os de maior interesse para o estudo do desenvolvimento de resposta imune contra essa molécula (BENMANSOUR et al., 1991). O sítio antigênico III

está presente apenas na forma trimérica da proteína, apontada como essencial para ligação da mesma a receptores celulares.

Na célula hospedeira, a RVGP é sintetizada pela tradução ribossomal associada ao retículo endoplasmático rugoso. Nas cisternas dessa organela, a proteína é translocada formando os trímeros e sofrendo as modificações pós-traducionais necessárias, como a glicosilação inicial. No complexo de Golgi, ocorre a glicosilação terminal com hidrólise parcial da fração glicídica e a adição de novos açúcares em um ou dois dos sítios de ligação N-link para oligossacarídeos (DIETZSCHOLD, 1977; GAUDIN, 1997,). Além da glicosilação, a RVGP sofre uma acetilação durante seu transporte para o Complexo de Golgi, e uma palmitolação em uma cisteína situada ao lado do carbono terminal da sua região transmembrana, sendo assim, uma proteína com necessidade de alterações pós traducionais para sua atividade antigênica (GAUDIN et al., 1992).

2.3 Sistemas de expressão de proteínas heterólogas

Atualmente, os estudos para desenvolvimento de vacinas se baseiam na utilização da tecnologia do DNA recombinante, de forma a utilizar como componente vacinal, apenas a proteína correspondente à geração de anticorpos neutralizantes, e não mais o patógeno como um todo. Sendo assim, é cada vez maior o número de trabalhos envolvendo avaliação de diferentes tipos de vetores, para realizar a entrega do gene de interesse em uma célula hospedeira, de forma que haja altos níveis de expressão protéica, e que a mesma seja qualitativamente adequada (ERTL, 2009).

Dependendo da proteína de interesse, existe um melhor sistema para que ela seja expressa, que compreende na escolha de um organismo ou tipo celular a ser usado, e qual vetor realizará a entrega gênica. Uma grande variedade de organismos vem sendo utilizados com sucesso na expressão de proteínas, incluindo plantas, algas, leveduras, bactérias, células de mamíferos, células de insetos, dentre outros (LANGER, 2009). Para cada sistema escolhido, haverá um vetor adequado, desde que apresente as características de ser estável, com um custo efetivo para sua produção e ser isento de toxicidade (CORTESI et al., 1996).

Após a inserção do gene de interesse na célula, a expressão pode ocorrer de maneira transiente ou estável. Na expressão estável, o material genético inserido é integrado de forma randômica ao material genético da célula, através de enzimas de recombinação, de forma que

pode ser herdado pelas células filhas. Marcadores de seleção são utilizados para que as células com o gene de interesse sejam selecionadas (WULHFARD, 2009). Tal abordagem tem como vantagens, o fato de que em teoria todas as células estão expressando a proteína, a necessidade de uma quantidade menor de material genético para transfecção, e que após a seleção tem-se uma fonte ilimitada de produção da proteína. Porém, as principais desvantagens são a necessidade de um marcador de seleção adequado, o longo tempo para realizar a correta seleção de clones produtores, e os níveis de expressão ser influenciados pelo sítio de integração (BOLLATI; COMINI, 2007). No caso da expressão transiente, as células expressam a proteína de interesse em pouco tempo após a inserção do material genético, não ocorrendo integração, alcançando bons níveis de expressão em um curto espaço de tempo (BOLLATI; COMINI, 2007; NETTLESHIP, 2010). O uso desta abordagem está relacionado à produção de proteínas de alto valor agregado, em diferentes linhagens celulares (PHAM et al., 2006). Como desvantagens desse sistema, têm-se o curto período de expressão, a grande quantidade de material genético necessário, e a necessidade de um processo de transfecção sempre que for utilizado. Como vantagens têm-se a possibilidade de utilização de fortes promotores gênicos, a não necessidade do extenso processo de seleção, pode-se alcançar altos níveis de expressão, e a possibilidade de uma mesma abordagem ser utilizada em diferentes linhagens celulares, permitindo assim, avaliar em qual célula uma determinada proteína pode ser melhor expressa (BOLLATI; COMINI, 2007).

Dentre os diversos sistemas utilizados para a expressão transiente de proteínas heterólogas, os vetores virais surgem como promissores candidatos. Um vírus para ser caracterizado como um vetor de expressão, geralmente sofre uma manipulação genética, alterando, por exemplo, seus riscos frente ao desenvolvimento de doenças, e possibilitando a inserção de genes de interesse, mas de modo que não perca sua capacidade inata de infectar células e liberar seu material genético (EL-ANEED, 2004). Diversos trabalhos relatam a utilização desses vetores na produção de proteínas terapêuticas (CASALES et al., 2010), e em terapia gênica, com pesquisas específicas para o tratamento de câncer (QUETGLAS et al., 2013). Nos trabalhos relacionados à terapia gênica, os vetores virais surgem como predominantes, sendo que os principais vírus utilizados como vetores são Adenovírus, Retrovírus, Vírus Adeno-associados, herpes vírus e poxvírus (vaccínia vírus) (VANNUCCI et al., 2013).

Os vetores virais se destacam frente aos não-virais, devido à sua alta taxa de expressão protéica e à sua grande capacidade de entrega gênica aos mais diversos tecidos. Entretanto,

existem limitações relacionadas ao tamanho dos genes que podem ser carreados, e a necessidade da utilização de cultura de células, cuja padronização pode ser difícil, além de ter custo mais elevado se comparada à produção de DNA plasmidial. Outro fato relevante, no caso de terapia gênica, seria a alta imunogenicidade de alguns vírus, o que dificultaria sua administração para efetuar a entrega gênica (PATIÑO SFS, 2011).

2.4 *Semliki Forest Virus* (SFV)

O SFV é um vírus envelopado, de RNA positivo simples fita, do gênero *Alphavirus*, e família *Togaviridae*, e vem sendo utilizado como um contundente sistema de expressão gênica. A infecção de células permissivas por vírus desse gênero tem demonstrado significativos resultados, tornando esse sistema um método de expressão gênica com grande potencial (LILJESTRÖM; GAROFF, 1991; PUSHKO et al., 1997).

Os vetores derivados de SFV têm sido largamente utilizados para obtenção de diversas proteínas recombinantes, para os mais variados fins, como caracterização da função celular, testes farmacológicos e estudos estruturais (HOFFMANN et al., 2001). Comumente, são expressas proteínas de membrana, receptores, enzimas e proteínas virais, sendo obtidos altos níveis de expressão protéica com esse sistema em células de mamíferos (BENMAAMAR et al., 2009; BIKKER et al., 1997; EIFLER et al., 2007; SHUKLA et al., 2006; SHUKLA et al., 2007). O rendimento deste sistema de expressão heteróloga pode ser de até 20 vezes mais do que outras abordagens de expressão transiente (SHUKLA et al., 2007).

O genoma do vírus é composto de duas regiões abertas de leitura (*open reading frames* - ORFs), sendo que a 5’ ORF codifica quatro proteínas não estruturais (nsp1-4), e a 3’ ORF codifica cinco proteínas estruturais que compõem o capsídeo e as glicoproteínas (E1, E2, E3 e 6K) (STRAUSS; STRAUSS, 1994; RAYNER et al., 2002). As proteínas não estruturais são traduzidas diretamente do RNA senso, e tem como função gerar o RNA anti-senso a partir deste (**Figura 2**). Desta fita RNA anti-senso serão geradas as proteínas estruturais do genoma, a partir do promotor 26S que é ativado pelas proteínas não estruturais. O RNA subgenômico, que originará as proteínas estruturais, será gerado até 10 x mais que o RNA genômico, graças ao forte promotor subgenômico 26S. A poliproteína gerada sofre posteriormente, modificações pós traducionais que permitem a cada proteína estrutural desempenhar a real função (LUNDSTRON, 2003).

Figura 2 - Ciclo de vida do *Semliki Forest virus* (SFV)

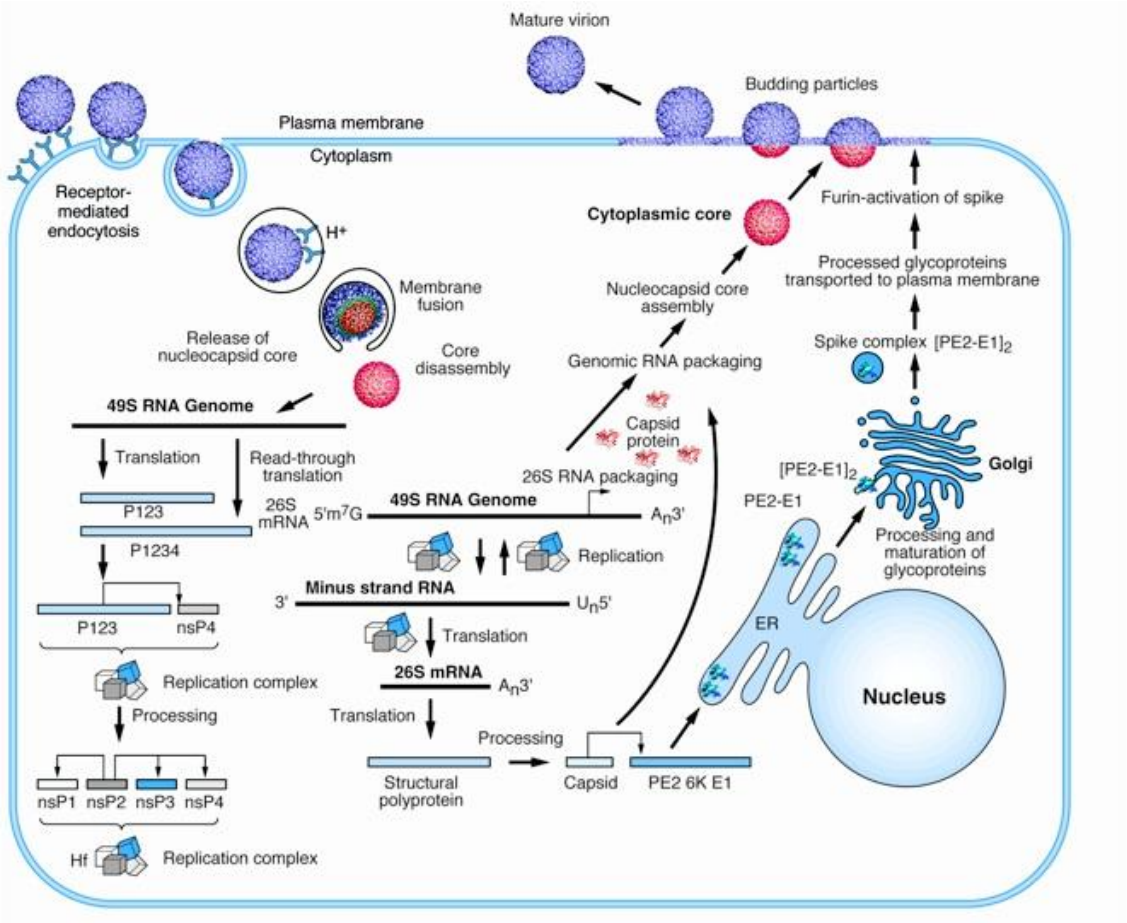

Fonte: http://bilbo.bio.purdue.edu/~viruswww/Kuhn_home/research.php

A utilização do SFV como vetor de expressão, envolve uma abordagem de engenharia genética para a construção de vetores baseados no seu genoma viral. Para a construção do vetor de expressão, o cDNA correspondente ao genoma do SFV foi dividido em dois plasmídeos diferentes: o plasmídeo de expressão, que contém os genes não estruturais do SFV e o promotor forte subgenômico SFV 26S, contendo ainda uma região de policlonagem para a introdução do gene de interesse, no caso a RVGP (pSFV-RVGP); e o plasmídeo auxiliar, contendo as proteínas estruturais do envelope viral (pSFV-Helper) (PUSHKO et al., 1997; KAMRUD et al., 2010). Após um processo de co-transfecção dos RNAs gerados *in vitro* referentes a ambos os plasmídeos, há a formação de partículas virais capazes de infectar uma ampla gama de células animais, notadamente as células de mamíferos. Entretanto, devido à

ausência do sinal de encapsidação no RNA codificante para as proteínas estruturais, apenas o RNA contendo o gene de interesse é empacotado nas partículas virais recém-formadas, constituindo o único RNA presente na partícula viral, o que na prática faz com que essas partículas sejam infecciosas, mas não replicativas (BERGLUND et al., 1993; GAROFF, 1991; LILJESTROM, 2003) Em uma abordagem de engenharia genética, visando aumentar a segurança do sistema, a proteína de envelope viral E2 foi mutada de forma que o vírus apenas possa realizar a fusão com a membrana plasmática da célula a ser infectada, quando previamente tratado com α-quimiotripsina (LUNDSTROM, 2003).

O presente estudo consiste em uma otimização de um trabalho realizado no laboratório, que avaliou o sistema SFV como potencial vetor para expressar a RVGP. Frente a outros trabalhos que avaliaram diferentes sistemas para expressar a RVGP, o sistema SFV se mostrou muito promissor. A expressão dessa proteína já foi estudada em sistemas utilizando tanto células eucarióticas, quanto procarióticas (**Tabela 2**) (LATHE et al., 1984; PREHAUD et al., 1989). Trabalhos com a RVGP expressa em bactérias mostraram que a proteína obtida e administrada em camundongos, não gerou proteção após o desafio, provavelmente por não realizarem as modificações pós-traducionais adequadas (YELVERTON et al., 1983). Morimoto et al. (1992), construíram um vetor derivado de retrovírus contendo o gene da RVGP, que foi capaz de expressá-la em células de neuroblastoma (NA) e células BHK-21, sendo corretamente glicosilada apenas em células BHK-21, sugerindo que as alterações pós-traducionais dependem também das condições celulares sob as quais a proteína é metabolizada. A RVGP também foi bem expressa em leveduras *Saccharomices cerevisiae* utilizando um vetor de expressão sob controle de um promotor indutível (metalotioneína) e um promotor constitutivo (triose desidrogenase) (KLEPFER et al., 1993, SAKAMOTO et al., 1999). Ramya et al., (2011) demonstraram através da construção de um baculovírus recombinante com o gene da RVGP, sob comando do promotor poliedrina, que a RVGP expressa em células de inseto *Spodoptera frugiperda* (Sf9), manteve as características estruturais e imunogênicas. Em células S2, a RVGP foi expressa utilizando um vetor plasmidial com o gene da proteína, sob um promotor constitutivo de actina, alcançando níveis de 300 ng / mL (YOKOMIZO et al., 2007). Em trabalho semelhante, utilizando o promotor indutível metalotioneína, foram alcançados maiores níveis de expressão chegando a 5,4 ug / 1E7 células, (LEMOS et al., 2009).

Tabela 2 - Sistemas utilizados para expressão de RVGP.

Sistemas de Expressão	Célula	Produção de RVGP	Conclusão	Referência
Bactérias	*Escherichia coli*	n.d.	A proteína expressa falhou na proteção de camundongos após o desafio	Yelverton, 1983
Leveduras	*Saccharomyces cerevisae*	30-40 ng / mL	RVGP não foi corretamente produzida, com baixa imunogenicidade	Sakamoto et al., 1999
Transfecção Estável	S2 (pAcRVGP2)	300 ng / mL	Expressão de RVGP em células S2 com correta atividade biológica	Yokomizo et al, 2007
Transfecção Estável	S2 (pAcRVGP2)	300-400 ng / 10^7	Cultivo em biorreator de 2L: Biostat MD System	Galessi et al, 2008
Transfecção Estável	S2 (pMtRVGPHy)	5,5 µg / 10^7 cel	Estratégias utilizando diferentes vetores, e uma nova pressão seletiva	Lemos et al, 2009
Transfecção Estável	S2 (pMtRVGPHy)	1,5-2 µg / 10^7 cel	Cultivo em biorreator de 1L: BioFlo 110	Ventini et al, 2010
Semliki Forest Virus (SFV)	BHK-21	18-22 µg / 10^7 cel	Bons índices de expressão de RVGP com esse sistema.	Benmaamar et al, 2009
Baculovírus	Sf-9	0,89 µg/10^7 cel	Expressão por esse sistema com alta imunogenicidade	Ramya et al, 2011
Baculovírus	BHK-21	n.d.	Expressão de RVGP utilizando esse sistema em células de mamíferos	Huang et al, 2011
Adenovírus	HEK-293	n.d.	Expressão de RVGP a baixos níveis.	Yarosh et al, 1996
Parainfluenza	MDBK	n.d.	Comprovado por Western blot, e boa imunogenicidade	Chen et al, 2013

Fonte: Adaptatado de Patiño (2011).

2.5 Quantificação viral através de qRT-PCR

Com o intuito de garantir a reprodutibilidade e maximizar a produção de proteínas, é importante uma estimativa do título do vírus recombinante que será utilizado em um processo de infecção. A utilização de um MOI (*Multiplicity of infection*) excessivamente alto de vírus pode ocasionar danos às células antes que a produção da proteína de interesse seja iniciada, e desperdiçar valiosos estoques de vírus (KOOL et al., 1991). Enquanto que o uso de poucas partículas virais por célula causa uma baixa produtividade da proteína de interesse.

Uma grande variedade de métodos alternativos para titulação foi desenvolvida nos últimos tempos, como a utilização de genes repórter, tais como β-galactosidase e proteína verde fluorescente de água viva, citometria de fluxo, medição das mudanças do diâmetro de células infectadas usando um contador de células e indicadores colorimétricos (CHA et al., 1997; JANAKIRAMAN et al., 2006; POULIQUEN et al., 2006; SHEN et al., 2002; YAHATA et al., 2000). O método de titulação em placa é uma alternativa para a quantificação viral, porém, tal método é trabalhoso e requer muito tempo, além de exigir um grau de especialização em cultura de células e manipulação viral, às vezes produzindo resultados que podem ser difíceis de interpretar (HUNT, 2005).

Lo e Chao (2004), descreveram uma técnica de PCR quantitativa (qPCR) para titulação de baculovírus, baseado na extração e quantificação do material genético viral. Sendo esse, um método que permite de uma maneira muito mais rápida e simples, determinar os títulos virais com base na intensidade de um sinal de fluorescência, geradas durante a amplificação da PCR.

Devido a sua alta sensibilidade, a transcrição reversa seguida pela qPCR é altamente utilizada para quantificar mudanças fisiológicas na expressão gênica. A técnica depende da sequência alvo, da quantidade de RNA esperada, do grau de precisão necessário e se a quantificação precisa ser relativa ou absoluta. Essa combinação de técnicas de biologia molecular (qRT-PCR), com a tecnologia do *SybrGreen*Master Mix (Applied Biosystems, Carlsbad, CA., U.S.A.) é capaz de fornecer resultados rápidos, precisos e confiáveis.

Em geral, duas curvas de calibração externas podem ser usadas, uma baseada no RNA recombinante, e outra baseada no DNA recombinante. Porém a curva baseada no DNA recombinante é mais estável que a de RNA, não sofrendo atividade de RNAses, e podendo ficar estocada por um período de tempo maior. Ao utilizar a curva baseada no DNA

recombinante, somente moléculas de cDNA derivadas de uma RT podem ser quantificadas com precisão, sendo que a eficiência de síntese do cDNA deve ser sempre confirmada (PFAFFL, 2001).

3 OBJETIVOS

3.1 Objetivo geral

Este trabalho tem como objetivo, o estudo de um sistema de expressão gênica, baseado em um *Alphavirus* (*Semliki Forest Virus* - SFV), utilizando diferentes linhagens de células de mamíferos. Para tanto, a proteína utilizada para avaliar a expressão, foi a glicoproteína do vírus rábico (RVGP).

3.2 Objetivos específicos

- estabelecer um protocolo de transcrição *in vitro* e transfecção de RNA, para produção de partículas virais SFV recombinantes (SFV-RVGP);

- analisar a expressão da RVGP no sistema de expressão SFV com diferentes métodos como ELISA, *Western blot* e imunofluorescência indireta (IFI);

- estabelecer um método de titulação/quantificação dos vírus recombinantes para otimizar a infecção viral e expressão da proteína heteróloga;

- determinar as melhores condições de cultivo celular e infecção viral para expressão da proteína heteróloga;

4 MATERIAIS E MÉTODOS

4.1 Células de mamíferos utilizadas para avaliar a expressão de RVGP

4.1.1 Baby Hamster Kidney (BHK-21)

Foram utilizadas nesse trabalho, células BHK-21 para a geração das partículas virais SFV-RVGP através de uma co-transfecção dos RNAs originados dos vetores pSFV-RVGP e pSFV-Helper. Esta linhagem é originária do organismo *Mesocricetus auratus* (*Syrian golden hamster*), passagem 87. Seu cultivo foi realizado em meio *Dulbecco's Modified Eagle Medium* (DMEM - Gibco, Grand Island, NY., U.S.A.) suplementado com 10% de soro fetal bovino (SFB), nas condições de 37 °C, com 5% de CO_2. A célula também foi utilizada para avaliar a expressão da RVGP a partir da infecção com o vírus SFV-RVGP.

4.1.2 BHK-21 suspensão

Células BHK-21 C-13 (Sigma-Aldrich *ECACCCell Lines*, Lyon, France), adaptadas a suspensão, generosamente doada pelo Dr. Renaud Wagner (*Ecole Superieure Biotecnologie, Universidade de Strasbourg*), utilizadas na passagem 137, foram cultivadas em meio IMDM (46,5%) (Gibco, Grand Island, NY., U.S.A); DMEM (46,5%); suplementado com Soro Fetal bovino inativado (5%) e solução de Glutamina 4 mM (2%). Foram avaliadas quanto à capacidAde de expressão de RVGP a partir da infecção com o vírus SFV-RVGP.

4.1.3 Células de Hepatocarcinoma humano (Human Hepato Cellular Carcinoma-HuH 7)

Células diferenciadas *in vitro* de hepatocarcinoma humano, passagem 118 foram utilizadas para avaliar a produção de RVGP após a infecção com o vírus SFV-RVGP. Condições de cultivo iguais às descritas para BHK-21.

4.1.4 Human Embrionic Kidney (HEK-293T)

Células derivadas do rim humano, utilizadas na passagem 123 também foram utilizadas para avaliar a produção de RVGP após a infecção com o vírus SFV-RVGP, sob as mesmas condições de cultivo das demais células. As células HEK-293T derivam da linhagem HEK-293, com o adicional de expressar o antígeno T, do vírus símio 40 (SV 40).

4.1.5 Green Monkey Kidney (VERO)

Também utilizamos a linhagem celular derivada do rim do macaco verde africano (*Cercopithecus Aethiops*), na passagem 62.

4.1.6 Linhagem L929 (ATCC – CCL-1)

A célula L929 é um subclone da linhagem parental L. Foi uma das primeiras linhagens celulares a serem estabelecidas em cultura contínua. A linhagem L é derivada do tecido aureolar subcutâneo e adiposo de um camundongo macho C3H/An de 100 dias. Foram utilizadas na passagem 18, sendo avaliada a produção de RVGP após a infecção por SFV-RVGP.

4.2 Obtenção do Semliki Forest Virus recombinante (SFV-RVGP)

Para a construção do vetor de expressão, o cDNA correspondente ao genoma do SFV foi dividido em dois plasmídeos distintos.O plasmídeo de expressão (pSFV-RVGP), contendo os genes não estruturais do SFV e o promotor subgenômico SFV26S, além de uma região de policlonagem para inserção do gene de interesse, no caso a RVGP. O cDNA da RVGP foi obtido a partir do plasmídeo RVGP/PV fornecido pelo Dr. Yves Jacob do Instituto Pasteur, de Paris. O outro plasmídeo, denominado como “auxiliar” (pSFV-Helper), contém a informação genética para as proteínas estruturais do vírus (**Figura 3**). Ambos os plasmídeos possuem como sinais de seleção bacteriana, o gene de resistência à ampicilina. O plasmídeo de expressão possui ainda um sinal de encapsidação, ausente no plasmídeo “auxiliar”, tendo essa sequência, a função de permitir que o plasmídeo/RNA que a possui seja incorporado pela

partícula viral recém gerada. A etapa de construção dos vetores foi realizada por um trabalho anterior a esse, no laboratório de Receptores de Proteínas Membranárias da Universidade Louis Pasteur em Strasbourg, França (BENMAAMAR et al., 2009).

Figura 3 - Vetores utilizados no trabalho.

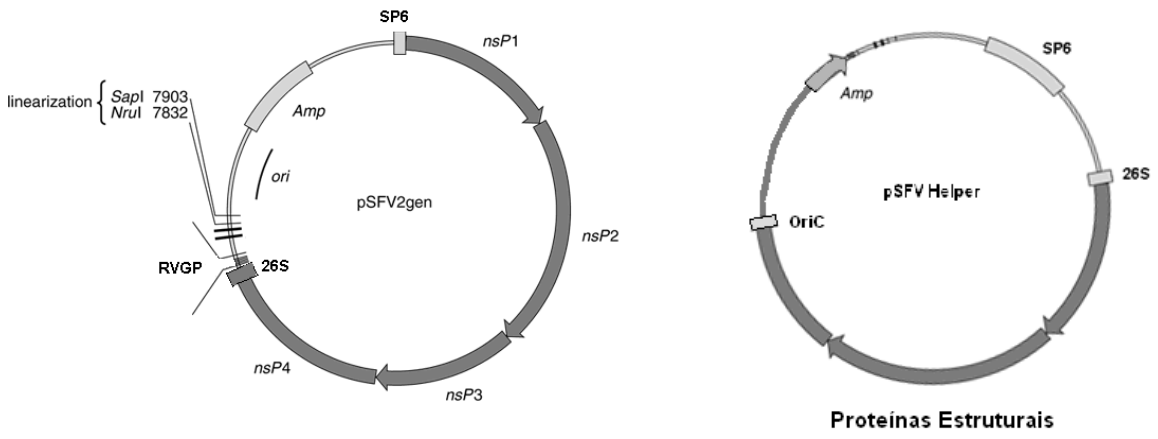

SP6 – Promotor para RNA polimerase
nsP1, nsP2, nsP3 e nsP4 – Proteínas não estruturais do SFV
Amp – Gene de resistência à ampicilina
26S – Promotor subgenômico viral
OriC – Origem de replicação bacteriana
RVGP – Glicoproteína do vírus rábico

4.2.1 Transformação bacteriana para amplificação dos vetores

Alíquotas de bactéria DH5α competentes foram descongeladas, e os vetores pSFV-RVGP e pSFV-Helper foram adicionados separadamente na proporção 3:30, sendo feito simultaneamente um controle negativo (sem plasmídeo). As misturas foram mantidas por 30 minutos no gelo. Em seguida, as bactérias foram mantidas a temperatura de 42 °C, 2 min, e imediatamente foram colocadas novamente no gelo por 5 minutos. O plaqueamento de todo volume da bactéria foi então feito em meio LB- ágar com antibiótico (ampicilina) e incubados a 37 °C, 20 h (*overnight*).

4.2.2 Obtenção dos plasmídeos

Colônias isoladas de bactérias contendo o vetor de interesse (pSFV-RVGP ou pSFV-Helper) foram inoculadas em 100mL de meio LB em um frasco *erlenmeyer* estéril e vedado, incubado a 37 °C, 20 h (*overnight*), sob agitação a 250 rpm. Após o período de incubação o DNA plasmidial foi extraído e purificado com o kit Maxiprep Plasmid (Qiagen, Valencia, CA., U.S.A.), conforme instruções do fabricante. A concentração dos vetores foi determinada por fluorimetria através do equipamento Qubit (Invitrogen, Carlsbad, CA., U.S.A) e confirmada por leitura em espectrofotômetro a 260 nm.

4.2.3 Transcrição in vitro

Primeiramente, os plasmídeos pSFV-RVGP e pSFV-Helper foram linearizados com as enzimas *Nru* I e *Spe* I, respectivamente, sendo o processo confirmado através de um procedimento de eletroforese em gel de agarose 0,8% (**Figura 5**). Após essa etapa, os mesmos foram então submetidos a um processo de transcrição *in vitro*, através do kit MAXIScript SP6® (Ambion, Carlsbad, CA., U.S.A.), conforme instruções do fabricante com algumas modificações, como a temperatura de incubação de 40 ºC, e o tempo de 2 h, além da adição dos reagentes CAPanalog (Invitrogen) e Ribolock (Thermo Scientific, Vilnius, Lituânia). Os RNAs gerados foram quantificados através de método fluorimétrico no equipamento Qubit, e um procedimento de eletroforese em gel de agarose (0,8%) foi feito, para verificar a eficiência da transcrição (**Figura 5**).

4.2.4 Transfecção por Eletroporação

O protocolo de eletroporação foi baseado em Karlsson e Liljestrom (2003), com algumas modificações. Os RNAs obtidos foram prontamente transfectados em células BHK-21 (8 x 10^6 células), repicadas no dia anterior, com 80% de confluência, utilizando o aparelho GenePulser II (Biorad, Hercules, CA., U.S.A.). A proporção entre os dois tipos de RNAs utilizados foi sempre de dois RNAs oriundos do pSFV-RVGP (RNA-RVGP), para cada um RNA obtido do pSFV-Helper (RNA-Helper). As condições de eletroporação utilizadas foram as seguintes: 360 v; 75 µF; resistência ∞, para cubetas de 0,2 cm. As células recém

eletroporadas foram colocadas em garrafa T-75, com 10 mL de meio DMEM, suplementado com 10% de soro fetal bovino, e incubadas a 37 ºC, 24 h, com 5% de CO_2. Após esse período, o sobrenadante das células foi coletado e centrifugado a 15550 g, 4 ºC, 30 min. O sobrenadante da centrifugação, contendo os vírus, foi então filtrado com filtros de 0,22 µm (Milipore, Billerica, MA., U.S.A.), aliquotados e armazenados a -80 ºC.

4.2.5 Transfecção utilizando o reagente comercial Transmessenger (Qiagen)

O processo de transfecção através do kit Transmessenger, foi realizado conforme instruções do fabricante, sendo realizada em garrafas T-75 com BHK-21 (80% confluentes) repicadas no dia anterior. Utilizou-se a proporção 1:4, de RNA com relação ao reagente, sendo que foram utilizados 12 µg de RNA total, dos quais 8 µg eram do RNA-RVGP, e 4 µg do RNA-Helper. A coleta das partículas virais foi realizada 24 h após a transfecção, através de centrifugação a 15550 g, 4 ºC, 30 min. O sobrenadante da centrifugação foi então filtrado com filtros de 0,22 µm, aliquotados e armazenado a -80 ºC.

4.3 Quantificação viral

Para determinar o título viral e, consequentemente, a quantidade de vírus a ser utilizada no processo de infecção (MOI), utilizou-se um protocolo de extração do RNA viral seguido de uma etapa de transcrição reversa, de forma que o cDNA obtido fosse então quantificado por qPCR.

4.3.1 Desenho de oligonucleotídeos

Através do aplicativo *Primer Express 3.0*, foram desenhados os oligonucleotídeos utilizados para o desenvolvimento do processo de quantificação viral (**Tabela 3**).

Tabela 3 - Características dos oligonucleotídeos

Nome	Seqüência	Tm (°C)	%GC
F-I-2	ACA GAC TGT CAC TGA GCA G	52	53
R-I-2	TCT CTG CAG TAG ATG GTC AC	54	50
SFV1	TGT GCC GCT ACG CAA TGA	64	56
SFV2R	CAT GCT TTT AAC TTG GTG TGA CCT A	62	40
SFV3	AGA CCA TGT GGA CCT CGA GAA	62	52
SFV4R	GAG GCA AGG TAT GCA GCT CTC T	62	55
R-E-2	CTC AAT GAT GAC GTG GAG CT	54	50

Tm - Temperatura de Melting.
GC – Par de bases nitrogenadas formado por Guanina e Citosina.

Foram utilizadas como alvo para anelamento, a região *nsp2* da poliproteína não estrutural do SFV, sendo desenhados três pares de oligonucleotídeos (F-I-2/R-I-2; SFV1/SFV2R; SFV3/SFV4R), cujas características estão dispostas na tabela.

4.3.2 Extração de RNA

O sobrenadante contendo as partículas virais foi submetido a um processo de extração do RNA viral, através do kit QIAmp Viral RNA (Qiagen), conforme instruções do fabricante.

4.3.3 Tratamento com DNase

O RNA obtido foi quantificado através do reagente Quant-it RNA assay kit (Invitrogen) e do fluorímetro Qubit (Invitrogen), sendo que esse reagente permite a quantificação em separado do RNA e do DNA presente na amostra. O material foi então tratado com a enzima DNase I (Promega, Madison, WI., U.S.A.), para eliminar possíveis DNAs contaminantes que possam existir na solução. Após a adição de 3 unidades da enzima para cada 3 microgramas do material, a solução foi incubada a 37ºC, 30 min. Terminado esse período, adicionou-se 2 µL de um inibidor enzimático à base de EGTA (*Stop Solution*), e a reação foi incubada a 65 ºC, 10 min. Este passo visa a inativação da enzima, para que não

haja ação da mesma no cDNA viral que será obtido posteriormente. O RNA tratado foi imediatamente submetido a uma reação de transcrição reversa.

4.3.4 Transcrição Reversa

O processo de transcrição reversa, visa obter o cDNA correspondente ao material genético viral para posterior quantificação do mesmo. Para essa etapa, foi utilizado o oligonucleotídeo R-E-2 (**Tabela1**), específico para a região *nsp2* do vírus.

Cada amostra de RNA livre de DNA foi então imediatamente submetida à reação de transcrição reversa com a enzima M-MLV (Invitrogen). Primeiramente, 200 ng de RNA tratado com DNase foram incubados a 65 ºC, 5 min, juntamente com 1 µM de oligonucleotídeos anti-senso específico (R-E-2), 0,5 mM de dNTPs e água livre de DNase e RNase. Em seguida, a mistura foi resfriada rapidamente no gelo e adicionou-se o tampão, juntamente com o DTT 0,1M e 200 U de M-MLV, em um volume total de 20 µL. A reação foi incubada a 37 ºC, 30 min, para a síntese do cDNA do SFV, sendo interrompida pela incubação a 70 ºC, 15 min. As amostras foram então armazenadas –20 ºC até a análise. Durante a padronização dos protocolos, as preparações de RNA tratadas com DNase foram testadas em reações de *nested*-PCR, utilizando os mesmos pares de *primers* (F-I-2 e R-I-2), para avaliar a eficácia da digestão do DNA contaminante. Somente após a confirmação da remoção do DNA contaminante, o cDNA de cada amostra viral foi submetido à qPCR, simultaneamente com os padrões da curva padrão. O cDNA obtido era utilizado imediatamente, ou armazenado a -20 ºC por no máximo 3 meses.

4.3.5 PCR e Nested PCR

A reação em cadeia da polimerase (PCR) foi desenvolvida com o kit comercial *Taq DNA Polymerase* (Invitrogen), seguindo recomendações do fabricante. Foram adicionados 5 µL de amostra, para 1 µL de cada *primer* (R-I-2 / F-I-2, a 5µM), 1 µL de $MgCl_2$ (1,5 mM), 0,5 µL dNTP (10 mM), 2,5 µL de Buffer 10x, 0,2 µL de enzima (1 U) e água para um volume final de 20 µL. A reação foi realizada no termociclador PTC-200 (MJ Research, St Bruno, Quebec, Canada) com o seguinte ciclo de amplificação: 94 ºC / 3 minutos, (94 ºC/ 15s, 53 ºC/

30s, 72 ºC/ 30s) x 34, 72 ºC/ 10 minutos. As mesmas condições foram utilizadas nas reações de *nested*-PCR, sendo as amostras provenientes da primeira PCR.

Os fragmentos amplificados puderam ser visualizados através de eletroforese em gel de agarose 1,5 % contendo 0,5 µg/mL de brometo de etídeo e revelação em transiluminador (TFX-20M, Life Technologies) sob luz ultravioleta, captura de imagem através de sistema fotodocumentador com câmera DC290 (Kodak,Rochester, NY, Estados Unidos) e análise com aplicativo *Alpha DigiDoc* (**Figura 4**).

4.3.6 Obtenção dos padrões para construção da curva-padrão para qPCR

Para realizar a quantificação do RNA genômico das partículas virais, foi construída uma curva-padrão, a partir do vetor de expressão (pSFV-RVGP). O vetor foi submetido à digestão através da enzima *Nru*I (Fermentas) para linearização, que foi confirmada através de eletroforese em gel de agarose 0,8% (**Figura 5**). Posteriormente, foi quantificado através do Qubit, e diluído em EGTA (1mM), para a obtenção de diversas quantidades de cópias em um mesmo volume de 3 µL (6×10^7, 6×10^6, 6×10^5, 6×10^4, 6×10^3, 6×10^2, e 60 cópias). Os padrões diluídos e aliquotados foram armazenados a -20 ºC até o momento do uso. Diversas amplificações da curva padrão foram realizadas em qPCR para determinar sua reprodutibilidade, avaliando três pares de oligonucleotídeos distintos (**Tabela1**), sendo os experimentos realizados em triplicatas para cada padrão (**Figura 8**).

4.3.7 qPCR

A qPCR foi realizada no equipamento *StepOne Real Time PCR System* (Applied Biosystem, Foster City, CA, U.S.A.). Utilizou-se o kit *Power Sybr Green* (Life Technologies), que contém uma mistura de dNTPs, $MgCl_2$, Taq DNA polimerase, e o reagente fluorescente intercalante de bases, *Sybr Green*, em tampão próprio, pronto para uso. Em 6,5 µL correspondente a esse reagente foram adicionados 0,65 µL de cada *primer* (R-I-2 / F-I-2, a 5 µM) e água para um volume final de 12 µL. A solução foi então distribuída na placa*MicroAmp*™ (Applied Biosystems), adicionando-se posteriormente 3 µL de amostra, totalizando 15 µL de volume final. A placa foi então vedada e brevemente centrifugada (45 g/ 5s) para coletar todo o volume no fundo do recipiente.

O ciclo de amplificação utilizado foi o mesmo já descrito (**Metodologia 5.3.5**). A leitura da fluorescência emitida era feita uma vez a cada ciclo após a elevação da temperatura a 80ºC. Ao final da amplificação era determinado o ponto de dissociação dos produtos da PCR ("*Melting point*"), através da elevação gradual da temperatura de 60 ºC a 95 ºC, com leitura a cada 1 ºC de elevação, para verificar a especificidade da reação, sendo que o fragmento amplificado deve apresentar dissociação à temperatura de 83 ºC ± 0.3 ºC, com base no seu tamanho (145 bp). Para cada análise das amostras oriundas do SFV-RNA, foi realizada na mesma placa a análise dos padrões para a construção da curva padrão de quantificação, sendo o experimento realizado em triplicata para as amostras e padrões.

O aplicativo *StepOne Software v2.2.2* foi utilizado para realizar a análise de dados obtidos durante a reação de qPCR. O nível de fluorescência, pelo qual passa a linha de amplificação exponencial ("*treshold*"), foi definido pela subtração do sinal de fundo ("*baseline*") pela média entre o sinal obtido no primeiro ciclo ao do décimo segundo ciclo. Posteriormente, visualizando o gráfico em modo suavizado ("*smooth*") na escala logarítmica, pode-se estabelecer o nível de fluorescência mais adequado, próximo ao início da curva exponencial de aumento da fluorescência. O ciclo de quantificação ("*cycle treshold*" - Ct), que é o parâmetro utilizado para realizar a análise, corresponde ao ponto de intersecção entre a curva de amplificação da fluorescência e o patamar fixado como ideal.

Para determinação do título viral, foram realizados alguns cálculos com base na equação da curva de quantificação. Sendo que, o número de cópias do SFV-RNA era determinado multiplicando-se o resultado fornecido pela qPCR por um valor obtido com base nas diluições efetuadas e pelo rendimento do processo de extração (**Figura 4**).

Figura 4 - Cálculos para determinação da titulação viral.

$$SFV = A \times B / C \times D / E$$

SFV – número de cópias de vírus por µl
A – resultado obtido pela qRT-PCR
B – volume total da RT
C – volume da amostra usada na qPCR
D – volume de eluição da coluna de extração
E – volume utilizado após tratamento com DNase para fazer RT

4.4 Ativação do vírus SFV-RVGP

Os vírus recombinantes são obtidos na forma inativa devido a uma mutação na proteína estrutural E1, sendo necessário um processo de ativação, para que a infecção seja realizada por eles. As partículas de SFV-RVGP são então tratadas com α-quimiotripsina (Sigma-Aldrich, St. Louis, MO, U.S.A.), 1,6 mg/mL de vírus, e incubadas à temperatura ambiente (TA), 30 min, sendo posteriormente submetidas a um processo de inativação dessa enzima, realizado com a adição de aprotinina (1 mg/mL) (Thermo Scientific, Vantaa, Finlândia), e incubação a TA, 5 min. Após esse processo, as partículas ativadas podem ser utilizadas ou armazenadas a -80ºC.

4.5 Infecção com o vírus SFV-RVGP

As diversas linhagens de células de mamíferos foram inoculadas em placas de 6 poços, com 3 x10^5 células por poço, um dia antes da infecção. No dia seguinte, as células recebiam os volumes de SFV-RVGP correspondentes aos MOIs determinados (1, 10, 15 e 50), sendo que no caso das células BHK-21 adaptadas a suspensão, utilizou-se apenas o MOI 15. Os tempos de coleta avaliados após a infecção foi de 24 e 48 horas.

Para o processo de infecção, as placas foram primeiramente lavadas com PBS estéril (0,8 mL/ poço), para retirar o meio de cultura contendo soro fetal bovino. Após a retirada do PBS, o vírus foi adicionado na quantidade desejada, previamente diluído em 0,5 mL de meio DMEM sem soro fetal bovino. As placas permaneceram a temperatura ambiente (24ºC)

durante duas horas, em agitador Kline. Após esse tempo, foram adicionados 1 mL de meio DMEM com soro fetal bovino (10%), e os cultivos colocados a 37 ºC em atmosfera contendo 5 % de CO_2.

Após 24 e 48 horas, o sobrenadante de cada poço foi coletado e centrifugado, enquanto que as células foram descoladas com PBS-EDTA (5 mM) e incubadas a 37ºC, 5 min, sendo posteriormente centrifugadas. Após centrifugação de ambos (800 g / 5 minutos), o sobrenadante e o pellet foram armazenados a -20ºC, para posterior avaliação quanto à presença de RVGP, através de ensaio imunoenzimático (ELISA) específico para a RVGP. A preferência pelo uso de PBS-EDTA se deve ao fato de que a utilização de tripsina diminui a concentração de RVGP presente (BENMAAMAR et al., 2009).

4.6 ELISA

A técnica de ELISA para detecção da RVGP foi realizada conforme descrito em trabalho anterior, para detecção da mesma proteína em células S2 (ASTRAY et al., 2008).

4.6.1 Reagentes e soluções

- Anticorpos monoclonais para a sensibilização das placas (IgG-D1): Imunoglobulina anti-sítio III da glicoproteína rábica.

- Anticorpos monoclonais conjugados com peroxidase (IgG-D1-Po): Imunoglobulina idêntica à utilizada para a sensibilização das placas, conjugada com peroxidase.

- Antígeno de referência: vírus rábico (linhagem Pasteur) inativado, purificado e liofilizado, apresentando 10 µg de RVGP.

- Tampão carbonato 0,05 M (pH 9,6): solução de bicarbonato de sódio 0,05 M, com pH 9,6 ajustado com solução de carbonato de sódio 0,05 M.

- Tampão de bloqueio: 0,3 % albumina de soro bovino (BSA) + 5% sacarose em tampão carbonato (pH 9,6).

- Tampão PBS (pH 7,0) concentrado 10x.

- Tampão de lavagem: PBS + 0,005% Tween 20.

- Tampão de diluição: PBS + 0,05% Tween 20 + 0,5% BSA (pH 7,0).
- Tampão citrato (pH 5,6):citrato de sódio + ácido cítrico + 0,1% peróxido de hidrogênio 40 v.
- Solução de substrato cromógeno: Tampão citrato + orto-phenylene diamine (2 mg/mL).
- Solução de parada: Ácido sulfúrico 4 N.

4.6.2 Procedimento

No dia anterior ao procedimento, as placas foram sensibilizadas com anticorpos monoclonais específicos para o sitio III antigênico da RVGP em seu estado trimérico, e armazenadas a 4 °C. No momento do uso, as placas foram bloqueadas com solução de bloqueio e incubadas por 30 minutos a 37 °C, sendo então lavadas 5x com tampão de lavagem. O antígeno de referência foi diluído em tampão de diluição nas concentrações 7,8 ng/mL, 14,6 ng/mL, 31,2 ng/mL, 62,5 ng/mL, 125 ng/mL, 250 ng/mL e 500 ng/mL, para definição da curva padrão do experimento. As amostras de lisado celular e sobrenadante foram primeiramente descongeladas, adicionou-se 500 uL de tampão T4, e foi feita homogeneização por vortex. Em seguida, foram colocados 500 uL de tampão de lise e nova homogeneização foi realizada, incubando em seguida as amostras a 4 °C, 1 h, com homogeneização a cada 15 minutos. Após esse período, foi feita centrifugação a 12000 g durante 10 minutos para separar os debris celulares. O sobrenadante e os padrões foram então aplicados na placa no volume de 200 uL em duplicatas e incubados por a 37^0C, 1 h, para permitir a ligação da RVGP aos anticorpos aderidos na placa. Após esse período, as placas foram novamente lavadas 5x e receberam o anticorpo monoclonal anti-RVGP conjugado com peroxidase, sendo incubadas a 37 °C, 1 h. Após serem lavadas 6x, a solução de cromógeno era adicionada e a reação incubada no escuro a 22 °C, 30 min, recebendo após esse tempo a solução de parada. A absorbância era lida no comprimento de onda de 492 nm em leitor de microplacas (Multiskan MJ-Labsystems). A determinação da concentração de RVGP em cada amostra era realizada com base na comparação das absorbâncias das amostras com a curva padrão.

4.7 *Western-Blot*

4.7.1 Reagentes e Soluções

- Anticorpo primário:IgG-D1 - Imunoglobulina policlonal contra a glicoproteína rábica.

- Anticorpo secundário:αIgG-D1 – Anti-rabbit conjugado com peroxidase.

- Solução de acrilamida 40%: 40% de acrilamida e 0,8% de bis acrilamida em água destilada.

- Tampão Tris-HCl 1,5 M – pH 8,8: 1,5 M de tris base em água destilada e pH 8,8 ajustado com solução de HCl 2N.

- SDS 20 %: 20 % de dodecil sulfato de sódio (SDS) em água destilada.

- Persulfato de amônio 10%: 10% de persulfato de amônio em água destilada.

- Tetrametiletilenodiamina (TEMED).

- Tampão de transferência – pH 8,3: 3 g de Tris-base, 14,4 g de Glicina, 1 g de SDS, 0,2 L de etanol e H2O qsp 0,8L.

- Tampão de bloqueio – pH 7,0: PBS com pH 7, leite em pó desnatado (3%) e Tween 20 (0,05%).

- Tampão de corrida – pH 8,3 (5x): 75,5 g de tris-base, 360g glicina, 25 g de SDS e H2O milli Q qsp 5L.

Os géis de separação (12%) e empilhamento (4%) foram preparados conforme a **Tabela 4**. Após polimerização, o gel foi mantido em tampão de corrida (*overnight*).

Tabela 4 - Composição dos géis utilizados no *Western blot*.

Reagentes	Gel de Separação (mL)	Gel de Empilhamento (mL)
Acrilamida/Bis 37 / 1 – 40%	1,5	0,312
Tris-HCl 1,5 M – pH 8,8	1,4	0,35
H_2O Milli Q	2,1	1,85
SDS 20%	0,025	0,0125
Persulfato de amônia - APS 10%	0,045	0,0125
Temed	0,0042	0,006

Temed – Tetrametiletilenodiamina
SDS - Dodecil sulfato de sódio

4.7.2 Procedimento

Foram montados dois géis de poliacrilamida (**Tabela 4**), para a realização simultânea dos procedimentos de *Western blot*, e da coloração do gel por prata. As amostras foram submetidas a um processo de lise, adicionando-se 500 uL de tampão T4, com posterior homogeneização por vortex. Em seguida, foram colocados 500 uL de tampão de lise e nova homogeneização foi realizada, deixando-as incubadas a TA, 30 min, sendo então posteriormente, centrifugadas a 1550 g, 5 min. Para o experimento de coloração por prata, foram utilizados 50 µL de amostra juntamente com 10 µL de Loading buffer 6x (5:1). Enquanto que, para o *Western blot*, utilizou-se 45 µL de amostra, com 15 µL de LDS Sample buffer non-reducing 4x (Thermo Scientific) (3:1). Todas as amostras foram então incubadas a 90°C, 5 min, sendo posteriormente aplicadas em seus respectivos géis. A corrida do gel foi realizada a 110V, 1,5 h. Em seguida, o gel contendo as amostras para o *Western blotting*, foi colocado em um aparato específico para realizar a transferência para membrana de nitrocelulose Amersham Hybond – ECL de 0,45 um (GE Healthcare, Piscataway, NJ, U.S.A.), sob as condições de 120V, 385 mA, 1,5 horas. Sendo posteriormente, a membrana transferida para a solução de bloqueio, e incubada *overnight* a 4°C. Enquanto que o gel para a coloração de prata foi primeiramente lavado 2x com água destilada por 10 minutos, fixado com solução contendo etanol 30%, e ácido acético 10%, e também incubado a 4 °C, *overnight*.

No dia seguinte, a membrana para *Western blot* foi lavada 3x por 10 minutos com TBS + Tween 20 (0,05%). Logo após, foi adicionado o anticorpo primário, diluído 1:1000 em 20

mL de tampão de bloqueio, sendo incubado por 1 h sob agitação. Três novos procedimentos de lavagem com TBS + Tween 20 (0,05%) foram realizados, e em seguida adicionou-se o anticorpo secundário, diluído 1:4000 em 25 mL de tampão bloqueio, sendo novamente incubado por 1 h sob agitação. O mesmo procedimento de lavagem já descrito foi realizado novamente.

Para o processo de revelação, primeiramente a membrana foi colocada sobre um papel celofane (*film*), com as bandas voltadas para cima. Foi adicionado o reagente Super Signal West Pico Chemiluminescent Substrate (Thermo Scientific, Rockford, IL, U.S.A.), deixando agir por 5 minutos. Posteriormente, foi montado o cassete de filmes raios X, contendo uma folha de transparência acoplada entre as faces. Na câmara escura de revelação, coloca-se a transparência em contato com a membrana, e o filme de raios X (Kodak) sobre a transparência, deixando em contato durante 5 minutos. Para concluir, é feita a revelação do filme utilizando o revelador e fixador (Kodak).

Com relação à coloração de prata, após o processo de parada, o gel é lavado 2x com etanol 10% por 5 minutos, e depois mais 2x com água destilada também por 5 minutos. O processo de coloração é então realizado com o kit Pierce silver stain (Thermo Scientific), conforme instruções do fabricante.

4.8 Dot Blot

O procedimento para realizar o *Dot blot* é realizado diretamente na membrana de nitrocelulose. O preparo das amostras é o mesmo que o do *Western blot*, até o momento de centrifugação das amostras. As amostras são então aplicadas à membrana Amersham Hybond – ECL de 0,45 µm (GE Healthcare), sendo então lavadas 3x com TBS. A membrana é então incubada em solução de bloqueio a 4 °C, *overnight*. No dia seguinte, todo o procedimento é o mesmo do *Western blot*, já descrito anteriormente, até a revelação em filme de raios X.

4.9 Imunofluorescência Indireta

4.9.1 Reagentes e soluções

- Anticorpo primário:IgG-D1 - Imunoglobulina anti-sítio III da glicoproteína rábica.
- Anticorpo secundário:αIgG-D1 – Anti-mouse conjugado com FITC.
- Azul de Evans
- Paraformoldeído (4%)
- Tampão PBS – pH 7,0
- Tampão PBS-Tween – pH 7,0: PBS + 0,05% Tween 20

4.9.2 Procedimento

No dia anterior ao procedimento, foi realizada uma infecção com SFV-RVGP em todas as linhagens estudadas, em placas de 6 poços com lamínulas, com os MOIs correspondentes (1 e 10). Após 24 horas, o meio de cultura foi retirado, e cada poço foi lavado sem homogeneização brusca, 3 vezes com PBS (1x). Para a fixação das células na lamínula, foram adicionados 0,5 mL de paraformaldeído (4%) em cada poço, sendo as placas incubadas sobre o gelo, 20 min. Passado esse tempo, cada poço foi novamente lavado 3 vezes com PBS (1x). O anticorpo primário (IgGD1) foi adicionado com diluição 1:400 (200 uL), através de gotejamento sobre a lamínula, e as placas incubada a TA, 1 h. Três novos procedimentos de lavagem foram realizados, utilizando 1 mL da solução de PBS-Tween. Para a adição do anticorpo secundário (αIgGD1), o mesmo foi diluído em solução de azul de Evans, sendo adicionado 200 uL por poço, e as placas incubadas a TA, 1 h, no escuro. Após esse tempo, cada poço foi novamente lavado 3 vezes com PBS (1x). As lamínulas foram então retiradas de cada poço, e colocadas em lâminas, que já haviam recebido 8 uL de *SlowFade Gold*® (Invitrogen), um reagente que preserva a fluorescência por um período maior de tempo, e que contem ainda o DAPI, um marcador de núcleo celular. A visualização foi feita em microscópio de fluorescência BX51 (Olympus, Tóquio, Japão), com auxílio do sistema de captação de imagem DP73 (Olympus), e do software CellSens Standard.

5 RESULTADOS

5.1 Avaliação dos métodos de linearização e transcrição *in vitro* dos vetores

Para a obtenção dos RNAs correspondentes aos vetores plasmidiais, são necessárias duas etapas, a linearização dos vetores e a transcrição *in vitro*. Após cada etapa, foi realizado um procedimento de eletroforese para verificar a efetividade do processo (**Figura 5**).

Figura 5 – Eletroforese em gel de agarose (0,8%)

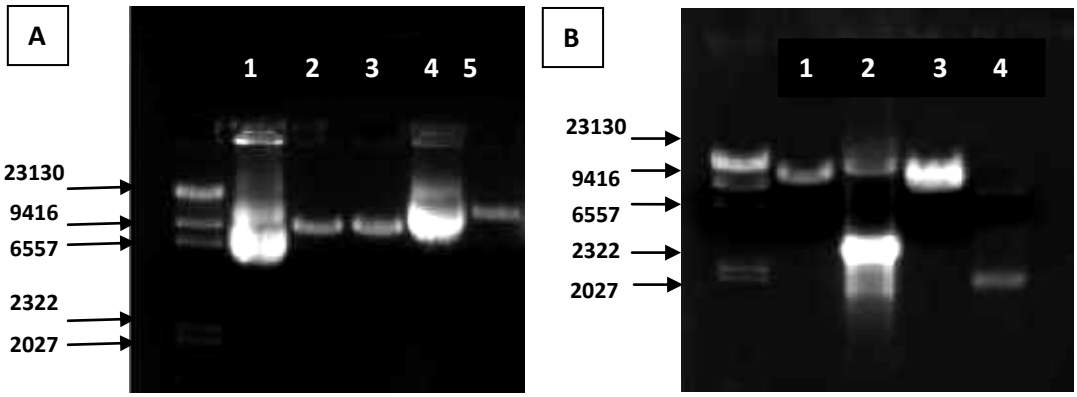

(A) Vetores linearizados; **1** – pSFV-Helper; **2** e **3** – pSFV-Helper linearizados; **4** – pSFV-RVGP; **5** – pSFV-RVGP linearizado; **(B)** RNA obtido pela transcrição *in vitro*; **1** – pSFV-RVGP linearizado; **2** – RNA- RVGP; **3** – pSFV-Helper linearizado; **4** – RNA-Helper;

No gel correspondente à linearização dos vetores, é possível verificar que a banda correspondente ao linearizado, se encontra entre as duas bandas do vetor circular (normal e *supercoiled*). Sendo o tamanho do pSFV-Helper linearizado de aproximadamente 8194 bp, e do pSFV-RVGP, de 11582 bp, correspondentes ao tamanho original dos vetores. Já com relação ao gel com o produto da transcrição *in vitro*, é possível verificar a banda do RNA gerado, bem abaixo das correspondentes aos vetores linearizados, fato esperado pelo menor tamanho e pela forma do RNA. Importante ressaltar, que o tamanho do RNA observado no gel não corresponde ao seu tamanho real, visto que devido às diferenças entre as moléculas de DNA e RNA, as bandas do marcador não representam a corrida da molécula de RNA.

5.2 Avaliação dos métodos de transfecção

Para a obtenção dos vírus recombinantes- SFV-RVGP, duas abordagens distintas foram avaliadas para a transfecção dos RNAs em células BHK-21. Um lipossomo comercial específico para RNA (Transmessenger) e o método de eletroporação. Em todos os casos, as partículas virais foram coletadas 24 h após a transfecção.

Os vírus obtidos dessas transfecções foram utilizados para ensaios de infecção em células BHK-21 e Huh 7, em placas de 6 poços com 7 x 10^5 células por poço. Utilizou-se 100 µL da suspensão viral, visto que o procedimento de quantificação das partículas virais foi realizado posteriormente. A coleta de RVGP foi realizada 24 e 48 h após a infecção e a quantificação da mesma foi realizada por ELISA (**Figura 6**).

Figura 6 - Expressão de RVGP a partir da infecção com o vírus SFV-RVGP obtido por diferentes métodos de transfecção.

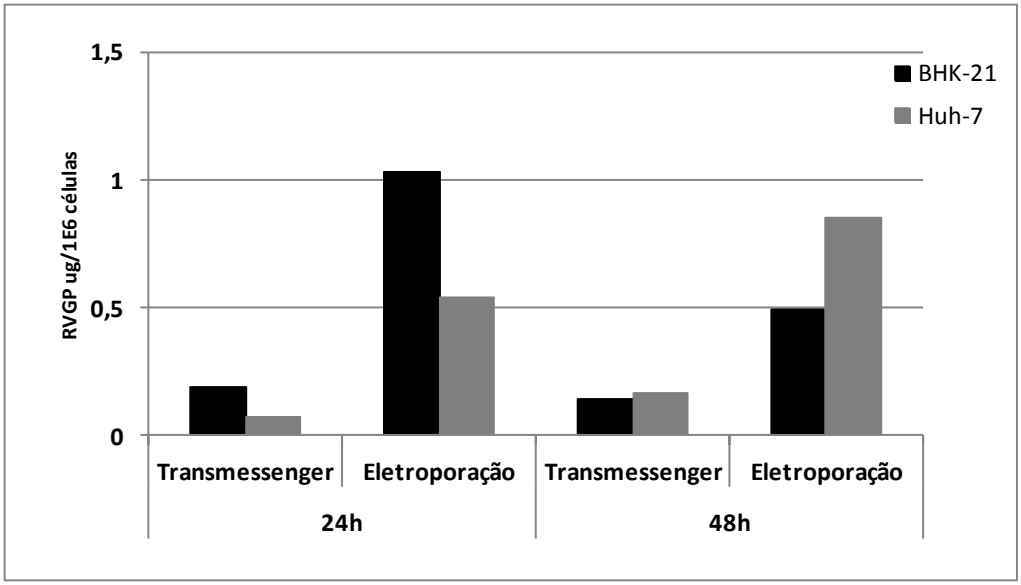

Os resultados apresentados demonstram uma clara evidência de que o método de eletroporação se mostrou mais eficaz que o método baseado no Transmessenger. O fato de ter sido obtido um maior nível de expressão de RVGP utilizando um mesmo volume de suspensão viral, indica que a abordagem utilizando eletroporação, foi capaz de produzir uma maior quantidade de partículas virais, fato comprovado posteriormente através da

quantificação viral por qRT-PCR (**Metodologia 5.3**). A partir dos cálculos de quantificação, pode-se determinar que foram utilizados valores de MOI de 0,2 e 2,9, para os vírus obtidos por Transmessenger e eletroporação, respectivamente.

Em ambos os protocolos de transfecção, foram utilizados RNAs obtidos de um mesmo protocolo de transcrição *in vitro* (**Metodologia 5.2.3**), com algumas modificações. Uma delas foi a adição do CAP analog, sendo que a presença de CAP no RNA gerado é reportado como determinante na regulação e estabelecimento de uma tradução eficiente dos RNAs recém transfectados (GALLIE, 1991). Outra modificação foi a adição de um inibidor de RNAse, com o propósito de retardar o processo de degradação do RNA. Como precaução com intuito de tornar o experimento padronizado, foi utilizada uma mesma linhagem celular oriunda de um mesmo banco, e em uma mesma passagem, para ambos os casos. Portanto, é válido dizer que fatores externos ou prévios não devem ter interferido no resultado, e que os dados expostos representam de maneira real a efetividade de cada processo.

Com relação às duas linhagens de células avaliadas (BHK-21 e Huh-7), os valores de RVGP expressos foram muito semelhantes em ambas, sendo alcançados entre 0,8 e 1 µg de RVGP/1E6 células. A linhagem BHK-21 apresentou uma maior expressão de RVGP no tempo de 24 horas após a infecção em ambas as abordagens, ao contrário da linhagem Huh-7 que apresentou maior expressão no tempo de 48 horas.

5.3 Padronização da qRT-PCR

Primeiramente, antes do procedimento de qPCR, foi realizado um experimento de PCR convencional (**Metodologia 5.3.5**), afim de verificar que o RNA extraído das partículas virais representava o material de interesse, e que o tratamento com DNase para eliminar possíveis contaminantes foi efetivo (**Figura 7**). Somente após a confirmação através do produto da PCR, é que o cDNA correspondente ao material genético viral foi submetido à qPCR para sua quantificação.

Figura 7 - Gel de agarose 1,5 % com os produtos da PCR-Nested

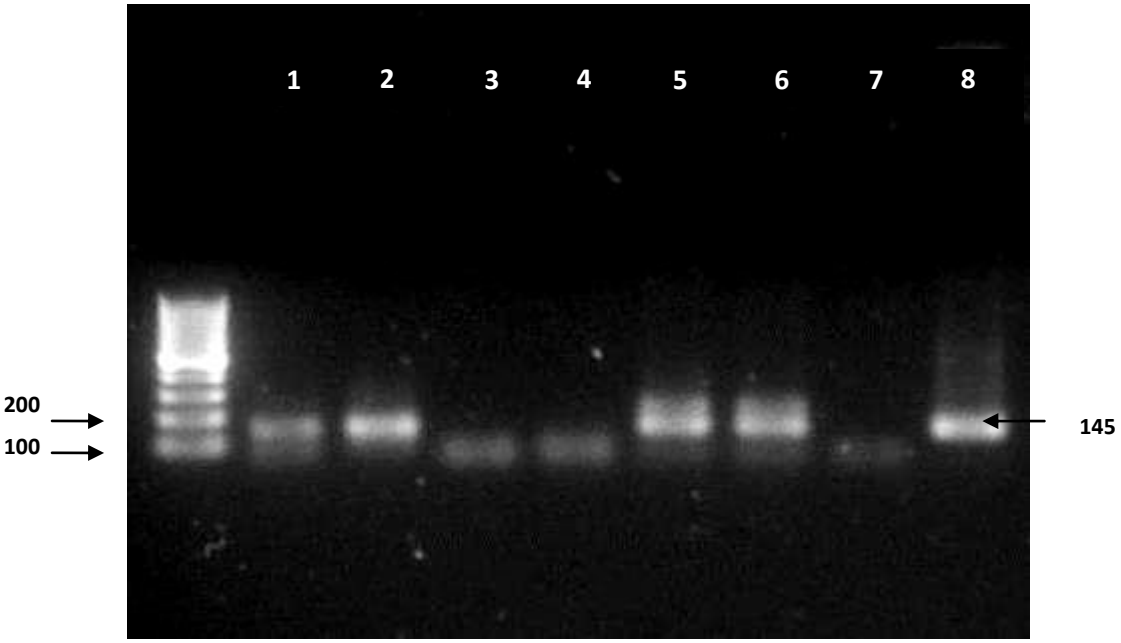

Marcador - 100bp**; (1 e 2)** RNA extraído das partículas virais; **(3 e 4)** RNA extraído tratado com DNase; **(5 e 6)** cDNAs; **(7)** Água; **(8)** pSFV-RVGP (C+)

Para realizar a padronização do procedimento de quantificação viral através de qPCR, foram realizadas diluições do plasmídeo pSFV-RVGP já linearizado, de forma que ficassem com os seguintes números de cópias 6×10^7, 6×10^6, 6×10^5, 6×10^4, 6×10^3, 6×10^2, e 60. Para avaliar a eficiência da curva padrão, três pares de oligonucleotídeos (**Tabela 1**) foram utilizados e os resultados estão expostos nos gráficos a seguir (**Figura 8**).

Figura 8 - Curva padrão obtida por qPCR através de diferentes pares de primers

A

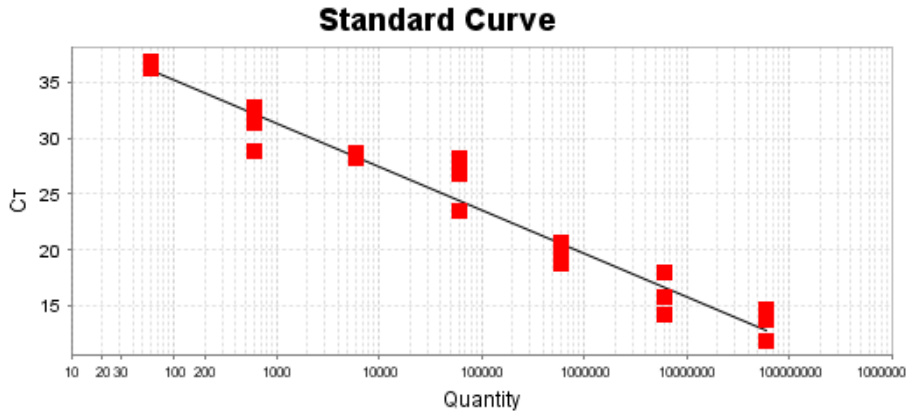

R^2 = 0,96 Slope = -3,871 Eficiência = 81,275

B

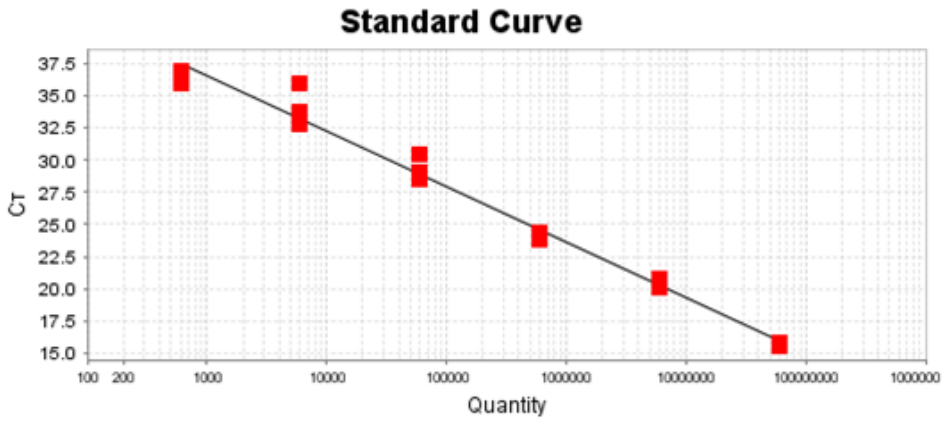

R^2 = 0,984 Slope =-4,318 Eficiência = 70,443

C

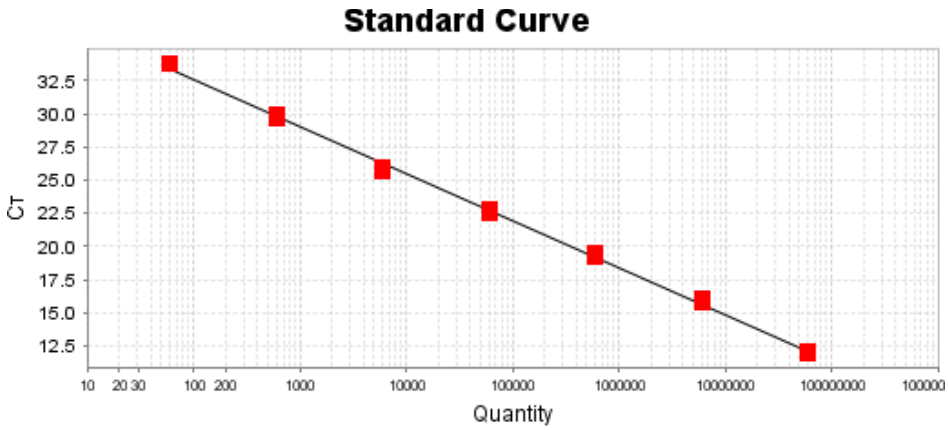

R^2 = 0,998 Slope =-3,538 Eficiência = 91,721

(A) SFV 1 / SFV 2R; **(B)** SFV 3 / SFV 4R e **(C)** F-I-2 / R-I-2.

Observamos que para os pares de oligonucleotídeos SFV1 e SFV2R, SFV3 e SFV4R, os CTs (*Cycle Threshold*) de cada ponto da curva foram detectados tardiamente (a amplificação do primeiro ponto ocorreu próximo ao 15º ciclo em ambas as curvas) e não houve reprodutibilidade entre as triplicatas. Também não houve amplificação do padrão contendo 60 cópias quando utilizado o par SFV3 e SFV4R. O par de *primers* R-I-2/F-I-2 apresentou a melhor curva padrão, com um valor elevado de R^2, e uma eficiência de cerca de 90%, sendo que o primeiro ponto, contendo $6x10^7$ cópias, foi detectado já no 12º ciclo, sendo assim, o par escolhido para desenvolver os procedimentos seguintes. Dois novos experimentos com esse par de *primers* foram realizados em dias diferentes, para verificar a reprodutibilidade da mesma.

Valores de CTs muito próximos entre as curvas produzidas em dias diferentes resultaram em valores praticamente iguais de R^2 e inclinação das curvas, o que comprova a reprodutibilidade da mesma e a estabilidade dos *primers* e padrões. Os desvios padrão médios calculados a partir de nove replicatas de uma mesma amostra de cDNA aplicada à reação de qPCR foram de 0,23 ± 0,06 Ct entre ensaios e de 0,10 ± 0,06 Cts intra ensaios. Esses dados permitem considerar a curva de quantificação e a metodologia, como sendo adequadas para a análise da quantidade de SFV – RNA nas amostras pretendidas (NOLAN et al., 2006).

5.4 Titulação viral

A partir da avaliação dos diferentes métodos de transfecção, um único lote foi desenvolvido para ser utilizado em ensaios de infecção com diferentes linhagens celulares. Foi obtido através de um procedimento de transfecção por eletroporação dos RNAs correspondentes aos vetores plasmidiais em células BHK-21, utilizando cubetas de 0,2 cm, com as seguintes condições: 360 v; 75 µF; resistência ∞. Sendo as partículas virais coletadas 24 h após o processo. Posteriormente, esse lote foi quantificado através de qRT-PCR, utilizando o par de *primers* que apresentou melhor resultado. Foram realizados três experimentos em dias diferentes com o lote em questão, e o valor médio da quantificação foi de 8×10^4 partículas virais por µL.

5.5 Avaliação da expressão de RVGP em diferentes linhagens celulares

5.5.1 BHK-21

A partir do lote de vírus SFV-RVGP, obtido através do método de eletroporação, foram realizados ensaios com diferentes MOIs de infecção (1, 10, 15 e 50) em células BHK-21. O experimento foi realizado em placas de seis poços, com 3 x 10^5 células por poço, sendo que a coleta de RVGP para análise foi realizada 24 e 48 h após a infecção (**Figura 9 - A**).

Figura 9 - Expressão de RVGP (µg / 1E6 células) em células BHK-21

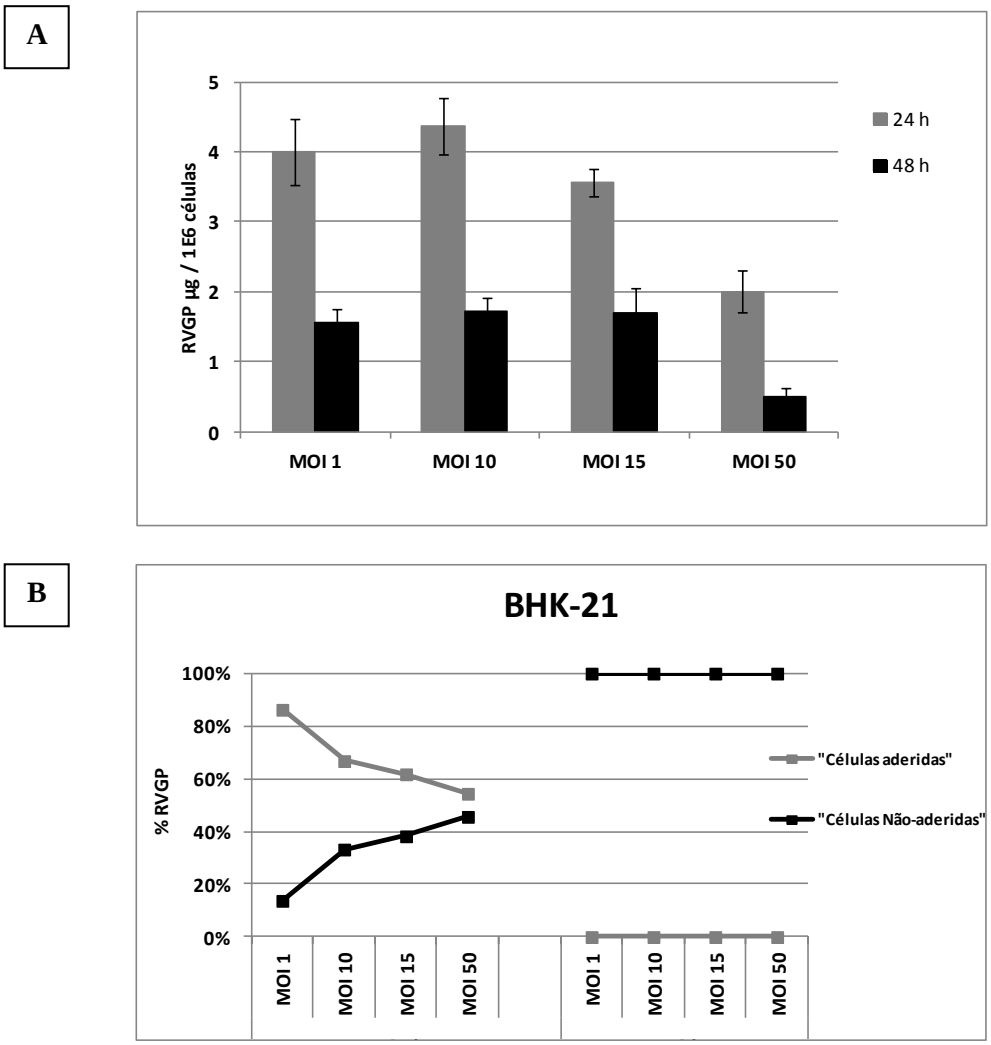

(A) Diferentes MOIs (1, 10, 15 e 50), com RVGP coletada 24 e 48 h após a infecção; **(B)** Porcentagem de RVGP encontrada em "células aderidas" e "células não-aderidas", para cada MOI, nos tempos de 24 e 48 h após a infecção.

Com base nos resultados obtidos, é possível verificar que o aumento na quantidade de vírus usada para a infecção, foi prejudicial à expressão da RVGP. Com coleta 24 h após a infecção, nota-se que quando utilizado o MOI 1, a quantidade de RVGP gerada foi igual a quando utilizou-se o MOI 10. Porém, há uma significativa diminuição de RVGP detectada, quando se compara a expressão do MOI 10, com a do MOI 15. O mesmo fato pode ser observado quando comparado o MOI 15, com MOI 50, sendo que esse último apresentou o menor valor dentre todos avaliados. No caso dos experimentos com tempo de coleta de 48 h após a infecção, o perfil é semelhante, exceto pelo fato de que os MOIs 1, 10 e 15, apresentaram quantidades iguais de expressão, mas novamente o MOI 50 apresentou o menor nível de expressão. Em todos os MOIs avaliados, a quantidade de RVGP expressa foi maior em 24 h, quando comparada com 48 h após a infecção.

Neste ensaio, vale ressaltar a grande quantidade de RVGP obtida quando a infecção foi feita com MOI 1, e a RVGP coletada após 24 h, chegando a níveis de 4,3 µg por 10^6 células, valor significativamente superior quando comparado a outros sistemas de expressão (**Tabela 2**). Outra observação importante é a proporção entre a quantidade de RVGP encontrada nas "células aderidas" e em "células não-aderidas". Com 24 h, a presença de RVGP em células aderidas, diminui conforme se aumenta o MOI. Sendo que no tempo de 48 h, toda a RVGP foi encontrada em "células não-aderidas". Fato já esperado, pois conforme o processo de infecção se estende, mais as células são lesadas devido à infecção viral e a RVGP acaba sendo detectada em restos celulares presente no sobrenadante (**Figura 9 - B**).

Imagens obtidas momentos antes da coleta da proteína revelam o estado morfológico da célula frente a cada MOI avaliado (**Figura 10**). Pode-se verificar, que conforme se aumenta a quantidade de vírus por célula, maior o efeito citopático ocasionado pelo processo de infecção. E também, no tempo de 24 h, as células apresentam melhor aspecto morfológico quando comparadas com o tempo de 48 h. Estes dados sustentam a ideia de que um maior MOI na infecção de células BHK-21, pode ocasionar um menor nível de expressão da RVGP, possivelmente devido ao forte efeito citopático desencadeado pela infecção.

Figura 10 - Efeito citopático em células BHK-21

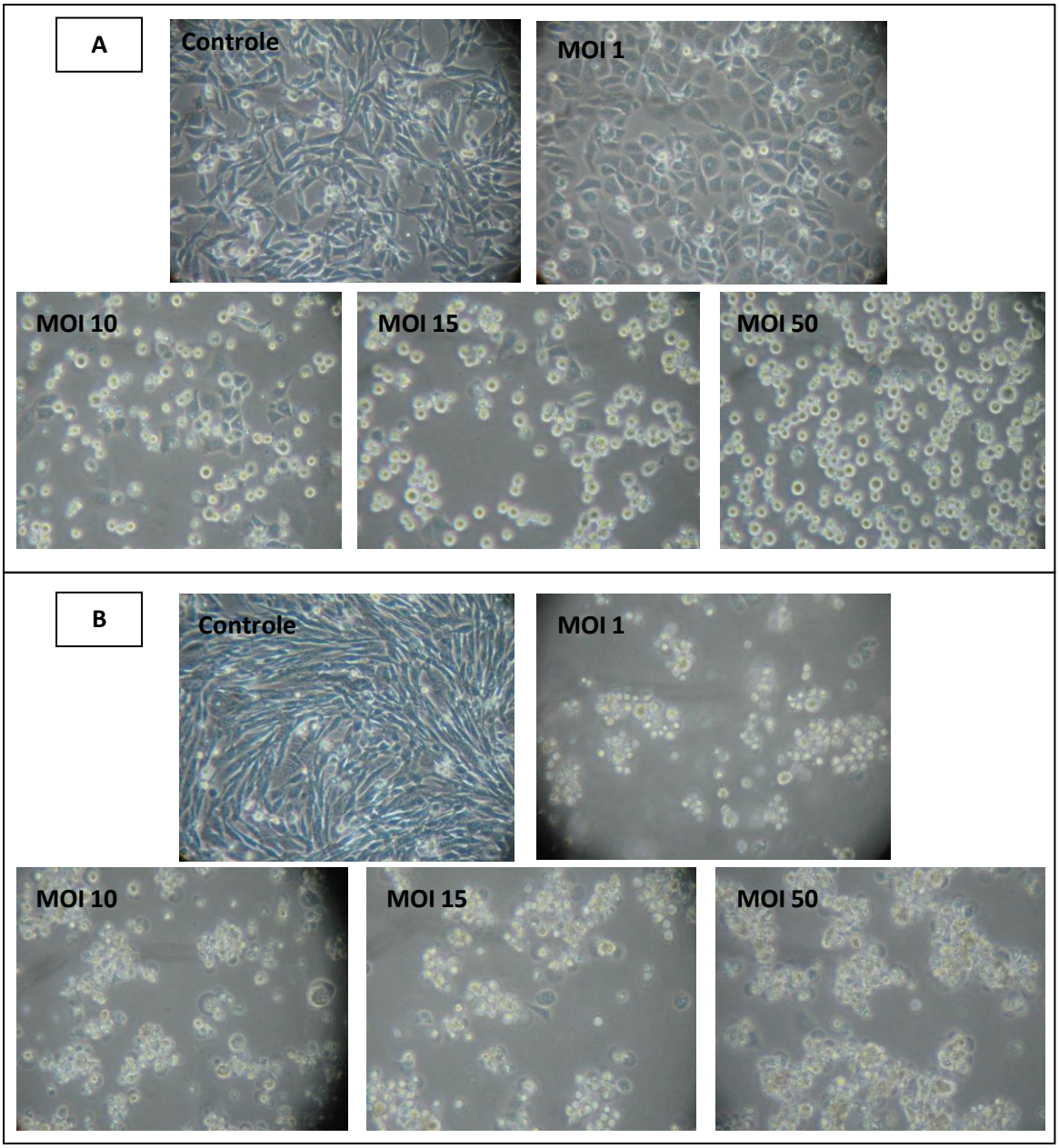

(**A**) 24 h após a infecção com SFV-RVGP; (**B**) 48 h após a infecção com SFV-RVGP.
MOI – *Multiplicity of infection*

Outros métodos de detecção da RVGP foram utilizados, como por exemplo, as técnicas de *Dot blot* e *Western blot*. Nos resultados do experimento de *Dot blot*, é possível a visualização de uma banda intensa na amostra correspondente às células BHK-21, evidenciando a presença de RVGP, fato não observado no controle negativo (**Figura 11**). No caso do *Western blot*, a banda gerada confirma que a proteína expressa pelo sistema possui o padrão de glicosilação adequado, sem a presença de formas distintas (**Figura 12**). O tamanho

da RVGP obtido por esse método foi de 65 kDa, valor já estabelecido por outros estudos que caracterizaram a mesma proteína (BENMAAMAR et al., 2008).

Foi realizado ainda, um experimento de imunofluorescência indireta (IFI) para detectar a proteína na célula. Conforme visto, a proteína se encontra nas membranas das células infectadas pelo vírus, fato já esperado por ser a RVGP, uma proteína transmembrânica (**Figura 13**). Conforme observado em dados anteriormente expostos, também pela técnica de IFI, é possível perceber que não há diferenças de expressão entre os MOIs 1 e 10. Vale ressaltar, que devido a dificuldades da técnica com relação à fixação das células, foram realizados experimentos apenas com MOI 1 e 10 em todas as linhagens.

Figura 11 - Dot blot para RVGP expressa em diferentes linhagens celulares infectadas com o vírus SFV-RVGP.

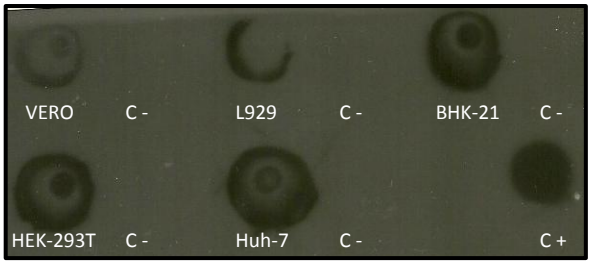

Figura 12 - *Western blot* para RVGP expressa em diferentes linhagens celulares infectadas com o vírus SFV-RVGP.

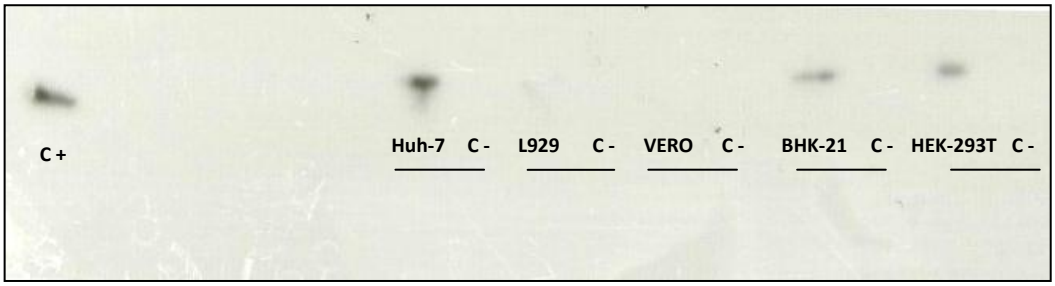

.

Figura 13 - Imagens de IFI com células BHK-21, 24 h após a infecção com SFV-RVGP.

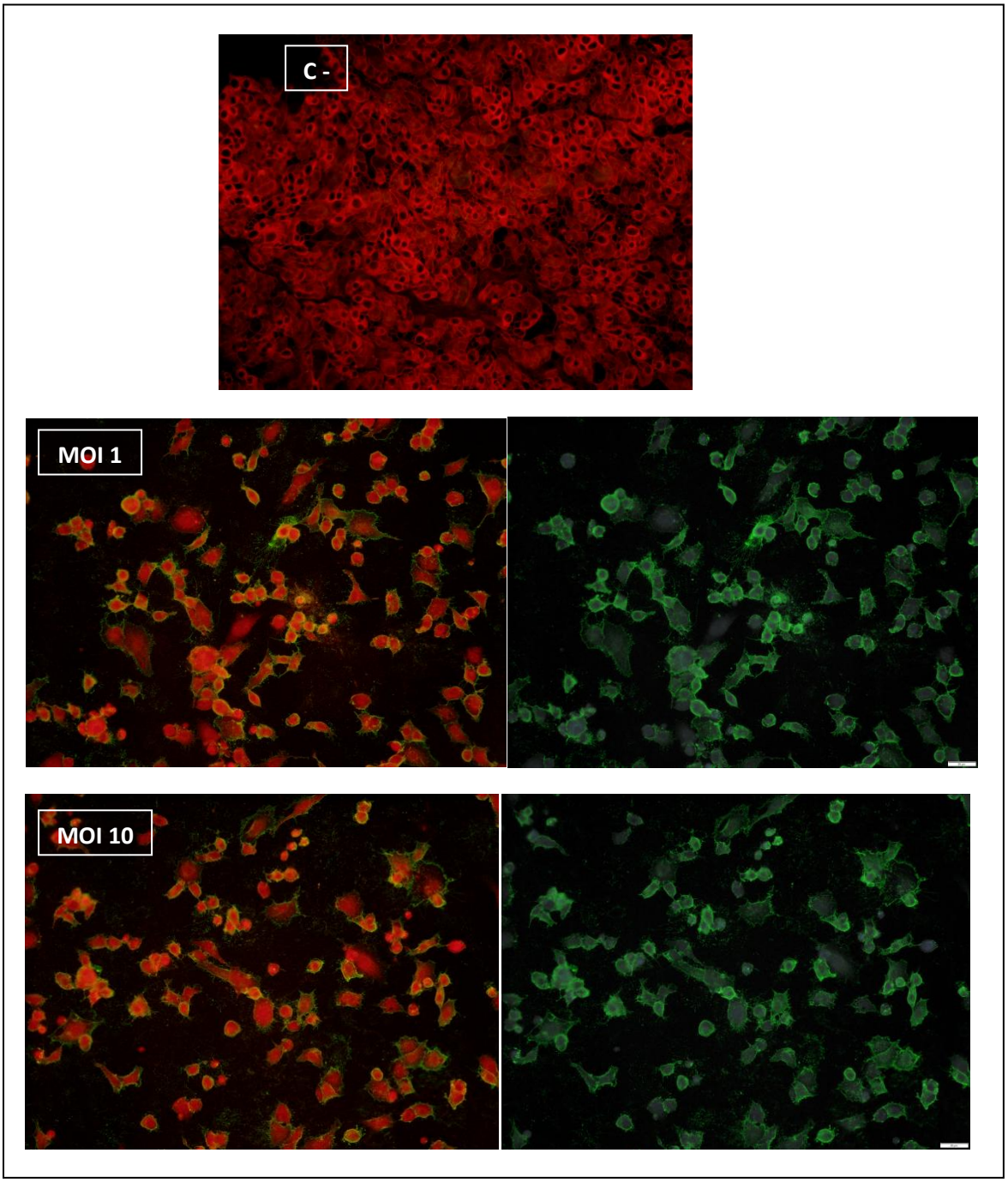

MOI – *Multiplicity of infection*

5.5.2 Huh-7

No processo de infecção com SFV-RVGP em células Huh-7, foram avaliados os mesmos MOIs já descritos anteriormente. Com base nos resultados (**Figura 14 - A)**, pode-se verificar que a quantidade de RVGP expressa, foi a mesma considerando o tempo de 24 h

após a infecção, para todos os MOIs, exceto o MOI 1, que mostrou maior expressão frente aos demais. Os MOIs 10, 15 e 50, obtiveram níveis iguais de expressão entre eles também no tempo de 48 h, com todos apresentando significativo aumento de expressão quando comparados com os respectivos ensaios no tempo de 24 h. Novamente a exceção é o MOI 1, que no tempo de 48 h apresentou um nível de expressão menor frente ao tempo de 24 h.

Figura 14 - Expressão de RVGP (µg / 1E7 celulas) em células Huh 7.

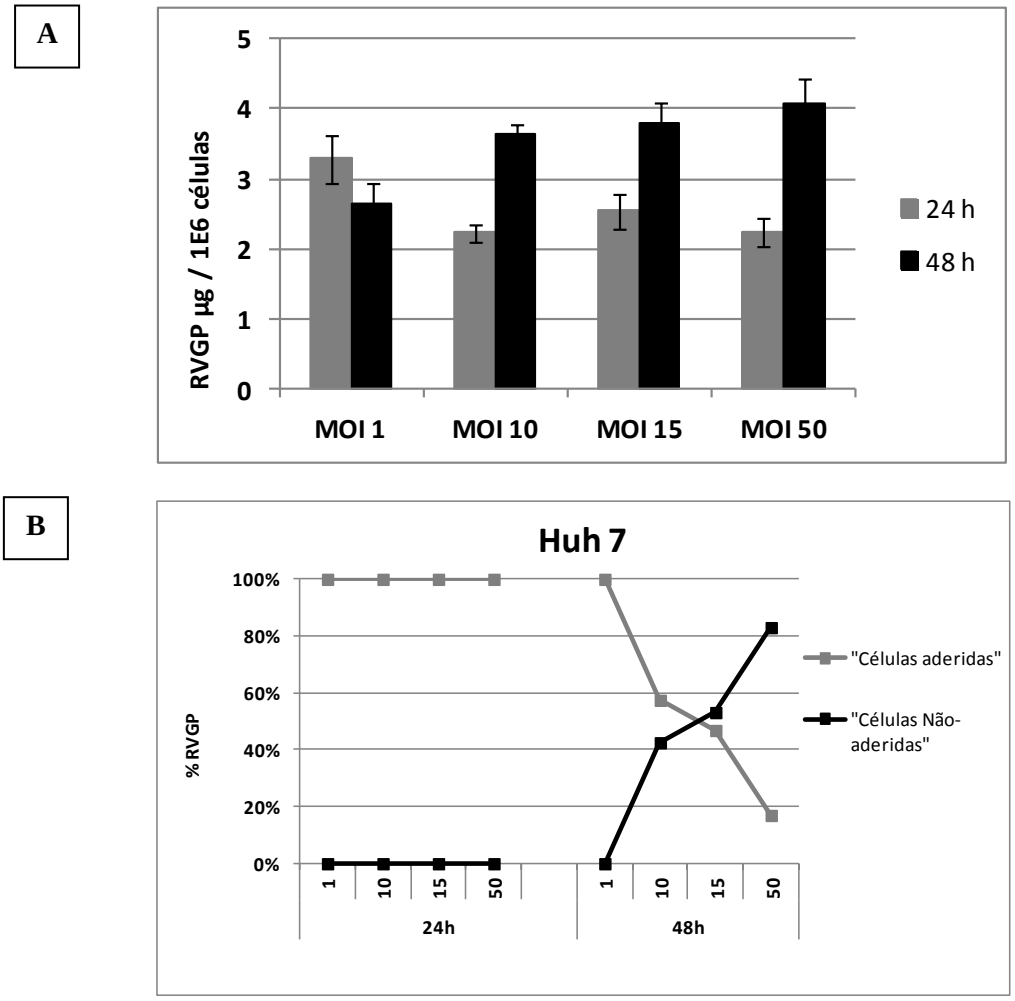

(A) diferentes MOIs (1, 10, 15 e 50), coletada 24 e 48 h após a infecção; **(B)** Porcentagem de RVGP encontrada em "células aderidas" e "células não-aderidas", para cada MOI, nos tempos de 24 e 48 h após a infecção;

A maior produção de RVGP 48 h após a infecção sugere que, ou o processo de infecção viral, ou a geração da proteína, nesse tipo de célula ocorre de maneira mais lenta, fato indicado pelo menor efeito citopático presenciado, onde mesmo com MOI 50 após 48 h, ainda pode ser verificado algumas células aderidas (**Figura 14– B)**. No tempo de 24 h após a

infecção, praticamente toda RVGP gerada é oriunda de amostras de “células aderidas”. Enquanto que somente após 48 h do processo de infecção, a quantidade de RVGP nas células aderidas decai gradativamente, conforme aumenta o MOI, aumentando o nível de RVGP presente nas “células não-aderidas”, que consiste nos restos celulares oriundos do processo de apoptose. O efeito citopático nessa linhagem se mostra menor no decorrer do processo de infecção, quando comparado as demais linhagens (**Figura 15**).

Figura 15 - Efeito citopático em células Huh 7 infectadas por SFV-RVGP.

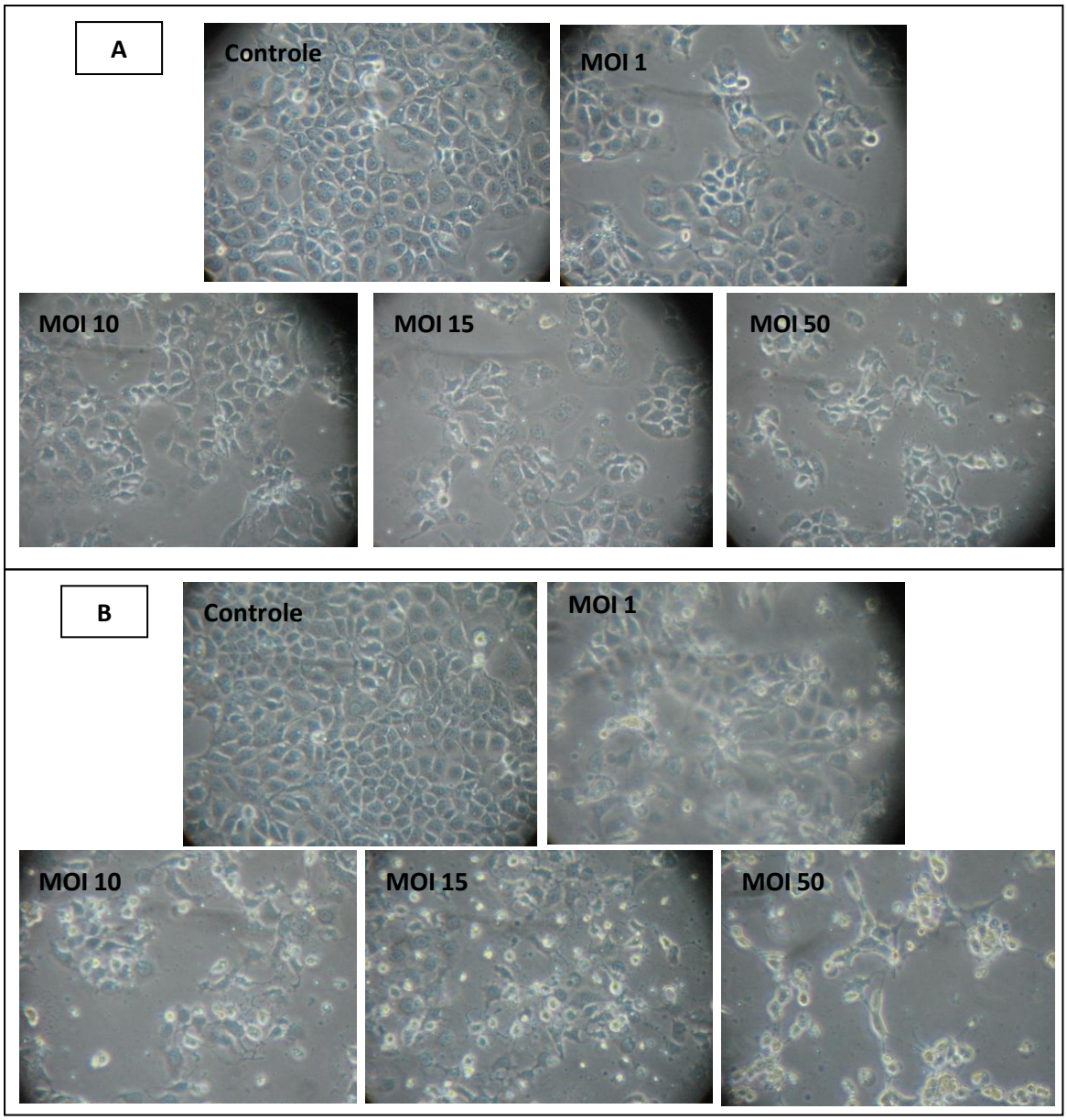

(**A**) 24 h após a infecção com SFV-RVGP; (**B**) 48 h após a infecção com SFV-RVGP.

Figura 16 - Imagens de IFI com células Huh-7, 48 h após a infecção com SFV-RVGP.

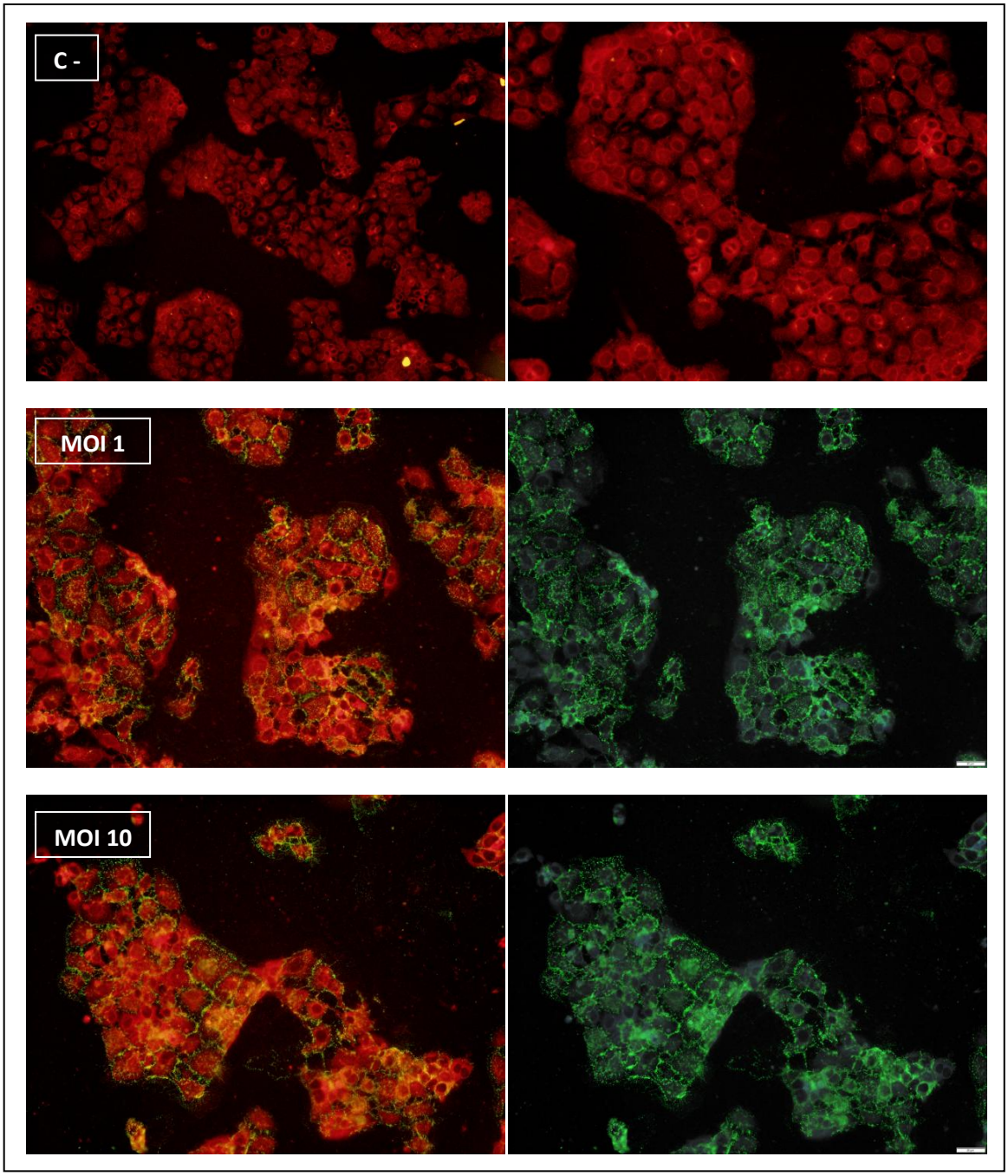

Também foram utilizados outros métodos para avaliar a expressão de RVGP nas linhagens Huh-7, como *Dot blot*, *Western blot* e imunofluorescência indireta (IFI). No experimento de *Dot blot*, é possível verificar uma intensa marcação na amostra oriunda dessa linhagem celular, e que não houve marcação no controle negativo (**Figura 11**). Na técnica de *Western blot*, houve geração de uma banda do tamanho correspondente à RVGP do controle positivo (**Figura 12**). No caso da avaliação por IFI, é possível verificar intensa marcação da

proteína nas membranas das células, e uma boa porcentagem de expressão por células totais (**Figura 16**).

5.5.3 L929

No experimento envolvendo células L929, foi verificado que a maior produção de RVGP foi utilizando o MOI1 (**Figura 17 - A**), com coleta 24 h após a infecção. Os demais MOIs também apresentaram expressão significativamente maior no tempo de 24 h, frente ao de 48 h, com valores semelhantes de expressão. Vale ressaltar o baixo nível de expressão obtido utilizando MOI 50, com coleta 48 h após a infecção.

O fato de apresentar melhores resultados 24 h após a infecção, juntamente com as imagens morfológicas das células no momento da coleta, evidenciam a grande suscetibilidade da linhagem L929 ao efeito citopático oriundo da infecção viral (**Figura 18)**. Nestas células, o momento em que a maior quantidade de RVGP passa a ser encontrada em "células não-aderidas" é em 24 h já com o MOI 10, sugerindo efeito de lise celular já com quantidades menores de vírus quando comparado com as demais linhagens (**Figura 17 – B**).

Figura 17 - Expressão de RVGP (µg / 1E7 células) em células L929.

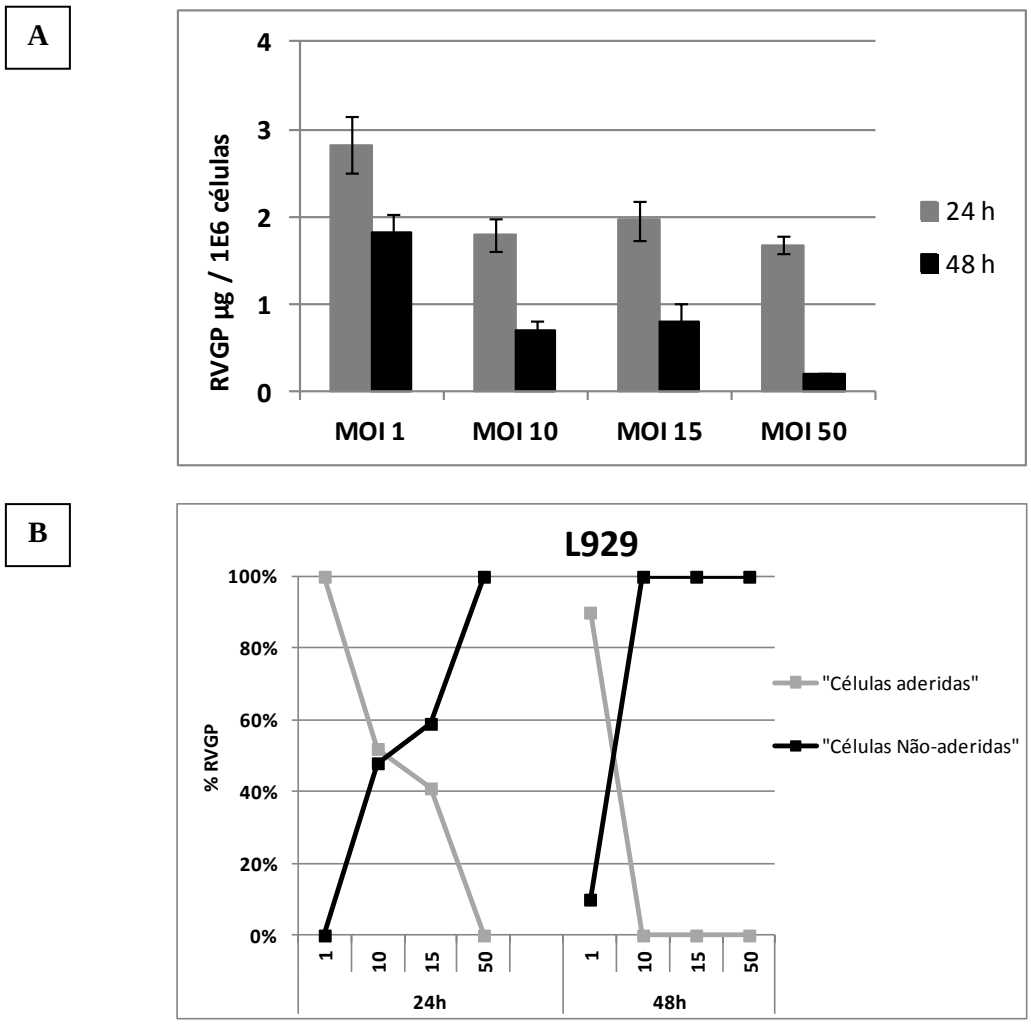

(A) Diferentes MOIs (1, 10, 15 e 50), coletas 24 e 48 h após a infecção; **(B)** Porcentagem de RVGP encontrada em "células aderidas" e "células não-aderidas", para cada MOI, nos tempos de 24 e 48 h após a infecção;

No experimento de *Dot blot*, é possível a visualização de uma marcação correspondente às células L929 infectadas, de forma que o controle negativo não a apresenta (**Figura 11**). Vale ressaltar, a menor intensidade de marcação quando comparada com as demais linhagens. Já com relação à técnica de *Western blot*, não foi visualizado banda que corresponda a RVGP, mas também não houve revelação de bandas inespecíficas (**Figura 12**). No procedimento de IFI, é possível a visualização com clareza da expressão de RVGP pelas células, sendo que, foi a linhagem que menos sofreu durante a execução da técnica, apresentando membranas mais integras e uma melhor marcação (**Figura 17**). Visto que através da mesma amostra de L929 infectada, foi possível confirmar a presença de RVGP por

ELISA e IFI, possivelmente houve algum problema no procedimento de lise da célula e obtenção de RVGP para a técnica de *Western blot*, não gerando a marcação correspondente.

Figura 18 - Efeito citopático em células L929.

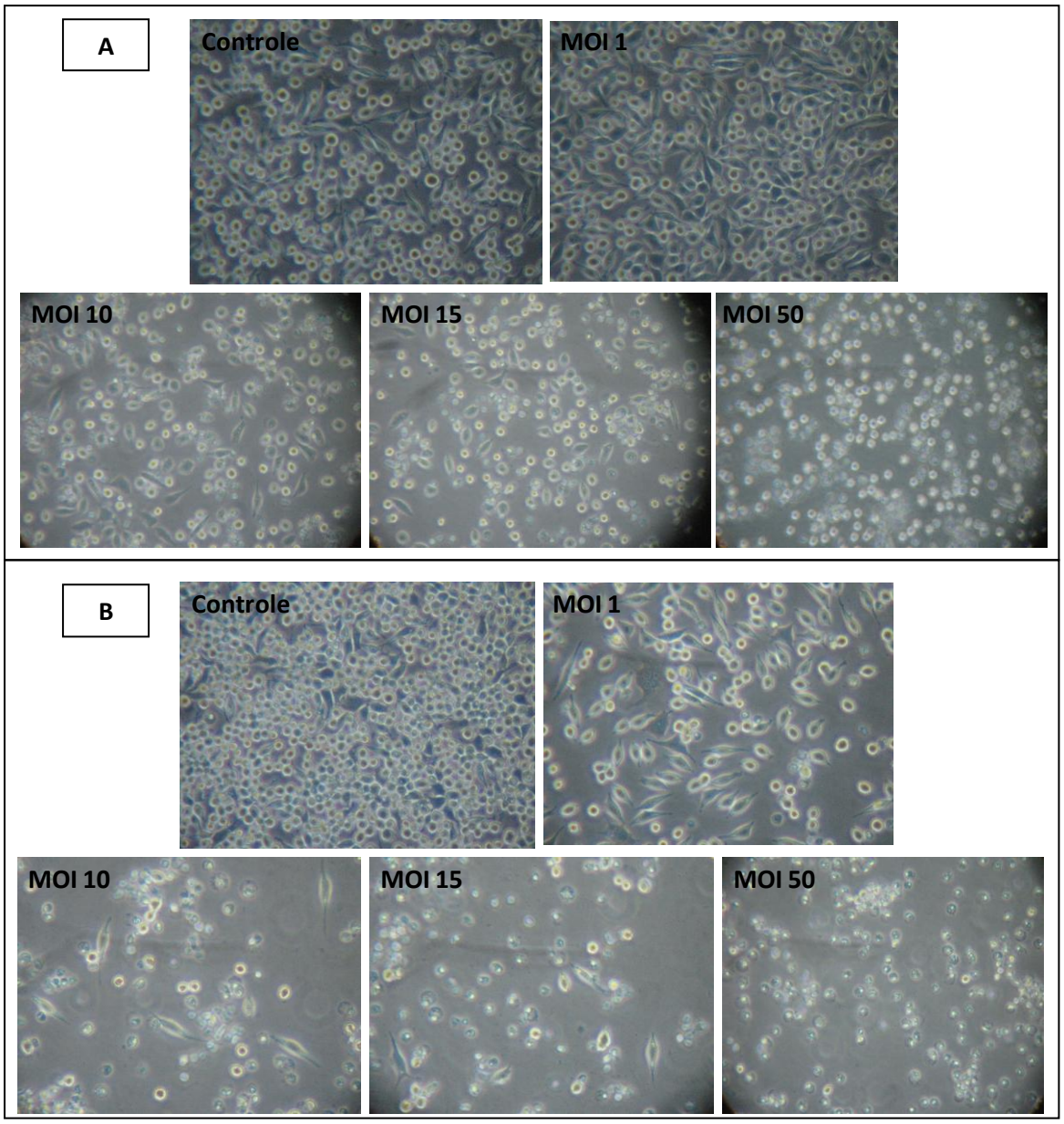

(**A**) 24 h após a infecção com SFV-RVGP; (**B**) 48 h após a infecção com SFV-RVGP.

Figura 19 - Imagens de IFI com células L929, 24 h após a infecção com SFV-RVGP.

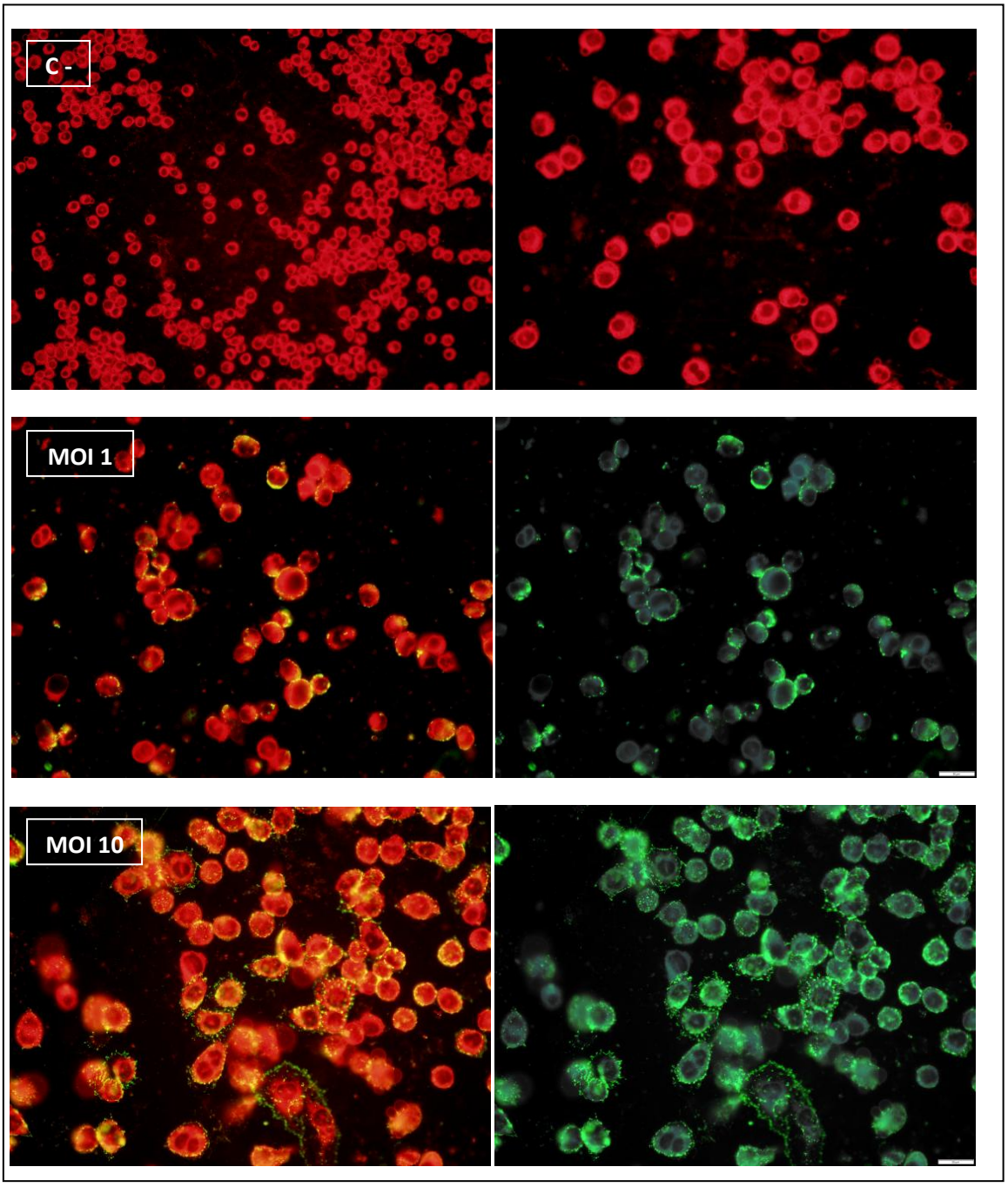

5.5.4 Vero

Nos ensaios envolvendo células Vero, pode-se verificar uma maior produção de RVGP no tempo de 24 h após a infecção (**Figura 20**), caso semelhante aos resultados das linhagens L929 e BHK-21. Tal fato pode ser explicado pela sensibilidade da linhagem a um processo de infecção, onde a geração de proteínas pela célula vai se tornando ineficaz com o passar do tempo. Também semelhante às linhagens L929 e BHK-21, o aumento do MOI acarretou na diminuição do nível de expressão de RVGP. Possivelmente, o aumento do número de partículas virais não acarrete necessariamente um aumento da produção protéica, pois o efeito citopático ocasionado na célula impede uma maior produção da proteína heteróloga (**Figura 21**). Curiosamente, toda a RVGP produzida foi encontrada em "células aderidas".

Figura 20 - Expressão de RVGP (µg / 1E6 células) em células Vero, utilizando diferentes MOIs (1, 10, 15 e 50), coletada 24 e 48 h após a infecção.

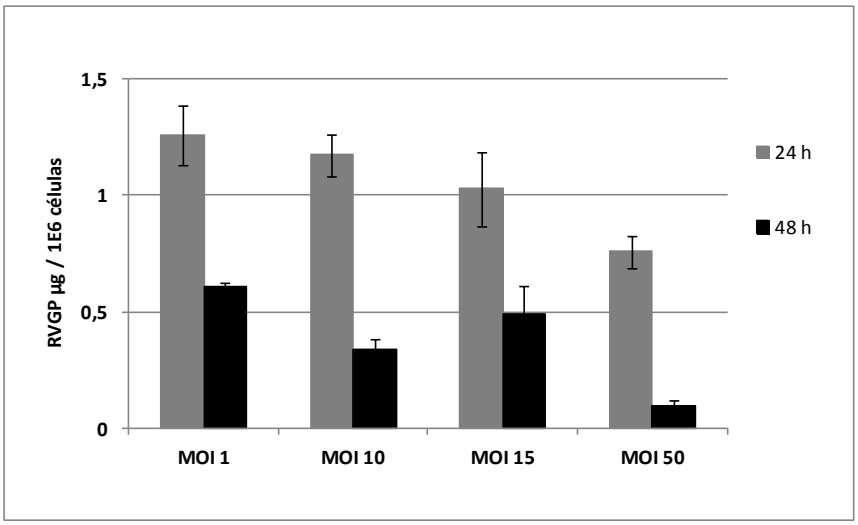

No experimento de *Dot blot* com amostras da linhagem VERO, é possivel verificar uma marcação menos intensa do que as das demais linhagens (**Figura 11**). Já com o experimento de *Western blot*, semelhante à linhagem L929, não houve geração de bandas, o que possibilita ser um problema da técnica, visto que RVGP foi encontrada através de outros métodos (**Figura 12**). No experimento de IFI, foi verificada a presença de RVGP nas

membranas das células, porém, foi a linhagem que mais sofreu com os procedimentos, mostrando membranas menos integras e células em grumos (**Figura 22**).

Figura 21 - Efeito citopático em células Vero.

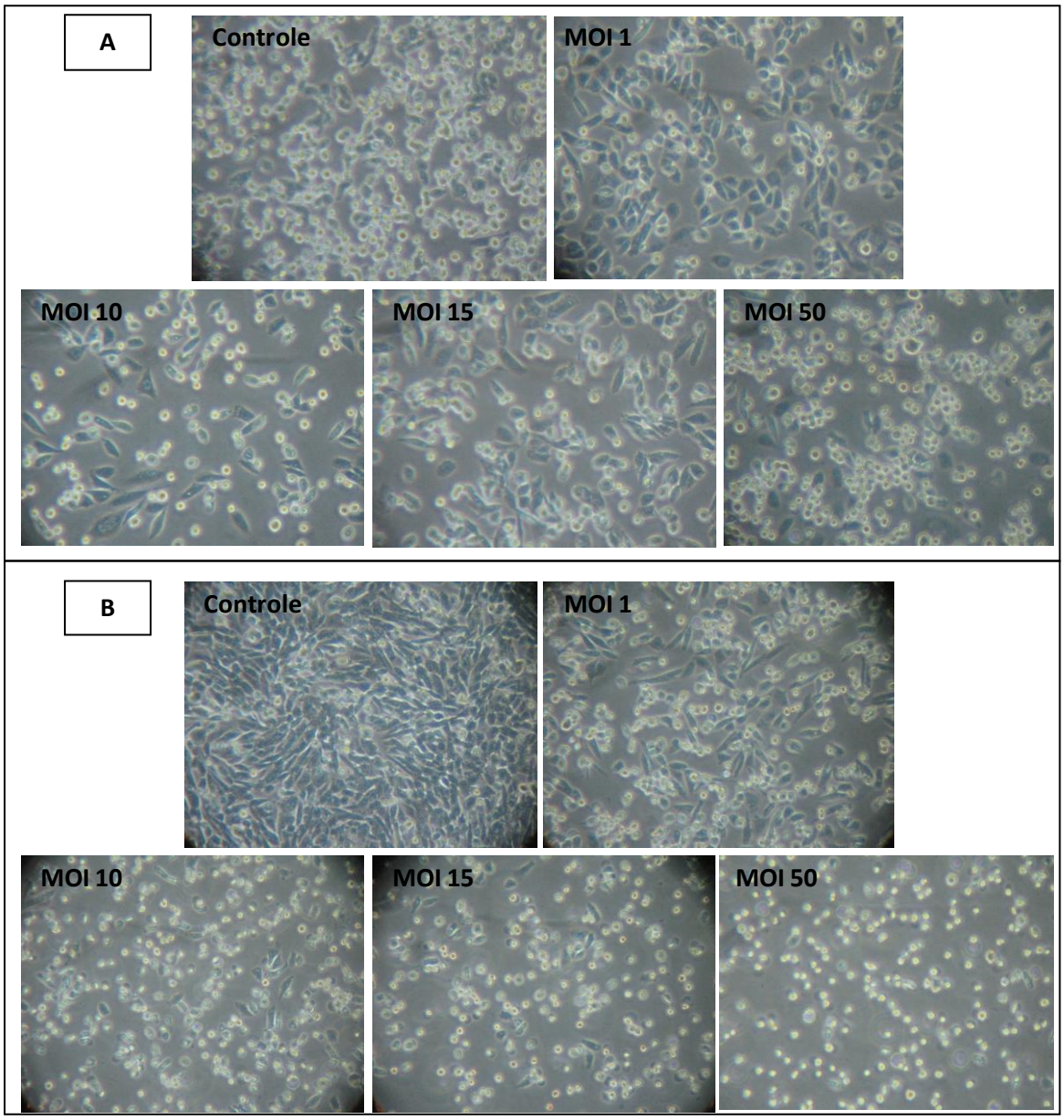

(**A**) 24 h após a infecção com SFV-RVGP; (**B**) 48 h após a infecção com SFV-RVGP.

Figura 22 - Imagens de IFI com células VERO, 24 h após a infecção com SFV-RVGP.

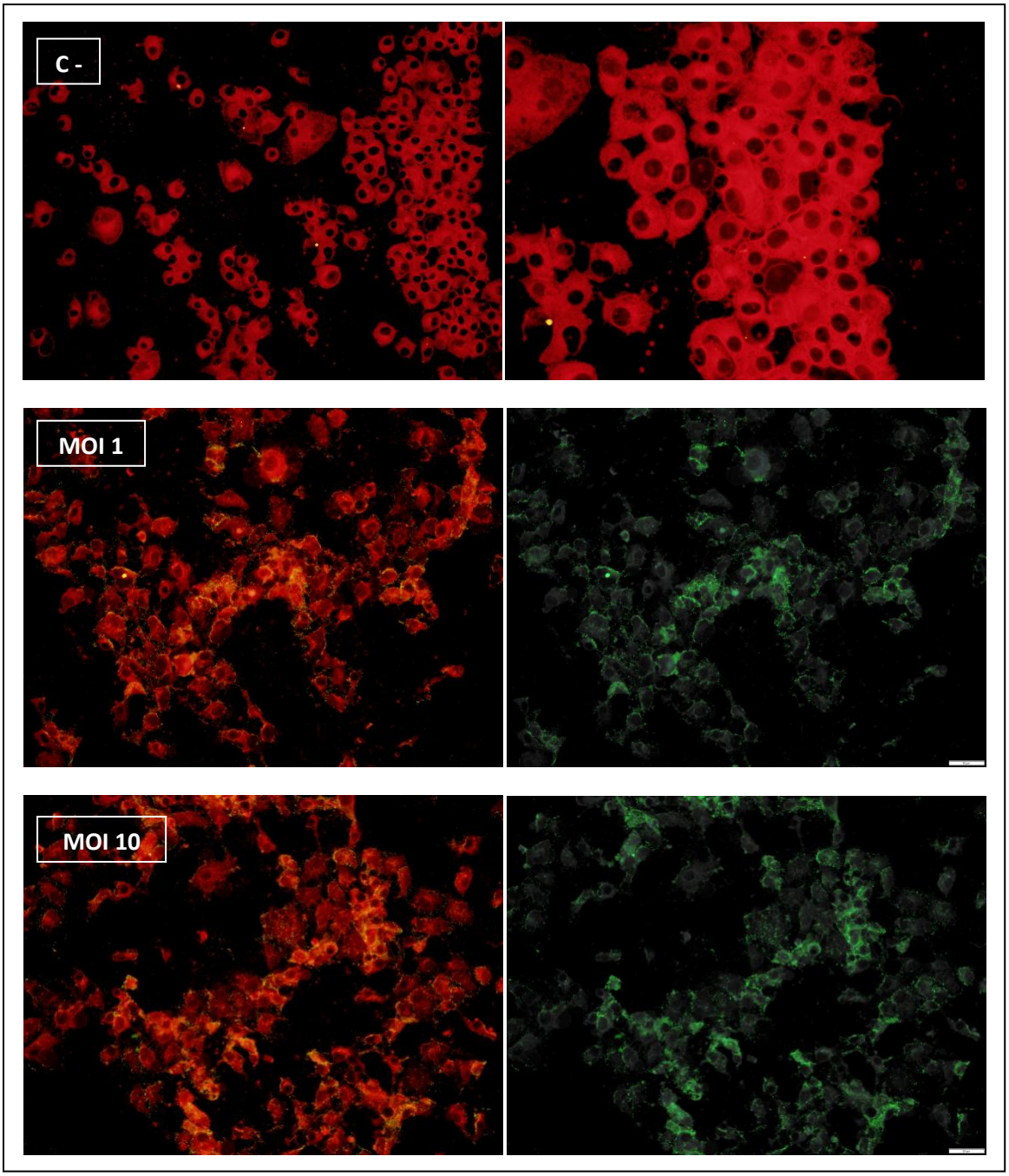

5.5.5 HEK 293T

Com base na avaliação da expressão de RVGP em células HEK-293T (**Figura 23**), pode-se verificar que há uma maior produção, quando elas são infectadas com uma quantidade menor de vírus. Isso se deve ao fato de ser uma linhagem semi aderente, e com isso ela se solta da superfície da placa muito precocemente, o que possivelmente, deva dificultar a penetração viral. Portanto, quanto maior a quantidade de vírus colocada (MOI),

mais as células tendem a se soltar, e assim, menor a possibilidade de ser infectada e produzir a RVGP. A produção de RVGP se mostrou bem maior quando coletada 24 h após a infecção, com relação a 48 h, em todos os MOIs avaliados. Conforme já visto em outras linhagens, não houve diferença significativa entre os MOIs 1 e 10, e entre os MOIs 10 e 15, sendo que no MOI 50, a produção da proteína foi substancialmente menor.

Figura 23 - Expressão de RVGP (µg / 1E6 células) em células HEK-293T, utilizando diferentes MOIs (1, 10, 15 e 50), coletada 24e 48 h após a infecção.

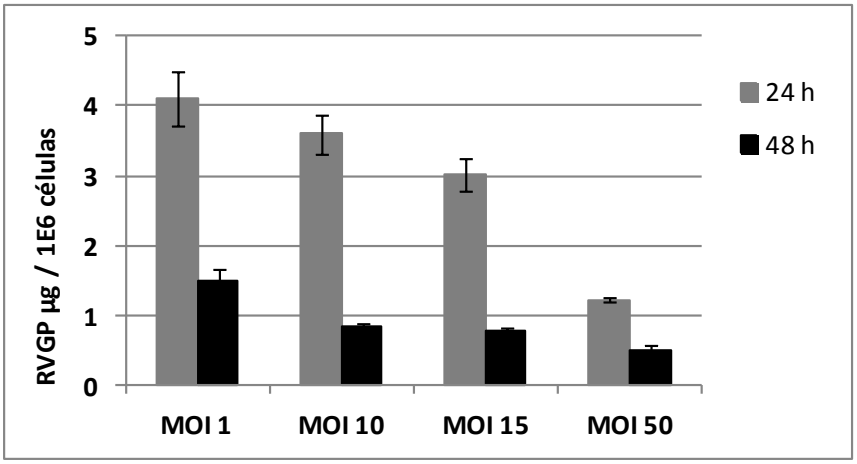

Com relação ao efeito citopático, a linhagem HEK-293T se mostrou com um comportamento semelhante as demais, onde o aumento do MOI, e o maior tempo de infecção, ocasionaram maiores danos na morfologia celular. Por se tratar de uma linhagem semi-aderente, as células se soltaram com mais facilidade mesmo com MOIs menores, ainda no tempo de 24 h. Porém, as células em suspensão, ainda aparentam estar vivas, e possivelmente, ainda estejam expressando RVGP.

Figura 24 - Efeito citopático em células HEK-293T.

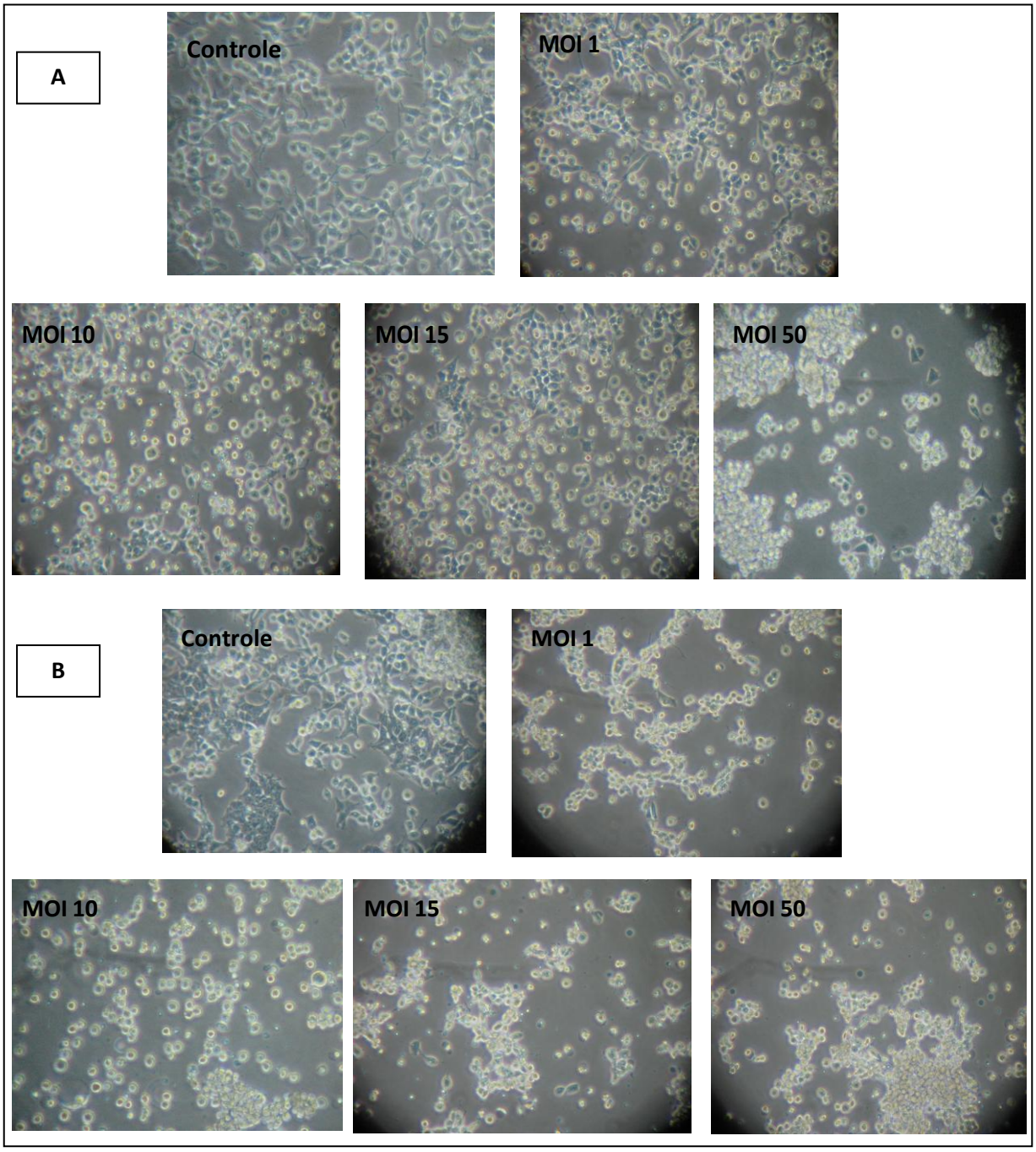

(**A**) 24 h após a infecção com SFV-RVGP; (**B**) 48 h após a infecção com SFV-RVGP.

No experimento de IFI é possível verificar a presença de RVGP nas células HEK-293T, com uma alta porcentagem de células infectadas (**Figura 25**). Conforme apresentado nos resultados do ELISA, não há diferença significativa entre os MOIs 1 e 10. No procedimento de *Dot blot*, a marcação gerada nas amostras dessa linhagen foi bastante intensa, semelhante às de BHK-21 e Huh-7 (**Figura 11**). O mesmo fato ocorreu no *Western*

blot, onde apenas essas linhagens apresentaram a banda correspondente a RVGP, mostrando o mesmo tamanho que a do controle positivo (**Figura 12**).

Figura 25 - Imagens de IFI com células HEK-293T, 24 h após a infecção com SFV-RVGP.

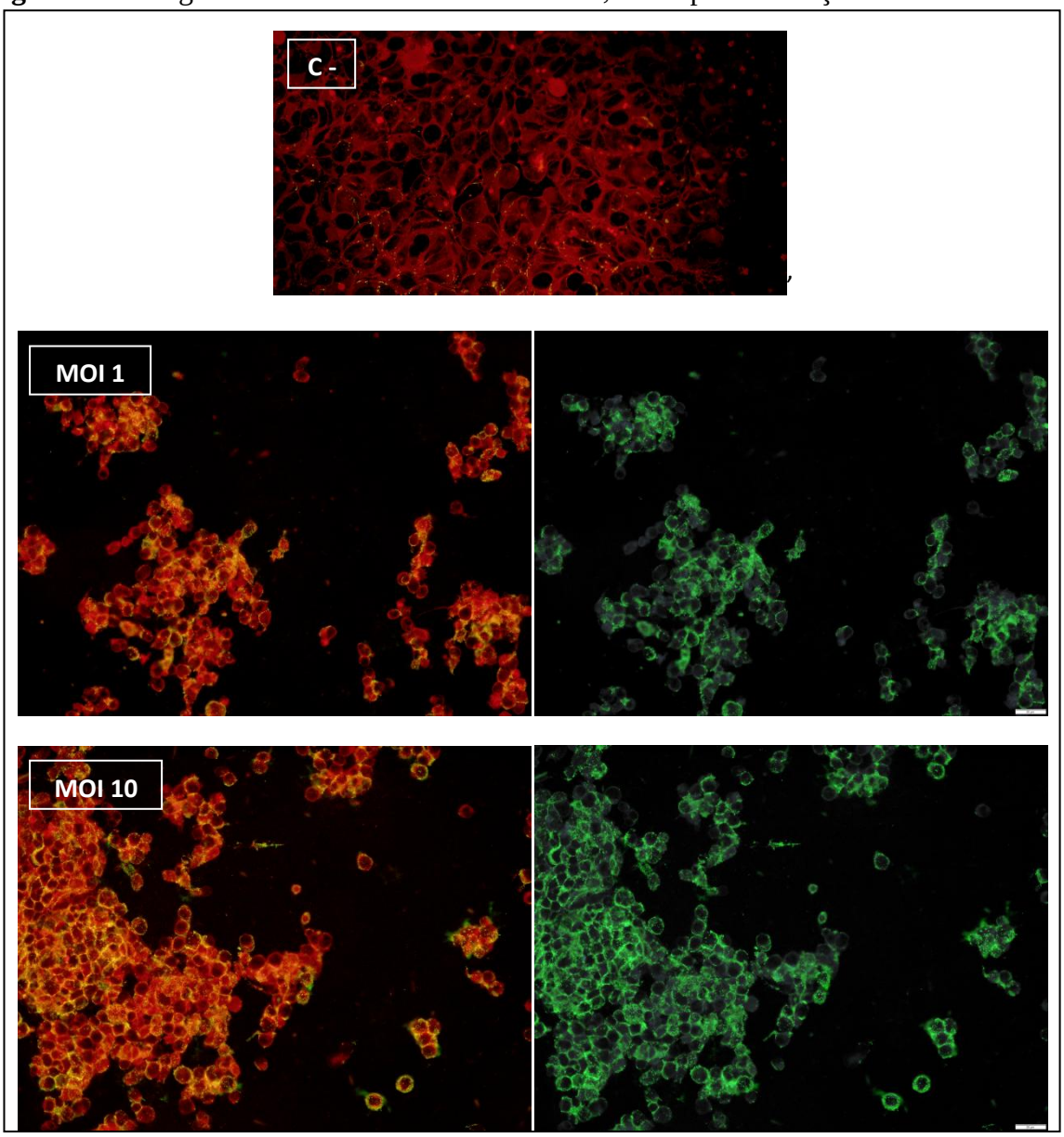

5.5.6 BHK-21 em suspensão

Simultaneamente, aos ensaios com as linhagens celulares já citadas, foi realizado um experimento com a linhagem BHK-21 adaptadas em suspensão (**Figura 26**). Nesse caso, foram utilizadas placas de 24 poços com 1,25 1E5 células por poço. Tal experimento corresponde a uma parceria com outro projeto do grupo, visando à expressão em linhagens BHK-21 em supensão, para uma possível aplicação em biorreatores.

Figura 26 - Expressão de RVGP (ng / 1E7 células) em células BHK-21 em suspensão, coletada 24 e 48 h após a infecção.

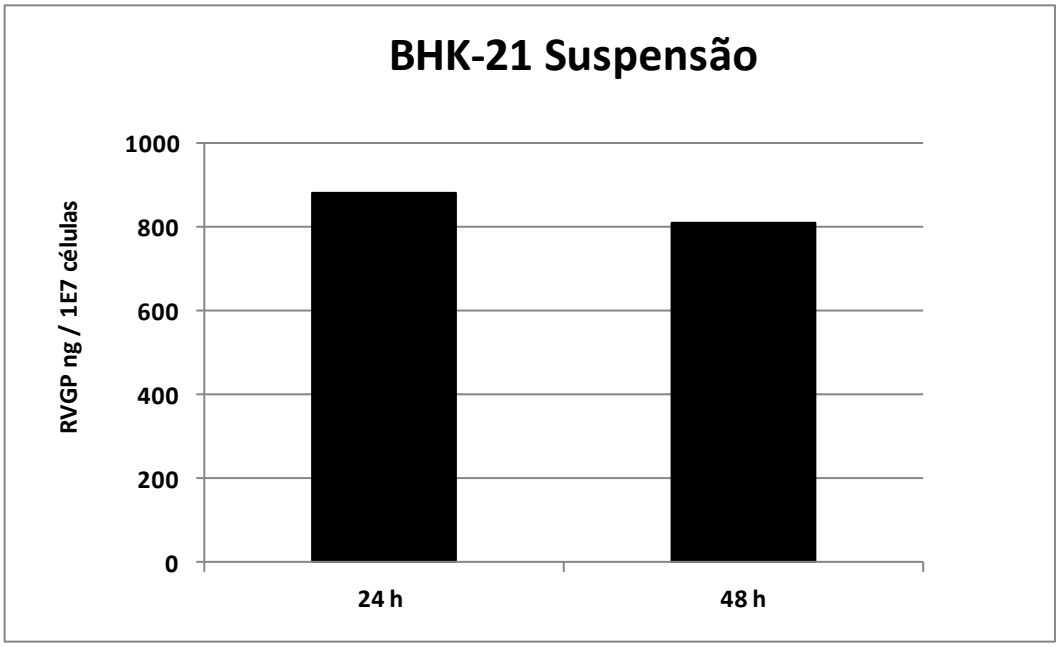

Tabela 5 - Resumo dos valores de RVGP (µg / 1E6 células) obtidos em cada linhagem

		MOI 1	MOI 10	MOI 15	MOI 50
BHK-21	**24 h**	4,00	4,37	3,56	2,00
	48 h	1,55	1,72	1,69	0,50
Huh-7	**24 h**	3,29	2,23	2,54	2,25
	48 h	2,65	3,65	3,80	4,08
HEK-293T	**24 h**	4,10	3,60	3,02	1,22
	48 h	1,48	0,86	0,77	0,49
L929	**24 h**	2,82	1,80	1,96	1,68
	48 h	1,81	0,70	0,80	0,20
Vero	**24 h**	1,26	1,17	1,03	0,76
	48 h	0,61	0,34	0,49	0,10

Valores de RVGP em µg / 1E6 células

6 DISCUSSÃO

O presente trabalho teve como objetivo otimizar o processo de produção de proteínas heterólogas utilizando o sistema de expressão SFV. Um trabalho anterior utilizando o sistema SFV para expressar a glicoproteína do vírus rábico (RVGP), já havia sido desenvolvido em nosso laboratório, em parceria com um laboratório na França (ASTRAY, 2009). Sendo que no presente estudo, avaliamos e padronizamos algumas variáveis que poderiam melhorar a produção da RVGP neste sistema. É importante ressaltar as dificuldades encontradas em estabelecer um protocolo baseado nesse sistema de expressão em nosso laboratório, visto que ocorrem algumas diferenças entre equipamentos e materiais disponíveis. O presente trabalho apresentou níveis de expressão de até 4,3 µg de RVGP por 1E6 células em células BHK-21, sendo um valor maior do que aquele apresentado no trabalho anterior, onde o máximo de expressão alcançado foi de 2,2 µg de RVGP por 1E6 células. Outro ponto importante, foi o fato de ter conseguido a expressão de RVGP em linhagens VERO e HEK-293T, o que não foi obtido no trabalho anterior. Ressaltando o alto nível de expressão em HEK-293T, ocorrendo o mesmo com a linhagem Huh-7. Além de uma nova linhagem avaliada, L929, que também apresentou resultados promissores.

Em relação ao trabalho anterior, nos propusemos a aperfeiçoar e padronizar a geração das partículas virais recombinantes (SFV-RVGP). Para tanto algumas modificações foram realizadas no processo, como na transcrição *in vitro*, onde um novo kit comercial foi utilizado, e necessitou de uma padronização para que fosse obtido um melhor rendimento de RNA, a partir dos vetores de expressão. Foram inseridos reagentes não disponíveis no kit, como o RNAcap analog, que fornece a 7-metil-guanosina, responsável pelo “capeamento” da extremidade 5’ do RNA recém gerado. A importância de inserção do CAP é amplamente discutida, sendo indicado como um mediador e potencializador em um processo de tradução protéica (GALLIE, 1991). E um inibidor de RNases, para diminuir sua degradação e consequentemente, aumentar a quantidade de RNA inserido na célula. O protocolo estabelecido para tal procedimento foi repetidamente utilizado, apresentando bons níveis de geração de RNA em todas às vezes. Sendo realizado sempre após cada procedimento, um gel de eletroforese para confirmar a transcrição, evidenciando uma banda intensa correspondente ao RNA gerado. Além de quantificação através de método fluorimétrico (Qubit), com valores de 1,5 µg / reação.

A partir do estabelecimento de um protocolo adequado de transcrição *in vitro*, os RNAs obtidos foram transfectados imediatamente em células BHK-21, através de duas abordagens distintas. Foram avaliados um kit comercial de transfecção de RNA, denominado Transmessenger (Qiagen), e também a técnica de eletroporação, já descrita em alguns trabalhos envolvendo SFV (LUNDSTROM, 2012). Com base na comparação dos dois métodos de transfecção utilizados, pode-se concluir que a abordagem utilizando a eletroporação se mostrou mais eficiente para gerar uma maior quantidade de vírus por experimento, visto que uma mesma quantidade de suspensão contendo as partículas virais (100 uL), possibilitou uma maior produção de RVGP nas células infectadas. Tal fato foi comprovado posteriormente com a quantificação de cada lote, fornecendo os valores de 2×10^4 e $1{,}35 \times 10^3$ partículas virais por microlitro, para eletroporação e Transmessenger, respectivamente.

A transfecção utilizando o kit comercial se mostrou inferior ao procedimento de eletroporação, mas seu uso não pode ser descartado visto que alguns procedimentos de padronização da técnica podem elevar a quantidade de vírus obtido por esse processo. Existem estudos específicos para a otimização do método de transfecção através desse reagente, que determinam a necessidade de padronização da quantidade de RNA utilizado para se complexar com o reagente, utilizando genes repórteres como a GFP, além da adição de reagentes como Yeast tRNA (Invitrogen) como inibidor da degradação do RNA (NARAYANASAMY et al., 2005). Porém, apesar de diversos trabalhos mostrarem a eficiência desse reagente, seu custo perante o método de eletroporação inviabilizaria sua utilização, além do fato de ser um procedimento muito mais laborioso, e estar mais sujeito a erros por parte do executante (GONZALEZ et al., 2007). Sendo assim, uma extensa padronização dessa técnica não foi realizada, visto que outro método apresentou melhores resultados em ensaios preliminares. Vale ressaltar que, mesmo a condição de eletroporação tendo mostrado ser mais eficiente, em termos de quantidade de vírus gerado, o método com Transmessenger obteve vírus de mesma qualidade, sendo esses capazes de expressar RVGP em quantidades proporcionais ao MOI que foi adicionado às células.

Após o processo de geração dos vírus recombinantes ter sido bem estabelecido, foi desenvolvido um método que fosse capaz de quantificar tais vírus de forma precisa e reprodutiva, sendo esse um procedimento de grande relevância em todo o processo, e que não havia sido bem estabelecido em outros trabalhos. Isso se faz necessário, para que o processo de infecção viral nas mais diversas linhagens celulares seja bem determinado, com uma real

comparação entre a quantidade de partículas virais utilizadas e o número de células infectadas. Com base em estudos recentes, foi utilizado a técnica de qPCR, onde o RNA extraído de cada vírus foi submetido a uma transcrição reversa e o cDNA obtido foi quantificado, e assim o título viral determinado (LO; CHAO, 2004).

Primeiramente, uma curva padrão foi construída com base no plasmídeo de expressão do SFV (pSFV-RVGP) linear. A utilização de um padrão de DNA para quantificar RNA se fez necessário, devido às dificuldades de se manter amostras de uma curva padrão de RNA, visto a instabilidade do mesmo (PFAFFL, 2001). Com as devidas diluições do padrão, foram testados três pares de oligonucleotídeos em um experimento de qPCR. A curva padrão obtida com os *primers* F-I-2 e R-I-2 se mostrou mais eficaz, obtendo valores dentro do desejado para os principais parâmetros que determinam uma boa curva e uma boa reprodutibilidade entre curvas que foram realizadas em dias distintos. Fato esse não verificado nos demais oligonucleotídeos, o que poderia comprometer uma possível quantificação que os utilizassem, sugerindo que a titulação viral deve ser padronizada para cada sistema viral utilizado. Nesse sentido, a nossa padronização da titulação viral através da qRTPCR permitiu ainda que esta seja utilizada para qualquer construção relacionada ao sistema SFV, independentemente do gene alvo inserido, já que utilizamos oligonucleotídeos específicos para regiões que não se alteram nessas construções, no caso a nsp1.

Alguns procedimentos de controle do processo de titulação viral foram realizados, como o tratamento com DNase do RNA recém extraído dos vírus, e a confirmação desse tratamento através de uma PCR convencional, com posterior corrida das amostras em gel de eletroforese. Somente as amostras que não apresentassem amplificação após o tratamento com DNase, eram submetidas ao procedimento de qPCR. Outro ponto importante, é a análise da curva de *Melting* obtida, sendo essa, uma ferramenta essencial para diferenciar possíveis produtos inespecíficos que tenham sido amplificados, e que podem influenciar no resultado, visto a alta sensibilidade da técnica (WITTWER, 2009). De forma que somente foram consideradas as titulações cujo as amostras não apresentassem picos inespecíficos, sendo que a temperatura de dissociação dos *primers* da sequência alvo, era de 83 ˚C.

Os experimentos e padronizações envolvendo o método de quantificação viral por qPCR, foram desenvolvidos simultaneamente com outro projeto do laboratório, que avaliava a produção de um vetor SFV expressando GFP. Como resultado, foi publicado um artigo em parceria (PUGLIA AL et al., 2013) (**ANEXO A**).

A partir da curva padrão selecionada, os lotes utilizados na comparação e determinação do melhor método de transfecção do RNA, foram titulados. Com a confirmação do método de eletroporação como melhor abordagem, um único lote foi desenvolvido através desse método, para que estudos relacionados ao MOI fossem realizados, sendo esse lote quantificado e fornecendo o valor de 8 x 10^4 partículas virais por µL, baseado em uma média de três experimentos de qRT-PCR.

Nos ensaios de infecção, foram avaliadas diferentes linhagens celulares de mamíferos, já utilizadas na literatura, como BHK-21; Huh-7; HEK-293T; VERO; L929;; BHK-21 CS adaptadas em suspensão, sendo as três primeiras as mais estudadas para o sistema em questão. A avaliação de células BHK-21 CS adaptadas em suspensão, foi realizada de forma simultânea por outro grupo do laboratório, baseado nas possibilidades de ampliação de escala do sistema para biorreatores.

Nos ensaios de infecção, foram utilizados os MOIs 1, 10, 15 e 50. Com exceção da BHK-21 CS em suspensão, onde foi utilizado o MOI 15, visto a viabilidade do processo, onde a utilização de diferentes MOIs ou um alto MOI em células em suspensão encareceria o processo, baseado na possibilidade de extrapolação do ensaio para *spinner* ou biorreator. A escolha desses MOIs se deve ao fato de tentar avaliar a influência da quantidade de vírus no processo de expressão, sendo assim, foram utilizados MOIs que pudessem representar um aumento significativo de vírus por célula, utilizando quantidades não tão grandes de lotes virais, conforme realizado em outros trabalhos com vetores virais (LEYVA et al., 2011).

As células BHK-21 mostraram uma grande expressão de RVGP nas primeiras 24 h, quando utilizado MOI 1 e 10. Sendo que os ensaios com MOI 15 mostraram níveis inferiores de expressão quando comparados com MOI 10, ocorrendo o mesmo decréscimo de expressão quando comparado o MOI 15 com MOI 50. Já com relação ao tempo de 48 h após a infecção, os MOIs 1, 10 e 15, mostraram resultados semelhantes frente ao desvio padrão, associado ao experimento. Enquanto que o MOI 50, novamente foi o que apresentou o menor nível de expressão. Todos os valores de expressão, de todas as linhagens, estão apresentados no **Tabela 5.**

Os dados obtidos mostram que o aumento no número de vírus utilizados na infecção fez com a expressão diminuísse, considerando o tempo de 24 h após a infecção. Possivelmente, isso ocorra devido ao grande efeito apoptótico desencadeado pela infecção viral (BARRY et al., 2010). Sendo assim, quanto mais vírus entrarem em uma determinada célula, maior e mais rápido será o processo de apoptose, e a maquinaria celular estaria menos

apta para produzir a proteína em questão. Estudos mostram que no *sindbis virus*, outro membro dos alphavirus, o processo de apoptose já é desencadeado logo no momento da ligação do vírus na célula, não sendo necessário todo o processo de replicação viral para que o evento ocorra (JAN; GRIFFIN, 1999). Portanto, seria válido a hipótese de que o efeito apoptótico desencadeado pela infecção viral, é influenciado tanto pela interação vírus-célula, quanto pelo tempo de infecção, o que explicaria o comportamento de expressão visto nessa linhagem, ou seja, mais vírus interagindo com mais receptores (MOI elevado), desenvolveriam o processo de apoptose mais rapidamente e, consequentemente, produziriam menos proteína.

Outra observação importante é a proporção entre a quantidade de RVGP encontrada no lisado celular e no sobrenadante, pois a RVGP encontrava-se mais presente no lisado celular no tempo de 24 h, enquanto que no tempo de 48 h toda a RVGP estava presente no sobrenadante, que corresponde na verdade, a restos celulares presentes no sobrenadante. Fato também comprovado pelas imagens obtidas momentos antes da coleta da proteína, onde fica evidente que células submetidas a um maior MOI, apresentam morfologia mais característica de células em apoptose.

No caso das células Huh-7, a produção de RVGP foi maior no tempo de 48 h após a infecção, e a maior produção de RVGP, ocorreu utilizando MOIs mais elevados, sendo que os resultados são considerados estatisticamente iguais para os MOIs 10, 15 e 50. Tendo esses mesmos MOIs, também resultados semelhantes no tempo de 24 h. Apenas no ensaio com MOI 1, a expressão foi maior a 24 h quando comparado com a coleta a 48 h. Essa diferença com o perfil de expressão da linhagem BHK-21 se deve possivelmente, ao menor dano causado pela infecção viral em células Huh-7, sendo que mesmo após as 48 h, ainda haviam células aderidas, fato que pode ser visualizado nas imagens obtidas no momento da coleta.

Uma possível explicação para esse comportamento descrito seria uma quantidade limitante de receptores que possam interagir com o vírus, dispostos nessa linhagem. Pois, sendo essa linhagem derivada de células tumorais, uma alteração na estrutura da membrana da mesma é um fato já explicitado. Estudos evidenciam a utilização de vetores SFV para infecção em algumas células tumorais, mostrando que a lise completa da célula ocorre somente após 72 h, o que reforça a hipótese de que esse tipo de linhagem se mostra mais “resistente” à ação viral (VAHA-KOSKELA et al., 2006). No mesmo estudo, é realizada uma comparação com células BHK-21, tendo como conclusão, que essa linhagem foi mais permissível à proliferação viral, do que as linhagens tumorais.

A utilização de MOI 50 e uma consequente produção de 4,08 µg por 1E6 células, sugere que a utilização de uma quantidade ainda maior de vírus, pode ocasionar uma maior produção de RVGP. Pois em diversos trabalhos envolvendo vetores virais, são utilizados MOIs de 100, ou até de 1000, para revisão veja Lee et al., 2007.

A linhagem L929 já foi previamente utilizada para expressão de proteínas utilizando o sistema SFV (MEINKOTH; KENNEDY, 1980). E no trabalho atual, apresentou expressão de RVGP no tempo de 24 h, alcançando níveis de até 2,82 µg por 1E6 células, enquanto que em 48 h, a produção menor com valores de no máximo 1,81 µg por 1E6 células. Tal fato, semelhante à BHK-21, se deve também à maior sensibilidade desse tipo de célula aos efeitos da infecção viral, refletindo em um grande efeito citopático. Possivelmente, porque a célula recém infectada produz grande quantidade de proteína devido ao forte promotor gênico do SFV, mas conforme a infecção avança, a célula não mais consegue manter a maquinaria de produção protéica e a mesma diminui abruptamente. Talvez a mesma quantidade de RVGP tenha sido gerada no ensaio de 48 h, mas houve uma degradação da mesma com o tempo e a quantificação tardia indicou um menor nível de expressão. Outro fato similar com a BHK-21, foi o aumento do MOI ocasionar uma menor produção de RVGP, podendo tal fato ser novamente relacionado ao desencadeamento de um processo mais intenso de apoptose, em células infectadas com uma maior quantidade de vírus (BARRY et al., 2010).

É interessante notar que as células BHK-21 foram as que menos sofreram durante o procedimento de IFI, gerando boas imagens e evidenciando a capacidade da célula em expressar RVGP. Ainda com relação a essas imagens, é possível verificar o alto percentual de células expressando a proteína, o que nos leva a crer, que no desenvolvimento de um vetor SFV com menor efeito citopático, ela se torna uma linhagem altamente recomendável para expressão das mais variadas proteínas (CASALES et al., 2008).

As células VERO, apresentaram o mesmo comportamento da linhagem BHK-21, apresentando uma maior produção de RVGP com MOI 1 no tempo de 24 h, diminuindo a produção com o aumento do MOI. Porém os valores obtidos foram inferiores aos encontrados com a célula BHK-21, mas ainda assim relevantes. Nesse tipo celular, toda a RVGP encontrada, independentemente do tempo de coleta, estava presente no lisado celular.

Dentre as linhagens avaliadas, a VERO, foi a que apresentou os piores resultados de expressão de RVGP, na análise por ELISA. Não possibilitando a detecção de bandas no experimento de *Western blot* e evidenciando a banda menos intensa no procedimento de *Dot blot*. Na técnica de IFI, foi evidenciada a presença de RVGP nas membranas, porém foi a

célula que mais sofreu no procedimento, apresentando membranas menos íntegras que as demais, e muita formação de grumos. Entretanto, é uma linhagem interessante já que é das mais utilizadas para produção de fármacos e vacinas, que envolvem cultura de células de mamíferos, sendo inclusive a células utilizadas para propagação do vírus rábico na atual vacina anti-rábica do Brasil, desenvolvida no Instituto Butantan (FRAZATTI-GALINA et al., 2004). Portanto, seria importante alcançar bons níveis de expressão com essa linhagem, por ser uma célula já preconizada em órgãos de regulamentação. O fato de não apresentar bons resultados nesse trabalho, não a descarta como substrato para utilização do sistema SFV, pois novos trabalhos com diferentes proteínas e diferentes metodologias podem reverter esse quadro.

Nos ensaios envolvendo células HEK-293T, também houve maior expressão de RVGP no tempo de 24 h, sendo que ela foi diminuindo conforme se aumentava o MOI. Já em 48 h, os níveis de expressão foram praticamente os mesmos para todos os MOIs, sendo significativamente mais baixos que aqueles apresentados a 24 h. Esse fato, também pode ser explicado pelo desencadeamento do processo de apoptose devido à infecção viral, fato que comprometeria a célula em continuar a produzir a proteína, na presença de grandes quantidades de vírus, ou por longos períodos.

Os resultados apresentados com as células BHK-21 CS, adaptadas em suspensão, são oriundos de um trabalho complementar, que foi realizado simultaneamente, em parceria com o Departamento de Engenharia Química da USP, onde foram utilizados os vírus produzidos por este trabalho. Para efeito de comparação, apenas estão expostos os dados obtidos com condições semelhantes às utilizadas para as demais células. Com base nisso, pode-se verificar que houve uma maior produção de RVGP no tempo de 24 h após a infecção. Entretanto, a produção nesse tipo celular, foi muito abaixo do que aquelas vistas em todas as demais linhagens, inclusive na BHK-21. Possivelmente, exista uma relação entre a infectividade do SFV e a necessidade da célula estar aderida, ou ser menos sensível ao processo de infecção. De qualquer forma, existe a necessidade de melhor entendimento desse processo e dessa relação, visto que uma possível aplicação desse método de expressão envolve diretamente uma extrapolação do sistema para biorreatores e com isso, a utilização de células em suspensão.

A semelhança entre o perfil de expressão obtido com a linhagem HEK-293T, com os obtidos com as células BHK-21, L929 e VERO, sustentam a hipótese de que o aumento de MOI, não necessariamente aumenta o nível de expressão de RVGP, sendo que em alguns

casos, ocorre até mesmo o contrário. E que, utilizando o sistema SFV, a proteína alvo é melhor expressa nas primeiras 24 h. Outra importante semelhança entre as linhagens BHK-21, HEK-293T e VERO, é que elas são oriundas de rins de diferentes espécies, explicando assim essa semelhança de comportamento. A exceção à esse perfil, é a linhagem Huh-7, que por ser derivada de células tumorais, é sabidamente detentora de um metabolismo distinto das demais. Entretanto, foi uma das linhagens que melhor expressaram a proteína, juntamente com a BHK-21 e HEK-293T.

Alguns trabalhos utilizando o próprio sistema SFV, relatam que o aumento do MOI pode estar relacionado ao aumento do nível de expressão, mas possivelmente, tal afirmação seja específica para o tipo de proteína expressa (BLASEY et al., 1997). Em um processo de produção de uma proteína diversos fatores são relevantes, quando se utiliza um procedimento *in vitro*, como temperatura, tempo de coleta, linhagem celular, composição do meio de cultura, pH, dentre outros. Sendo que os resultados apresentados nesse trabalho correspondem aos índices de expressão de proteínas, que foram detectadas pelo método utilizado, no tempo específico. Portanto, visto que em alguns casos a expressão protéica foi melhor no tempo de 24 h, frente a 48 h, é prudente afirmar que a proteína foi produzida em quantidades iguais em ambos os sistemas, o que os diferencia é o tempo que a proteína levou para ser detectada. Sendo assim, pequenas mudanças que alterem a conformação protéica, podem alterar os resultados finais, pois cada linhagem cria seu próprio microambiente, com metabólitos específicos, que podem agir na proteína gerada, através, por exemplo, de uma mudança de pH (GAUDIN et al., 1991). O MOI utilizado pode também interferir nessa relação da proteína gerada com o ambiente em que está, sendo que a presença de uma quantidade maior de vírus pode vir a afetar a posterior detecção da proteína.

Como conclusão, pode-se destacar o sistema SFV como um método eficaz e promissor, sendo capaz de bons níveis de expressão, e podendo utilizar diferentes linhagens celulares. Seu principal ponto positivo é sua versatilidade, pois pode expressar proteínas diversas em linhagens que sejam específicas para cada uma. Portanto, após estabelecida a plataforma mais adequada para esse sistema, é possível estende-la para diversas outras vertentes e produtos.

A desvantagem da aplicação do sistema baseado no SFV, especialmente para a produção em larga escala, é que a produção de estoque de vírus é relativamente cara. Os custos elevados estão relacionados com o processo de transcrição *in vitro*. Sendo que tentativas para facilitar e reduzir os custos de produção desses vírus são introduzidos

constantemente através do desenvolvimento de novos sistemas baseados no SFV (POLO et al., 1999). Outra preocupação tem sido a segurança relacionada ao SFV, especialmente para a produção em larga escala, que obviamente requer grandes volumes de vírus. Mas com abordagem atual utilizada para o SFV, os riscos são bastante baixos, ainda mais se comparado a outros sistemas semelhantes.

Por fim, os dados obtidos por esse trabalho são de grande importância para o entendimento desse promissor sistema de expressão, visto a possibilidade de expressão em diferentes linhagens e assim, obter as mais diversas proteínas para diferentes aplicações. O SFV se mostrou muito eficiente para infectar todas as células estudadas, quando comparado com o nível de expressão de outros sistemas, e as informações obtidas são muito relevantes, devido ao fato de que diferentes proteínas a serem expressas, podem necessitar de linhagens específicas, e esse estudo preconiza que o sistema se comporta de maneira distinta conforme a linhagem utilizada.

7 CONCLUSÕES

Neste trabalho estabelecemos um protocolo de transcrição *in vitro* e transfecção de RNA, para produção de partículas virais SFV recombinantes (SFV-RVGP) em células BHK-21. Estabelecemos também uma metodologia baseada em qRT PCR para quantificar as partículas virais obtidas e a partir daí pudemos obter um lote de vírus recombinante e padronizar as melhores condições de infecção celular (MOI e tempo de coleta) para produção da RVGP em diferentes linhagens celulares de mamíferos.

Os resultados obtidos demonstram uma diferença evidente entre os níveis de expressão utilizando as diferentes linhagens, sugerindo que o sistema SFV, possui um comportamento de infecção específico para cada tipo celular. Pode-se admitir também, que cada linhagem possui diferenças no processamento da proteína, obtendo índices de expressão distintos não somente na quantidade, como também no tempo após a infecção com o vetor viral SFV.

O trabalho consiste em uma abordagem preliminar sobre o comportamento desse vetor viral em diferentes linhagens de mamíferos, sendo que estudos complementares podem possibilitar seu emprego, para expressão de diferentes proteínas, utilizando uma linhagem celular específica para a mesma.

REFERÊNCIAS*

ASTRAY, R. M. et al. Analytical approach for the extraction of recombinant membrane viral glycoprotein from stably transfected Drosophila melanogaster cells. **Biotechnol. J.**, v. 3, n. 1, p. 98-103, 2008.

ASTRAY, R. M. et al. Kinetic studies of recombinant rabies vírus glycoprotein (RVGP) cDNA transcription and mRNA translation in Drosophila melanogaster S2 cell. **Cytotechnology**., v. 65, n. 5, p. 829-838, 2013.

ASTRAY, R. M. **Expressão da glicoproteína recombinante do vírus rábico em sistemas Drosophila melanogaster (S2) e Semliki Forest Virus (SFV).** 2009, 161 f. Tese (Doutorado em Biotecnologia) - Universidade de São Paulo (USP), São Paulo, Brasil, 2009.

BALDI, L. et al. Recombinant protein production by large-scale transiente gene expression in mammalian cells: state of the art and future perspectives. **Biotechnol. Lett.,** v. 29, n. 5, p. 677-684, 2007.

BARRY, G. et al. Semliki forest virus-induced endoplasmic reticulum stress accelerates apoptotic death of mammalian cells. **J. Virol.**, v. 84, n. 14, p.7369-7377, 2010.

BENMAAMAR, R. et al. High-level expression of rabies virus glycoprotein with the RNA-based Semliki Forest Virus expression vector. **J. Biotechnol.,** v. 139, n. 4, p. 283-290, 2008.

BENMANSOUR, A. et al. Antigenicity of rabies virus glycoprotein. **J. Virol.,** v. 65, n. 8, p. 4198-4203, 1991.

BERGLUND, P. et al. Semliki Forest Virus expression system: production of conditionally infectious recombinant particles. **Biotechnology**., v. 11, n. 8, p.916-920, 1993.

BIKKER, H. et al. Molecular analysis of mutated thyroid peroxidase detected in patients with total iodide organification defects. **J. Clin. Endocrinol. Metab.,** v. 82, n. 2, p. 649-653, 1997.

BLASEY, H. D. et al. Recombinant protein production using the Semliki Forest Virus expression system. **Cytotechnology**., v. 24, n. 1, p. 65–72, 1997.

BOLLATI-FOGOLIN, M; COMINI, M. Clonagem e expressão de proteínas heterólogas em células animais. Em: Leda Castilho; Angela Moraes; Elisabeth Augusto. **Tecnologia do cultivo de células animais: de biofármacos à terapia gênica**. 1 ed. São Paulo: Editora Roca LTDA, v.1, p. 42-73, 2007.

BRASIL, MINISTÉRIO DA SAÚDE. Disponível em: <http://portal.saude.gov.br/portal/arquivos/pdf/mapas_atual_raiva_2012_08_05_2013.pdf>, acessado em 04 de Novembro de 2013.

*De acordo com:
ASSOCIAÇÃO BRASILEIRA DE NORMAS TÉCNICAS. NBR 6023: informação e documentação: referências: elaboração. Rio de Janeiro, 2002.

BRASIL, MINISTÉRIO DA SAÚDE. Disponível em: <http://www.brasil.gov.br/saude/2012/10/brasil-e-exemplo-na-erradicacao-da-raiva-animal-e-humana-no-mundo>, acessado em 04 de Novembro de 2013.

CASALES, E. et al. A novel system for the production of high levels of functional human therapeutic proteins in stable cells with a Semliki Forest virus noncytopathic vector. N **Biotechnol.,** v. 27, n. 2, p. 138-148, 2010.

CASALES, E. et al. Development of a new noncytopathic Semliki Forest virus vector providing high expression levels and stability. **Virology**, v. 376, n. 1, p. 242-251, 2008.

CHA, H. J; GOTOH, T; BENTLEY, W. E. Simplification of titer determination for recombinant baculovirus by green fluorescent protein marker. **Biotechniques,** v. 23, n. 5, p. 782-786, 1997.

CHEN, Z. et al. A novel rabies vaccine based on a recombinant parainfluenza virus 5 expressing rabies virus glycoprotein. **J. Virol**., v. 87, n. 6, p. 2986-2993.

CORTESI, R. et al. Effect of cationic liposome composition on in vitro cytotoxicity and protective effect on carried DNA. **Int. J. Pharmaceut.,** v. 139, n. 1, p. 69-78, 1996.

DE JESUS, M; WURM, F. M. Manufacturing recombinant proteins in kg-ton quantities using animal cells in bioreactors. **Euro. J. Pharm. Biopharm.,** v. 78, n. 2, p.184-188, 2011.

DIETZSCHOLD, B. Oligosaccharides of the glycoprotein of rabies virus. **J. Virol.**, v. 23, n. 2, p. 286-293, 1977.

EIFLER, N. et al. Functionalexpression of mammalianreceptors and membrane channels in different cells. **J. Struct. Biol.,** v. 159, n. 2, p.179-193, 2007.

EL-ANEED, A. An overview of current delivery systems in cancer gene therapy. **J Control Release**, v. 94, n. 1, p. 1-14, 2004.

ERTL, H. C. Novel vaccines to human rabies. **PLoS. Negl. Trop. Dis**., v. 3, n. 9, p. 515, 2009.

European Medicines Agency (EMA). **Sciences Medicines Health**. 2010. Disponível em : http://www.ema.europa.eu/docs/pt_PT/document_library/EPAR_-_Summary_for_the_public/veterinary/002003/WC500104120.pdf

FRAZATTI-GALLINA, N. M. et al. Vero-cell rabies vaccine produced using serum-free medium. **Vaccine,** v. 23, n. 4, p. 511-517, 2004.

GALESSI, A. L. et al. Growth of recombinant drosophila melanogaster Schneider 2 cells producing rabies virus glycoprotein in bioreactor employing serum-free medium. **Cytotechnology**, v. 57, n. 1, p. 73-81, 2008.

GALLIE, D. R. The cap and the poly(A) tail function synergistically to regulate mRNA translational efficiency. **Genes Dev**., v. 5, n. 11, p. 2108-2116, 1991.

GAUDIN, Y. et al. Rabies virus glycoprotein is a trimer. **Virology**, v. 187, n. 2, p. 627-632, 1992.

GAUDIN, Y. et al. Reversible conformational changes and fusion activity of rabies virus glycoprotein. **J. Virol.,** v. 65, n. 9, p. 4853–4859, 1991.

GAUDIN, Y. et al. Soluble ectodomain of rabies virus glycoprotein expressed in eukaryotic cells folds in a monomeric conformation that is antigenically distinct from the native state of the complete, membrane-anchored glycoprotein. **J. Gen. Virol**., v. 80, n. 7, p 1647-1656, 1999.

GAUDIN, Y. Folding of rabies virus glycoprotein: epitope acquisition and interaction with endoplasmic reticulum chaperones. **J. Virol.**, v. 71, n. 5, p. 3742-3750, 1997.

GONZALEZ, G. et al. Selection of an optimal RNA transfection reagent and comparison to electroporation for the delivery of viral RNA. **J. Virol. Methods,** v. 145, n. 1, p. 14–21, 2007.

HOFFMAN, M. et al. Recombinant Semliki Forest virus for over-expression and pharmacological characterization of the histamine H(2) receptor in mammalian cells. **Euro. J. Pharmacol.,** v. 427, n. 2, p. 105-114, 2001.

HUANG, H. et al. Construction and immunogenicity of a recombinant pseudotype baculovirus expressing the glycoprotein of rabies virus in mice. **Arch. Virology**, v. 156, n. 5, p. 753-758.

HUNT, I. From gene to protein: a review of new and enabling technologies for multi-parallel protein expression. **Protein Expr. Purif.,** v. 40, n. 1, p. 1-22, 2005.

JAN, J. T., GRIFFIN, D. E. Induction of apoptosis by Sindbis virus occurs at cell entry and does not require virus replication. **J. Virol.***,* v. 73, n. 12, p. 296-302, 1999.

JANAKIRAMAN, V. et al. A rapid method for estimation of baculovirus titer based on viable cell size. **J. Virol. Methods**, v. 132, n. 1-2, p. 48-58, 2006.

JORGE, S. A. C. et al. Expression of the hepatitis B virus surface antigen in mammalian cells using an Epstein-barr-virus-derived vector. **Appl. Microbiol. Biotechnol.,** v. 46, n. 5-6, p. 533-537, 1996.

JORGE, S. A. C. et al. Transient expression of hepatitis B virus surface antigen (HBsAg) gene in monkey cells by a SV40-based virus vector. **Biotechnology Letters,** v. 17, n. 12, p. 85-90. 1995.

JOSE, J.; SNYDER, J. E.; KUHN, R. J. A structural and functional perspective of alphavirus replication and assembly, **Future Microbiol**., v. 4, n. 7, p. 837-856, 2009.

KAMRUD, K. I. et al. Development and characterization of promoterless helper RNAs for the production of alphavirus replicon particle. **J. Gen. Virol**., v. 91, n. 7, p. 1723-1727, 2010.

KARLSSON, G. B.; LILJESTROM, P. Live viral vectors: Semliki Forest Virus. **Method Mol. Med**., v. 87, p. 69-82, 2003.

KLEPFER, S. R. et al. Characterization of rabies glycoprotein expressed in yeast. **Arch. Virol**., v. 128, n. 3-4, p. 269-286, 1993.

KOOL, M. et al. Detection and analysis of Autographa californica nuclear polyhedrosis virus mutants with defective interfering properties. **Virology,** v. 183, n. 2, p. 739-746, 1991.

LANGER, E. S. On the horizon: new expression systems to become common industry platforms new expression systems compete for attention. **BioPharm. International.,** v. 22, n. 6, p. 4-9, 2009.

LATHE, R. F. et al. M13 bacteriophage vectors for the expression of foreign proteins in *Escherichia coli*: The rabies glycoprotein. **J. Mol. Appl. Genet**., v. 2, n. 4, p. 331-342, 1984.

LEE, H. S. et al. Efficient gene expression by self-complementary adeno-associated virus serotype 2 and 5 in various human cancer cells. **Oncol. Rep.**, v. 18, n. 3, p. 611-616, 2007.

LEMOS, M. A. N. et al. Rabies virus glycoprotein expression in Drosophila S2 cells. I: design of expression/selection vectors, subpopulations selection and influence of sodium butyrate and culture medium on protein expression. **J. Biotechnol.**, v. 143, n. 2, p. 103-110, 2009.

LEYVA, F. J. et al. Evaluation of transduction efficiency in macrophage colony-stimulating factor differentiated human macrophages using HIV-1 based lentiviral vectors. **BMC. Biotechnol.,** v. 11, n.13, p. 30-37, 2011.

LILJESTROM, P.; GAROFF, H. A new generation of animal cell expression vectors based on the Semliki Forest virus replicon. **Biotechnology,** v. 9, n. 12, p. 56-61, 1991.

LO, H. R.; CHAO, Y. C. Rapid titre determination of baculovirus by quantitative real-time polymerase chain reaction. **Biotecnol. Prog.,** v. 20, n. 1, p. 354-360, 2004.

LUNDSTROM, K. Alphavirus vectors for vaccine production and gene therapy. **Expert. Rev. Vaccines**, v. 2, n. 3, p. 47-59, 2003.

LUNDSTROM, K. Expression of mammalian membrane proteins in mammalian cells using Semliki Forest virus vectors. **Method Mol. Biol.,** v. 601, n. 1, p. 49-63, 2010.

LUNDSTROM, K. Generation of Recombinant Alphaviral Vectors. **Cold. Spring. Harb. Protoc**., v. 7, p. 825-831, 2012.

MORATO, F.; IKUTA, C. Y.; ITO, F.H. Raiva: uma doença antiga, mas ainda atual. **Rev. Educ. Cont. Med. Vet. Zootec. CRMV-SP,** v. 9, n. 3. p. 20–29, 2011.

MORIMOTO, K.; KAWAI, A.; MIFUNE, K. Comparison of rabies virus G proteins produced by cDNA-transfected animal cells that display either inducible or constitutive expression of the gene. **J. Gen. Virol.,** v. 73, n. 2, p. 335-345, 1992.

NARAYANASAMY, E. et al. Optimized transfection of mRNA transcribed from a d(A/T)100 tail-containing vector. **Biochem Bioph Res Co.,** v. 330, n. 3, p. 958–966, 2005.

NATHANSON, N.; LANGMUIRAD. The cutter incident: poliomyelitis following fobmaldehybe-inactivated poliovirus vaccination in the United States during the spring of 1955: ii. relationship of poliomyelitis to Cutter vaccine. **Am. J. Epidemiol.**, v. 142, n. 2, p. 109-140, 1995.

NETTLESHIP, J. E. et al. Recent advances in the production of proteins in insect and mammalian cells for structural biology. **J. Struct. Biol.**, v. 172, n. 1, p. 55-65, 2010.

NOLAN, T.; HANDS, R. E.; BUSTIN, S. A. Quantification of mRNA using real-time RT-PCR. **Nat. Protoc.,** v. 1, n. 3, p. 1559-1582, 2006.

PATIÑO, S. F. S. **Avaliação da expressão transiente do gene da glicoproteína do vírus da raiva (RVGP) em células de inseto da linhagem *Drosophila melanogaster* S2.** 2011, 121 f. Dissertação (Mestre em Biotecnologia) - Universidade Federal de São Carlos (UFSCAR), São Carlos, Brasil, 2011.

PAUL, N. L. et al. Expression of HIV-1 envelope glycoproteins by Semliki Forest virus vectors. **AIDS Res. Hum. Retrov.,** v. 9, n. 10, p. 963-970, 1993.

PERRIN, P.; THIBODEAU, L.; SUREAU, P. Rabies immunosome (subunit vaccine) structure and immunogenicity. Pre- and post-exposure protection studies. **Vaccine**., v. 3, n. 3, p. 325-332, 1985.

PFAFFL, M. W. et al. Validities of mRNA quantification using recombinant RNA and recombinant DNA external calibration curves in real-time RT-PCR. **Biotechnol. Letters**, v. 23, n. 4, p. 275-282, 2001.

PHAM, P. L; KAMEN, A.; DUROCHER, Y. Large cale transfection of mammalian cells for the fast production of recombinant protein. **Mol. Biotechnol.**, v. 34, n. 2, p. 225-237, 2006**.**

POULIQUEN, Y. et al. Automated baculovirus titration assay based on viable cell growth monitoring using a colorimetric indicator. **Biotechniques,** v. 40, n. 3, p. 282-286, 2006.

PREHAUD, C. et al. Characterization of a new temperature-sensitive and avirulent mutant of the rabies virus. **J. Gen. Virol.,** v. 70, n.1, p. 133-143, 1989.

PUGLIA, A. L. et al. Quantitative RT-PCR for titration of replication-defective recombinant Semliki Forest virus. **J. Virol. Methods,** v. 193, n. 2, p. 647-652, 2013.

PUSHKO, P. et al. Replicon-helper systems from attenuated Venezuelan equine encephalitis virus: expression of heterologous genes in vitro and immunization against heterologous pathogens in vivo. **Virology**, v. 239, n. 2, p. 389-401, 1997.

QUETGLAS, J. I. Eradication of liver-implanted tumors by Semliki Forest virus expressing IL-12 requires efficient long-term immune responses. **J. Immunol**., v. 190, n. 6, p. 2994-3004, 2013.

RAMYA, R. et al. Expression and solubilization of insect cell-based rabies virus glycoprotein and assessment of its immunogenicity and protective efficacy in mice. **Clin. Vaccine Immunol.,** v. 18, n. 10, p. 1673-1679, 2011.

RAYNER, J.O.; DRYGA, S. A.; KAMRUD, K. I. Alphavirus vectors and vaccination. **Rev. Med. Virol.,** v. 12, n. 5, p. 279-296, 2002.

SAKAMOTO, S. et al. Studies on the structures and antigenic properties of rabies virus glycoprotein analogues produced in yeast cells. **Vaccine**, v. 17, n. 3, p. 205-218, 1999.

SCHNELL, M. J. et al. The cell biology of rabies virus: using stealth to reach the brain. **Nat. Rev. Microbiol**., v. 8, n. 1, p. 51-61, 2010.

SHEN, C. F.; MEGHROUS, J.; KAMEN, A. Quantitation of baculovirus particles by flow cytometry. **J. Virol. Methods**, v. 105, n. 2, p. 321-330, 2002.

SHUKLA, A. K. et al. Biochemical and pharmacological characterization of the human bradykinin subtype 2 receptor produced in mammalian cells using the Semliki Forest virus system. **Biol. Chem**., v. 387, n. 5, p. 569-576, 2006.

SHUKLA, A. K. et al. Heterologous expression and comparative characterization of the human neuromedin U subtype II receptor using the methylotrophic yeast Pichia pastoris and mammalian cells. **Int. J. Biochem. Cell Biol.,** v. 39, n. 5, p. 931-42, 2007.

STRAUSS, J. H.; STRAUSS, E. G. The alphaviruses: gene expression, replication, and evolution. **Microbiol. Rev.,** v. 58, n. 3, p. 491–562, 1994.

TORDO, N. et al.Completion of the rabies virus genome sequence determination: highly conserved domains among the L (polymerase) proteins of unsegmented negative-strand RNA viruses.**Virology,** v. 165, n. 2, p. 565-576, 1988.

TWYMAN, R. M. Gene transfer using viral vectors. In: _____ **Gene transfer to animal cells**. New York: Garland BIOS Scientific Publishers**,** 2005. cap. 4, p. 70-119.

VÄHÄ-KOSKELA, M. J. et al. Oncolytic capacity of attenuated replicative semliki forest virus in human melanoma xenografts in severe combined immunodeficient mice. **Cancer Res**., v. 66, n. 14, p. 7185-7194, 2006.

VENTINI, D. C. et al. Recombinant rabies virus glycoprotein synthesis in bioreactor by transfected Drosophila melanogaster S2cells carrying a constitutive or an inducible promoter. **J. Biotechnol**., v. 146, n. 4, p. 169-172.

WALSH, G. Post-translational modifications of protein biopharmaceuticals. **Drug. Discov**. **Today.,** v. 15, n. 17, p. 773-780, 2010.

WITTWER, C.T. High-resolution DNA melting analysis: advancements and limitations. **Hum. Mutat.**, v. 30, n. 6, p. 857-859, 2009.

WORLD HEALTH ORGANIZATION (WHO). **Rabies**. <www.who.int/rabies>, acessado em 26 de Março de 2013.

WU, X; SMITH, T.G; RUPPRECHT, C.E. From brain passage to cell adaptation: the road of human rabies vaccine development. **Expert Rev. Vaccines,** v. 10, n. 11, p. 1597-1608, 2011.

WULHFARD, S. **Transient recombinant protein expression in mammalian cells: the role of mRNA level and stability.** 2009, 145 f. Tese (Doutorado em Ciências) – École Polytechnique Fédérale de Lausanne, Lausanne, 2009.

YAHATA, T. et al. Estimation of baculovirus titer by beta-galactosidase activity assay of virus preparations. **Biotechniques**, v. 29, n. 2, p. 214-215, 2000.

YAROSH, O. K. et al. Human adenovirus type 5 vectors expressing rabies glycoprotein. **Vaccine**, v. 14, n. 13, p. 1257-1264.

YELVERTON, E. et al. Rabies virus glycoprotein analogs: biosynthesis in Escherichia coli. **Science**, v. 219, n. 4585, p. 614-620, 1983.

YOKOMIZO, A.Y. et al. Rabies virus glycoprotein expression in Drosophila S2 cells. I. Functional recombinant protein in stable co-transfected cell line. **Biotechnol. J**., v. 2, n. 1, p.102-109, 2007.

ANEXO – TRABALHOS PUBLICADOS

ANEXO A – Quantitative RT-PCR for titration of replication-defective recombinant Semliki Forest virus.

ANEXO B – Using Statistical Tools for Improving Bioprocesses.

ANEXO C – Semliki Forest Virus as a Vector: Pros and Cons for Its Use in Biopharmaceuticals Production.

ANEXO D – Influence of aeration–homogenization system in stirred tank bioreactors, dissolved oxygen concentration and pH control mode on BHK-21 cell growth and metabolism. Cytotechnology.

ANEXO E – A multivariate calibration procedure for UV/VIS spectrometric monitoring of BHK-21 cell metabolism and growth.

G Model
VIRMET 12261 1–6

ARTICLE IN PRESS

Journal of Virological Methods xxx (2013) xxx–xxx

Contents lists available at ScienceDirect

Journal of Virological Methods

journal homepage: www.elsevier.com/locate/jviromet

Quantitative RT-PCR for titration of replication-defective recombinant Semliki Forest virus

Q1 Ana L.P. Puglia[a,1], Alexandre G. Rezende[a,1], Soraia A.C. Jorge[a,1], Renaud Wagner[b,2], Carlos A. Pereira[a,1], Renato M. Astray[a,*]

[a] Laboratório de Imunologia Viral, Instituto Butantan, Av. Vital Brasil 1500, CP 05503-900 São Paulo, Brazil
[b] Institut de Recherche de l'Ecole de Biotechnologie de Strasbourg, University of Strasbourg, CNRS, Bd. Sébastien Brandt, CP 10413, F-67412 Illkirch, France

Article history:
Received 14 May 2013
Received in revised form 17 July 2013
Accepted 22 July 2013
Available online xxx

Keywords:
Semliki Forest virus
qRT-PCR
Virus titration

ABSTRACT

Virus titration may constitute a drawback in the development and use of replication-defective viral vectors like Semliki Forest virus (SFV). The standardization and validation of a reverse transcription quantitative PCR (qRT-PCR) method for SFV titration is presented here. The qRT-PCR target is located within the nsp1 gene of the non-structural polyprotein SFV region (SFV RNA), which allows the strategy to be used for several different recombinant SFV constructs. Titer determinations were carried out by performing virus titration and infection assays with SFVs containing an RNA coding region for the rabies virus glycoprotein (RVGP) or green fluorescent protein (GFP). Results showed that the standardized qRT-PCR is applicable for different SFV constructs, and showed good reproducibility. To evaluate the correlation between the amount of functional SFV RNA in a virus lot and its infectivity in BHK-21 cell cultures, a temperature mediated titer decrease was performed and successfully quantitated by qRT-PCR. When used for cell infection at the same multiplicity of infection (MOI), the temperature treated SFV-RVGP samples induced the same levels of RVGP expression. Similarly, when different SFV-GFP lots with different virus titers, as accessed by qRT-PCR, were used for cell infection at the same MOI, the cultures showed comparable amounts of fluorescent cells. The data demonstrate a good correlation between the amount of virus used for infection, as measured by its SFV RNA, and the protein synthesis in the cells. In conclusion, the qRT-PCR method developed here is accurate and enables the titration of replication-defective SFV vectors, an essential aid for viral vector development as well as for establishment of production bioprocesses.
© 2013 Published by Elsevier B.V.

1. Introduction

The Semliki Forest virus (SFV) is an enveloped, single-stranded RNA virus of positive polarity belonging to the genus *Alphavirus*, family Togaviridae. The viruses of this family comprise a single non-segmented RNA molecule, which acts as a messenger RNA (Schlesinger and Schlesinger, 1991). The finding that the SFV was able to infect many cell types with high efficiency in gene delivery and that the use of a strong viral promoter allowed the amplification of heterologous RNA into the host cell led to the development of the SFV expression vector (Liljeström and Garoff, 1991). For this purpose, the cDNA corresponding to its genome was cut and inserted into two different plasmids. The expression plasmid contains the genes for SFV non-structural proteins (nsp1-4) and the strong subgenomic SFV 26S promoter located upstream of a polycloning site. The helper plasmid contains the genes for the structural proteins (Liljeström and Garoff, 1991; Smerdou and Liljeström, 1999). In order to obtain SFV particles, both plasmids are linearized and transcribed *in vitro* in expression and helper RNAs. After the electroporation of the RNAs in mammalian cells, infectious but non-replicative virus particles are formed, which can be collected from the supernatant (for review see Lundstrom et al., 2001; Rayner et al., 2002). These particles can be used for infecting several cell types *in vitro* or for *in vivo* gene delivery. Infected cells can then translate the heterologous RNA and synthesize the recombinant protein. In a previous study, an SFV vector carrying the rabies virus glycoprotein (SFV-RVGP) was constructed. Upon baby hamster kidney (BHK-21) cell infection with SFV-RVGP, RVGP mRNA amplification took place and high levels of RVGP could be produced (Benmaamar et al., 2009).

An essential step in using recombinant SFV particles is the virus titration. Traditional methods for assessing cytopathic effects in plaque assays are often used for the titration of replicative wild

* Corresponding author. Tel.: +55 11 26 27 96 21.
E-mail addresses: analiapp@butantan.gov.br (A.L.P. Puglia), alexandre.biotecjuruaia@gmail.com (A.G. Rezende), sacjorge@butantan.gov.br (S.A.C. Jorge), renaud.wagner@unistra.fr (R. Wagner), grugel@butantan.gov.br (C.A. Pereira), renatoastray@butantan.gov.br, renatoastray@yahoo.com (R.M. Astray).
[1] Tel.: +55 11 26 27 96 21.
[2] Tel.: +33 03 68 85 47 31.

0166-0934/$ – see front matter © 2013 Published by Elsevier B.V.
http://dx.doi.org/10.1016/j.jviromet.2013.07.058

Please cite this article in press as: Puglia, A.L.P., et al., Quantitative RT-PCR for titration of replication-defective recombinant Semliki Forest virus. J. Virol. Methods (2013), http://dx.doi.org/10.1016/j.jviromet.2013.07.058

or modified strains of SFV (Liljestrom et al., 1991; Zusinaite et al., 2007), but these methods are not applicable to non-replicative SFV vectors, which do not develop plaques. The titration of replication-deficient SFV vectors has traditionally been accomplished by the use of methods such as virus infection of plated cells with subsequent detection by immunofluorescence using primary antibodies against the protein of interest (Karlsson and Liljestrom, 2003; Hubby et al., 2007) or against the viral replicase (Klimpi et al., 2001), or even using a reporter gene like green fluorescent protein (GFP) or β-galactosidase (Ni et al., 2005; Zusinaite et al., 2007; Lundstrom, 2012). The viral titration can also be performed by dot-blotting technique, using radioactively labeled DNA probes (Wahlfors and Morgan, 2002). Nevertheless, these methods are time-consuming and often not sensitive enough. It is clear that the titration of SFV vectors still lacks a simple and sensitive technique for an accurate evaluation of the system. A similar demand led to the standardization of a qPCR approach for baculovirus titration (Lo and Chao, 2004; Hitchman et al., 2007). The qRT-PCR technique is a good alternative for the titration of SFV vector particles since the diffusion of qRT-PCR technology and prior knowledge about its use in viral titration provide considerable support for this approach (Rohr et al., 2002; Hitchman et al., 2007; Morsy El-Senousy et al., 2007; Zhang et al., 2008; Zhao et al., 2007).

This study presents the standardization of a method for qRT-PCR titration of non-replicative SFV particles. The method proposed here could be applicable to virtually any non-replicative SFV particles since the target for amplification is a conserved region of the gene coding for the nonstructural protein 1 (nsp1). Results of using different SFV constructs show that qRT-PCR is a suitable method for SFV titration since there is a good correlation between the amount of SFV containing RNA used for cell infection, the amount of infected cells, and the production of the recombinant protein.

2. Materials and methods

2.1. SFV vectors

Different recombinant SFV vectors were obtained by cloning the gene of interest under the control of the strong subgenomic promoter, SFV 26S, into the pSFVgen2C plasmid, which code for non-structural SFV proteins as already described (Karlsson and Liljestrom, 2003; Benmaamar et al., 2009). SFV vectors carrying genes coding for membrane proteins were used: SFV-RVGP, SFV-melatonin A1 receptor (Mta-1), SFV-modified adenosine receptor (Ala-80) and SFV-adenosine receptor A2A (20A2). An SFV-GFP vector expressing cytoplasmic GFP was also used. For obtaining SFV particles, the genes coding for structural proteins were supplied by SFV-Helper2 plasmid (Berglund et al., 1993). Briefly, helper and different expression plasmids were linearized using Spe I and Nru I restriction enzymes, respectively. Linearized plasmids were transcribed *in vitro* using SP6 RNA polymerase and the MAXIScript® SP6 kit (Life Technologies, Carlsbad, USA) at 40 °C for 2 h. RNA was then quantitated by fluorimetry using the Quant-it™ RNA assay kit (Life Technologies, Eugene, USA). Expression and helper RNAs were used for co-transfect of BHK-21 cells by electroporation. After 24 h recombinant SFV particles were harvested from supernatant. Before utilization, SFV particles were activated with α-chemotrypsin 0.5 mg/mL (Sigma–Aldrich, Saint Louis, USA) followed by enzymatic inactivation with aprotinin 1 mg/mL (Thermo Fisher Scientific, Rockford, USA). Activated SFV particles were titrated and used for BHK-21 infection. All virus stocks were maintained at −80 °C until the moment of activation and utilization. Alternatively, activated SFV-RVGP aliquots were submitted to temperatures of 24 °C or 37 °C for 1 h or 3 h and then titrated and utilized for infection.

2.2. RNA extraction from SFV samples

RNA extraction from SFV samples was performed using the RNeasy kit (Qiagen, Maryland, USA), following the manufacturer's instructions. First, three SFV-RVGP sample volumes were assayed (50 μL, 100 μL, and 200 μL) to determinate the best sample size, based on the amount of RNA required for analysis. The best qRT-PCR amplification performance was found using 100 μL. As the amount of total RNA in any SFV sample was below the limit of quantitation of our available quantitation methodologies, the RNA recovery after extraction was evaluated by the introduction of 3 μg yeast tRNA (Life Technologies, Carlsbad, USA) in each SFV sample. After the extraction process, total extracted RNA was quantitated by fluorimetry, and the RNA extraction yield was calculated.

2.3. DNase treatment and cDNA synthesis

For contaminant DNA removal, 1 μg of total RNA was treated with 1 U of DNase I (Promega Corporation, Fitchburg, USA) and 1 U of RNase inhibitor (Life Technologies, Carlsbad, USA) for 30 min at 37 °C, followed by incubation with ethylene glycol tetraacetic acid (EGTA) for 10 min at 65 °C for DNase I inactivation. Each 600 ng sample of DNA-free RNA was then reverse transcribed with 200 U M-MLV (Life Technologies, Carlsbad, USA), 1 μM reverse specific primer SFV-R1 (5′-CTCAATGATGACGTGGAGCT), 0.5 mM dNTPs, 0.1 M DTT, and RNase-free water. The reaction was incubated at 37 °C for 30 min, followed by enzyme inactivation at 70 °C for 15 min. cDNA samples were stored at −20 °C until processed.

2.4. qPCR

qPCR runs were performed in a StepOne™ (Life Technologies, Singapore) real-time fluorescence detector thermocycler. The reaction was set-up using the Power SYBR® Green kit (Life Technologies, Foster City, USA), 3 μL cDNA sample, 50 nM forward primer SFV-S2 (5′-ACAGACTGTCACTGAGCAG), 50 nM reverse primer SFV-R2 (5′-GTGACCATCTACTGCAGAGA) in 15 μL total reaction volume. After distribution of samples and standards, the optic plates (Life Technologies, Foster City, USA) were sealed and briefly centrifuged (1200 rpm for 3 min). qPCR was performed at 95 °C for 10 min, 34 × (95 °C/15 s, 55 °C/15 s, 60 °C/15 s), and the fluorescence was measured at 60 °C. The threshold fluorescence level for quantification was set within the exponential phase where all amplification curves exhibited the most significant signal increase. The cycle threshold (Ct) was obtained by recording the number of cycles required for the fluorescent signal to cross the threshold. After amplification, the melting curve (60–95 °C) was developed in order to verify reaction specificity, with the amplified fragment (145 bp) presenting dissociation at 83 ± 0.3 °C.

2.5. Standard curve

The standard curve for SFV-RNA quantitation was obtained by serial dilution of pSFV-RVGP plasmid. pSFV-RVGP was produced in bacteria, extracted, and purified using the Plasmid Maxi-Prep kit (Qiagen, Maryland, USA). Plasmid was treated with DNase-free RNase, quantitated by spectrophotometry and subsequently 2 μg of pSFV-RVGP was linearized by Not I digestion and quantitated by fluorimetry using the Quant-it™ DNA assay kit (Life Technologies, Carlsbad, USA). The concentration required for a specific number of the target sequence was calculated based on the mass of a single plasmid molecule and the mass of plasmid containing the copy number of interest. Six dilutions were performed in 10 mM Tris + 1 mM EGTA buffer, generating the standard dilutions containing 6×10^7, 6×10^6, 6×10^5, 6×10^4, 6×10^3 or 6×10^2 copies in each 3 μL. Four independent runs with three replicates of each

Please cite this article in press as: Puglia, A.L.P., et al., Quantitative RT-PCR for titration of replication-defective recombinant Semliki Forest virus. J. Virol. Methods (2013), http://dx.doi.org/10.1016/j.jviromet.2013.07.058

standard dilution were performed, and each standard curve was defined as the regression line of the logarithm of standard copy number *versus* Ct. A mean standard curve was calculated from previous curves and data was plotted. All curves were evaluated in accordance with published guidelines (Nolan et al., 2006). Efficiency was determined by the formula (Pfaffl, 2001)

$$E = 10^{(-1/S)}$$

where "E" is efficiency and "S" is the slope of the standard curve.

2.6. Titration of SFV RNA

cDNA obtained after reverse transcription of SFV RNA samples were amplified together with standard curve dilutions, in three replicates each. Mean Cts were applied to the standard curve equation to determinate the cDNA copy number in each sample. The total SFV RNA copy number present in the original SFV sample was calculated by the multiplication of the cDNA copy number by a conversion factor specific to each sample, which considered all dilutions made and the yield of RNA extraction. Each SFV RNA copy was considered to belong to one potentially infective particle, so virus titer was expressed in virus particle per milliliter (VP/mL).

2.7. Cell cultures and infection

BHK-21 cells were cultivated in α-MEM medium (Life Technologies, Carlsbad, USA) containing 10% fetal calf serum (FCS), at 37 °C and 5% CO_2. For infection studies, cells were seeded in six-well plates at a concentration of 7×10^5 cells/well; the medium was replaced with α-MEM containing the desired amount of recombinant SFV. The multiplicity of infection (MOI), or the amount of SFV/cell, was calculated based on the SFV titer and the cell number. To provide a homogeneous infection and avoid temperature-mediated degradation of viruses, the cultures were kept under gentle agitation at room temperature (24 ± 2 °C) for 2 h. The culture medium was then replaced with 1.5 mL of α-MEM with FCS, and cells were incubated at 37 °C. At different time points after infection, cells were resuspended in PBS + 5 mM EDTA by incubation at 37 °C for 5 min. Samples containing 3×10^5 cells were analyzed by ELISA (Perrin et al., 1996) for determination of RVGP production following previously published procedures of sample treatment (Astray et al., 2008; Benmaamar et al., 2009). For RVGP mRNA quantitation, samples of 8×10^5 cells were RNA-extracted and the procedures of DNase treatment, reverse transcription, and qPCR were followed as previously described (Benmaamar et al., 2009).

2.8. Flow cytometry analysis

To analyze the relationship between the MOI used for infection and the relative amount of infected cells, three different lots of SFV-GFP were produced and titrated by qRT-PCR. Following titration, virus lots were used for BHK-21 infection with MOI 1, 3, 5, 10, or 15. After 24 h cells were harvested with PBS + 5 mM EDTA, washed and fixed with PBS + 0.2% para-formaldehyde. The proportions of fluorescent cells were determined by counting 10,000 events on a FACSCalibur™ flow cytometer (Becton Dickinson, San Jose, USA). The equipment was calibrated with a mock infected BHK-21 as negative control, and samples were read at wavelength of 530 nm.

2.9. Fluorescence microscopy

The kinetics of GFP expression was evaluated by infecting BHK-21 cells with SFV-GFP (MOI 10) and incubation at 37 °C in a MIU-IBS CO_2 chamber coupled to an IX-81 fluorescence microscope (Olympus, Tokyo, Japan). Photomicrographs were taken automatically

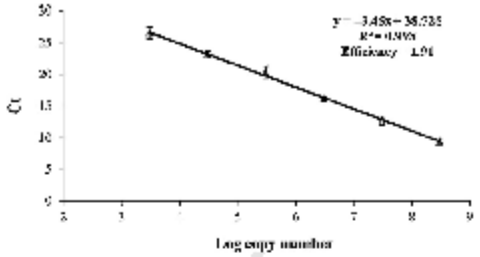

Fig. 1. qRT-PCR standard curve for the titration of SFV. Four qRT-PCR standard curves were obtained in parallel from six 10-fold dilutions of a reference DNA. Mean values of cycle tresholds (Ct) corresponding to each logarithm of standard copy number were plotted. Equation of regression line shows the slope (−3.45) used for calculation of amplification efficiency as indicated above (1.91) and the correlation coefficient R^2 (0.998). Error bars show SD.

from the same observation field at several time points after infection using the OV100 *in vivo* imaging system (Olympus, Tokyo, Japan).

2.10. Statistical analysis

The ANOVA test with a confidence interval of 95% ($p < 0.05$) was used for the RVGP and RVGP mRNA expression studies.

3. Results

The initial steps for standardizing the best conditions for analysis included the determination of the following parameters: amount of sample for RNA extraction, DNase treatment efficacy, primer concentration, cDNA sample quantity, and qPCR amplification cycle. A qRT-PCR standard curve for SFV RNA titration was then established after four amplifications to confirm the reproducibility between different runs and to calculate the average efficiency of amplification (Fig. 1). The standard curve showed the basic requirements necessary for qRT-PCR, namely, the use of at least five dilutions of standard and a slope of standard curve preferably between −3.3 and −3.8 and R^2 value of 0.99. The reproducibility of qRT-PCR was accessed by the amplification of a single cDNA sample obtained from an SFV pool, in nine replicates, in each one of two independent PCR runs. The average standard deviations were 0.23 ± 0.06 Ct interassays and 0.10 ± 0.06 Ct intra-assays. These data indicated that the standardized method was reproducible and the assay suitable for analyzing the amount of SFV RNA in intended samples. To prove that the proposed method actually applies to all SFV constructs, three separate samples of each different SFV stock (SFV-Mta-1, SFV-Ala-80, SFV-20A2, SFV-GFP, and SFV-RVGP) were titered. All viruses were efficiently amplified, with an average accumulated coefficient of variation (CV) of 15.1% (*i.e.* for the whole process of RNA extraction, DNase treatment, and qRT-PCR). Virus titers ranged from 3.2×10^7 VP/mL to 8.3×10^8 VP/mL, a difference of approximately 26 times between viral lots obtained by the same molecular biology and transfection procedures (Table 1).

To demonstrate the correlation between the amount of viral RNA used for cell infection and the amount of recombinant protein produced, BHK-21 cells were infected with different amounts of a single lot of SFV-RVGP and then the mRNA accumulation was measured; the RVGP produced is shown in Fig. 2A and B shows the cell growth kinetics. Infections at MOIs of 0.15, 1.5 or 15 SFV RNA/cell produced similar profiles of RVGP mRNA exponential accumulation into cells, leading to maximum quantities statistically different between 12 h and 24 h. RVGP accumulation was proportional to RVGP mRNA levels and reached the highest

UNCORRECTED PROOF

Please cite this article in press as: Puglia, A.L.P., et al., Quantitative RT-PCR for titration of replication-defective recombinant Semliki Forest virus. J. Virol. Methods (2013), http://dx.doi.org/10.1016/j.jviromet.2013.07.058

Table 1
qRT-PCR titration of different recombinant SFV.

Virus	Viral titer (VP/mL)	Standard deviation	CV (%)
SFV-Mta-1	6.31×10^8	5.6×10^7	9.0
SFV-Ala-80	8.20×10^8	1.4×10^8	17.6
SFV-20A2	0.32×10^8	6.2×10^6	19.3
SFV-GFP	1.45×10^8	2.2×10^7	15.2
SFV-RVGP	8.30×10^8	1.2×10^8	14.4

SFV-RVGP, rabies virus glycoprotein; SFV-GFP, green fluorescent protein; SFV-Mta-1, melatonin A1 receptor; SFV-Ala-80, modified adenosine receptor and SFV-20A2, adenosine receptor A2A. CV, coefficient of variation. Data represent the mean value of three independent assays.

concentrations at 30 h post-infection. After 30 h the amounts of transcript and RVGP decreased, mainly in cells infected with MOI 15 (Fig. 2A). At this time, viable cell concentration started to increase due to the multiplication of uninfected cells (Fig. 2B). These data also showed that when less than MOI 15 was used for infection, many cells were not infected and continued to divide, which was evident mainly after 24 h post-infection. Surprisingly, a large number of BHK-21 cells infected with an MOI 0.15 showed high cytotoxicity despite low RVGP expression levels, reaching 24 h of infection with only 59.7% of initial culture viability, while the cultures infected with MOI 1.5 and 15 presented viabilities of 51.8% and 29.7%, respectively.

In order to show further the correlation of qRT-PCR titrated virus input and the amount of RVGP produced in infected cells, aliquots of a single lot of SFV-RVGP were subjected to different temperature treatments and then qRT-PCR titrated in five replicates (mean CV = 15%). Subsequently, temperature-treated virus aliquots were

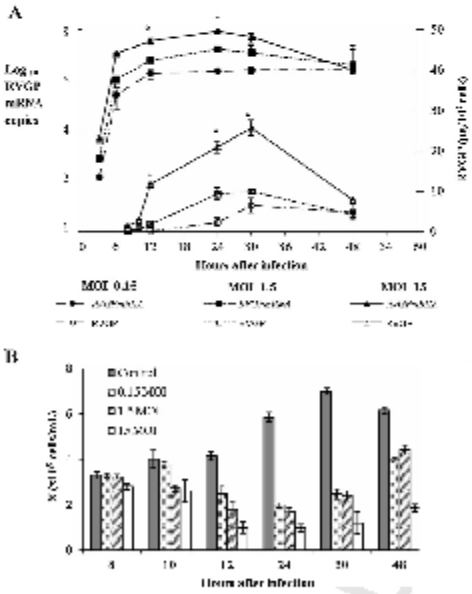

Fig. 2. Kinetics of RVGP mRNA copy number, RVGP expression, and growth in cultures of BHK-21 infected with different MOI (0.15, 1.5, and 15) of SFV-RVGP. RVGP mRNA was determined by qRT-PCR in 90 ng of total RNA and expressed in Log_{10} copy number; RVGP was determined by ELISA and expressed as µg of RVGP/10^6 cells (A); viable cell concentration was determined by cell counting in a hemocytometer by a trypan exclusion method. X, cells/mL × 10^6 (2B). *Statistically different from other values ($p < 0.05$).

Table 2
Effect of temperature treatment on SFV-RVGP inactivation. SFV-RVGP titration by qRT-PCR, and RVGP synthesis in infected BHK-21 cells.

SFV-RVGP inactivation			SFV-RVGP infection
Incubation	Titer (VP/mL)	Titer decrease (%)	RVGP (ng/mL)
24 °C/1 h	8.12×10^8	2.2	265.3 ± 25.1
24 °C/3 h	7.66×10^8	7.7	260.8 ± 14.6
37 °C/1 h	3.61×10^8	56.5	241.3 ± 22.2
37 °C/3 h	1.45×10^8	82.5	244.4 ± 15.9
−20 °C (stock)	8.30×10^8	–	302.1 ± 9.6

Identical SFV-RVGP samples were incubated at different temperatures for different times and then submitted to qRT-PCR titration, and used for BHK-21 infection (MOI 10) in three replicates. Virus inactivation is expressed in % related to the viral stock at −20 °C. RVGP synthesis in the different groups ($n = 3$) was measured by ELISA and was considered statistically equivalent ($p = 0.015$).

used for infection of BHK-21 cells at MOI 10, and RVGP production was measured (Table 2). The results show that the incubation of virus suspensions at temperatures of 25 °C or 37 °C, for 1 h or 3 h, led to the partial SFV RNA degradation since virus titers decreased as compared to virus stock maintained at −20 °C. The treatment at 37 °C for 3 h, especially, resulted in a significant loss of viral titer (82.4%). In comparing RVGP production among the cultures infected with an MOI 10 of the temperature-treated SFV particles, results were very similar (standard deviation [SD] = 11.87 ng/mL; CV = 4.69%), demonstrating a correlation between the amount of SFV RNA used for infection and the RVGP expression, which reinforces the applicability of qRT-PCR for titration of SFV constructs. Cultures infected with SFV stocked at −20 °C presented RVGP values 14–20% higher than temperature-treated cultures, raising variation values (SD = 24.26 ng/mL; CV = 9.23%).

Finally, the qRT-PCR method was used for the titration of different lots of SFV-GFP, which were used to infect BHK-21 cells with different MOIs. Infected cells expressed the GFP and were analyzed by fluorescence microscopy or flow cytometry (Fig. 3). Fluorescence microscopy analysis was used for defining the best time after infection for measuring the amount of infected cells in a kinetic study of GFP expression after BHK-21 infection with SFV-GFP with MOI 10 (Fig. 3A). Photomicrographs show the first signs of GPF expression at 1 h of infection. Increased amounts of fluorescent cells were observed until 24 h of infection, so this time point was chosen for analysis of GFP expression after infecting cells with different MOIs (Fig. 3B). The results show that an increase in the MOI corresponded to an increase, although not proportionally, in the percent of infected cells. Most importantly, when three different SFV-GFP lots were used with the same MOIs, similar amounts of cells were shown to express GFP, as indicated by the low SD observed in the assays. From the equation on the data graph, the predicted MOI for attaining 100% of infected cells would be 22.9.

4. Discussion

The SFV expression system has been used widely for recombinant protein expression in mammalian cells, markedly for membrane proteins (Hassaine et al., 2006). This system is also a promising vector for studies of immunization, cancer therapy (Riezebos-Brilman et al., 2006), and for neuroscience investigations (Lundstrom et al., 2001). The application of an qRT-PCR method for easy and reliable recombinant SFV titration is suggested. First, a standard curve was established based on the linearized SFV expression plasmid, and its characteristics were evaluated, which corresponded to the basic requirements needed to validate the qRT-PCR (Nolan et al., 2006). The amplification of different SFV constructs confirmed that the standardized method is applicable to any SFV with a conserved *nsp1* gene in the non-structural polyprotein region. Furthermore, the large difference in viral titers between

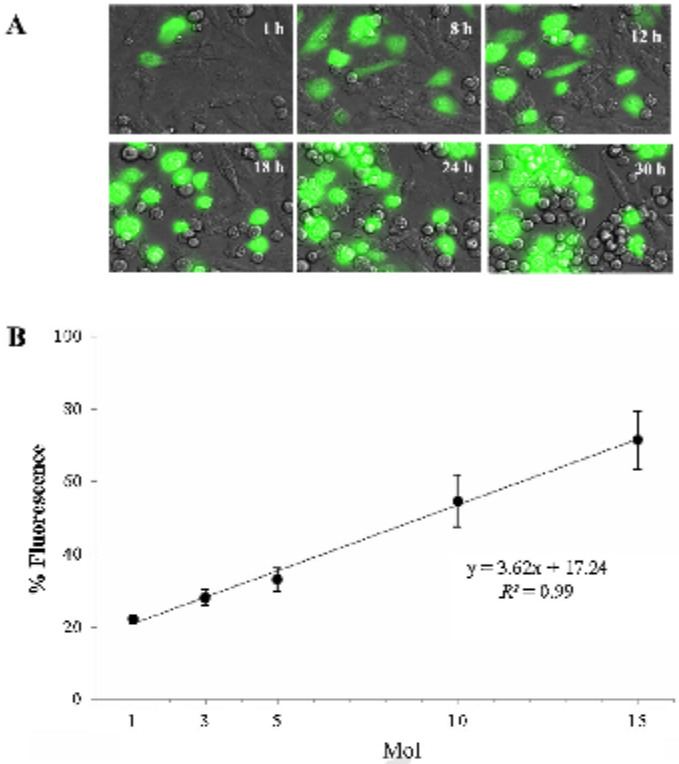

Fig. 3. Correlation between MOI and infection of BHK-21 cells with SFV-GFP. Microphotographs of the same observation field were taken at several time points for the study of GFP expression kinetics on SFV-GFP (MOI 10) infected BHK-21 cells. Amounts of infected cells increased until 24 h after infection (400×) (A). Three lots of SFV-GFP were used for BHK-21 infection with different MOI for 24 h. Amounts of fluorescent cells were determined by flow cytometry. Data show mean fluorescence (●). Error bars show SD. Fluorescence CV were 5.7%, 7.5%, 9.6%, 13.1%, and 11.4%, for MOIs 1, 3, 5, 10, and 15, respectively (B).

these constructions showed that even if the same steps are followed for producing recombinant SFV particles, a broad range of viral titers can be obtained after completion of all processes of molecular biology, transfection, cultivation of cells, and virus harvesting. The qRT-PCR method is able to determine the virus titer on the interval between 600 and 60 million copies of SFV RNA per sample, in one reaction in a few hours. This is an advantage if compared to quantitation by immunofluorescence, which is not sensitive enough and requires performing several virus dilutions, cell cultivation, antibody labeling, and a few days to complete. In addition, large stocks of SFV, even stored under the best conditions, are subjected to potency loss due to the labile nature of RNA. When different aliquots of the same batch of SFV-RVGP were treated at different temperatures to promote partial degradation of the SFV RNA, the standardized qRT-PCR titration method was able to measure with accuracy the extent of degradation. When the temperature-treated viruses were used for BHK-21 infection with the same MOI, very similar amounts of RVGP were produced, demonstrating that there was a good correlation between the amount of SFV-containing preserved RNA used for infection and the RVGP expression. The difference between the amounts of RVGP produced by cultures infected with freezer stock SFV-RVGP and temperature-treated stock, although not statistically significant, may represent the effect of virus degradation due to an additional freeze-thaw step of SFV particles which were frozen after temperature treatment while qRT-PCR titration was performed. Therefore, it is important to have aliquots of an SFV stock available for titration, as repeated freeze–thaw cycles can interfere with the determination of the correct virus titer and MOI. Taking this into consideration, virus samples may be titrated accurately before use, allowing a precise and reliable calculation of the amount of SFV particles under optimal conditions. This finding is important because it demonstrates that the degradation of a viral batch can be measured effectively. It is different from the titration of DNA virus vectors, whose degradation sometimes are not apparent by qPCR analysis because DNA is more stable than RNA and can remain in suspension, resulting in overestimation of viral titer (Hitchman et al., 2007).

The reproducibility of this method was evaluated by assays using SFV-GFP. Three different SFV-GFP batches were titrated by qRT-PCR, showing very different amounts of SFV RNA. When they were used for infecting cells with the same MOI, the rates of fluorescent cells were very similar. Therefore, with the qRT-PCR titration approach, the titer variability between SFV batches can be well-identified by evaluating the number of active virus particles. qRT-PCR virus titers can then be accurately used to calculate the virus input based on the desired MOI, obtaining reproducible results. Finally, when an SFV-RVGP batch was titrated based on the SFV RNA content and then used for infection in three log different

MOIs, the amount of virus used was shown to be proportional to the amount of RVGP mRNA produced by cells, and consequently, proportional to RVGP production.

5. Conclusion

In conclusion, SFV titers determined by qRT-PCR can be accurately used to calculate the virus input based on the desired MOI, obtaining reproducible results. Also, qRT-PCR methods targeting viral RNA of non-structural proteins, as the method established here, can be accurate and reliable tools for the titration of any replication-defective viral vector.

Conflict of interest

The authors declare no conflict of interest.

Q3 Uncited references

Lundstrom, 2003 and Strauss and Strauss, 1994.

Acknowledgements

We thank Dr. Jorge Mário da Costa Ferreira Jr., Laboratório de Imunoquímica, Instituto Butantan, São Paulo, SP, Brazil, for flow cytometry analysis. This work was financially supported by grants from FAPESP (2010/08742-8 and 2011/15269-0), CNPq and Butantan Foundation. C.A. Pereira is recipient of a CNPq 1A senior fellowship.

References

Astray, R.M., Augusto, E.F., Yokomizo, A.Y., Pereira, C.A., 2008. Analytical approach for the extraction of recombinant membrane viral glycoprotein from stably transfected *Drosophila melanogaster* cells. Biotechnology Journal 3, 98–103.
Benmaamar, R., Astray, R.M., Wagner, R., Pereira, C.A., 2009. High-level expression of rabies virus glycoprotein with the RNA-based Semliki Forest virus expression vector. Journal of Biotechnology 139, 283–290.
Berglund, P., Sjöberg, M., Garoff, H., Atkins, G.J., Sheahan, B.J., Liljeström, P., 1993. Semliki Forest virus expression system: production of conditionally infectious recombinant particles. Biotechnology 11, 916–920.
Hassaine, G., Wagner, R., Kempf, J., Cherouati, N., Hassaine, N., Prual, C., André, N., Reinhart, C., Pattus, F., Lundstrom, K., 2006. Semliki Forest virus vectors for overexpression of 101 G protein-coupled receptors in mammalian host cells. Protein Expression and Purification 45, 343–351.
Hitchman, R.B., Siaterli, E.A., Nixon, C.P., King, L.A., 2007. Quantitative real-time PCR for rapid and accurate titration of recombinant baculovirus particles. Biotechnology and Bioengineering 96, 810–814.
Hubby, B., Talarico, T., Maughan, M., Reap, E.A., Berglund, P., Kamrud, K.I., Copp, L., Lewis, W., Cecil, C., Norberg, P., Wagner, J., Watson, A., Negri, S., Burnett, B.K., Graham, A., Smith, J.F., Chulay, J.D., 2007. Development and preclinical evaluation of an alphavirus replicon vaccine for influenza. Vaccine 25, 8180–8189.
Karlsson, G.B., Liljestrom, P., 2003. Live viral vectors – Semliki Forest virus. In: Robinson, A., Hudson, M., Cranage, M.P. (Eds.), Vaccine Protocols. Humana press, Totowa NJ, pp. 69–82.
Klimpi, A.H., Vaart, E., Lansinki, P.O., Withoff, S., Vries, E.G.E., Scherphof, G.L., Wilschut, J., Daemen, T., 2001. Activation of peritoneal cells upon in vivo transfection with a recombinant alphavirus expressing GM-CSF. Gene Therapy 8, 300–307.
Liljeström, P., Garoff, H., 1991. A new generation of animal cell expression vectors based on the Semliki Forest virus replicon. Biotechnology (NY) 9, 1356–1361.
Liljestrom, P., Lusa, S., Huylebroeck, D., Garoff, H., 1991. In vitro mutagenesis of a full-length cDNA clone of Semliki Forest virus: the small molecular-weight membrane protein modulates virus release. Journal of Virology 65, 4107–4113.
Lo, H.R., Chao, Y.C., 2004. Rapid titre determination of baculovirus by quantitative real-time polymerase chain reaction. Biotechnology Progress 20, 354–360.
Lundstrom, K., Schweitzer, C., Rotmann, D., Hermann, D., Schneider, E.M., Ehrengruber, M.U., 2001. Semliki Forest virus vectors: efficient vehicles for in vitro and in vivo gene delivery. FEBS Letters 504, 99–103.
Lundstrom, K., 2003. Semliki Forest virus vectors for rapid and high-level expression of integral membrane proteins. Biochimica et Biophysica Acta 1610, 90–96.
Lundstrom, K., 2012. Determination of alphaviral titers. Cold Spring Harbor Protocols 2012 (7), 835–837.
Morsy El-Senousy, W., Guix, S., Abid, I., Pintó, R.M., Bosch, A., 2007. Removal of astrovirus from water and sewage treatment plants, evaluated by a competitive reverse transcription-PCR. Applied and Environment Microbiology 73, 164–167.
Ni, B., Wenda, G., Zhu, B., Lin, Z., Jia, Z., Zhou, W., Zhao, J., Wang, L., Wu, Y., 2005. Induction of specific human primary immune responses to a Semliki Forest virus-based tumor vaccine in a Trimera mouse model. Cancer Immunology, Immunotherapy 54, 489–498.
Nolan, T., Hands, R.E., Bustin, S.A., 2006. Quantitation of mRNA using real-time RT-PCR. Nature Protocols 3, 1559–1582.
Pfaffl, M.W., 2001. A new mathematical model for relative quantitation in real-time RT–PCR. Nucleic Acids Research 29, 2002–2007.
Perrin., P., Lafon, M., Sureau, P., 1996. Enzyme linked immuno-sorbent assay (ELISA) for the determination of glycoprotein content of rabies vaccines. In: Meslin, F.X., Kaplan, M.M., Koprowaski, H. (Eds.), Laboratory Techniques in Rabies. WHO, Geneva, pp. 383–388.
Rayner, J.O., Dryga, S.A., Kamrud, K.I., 2002. Alphavirus vectors and vaccination. Reviews in Medical Virology 12, 279–296.
Riezebos-Brilman, A., de Mare, A., Bungener, L., Huckriede, A., Wilschut, J., Daemen, T., 2006. Recombinant alphaviruses as vectors for anti-tumour and anti-microbial immunotherapy. Journal of Clinical Virology 35, 233–243.
Rohr, U.P., Wulf, M.A., Stahn, S., Steidl, U., Haas, R., Kronenwett, R., 2002. Fast and reliable titration of recombinant adeno-associated virus type-2 using quantitative real-time PCR. Journal of Virological Methods 106, 81–88.
Schlesinger, S., Schlesinger, M.J., 1991. Replication of Togaviridae and Flaviviridae. In: Fields, B.N., Knipe, D.M., Chanock, R.M., Melnick, J.L., Martin, S.H., Monath, T.P., Roizman, B. (Eds.), Fundamental Virology. Raven Press, New York, pp. 453–467.
Smerdou, C., Liljeström, P., 1999. Two-helper RNA system for production of recombinant Semliki Forest virus particles. Journal of Virology 73, 1092–1098.
Strauss, J.H., Strauss, E.G., 1994. The alphaviruses: gene expression, replication and evolution. Microbiological Reviews 58, 491–562.
Wahlfors, J., Morgan, R.A., 2002. Viral vectors for gene therapy: methods and protocols. In: Machida, C.A. (Ed.), Methods in Molecular Medicine. Humana Press, Totowa, NJ, pp. 564–678.
Zhang, X., Wang, X., Zhou, G., 2008. A one-step real time RT-PCR assay for quantifying rice stripe virus in rice and in the small brown planthopper (*Laodelphax striatellus* Fallen). Journal of Virological Methods 151, 181–187.
Zhao, X., Bailey, M.R., Emery, W.R., Lambooy, P.K., Chen, D., 2007. Evaluation of viral removal by nanofiltration using real-time quantitative polymerase chain reaction. Biotechnology and Applied Biochemistry 47, 97–104.
Zusinaite, E., Tints, K., Kiiver, K., Spuul, P., Karo-Astover, L., Merits, A., Sarand, I., 2007. Mutations at the palmitoylation site of non-structural protein nsP1 of Semliki Forest virus attenuate virus replication and cause accumulation of compensatory mutations. Journal of General Virology 88, 1977–1985.

UNCORRECTED PROOF

Please cite this article in press as: Puglia, A.L.P., et al., Quantitative RT-PCR for titration of replication-defective recombinant Semliki Forest virus. J. Virol. Methods (2013), http://dx.doi.org/10.1016/j.jviromet.2013.07.058

Asian Journal of Biotechnology 5 (1): 1-20, 2013
ISSN 1996-0700 / DOI: 10.3923/ajbkr.2013.1.20
© 2013 Knowledgia Review, Malaysia

Using Statistical Tools for Improving Bioprocesses

[1]Eutimio Gustavo Fernández Núñez, [2]Rodolfo Valdés Veliz, [1]Bruno Labate Vale da Costa, [3]Alexandre Gonçalves de Rezende and [1]Aldo Tonso
[1]Departamento de Engenharia Química, Universidade de São Paulo, São Paulo, SP, Brazil
[2]Monoclonal Antibody Department, Center for Genetic Engineering and Biotechnology (CIGB), Ave. 31 / 158 and 190, Cuabanacan, Playa, P.O. Box 6162, CP 10600, Havana, Cuba
[3]Laboratório de Imunologia Viral, Instituto Butantan São Paulo, SP, Brazil

Corresponding Author: Eutimio Gustavo Fernández Núñez, Departamento de Engenharia Química, Universidade de São Paulo, Av. Prof. Luciano Gualberto, trav. 3, 380 Butantã, 05508-900, São Paulo, SP, Brazil Tel: (55)-11-3091 2282

ABSTRACT

In this review most of statistical tools currently applied in the bioprocess area were discussed and classified. The main three categories were: fair comparison of results, mathematical modeling for little studied systems and taking advantage of large volume of data for enhance robustness and efficiency. For each statistical technique, an example from literature was commented to demonstrate its utility in bioprocess problems. Besides, others statistical tools without a wide application, at the moment, in bioprocess were also discussed, taking into consideration the near future use of them. As a conclusion, a chart was constructed for guiding researchers to select the correct statistical technique according to the specific bioprocess problem.

Key words: Artificial neural network, bioprocess, experimental design, multivariate methods

INTRODUCTION

Bioprocesses are currently used to produce a wide variety of chemicals from alcohols, organic compounds and amino acids, to antibiotics and therapeutically active recombinant proteins (Clementschitsch and Bayer, 2006). This kind of processes is characterized by the industrial application of biological pathways or reactions mediated by living cells of animal, plants and microorganisms or enzymes under controlled conditions for the biotransformation of raw material into products (Nair, 2008). Bioprocess technology is typically made up of three parts: upstream process, bioreactions and downstream processing (Nair, 2005).

In the upstream step or pretreatment, the raw material from biological or non-biological origin is first converted to a form suitable for processing. Subsequently, one or more bioreaction stages are performed. The biochemical reactors or bioreactors are the core of the bioreaction step. In this stage, the following operations are carried out: production of biomass, metabolize biosynthesis and biotransformation. Finally, the material produced in bioreactors must be further processed in the downstream section. Downstream processing consists of basically physical separations in order to purify and concentrate the product of interest (Jana, 2008).

Bioprocess goals are influenced by several parameters, being the definition of best values for them, an important and complex task for biochemical engineers. For economic reasons, large-scale established bioprocess should not be disturbed and any modification to any parameter may be not

considered (Najafpour, 2006). Thus, on lab-scale is performed an intensive experimental work for understanding and optimizing the individual operation units and the process as a whole, both novel and established bioprocesses (Najafpour, 2006; Dubey and Behera, 2011). At the same time a high amount of data is stored from bioprocesses on large-scale equipped with sophisticated control, data logging and archiving systems; these could be also used to improve them (Charaniya *et al.*, 2008).

The statistical tools have demonstrated that are useful to solve this task, decreasing time and resource. The aim of this review is to expose the principal statistical techniques with applications in bioprocesses through the examples extracted from literature as well as a philosophy of work without mathematical details in order to identified what statistical method should be used as the classification of the problem under study.

DEFINING KEY TERMS

The definitions of three key statistical terms (factors, levels and responses) are necessary to facilitate the readership understanding of this text, mainly for poor trained professionals in statistical tools. This is the first step of the stair for helping bioprocess researchers to choose by themselves with a minimal statistical knowledge, the right technique for their specific problem.

Factors correspond to the independent variables of the system which we are interested in knowing as they influence the process outputs. The levels are some values in the study range of factors, when factor is a numeric variable or different categories, in the case of qualitative variable. For instance, the pH and nitrogen source could be studied for improving the yield of a fermentative process. The range of interest for factor pH (6.0-8.0), a numeric variable, could be explored at three levels: 6.0, 7.0 and 8.0. On the other hand, for nitrogen source, a qualitative variable, nitrate and urea could be two levels for this factor.

Responses are the properties of the system that are being measured and they are modified as a consequence of changes in factor values. They are also defined as dependent variables. Retaking the previous example, yield would be the response in this study case.

PROBLEM DEFINITION

Once defined the basic statistical vocabulary, we have the primary elements to understand what kind of problem we need to resolve in statistical terms. This is the first question to answer in order to choose the right statistical tool in any scientific work and as a consequence in bioprocesses too. In general, problems in bioprocesses might be statistically classified in three categories:

- Fair comparison of results
- Mathematical modeling for little-studied systems or processes
- Take advantage of large volume of data for enhance robustness and efficiency

The first one is used to determine whether or not one or more factors can affect the system outcomes (responses). The main goal is to define in qualitative way the effects of variables and levels of them on responses of a well-know system (control) or among their own responses for non-established systems. In other words, as a result of this statistical problem are identified relationships of equality, superiority or inferiority among alternatives or treatments considered (Boos and Brownie, 1995).

Statistical modeling or design of experiment methodology for little-studied systems or processes is useful when a mathematical function which connects individual factors under study and their

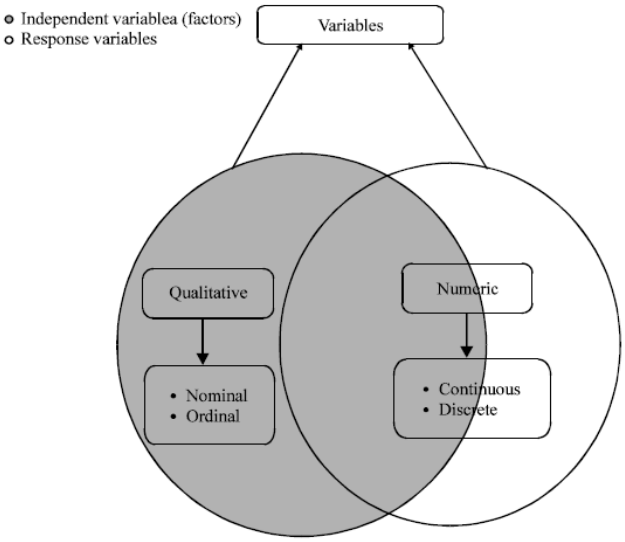

Fig. 1: Classification of variables and most frequently types of factors and response in bioprocesses

interactions with responses of the system, is desired. This is used for rapid variable screening, understanding and optimization of systems without phenomenological models associated. This general statistical tool has been boosted by Food and Drug Administration through Process Analytical Technology (PAT). PAT aims to enhance the necessary deeper understanding of the manufacturing bioprocess in the pharmaceutical field, with the purpose of adjusting manufacture online and eliminating delays in product release. However, the applications of PAT might be helpful in any other bioprocess application, beyond pharmaceutical industry (Mandenius and Brundin, 2008).

For first two types of problems, it is critical the definition of factor levels (values of independent variables) under study (Ryan, 2007). The correct definition of them can be performed by a previous revision of literature about the systems of interest or similar, through theoretical considerations or preliminary experiments. When this step is done correctly, time and resources are saved and properly results can be achieved.

Another important moment (for problems type 1 and 2) when researchers are programming their experimental work in bioprocess on lab-scale is the definition of variable types included in the system under study. The type of variable defines the appropriated statistical design and data analysis technique. Variable classification is divided in two large groups: qualitative and numeric variables (Mendenhall *et al.*, 2009). Most of the problems in bioprocess include numeric variables for process responses, either continuous or discrete (e.g., yield, productivity and variables related with final product quality) and for independent variables, qualitative factors are also included, for instance: types of carbon and nitrogen sources in culture medium (Fig. 1).

Nowadays, bioprocesses are well automated and they have a comprehensive data collection and archiving. These archives represent an enormous opportunity for using multivariate methods and artificial neural networks in order to enhance the robustness and efficiency of manufacturing processes (Charaniya *et al.*, 2008, 2010; Albert and Kinley, 2001).

FAIR COMPARISON OF RESULTS

This kind of statistical problem could be classified according of the number of factors under consideration that could have impact in outcome parameter(s), their number corresponding levels and if levels (samples) are independent or paired. Independent samples belong to different populations; no connection exists among experimental units. On the other hand, paired samples are samples which each data point in the first sample is uniquely matched to a data point in the subsequent samples (Gerstman, 2008).

When one independent variable is being investigated, the proper experimental design to detect difference among levels is completely randomized (one-way) design (Michelson and Schofield, 1996). As a rule the sample size (N) for assessing each level or treatment is the same and N is greater or equal to three. Larger sample size is better but this will depend on cost criteria and time. These problems with one variable are subdivided according to number of levels, because they define statistical technique to analyze experimental data. If only two levels are assessed two-sample t-test or its equivalent non-parametric Mann-Whitney test could be used. Problems with three or more levels are solved by one-way Analysis of Variance (ANOVA) or the Kruskal-Wallis non-parametric test (Michelson and Schofield, 1996; Aleman *et al.*, 2007). In bioprocess experimentation, parametric test are more frequently used (Table 1). If statistical differences are detected (dispersion caused by levels is higher than dispersion caused by experimental errors or noise) the other step is for determining which levels or treatments differ from each other. For this purpose a multiple comparison procedure (multiple range tests) must be applied. Among the existing methods are: least significant difference test, Bonferroni t-statistics, Tukey Honest Significant Difference (HSD) and Duncan's multiple range test (Hinkelmann and Kempthorne, 2008). Tukey HSD test is one of the most conservative methods and produces more reliable results (Compton, 2011); this makes it one of the most used multiple range test in bioprocesses. For paired samples, paired t-test and two-way ANOVA are useful to perform fair comparisons with two and three or more levels, considering only one variable as (Rao, 2007).

In problems which are influenced by two or three factors with several levels each one, randomized complete blocks and Latin squares and related designs are used (Kowalski and Montgomery, 2011). In principle, these experimental strategies assume that interactions among variables are nonexistent. The data analysis using these statistical tools could be carried out by two, three-way ANOVA (Henderson, 2011; Taneja, 2009) (Table 1). If any factor significantly modified the response under study, a multiple range test must be performed to detect differences among levels of this factor.

Over the course of last decade, several papers in the bioprocess field have used any of these statistical techniques for fair comparison of results. For instance, a completely randomized design was performed to define the effects of three levels of one independent variable, tween 80

Table 1: Main experimental designs for fair comparison of results used in bioprocess experimentation

Experimental design	Parametric methods for data analysis	Type of sample	No. of factors	No. of levels
Completely randomized	t-student test	Independent	1	2
	Paired t-test	Paired		
	One-way ANOVA	Independent		3 or more
	Two-way ANOVA	Paired		
Randomized complete blocks	Two-way ANOVA	Independent	2	2 or more
Latin squares	Three-way ANOVA	Independent	m	n

Table 2: Latin square designs (3 factors and 3 levels) used to optimize medium composition in RB 5 decolorization by *Funalia trogii*

	X_1	X_2	X_3
Y_1	Z_1 (1)	Z_2 (2)	Z_3 (3)
Y_2	Z_3 (4)	Z_1 (5)	Z_2 (6)
Y_3	Z_2 (7)	Z_3 (8)	Z_1 (9)

X, Y and Z are independent variables (factors), for first experiment: Carbon, nitrogen and phosphate sources and for the second one: Concentration of each selected ingredient from the first Latin square, RRB 5: Reactive black 5

percentage (0, 0.1, 1.0%) on growth, lipid accumulation and fatty acid composition in *Thraustochytrium aureum* (response variables). Sample size for each assessed tween 80 percentage was 3. Data were statistically compared using one-way analysis of variance (ANOVA) and significant differences were identified by Tukey's test (Taoka *et al.*, 2011).

As another example, a completely randomized block design was utilized to determine effects of two factors in pulse ultraviolet light technology (distance from the central axis of the lamp and exposition time) on major allergens mitigation. Both variables were studied at 3 levels each, 10.8, 14.6 and 18.2 cm and 2, 4 and 6 min, respectively. Comparison of level for each variable was done by the Tukey's test. It was demonstrated that reduction of the protein band intensity for peanut allergens increased with treatment time but decreased with increased distance from the pulse ultraviolet light lamp (Yang *et al.*, 2011).

In one of the papers where Latin square method was used, two applications were performed in order to define the better medium composition for decolorizing of reactive black 5 (RB 5), a wastewater contaminant from textile industry, by *Funalia trogii*. Firstly, it was carried out a Latin square design to optimize three media components (carbon, nitrogen and phosphate source) at three levels of them (carbon: fructose, glycerol, starch; nitrogen: ammonium tartrate, yeast extract, peptone and phosphate: KH_2PO_4, $KHPO_4$, Na_2HPO_4). The concentration of each element resource was kept constant. Secondly, another Latin square design was performed to optimize concentrations of selected medium ingredients from first experimental plan. The variables were fructose, peptone and Na_2HPO_4 concentrations at three levels each. The response variable in both cases was decolorization percentage of RB 5. Nine combinations in both designs were done (Table 2). Authors did not consider interactions among components for reducing the experimental work and avoid inaccurate results, this justify Latin square design choice. No statistical data analysis technique was performed to define better ingredient sources and their concentrations; Latin square design was just employed for programming experimentation (Park *et al.*, 2007).

STATISTICAL MODELING OF LITTLE KNOWN SYSTEMS

When we are interested in getting a rapid mathematical modeling of little known systems in bioprocess field in order to screen or optimize factors which are suspected to be important, design of experiment methodology (DoE) have been extensively used. DoE is a collection of predetermined setting of the process variables of interest which provides an efficient procedure for programming experiments (Lee and Gilmore, 2006). This general approach after experimentation allows definition of mathematical relationships between input (factors) and output (response) variables of a given system. Besides, with DoE the effects of input variables interactions can be studied as considered factors can change simultaneously and experimental biases are avoided (Mandenius and Brundin, 2008).

As a rule when it is trying to optimize a new system, firstly it is carried out experimental designs for factors screening and after that it is performed experimental plans for optimizing the most significant factors (Xu *et al.*, 2010; Arutchelvi *et al.*, 2011). This strategy reduces the required number of experiments and as consequence experimentation cost and time. Below, it will be addressed the experimental designs for screening and optimizing process variables in theory and their applications in bioprocesses.

SCREENING

Among the most used experimental designs for screening process variables in bioprocesses are: two-level factorial, fractional factorial and Plackett-Burman designs. The first design allows for the estimation of all factor effects and all interaction effects among factors. The application of two-level factorial design is limited for high number of independent variables because the experimentation could require a considerable time and financial resources (Sower, 2011). The number of experimental runs is defined by all combinations among factor levels (2^k), where k is the number of factors, 2 is the number of levels. Generally, this experimental plan is used up to 5 independent variables, where the runs number associated with this design is 32 (2^5) (Eriksson *et al.*, 2008). The response is described as a polynomial function which is defined according to the selected design and the exploration of experimental domain is peripheral (Fig. 2).

Both experimental designs for screening and optimizing variables, the actual values of levels are usually changed to a scale from -1 (minimum value) to 1 (maximum value), in order to eliminate effects of different variable ranges; facilitate the data analysis and inferences (Mills *et al.*, 2010). Besides, repetitions of experimental points included in statistical design or in the central point of the experimental domain are performed to evaluate the statistical significance of model and parameters (Brue and Howes, 2005; Santos *et al.*, 2011).

When the number of factor to asses is large, two-level fractional factorial or Plackett-Burman designs are applied. Fractional factorial design is a fraction of an original two-level full factorial design for a defined number of factors. The reduction of experimental runs with these experimental plans sacrifice the non-confused effects determination of individual factors and their interactions. Therefore, they are applied when it is assumed that some interactions between factors are not significant. Two-level fractional factorial designs are classified in resolution III, IV or V, according

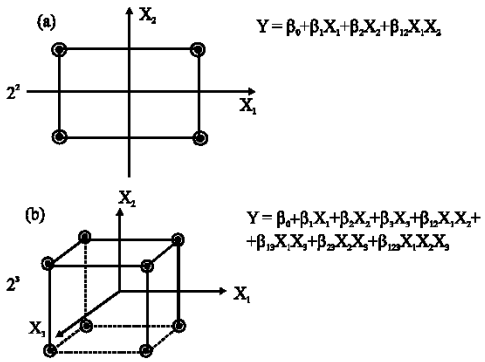

Fig. 2(a-b): Experimental domains and runs distribution for two-level full factorial design as well as their corresponding polynomial model with (a) Two factors and (b) Three factors

Table 3: Resolutions of two-level fractional factorial design and their respective grades of confusion among interactions

Resolution	Aliasing of interactions
III	Evaluate the main effects, which are confounded with two-factor interaction
IV	Evaluate the main effects and confounded two-factor interactions (there is aliasing of the two-factor interactions)
V	Evaluate the main effects and two-factor interactions independently (there is aliasing of the two-factor with three-factor interactions)

the confusion among interactions (Table 3) (Breyfogle, 1992). In general fractional factorial designs with resolution V are widely used because rarely interactions of three-factors have significant influence on system responses.

Plackett-Burman design is another experimental plan where factors are studied at two-levels. It is also useful for screening factors, when the number of them is fairly large. This experimental strategy shows resolution III. The number of experiment is a multiple of four. Hence, designs exist for 4, 8, 12, 16, 20 and 24 etc., experiments. The number of experiments exceeds the number of factors, k, by one. Standard Plackett-Burman designs exist for 7, 11, 15, 19 and 25 factors. In cases where the number of experimental factors is less than number defined for standard design (a multiple of 4 minus 1), the final factors are dummy ones (Brereton, 2003).

After experimentation for screening variables and also for optimizing (next section), polynomial models are adjusted by matrix calculations. In order to demonstrate and improve the quality of statistical model, four tests are mainly performed:

- Goodness of fit
- Lack of fit
- Statistical significance of model coefficients
- Residues analysis

Goodness of fit test describes how well current runs can be reproduced in the proposed polynomial model. Lack of fit allows for determining whether or not errors associated to model for experimental points not included in basic design are similar to experimental errors or noise (Onsekizoglu *et al.*, 2010). On the other hand, the significance of model coefficients is useful to identify the independent variables with real effects on responses, to reduce the polynomial equation and to facilitate the inferences about the system under study (Deming and Morgan, 1993). Finally, residues analysis should be performed to confirm no patterns as well as if they are normally distributed to ensure that residuals are randomly placed around the model (Harry *et al.*, 2011), otherwise a mathematical transformation response values could be necessary in order to improve model fit to experimental data.

Screening experimental designs are applied in bioprocess area as first step in two-stage methodology for optimizing culture media (ingredient concentrations), process variables (temperature, time, agitation, linear flow, etc.) or a combination of both. The other remarkable applicability of this type of experimental plans is to demonstrate process robustness or to validate process in the biopharmaceutical industry (Jakobsson *et al.*, 2005). In general, more than three factors are included in these two-level designs when they are used in bioreactions or downstream procedures.

As example: Plackett-Burman design was utilized during the first step for optimizing production of lipases from a newly isolated *Penicillium* sp. Six variables at two-levels were considered in 12 experiments, three repetition on the center of the experimental domain were added.

Independent variables were temperature (28-36), inoculums (25-125 ml L^{-1}), peptone (20-80 g L^{-1}), yeast extract (5-30 g L^{-1}), NaCl (5-30 g L^{-1}) and olive oil (10-30 g L^{-1}). The response variables were lipase activity after 48, 72 and 96 h of fermentation. Temperature, olive oil concentration and NaCl concentration, were the significant factors on lipase activity, with negative effects for first variables and positive for the last one. In optimization step, temperature was set at 28°C because previous results confirmed similar optimal temperatures. Olive oil and NaCl concentration were studied deeply in the optimization design according to physiological criteria (Wolski *et al.*, 2009).

Another example of screening experimental design was the application of a fraction factorial design (Resolution III) as a first stage to optimize culture media for production of phycobiliprotein by *Synechocystis* sp. PCC 6701. Seven factors (KNO_3, $NaNO_3$, $Na_2H_2PO_4$, Na_2HPO_4, $Ca(NO_3)_2$, FeEDTA, $MgSO_4$ concentrations) with two levels were studied. Addition two central point replicates were included to original design (8 runs in duplicates = 16 runs), 18 runs were performed. The response variable was specific growth rate. Nitrate and phosphate were identified as significant factors. The other factors were discarded for the optimization step (Hong and Lee, 2008).

SURFACE RESPONSE METHODOLOGY

Full factorial three-level, Central composite and Box-Behnken designs for symmetrical domains have been extensively used as surface response methods of choice in bioprocess. The central goal in these methods is to find the best combination of factors values in order to optimize the system response(s).

Full factorial three-level are used for investigating two or three factors. In the case of many factors the same problem as with a two-level design arises, the number of experiments becomes high. They can be represented in the same way as previous described for two-level designs, 3^k, k means number of factors and 3 is the number of levels (Otto, 2007; Fernandez-Nunez *et al.*, 2011). The number of experiment is 3^k. For instance, in problem with 3 factors, 27 experimental runs must be carried out (Fig. 3).

When high number of factors is required for system statistical modeling with optimizing purposes or the experimentation cost is elevated, central composite and Box-Behnken design should be used.

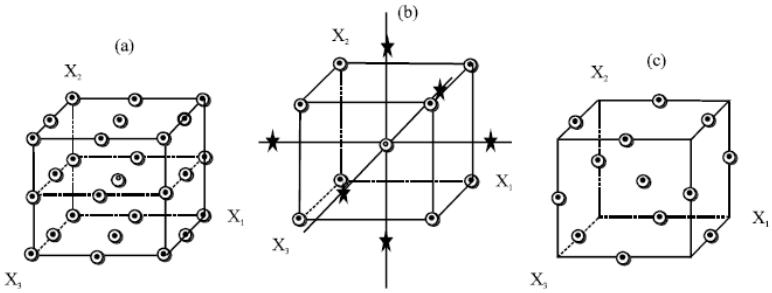

Fig. 3(a-c): Geometrical representations of experimental points arrange for (a) Full three-level, (b) Central composite and (c) Box-Behnken designs with three factors

Central composite design is generated from full factorial two-level design link to a star design. The number of run (n) is calculated by the following equation:

$$n = 2^k+2k+n_o$$

where, n_o is the number of runs in the geometrical center of the experimental domain. For three factors, the number of experiments is 15, when repetitions number of the central point is 1 (Fig. 3). Most of the composite central designs with applications in bioprocesses are circumscribe, the distance of the star points (α) from the center can be calculated by this equation: $\alpha = 2^{k/4}$ (Anderson and Whitcomb, 2004). The experimental disadvantage of this design is the position of star point outside the hypercube, as a consequence the number of levels is higher than 3 (Fig. 3). The alternative of solution for this drawback is the Box-Behnken design.

The experimental points in Box-Behnken experimental plan lie on a hypersphere equidistant from the center point. The total number of experiment is even lower than those required in central composite designs because need few factor combinations (Otto, 2007) (Fig. 3).

Quadratic polynomials are adjusted for data provided by these experimental plans, for this reason quadratic terms for each factor are included in equation describing response(s) (Anderson and Whitcomb, 2004). This allows the local maximum and minimum detection.

Several works using three levels factorial design for two or three factor in bioprocess have been published. As example a 3^2 full factorial design was conducted to locate the optimum concentrations of yeast extract (2.5-10 g L^{-1}) and peptone (2.5-10 g L^{-1}) for the maximum cell growth of *Bacillus fusiformis* CICC 20463, used to transform 4´-demethyl epipodophyllotoxin (DMEP) into 4´-demethyl epipodophyllic acid (DMEPA), at the same DMEP consumption and DMEPA accumulation were considered as response variables (y) too. Three y variables were modeled by quadratic polynomial, the number of experimental points was 10, one central point was added to 9 initial runs for a 3^2 design. Each model was statistically analyzed and non-significant coefficients were eliminated. As example: the DMEP consumption was defined by the following Eq. 1. Then, each combination for maximum cell growth, DMEP consumption and DMEPA accumulation were defined (Tang *et al.*, 2010):

$$Y_{DMEP} = 23.64X_1-1.83X^2_1 \quad (1)$$

where, Y_{DMEP} is the DMEP consumption response and X_1 is the yeast extract concentration.

Central composite designs are frequently used in bioprocess problems too. Exemplifying, this type of experimental plan was applied to model the purification of α-amylase from the cultivation of *Bacillus subtilis* in a polyethylene glycol-citrate aqueous two-phase system. The PEG3350, citrate and sodium chloride concentrations were selected as variables to evaluate partition coefficients of α-amylase, total protein, purification factor and α-amylase yield. Value of α for this problem (k = 3) was 1.68 ($2^{k/4} = 2^{3/4}$). The experimental plan was composted by 8 runs associated to the factorial design, 6 runs associated to the star points and 5 repetitions of the central point of the experimental domain. At the end of the work, the optimal values for three factors determined by the statistical models were confirmed experimentally (Zhi *et al.*, 2005). This is an important step when the results on small scales based on empiric models are going to be used on large-scale in order to decrease risks in scale-up decisions.

In general the Box-Behnken designs are suggested in bioprocess field when experiments are costly or there is not much time for a large number of experimental runs. For instance, Box-Behnken design was used to optimize the levels of four factors (maltose, beef extract, $MgSO_4$ concentrations and incubation time) for chitosanase production by *Bacillus* sp. RKY3 (Wee *et al.*, 2009).

MIXTURE DESIGN

Mixtures designs constitute a category within the experimental designs, specifically fitted to problems where factors are proportions or fractions (mass, volumetric and molar). They have found applications in different areas of knowledge. However, the number of papers with this statistical tool for optimizing pharmaceutical formulations is significant (Gabrielsson *et al.*, 2002). In bioprocess, mixture designs have been also utilized for optimizing proportion of components of culture media, mainly in bioremediation processes (Prakasham *et al.*, 2009) and they could be also utilized to seek best composition of liquid mixtures for metabolites extractions or chromatographic mobile phases in downstream steps. It is prudent to clarify that mixtures design cannot be applied for optimizing culture media if components are expressed in concentrations units, in these cases experimental designs with process variables (screening and surface response) are suitable.

The factors in this type of problems are not totally independent like those discussed for problems with process variables. Fractions (x_i) must sum to unity and then the effective number of variables is the total number minus 1 (Cornell, 2002). This has implications in the domains under investigations. The geometrical domains in mixture problem are different to those for process variable problem with the same number of factors, for this reason the experimental point arrange discussed in previous sections cannot be used in mixture problems. For instance, mixtures with three components are represented as equilateral triangle whereas a problem with three process variables defines a cube (Fig. 4) (Fernandez *et al.*, 2008a).

Problems with mixtures are divided in two main categories: without constrains and with constrains. The first one encompasses mixtures in which all components (factors) are studied in

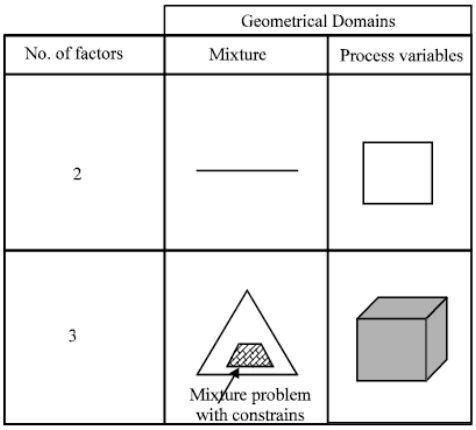

Fig. 4: Geometrical domains related to two or three factors for problems with mixture and process variable. Arrow indicates a mixture problem with constrains, describing no similar experimental area respect to original domain without constrains

0-1 range. They are defined by symmetric geometrical areas (Fig. 4). Nevertheless, mixtures with ingredients constrains ($a \leq x_i \leq b$; $a \neq 0$ or $b \neq 1$) could generate irregular experimental areas (Fig. 4), as a consequence different statistical design must be applied in each case. Simplex lattice designs and simplex centroid designs are utilized in problems without constrains whereas D-optimal designs are the experimental plans of choice for modeling response in mixtures studies with constrains describing irregular areas (Fernandez *et al.*, 2008a). When formulation with component constrains lead to an experimental area being analogous to original ($0 \leq x_i \leq 1$), simplex lattice and simplex centroid designs can be used.

The mathematical models for responses in mixtures could be linear, quadratic, special cubic and cubic. The linear models are usually employed for screening mixture ingredients and the others are used to find the best combination of factors which satisfy the response(s) goal (Cornell, 2002). The decision among quadratic, special cubic and cubic model is taken balancing the level of precision for describing response and the experimental time and cost.

In bioprocess, non-constrains problems have been the most discussed. As example, an augmented simplex-centroid design for three components was used to improve glutaminase production in solid-state fermentation by isolated *Bacillus* sp. RSP-GLU. Wheat bran, Bengal gram and Palm seed fiber were de ingredients under study and the response variable was glutaminase activity. A quadratic model described satisfactorily glutaminase activity. Two combinations of factors were identified in order to maximize glutaminase production, 100% of Bengal gram husk or a mixture of Bengal gram husk and wheat bran (66:34%) (Sathish *et al.*, 2008).

Sometime, bioprocess professional need to define a polynomial equation for describing a response as a function of ingredients proportions and process variables. In this case, crossed experimental design is recommended (Lee and Gilmore, 2006). On the other hand, there exist problems where a mixture inside another mixture should be optimized; in this situation crossed mixture design must be applied (Delaroza and Scarminio, 2008). Recently, the last statistical tool was used for improving a recombinant protein in continuous culture (Didier *et al.*, 2009).

In near future, mixture design could be more utilized in bioprocess because there are many challenges involving optimization of ingredient proportions like definition of culture media and composition of liquid phase in bioseparations.

UNIFORM DESIGN

Uniform designs were created by Fang at the end of 70's to solve an industrial problem where 6 factors with at least 12 levels each should be considered. Nevertheless, the experimental runs could not exceed 50 because of cost limitations. Using, the classical experimental designs for polynomial modeling of systems described in previous sections, the number of runs generated by these techniques would have been impossible for carrying out. Then, this problem was overcome using Uniform design with only 31 experiments and each factor with 31 levels (Liang *et al.*, 2001). This experimental plan produces uniform scattering of the design points over the experimental domain (Fang and Chan, 2006). If point distribution in screening and surface response experimental designs inside experiment domain is observed, it will be noticed that most of the points are placed on the periphery of experimental domain. Therefore, the sample to be experimented for generating inferences could be not representative. Classical experimental designs show uniform scattering of designs point in their dimensions but not in the geometrical area defined by factor and

their levels. One of the most important advantages of Uniform design over traditional experimental design is that, even when factors number and their corresponding levels are large, the experiment can be performed in a relatively small number of runs (Fang and Chan, 2006).

Most of experimental designs are based on model assumptions. However, experimental plans insensitive to this assumption are desired. In other words, changes in the underlying distribution or model should cause small change in the performance of the design (Liang *et al.*, 2001). Uniform designs do not have a mathematical model associated, thus it is particular suitable for studying systems with an unknown underlying model. Artificial neural networks and multiple linear regressions could be used to model non-linear and linear systems, respectively, after experimentation and data collection with uniform designs.

For programming experimentation (point arrange) in common problems by means of uniform design, softwares and tables (http://www.math.hkbu.edu.hk/UniformDesign/) are available (Sun *et al.*, 2010; Zhou *et al.*, 2011). The choice of particular experimental [U_n (q^s)] is defined by number of runs (n), number of factors (s) and number of levels (q). Both process and mixture variables can be studied through this kind of experimental design (Fang and Chan, 2006).

Uniform design is very attractive for statistical system modeling in bioprocess where the experimentation is very expensive. In general, it has been used for optimizing concentration of culture medium components and process variables related to bioreactions step (Hua and Xu, 2011; Wei *et al.*, 2009; Xu *et al.*, 2006).

As example: A uniform design was used to optimize medium composition in order to improve the ethanol tolerance of self-flocculating yeast. Seven component were studied at 6 levels each in experimental plan with 12 runs [U_{12} (7^6)]. The ingredients were vitamins (x base), $(NH_4)_2SO_4$ (g L^{-1}), K_2HPO_4 (g L^{-1}), $MgSO_4.7H_2O$ (g L^{-1}), $CaCl_2.2H_2O$ (g L^{-1}), $ZnSO_4.7H_2O$ (mg L^{-1}), $CoCl_2.6H_2O$ (mg L^{-1}) and the response variables were viability and ethanol concentration. The statistical model was adjusted by means a linear-regression method. The optimization of medium component led to 90.2% of cell viability which demonstrated noteworthy improvement of ethanol tolerance of the self-flocculating yeast (Xue *et al.*, 2008).

MULTIPLE RESPONSE OPTIMIZATIONS

Finding optimal values of factors is a major goal in statistical modeling of little known systems, in general research and therefore in bioprocess field too. However, in most of the cases systems need to be evaluated by more than one response variable (Hendriks *et al.*, 1992). Sometimes models for response differ greatly and then optimal values could be quite different for each particular response. Besides, outcome parameters could have dissimilar positive criteria on the system, for instance: in group of response variable, one of them would need to be maximized and another could need minimized or set in a range to guarantee the best system performance comprehensively. Thus, professionals in bioprocess research and development area must be trained in multiresponse optimization. The main issue related to this kind of optimization is to make a selection out of a set of factor values that result in a compromise solution of a multicriteria problem (Hendriks *et al.*, 1992).

A large number of statistical techniques with this purpose are now available. These include: overlay plots, pareto optimality, utility functions, desirability functions and methods based on the

standardized Euclidian distance between the predicted value of each response and the optimum one that was obtained individually (Hendriks *et al.*, 1992; Sivakumar *et al.*, 2007; Takayama *et al.*, 2003). Among them, the most employed in bioprocesses is the desirability function.

Desirability function includes all the response variables into a single function in order to consider all of them simultaneously. This method requires minimum and maximum acceptable values for each outcome variable. The individual response can be normalized to the desirability functions (d_k, k = 1, 2, 3,..., n) with values inside the interval [0,1] using the distance between minimum and maximum acceptable values. The d_i functions are then combined to obtain a global desirability function D which should be maximized choosing the best conditions of the designed variables. D is calculated by the following equation (Takayama *et al.*, 2003; Moreira *et al.*, 2007):

$$D = (d_1^{r1} \times d_2^{r2} \times d_3^{r3} \times \ldots \times d_n^{rn})^{1/(r1+r2+r3 \cdots m)}$$

where, r_i is the relative importance assigned to each response.

The application of this method for multiresponse optimization is performed mainly in bioprocess for defining best values of factors associated to bioreaction step (Moreira *et al.*, 2007; Liu and Tang, 2010). For instance: Desirability function was used to find the best combination of four medium component concentrations (sucrose, yeast extract, peptone, Mg^{2+}) in order to maximize three response variables: dry cell weight, extracellular and intra cellular polysaccharides. The relative importance for three outcome variables was the same. The optimal values were 73, 11, 8 g L^{-1} and 46 mM of sucrose, yeast extract, peptone and Mg^{2+}, respectively. Under these conditions the predicted values for dry cell weight, extracellular and intra cellular polysaccharides were 24.50, 4.10 and 3.20 g L^{-1}, respectively (Liu and Tang, 2010).

HOW TO TAKE ADVANTAGE LARGE VOLUME OF DATA

The statistical techniques included in categories: fair comparison of results and statistical modeling of little known systems are applied almost always on lab scale, for further application on large-scale, scale-up criteria should be considered. However, nowadays modern bioprocess plants are equipped with proper automation systems for capturing and recording material input, process output, control action as well as physical parameters (Charaniya *et al.*, 2008; Alford, 2006). These data might provide the cause of process response variables fluctuations. Besides, industrial bioprocess data allows for improving process robustness and efficiency (Charaniya *et al.*, 2008).

To identify novel and useful relations and patterns that associate process factors with different process response, a methodology involving four interactive steps is commonly used. These steps are: data processing, feature selection and/or dimensionality reduction, data mining and expert analysis for interpretation of the results. Multivariate methods and artificial neuronal networks have been extensively used in dimensionality reduction and data mining steps (Charaniya *et al.*, 2008, 2010).

Among multivariate methods for improving bioprocesses from production plant data, Principal Component Analysis (PCA) and Partial Least Squares (PLS) are the most used (Charaniya *et al.*, 2010).

Specifically, PCA is applied to get a quick overview and to detect deviations from the desired bioprocess behavior. Its main purpose is to reduce the dimension of the space of the inter-correlated variables to a lower dimensional representation space with less correlated variables. The PCA is

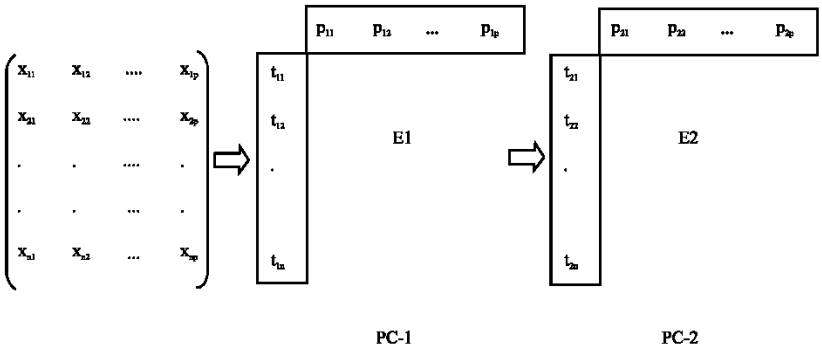

Fig. 5: Principal component analysis: representation of matrix X decomposition in principal components (PC), E: Matrix containing residuals

applied to bi-dimensional data structures (matrix-X) defined by p columns (number of variables) and n rows (number of observations). Matrix-X is discomposed into a number of principal components that maximize explained variance in data on each successive component under the constraint of being orthogonal to the previous principal components (Nucci *et al.*, 2010). A bilinear model is the result of this latent variable projection method, a product of scores T and the loadings P matrices (Fig. 5). Two main graphics are generated from PCA, score and loading plots. Each observations gets a score value on each principal component, then observations can be represented in scores plots. This graph reveals clusters, trends and outliers in data. Similarly, variables are represented in loading plots, allowing to detect correlations among variables and to interpret patterns observed in the score plot (Rajalahti and Kvalheim, 2011). For instance: PCA was applied to identify key variables from cell culture data related to a fed-batch culture of mouse hybridoma by reducing their dimensionality. For each observation was defined: cell density, concentration of amino acids, major carbon sources and by-products. PCA identified three major clusters characterized by a particular amino acids consumption/production rates (Selvarasu *et al.*, 2010).

Regression method based on PLS in bioprocess has been used to identify predictive correlations between output parameters (Y) and factors (X) as well as detect process abnormalities (Charaniya *et al.*, 2008). PLS takes PCA one step further, as it deals with two matrixes (X and Y). Each observation is represented in both spaces X and Y. In PLS, firstly a PCA is carried out for both the descriptive (X) and the response (Y) variables. Then, the best correlation between X and Y is calculated using least square technique. Therefore, the resulting PLS model is not always the best description of X and Y but rather of the relation between them. Summarizing, the emphasis in PLS is both on the correlation between X and Y and a good description of X and Y (Gabrielsson *et al.*, 2002). As a bioprocess example: a PLS regression was used to calibrate models in order to predict volatile fatty acid concentrations from near infrared spectra obtained in biogas test plants. These Volatile Fatty Acids (VFA) should be well controlled to guarantee a stable biogas production. The model displayed acceptable to very good prediction performances for total VFA as well as for three other essential individual acids based on test set validations. This PLS application was useful for improving the bioreaction control (Holm-Nielsen and Esbensen, 2011).

Another predictive approach used to analyze bioprocess data is Artificial Neural Networks (ANN). Especially, it has been applied to predict the output of a fermentation process as a nonlinear function of the process inputs. This artificial intelligence approach can be used together with optimization methods to identify the optimal factor values to maximize the desire process response (Charaniya *et al.*, 2008). The inputs to the model are process measurements, then data are weighted individually or in groups, after that combined using a nonlinear activation function at a node referred to as a neuron. A process ANN model is often composed of an input layer, an output layer and one or more hidden layers of nodes (Komives and Parker, 2003). There are many types of ANN, the most often used ANN is a fully connected, supervised network with backpropagation learning rule. This type of ANN is excellent at prediction and classification tasks (Agatonovic-Kustrin and Beresford, 2000). A concrete example of ANN application in bioprocess for taking advantage large volume of data was the satisfactory dynamic modeling of biochemical oxygen demand, chemical oxygen demand, suspended solid and total nitrogen removal in a Waste Water Treatment Plant (WWTP) using a data set collected from a full-scale WWTP (Lee *et al.*, 2011).

COMBINING STATISTICAL MODELING OF LITTLE KNOWN SYSTEMS AND MULTIVARIATE METHODS

To finish this review, it is appropriated to note that a useful statistical tool with wide applications in pharmaceutical industry, it has not found the same application in bioprocess, the multivariate designs. They are a combination of classical methods for modeling of little known systems and multivariate methods (PCA and PLS). In pharmaceutical formulation, this experimental strategy has been used to optimize type of ingredients and their concentrations (Fernandez *et al.*, 2010). Ingredient types for the same purpose were characterized by several descriptive variables and then PCA was applied to turn this categorical variable into numeric variables (scores) (Gabrielsson *et al.*, 2002). Subsequently, a higher number of ingredients could be considered, even for new ones non evaluated, the developed models could estimate the responses associated to the system under study. This application would be interesting for culture media optimization where most of the time different resources of nutrients are assessed.

Another application of the multivariate design is related to multi-stages processes which has not frequently used in bioprocesses. In general, most of the time just one system unit is optimized and it is not considered the system as a whole. Multivariate design allows for considering the previous step by means of latent variables generate from PCA and integrate them to the own variables of the system unit being optimize (Bergman *et al.*, 1998). This would be very useful to connect bioreaction and downstream steps. Specially for connecting bioreaction with the first downstream operation unit.

INFERENCE

In this review, the statistical tools were classified so that professionals with low statistics expertise involved in bioprocess research can choose the correct technique for a similar investigation problem. Figure 6 is a graphical guide for this purpose. Examples from literature were also commented in order to help the understanding of theoretical issues of each statistical technique. Besides, some statistical tools without wide application at the moment in bioprocess were also discussed, taking into consideration the near future use of them.

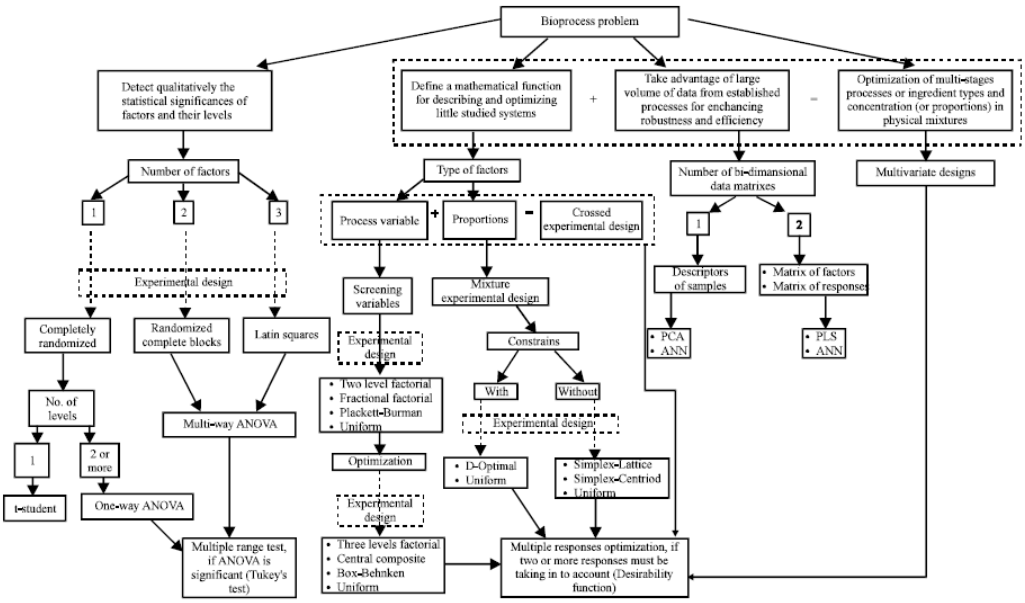

Fig. 6: Guide for choosing statistical tools in bioprocess problems

ACKNOWLEDGMENTS

First author gratefully acknowledges his wife and daughter, Relma and Giovanna as well as Ph.D. students: Bruno Oliva Oishi and Hector Aguilar Vitorino, for the inspiration to write this study.

REFERENCES

Agatonovic-Kustrin, S. and R. Beresford, 2000. Basic concepts of Artificial Neural Network (ANN) modeling and its application in pharmaceutical research. J. Pharm. Biomed. Anal., 22: 717-727.

Albert, S. and R.D. Kinley, 2001. Multivariate statistical monitoring of batch processes: An industrial case study of fermentation supervision. Trends Biotechnol., 19: 53-62.

Aleman, M.D.R., E. Noa, A. Tamayo, M. Dubed and S. Padilla *et al.*, 2007. Downstream processing: A revalidation study of viral clearance in the purification of monoclonal antibody CB.Hep-1. BioPharm Int., 20: 46-55.

Alford, J.S., 2006. Bioprocess control: Advances and challenges. Comput. Chem. Eng., 30: 1464-1475.

Anderson, M.J. and P.J. Whitcomb, 2004. RSM Simplified: Optimizing Processes Using Response Surface Methods for Design of Experiments. Productivity Press, USA., ISBN-13: 9781563272974, Pages: 292.

Arutchelvi, J., C. Joseph and M. Doble, 2011. Process optimization for the production of rhamnolipid and formation of biofilm by *Pseudomonas aeruginosa* CPCL on polypropylene. Biochem. Eng. J., 56: 37-45.

Bergman, R., M.E. Johansson, T. Lundstedt, E. Seifert and J. Aberg, 1998. Optimization of a granulation and tabletting process by sequential design and multivariate analysis. Chemometr. Intell. Lab., 44: 271-286.

Boos, D.D. and C. Brownie, 1995. ANOVA and rank tests when the number of treatments is large. Stat. Probab. Lett., 23: 183-191.

Brereton, R.G., 2003. Chemometrics Data Analysis for the Laboratory and Chemical Plant. John Wiley and Sons Ltd., USA., ISBN-13: 9780470845745, Pages: 504.

Breyfogle, F.W., 1992. Statistical Methods for Testing, Development and Manufacturing. John Wiley and Sons Inc., USA., ISBN-13: 9780471540359, Pages: 516.

Brue, G. and R. Howes, 2005. The McGraw-Hill 36-Hour Course Six Sigma. The McGraw Hill Companies, USA., ISBN-13: 9780071430081, Pages: 304.

Charaniya, S., H. Le, H. Rangwala,, K. Mills, K. Johnson, G. Karypis and W.S. Hu, 2010. Mining manufacturing data for discovery of high productivity process characteristics. J. Biotechnol., 147: 186-197.

Charaniya, S., W.S. Hu and G. Karypis, 2008. Mining bioprocess data: Opportunities and challenges. Trends Biotechnol., 26: 690-699.

Clementschitsch, F. and K. Bayer, 2006. Improvement of bioprocess monitoring: Development of novel concepts. Microb. Cell Factories, Vol. 5. 10.1186/1475-2859-5-19

Compton, M.E., 2011. Elements *In vitro* Research. In: Plant Tissue Culture, Development and Biotechnology, Trigiano, R.N. and D.J. Gray (Eds.). CRC Press/Taylor and Francis Group, USA., pp: 57-74.

Cornell, J.A., 2002. Experiments with Mixtures: Designs, Models and the Analysis of Mixture Data. 3rd Edn., John Wiley and Sons Ltd., New York, USA., ISBN-13: 9780471393672, Pages: 649.

Delaroza, F. and I.S. Scarminio, 2008. Mixture design optimization of extraction and mobile phase media for fingerprint analysis of *Bauhinia variegata* L. J. Sep. Sci., 31: 1034-1041.

Deming, S.N. and S.L. Morgan, 1993. Experimental Design: A Chemometric Approach. 2nd Edn., Elsevier Science Publishers, USA., ISBN-13: 9780444891112, Pages: 437.

Didier, C., G. Forno, M. Etcheverrigaray, R. Kratje and H. Goicoechea, 2009. Novel chemometric strategy based on the application of artificial neural networks to crossed mixture design for the improvement of recombinant protein production incontinuous culture. Anal. Chim. Acta, 650: 167-174.

Dubey, K.K. and B.K. Behera, 2011. Statistical optimization of process variables for the production of an anticancer drug (colchicine derivatives) through fermentation: At scale-up level. New Biotechnol., 28: 79-85.

Eriksson, L., E. Johansson, N. Kettaneh-Wold, C. Wikstrom and S. Wold, 2008. Design of Experiments: Principles and Applications. 3rd Edn., Umetrics Academy, USA., ISBN-13: 9789197373043, Pages: 459.

Fang, K.T. and L.Y. Chan, 2006. Uniform Design and its Industrial Applications. In: Springer Hanbook Engineering Statistics, Pham, H. (Ed.). Springer-Verlag, USA., pp: 228-248.

Fernandez, E.G., M. Fernandez, R.T. Oliveira, B. Bermudez and I. Perez *et al.*, 2008a. Disenos de experimentos en tecnologia y control de los medicamentos (Design of experiments in technology and medication management). Lat. Am. J. Pharm., 27: 286-296.

Fernandez, E.G., R. Valdes, J.A. Montero, A. Figueroa and T.A. Alvarez *et al.*, 2008b. Application of the partial least square technique to identify critical variables in the immunosorbent manufacturing. Chormatographia, 68: 375-380.

Fernandez, E.G., M. Fernandez, H.M. Hoang, I. Perez and D. Guerra *et al.*, 2010. A multivariate strategy for tablet manufacturing optimization. Latin Am. J. Pharm., 29: 1336-1344.

Fernandez-Nunez, E.G., B.L. Faintuch, R. Teodoro, D.P. Wiecek and N.G. da Silva *et al.*, 2011. Parameters optimization defined by statistical analysis for cysteine-dextran radiolabeling with technetium tricarbonyl core. Applied Radiat. Isot., 69: 663-669.

Gabrielsson, J., N.O. Lindberg and T. Lundstedt, 2002. Multivariate methods in pharmaceutical applications. J. Chemom., 16: 141-160.

Gerstman, B.B., 2008. Basic Biostatistics: Statistics for Public Health Practice. Jones and Bartlett Publishers Inc., USA., ISBN-13: 9780763735807, Pages: 557.

Harry, M.J., P.S. Mann, O.C. De Hodgins, R.L. Hulbert and C.J. Lacke, 2011. Practitioner's Guide to Statistics and Lean Six Sigma for Process Improvements. John Wiley and Sons Inc., USA., ISBN-13: 9781118210215, Pages: 800.

Henderson, G.B., 2011. Six Sigma Quality Improvement with Minitab. 2nd Edn., John Wiley and Sons Ltd., USA., ISBN-13: 9781119976189, Pages: 528.

Hendriks, M.M.W.B., J.H. de Boer, A.K. Smilde and D.A. Doornbos, 1992. Multicriteria decision making. Chemom. Intell. Lab. Syst., 16: 175-191.

Hinkelmann, K. and O. Kempthorne, 2008. Design and Analysis of Experiments Volume 1: Introduction to Experimental Design. 2nd Edn., John Wiley and Sons, USA., ISBN-13: 9780471727569, Pages: 631.

Holm-Nielsen, J.B. and K.H. Esbensen, 2011. Monitoring of biogas test plants: A process analytical technology approach. J. Chemom., 25: 357-365.

Hong, S.J. and C.G. Lee, 2008. Statistical optimization of culture media for production of phycobiliprotein by *Synechocystis* sp. PCC 6701. Biotechnol. Bioprocess. Eng., 13: 491-498.

Hua, D. and P. Xu, 2011. Recent advances in biotechnological production of 2-phenylethanol. Biotechnol. Adv., 29: 654-660.

Jakobsson, N., M. Degerman and B. Nilsson, 2005. Optimisation and robustness analysis of a hydrophobic interaction chromatography step. J. Chromatogr. A., 1099: 157-166.

Jana, A.K., 2008. Chemical Process Modeling and Computer Simulation. Prentice Hall of India Private Limited, New Delhi, India, ISBN-13: 9788120331969, Pages: 273.

Komives, C. and R.S. Parker, 2003. Bioreactor state estimation and control. Curr. Opin. Biotechnol., 14: 468-474.

Kowalski, S.M. and D.C. Montgomery, 2011. Design and Analysis of Experiments. 7th Edn., John Wiley and Sons Inc., USA.

Lee, J.W., C. Suh, Y.S.T. Hong and H.S. Shin, 2011. Sequential modelling of a full-scale wastewater treatment plant using an artificial neural network. Bioprocess. Biosyst. Eng., 34: 963-973.

Lee, K.M. and D.F. Gilmore, 2006. Statistical experimental design for bioprocess modeling and optimization analysis: Repeated-measures method for dynamic biotechnology process. Applied Biochem. Biotechnol., 135: 101-115.

Liang, Y.Z., K.T. Fang and Q.S. Xu, 2001. Uniform design and its applications in chemistry and chemical engineering. Chemom. Intell. Lab. Syst., 58: 43-57.

Liu, R.S. and Y.J. Tang, 2010. *Tuber melanosporum* fermentation medium optimization by Plackett-Burman design coupled with Draper-Lin small composite design and desirability function. Bioresour. Technol., 101: 3139-3146.

Mandenius, C.F. and A. Brundin, 2008. Bioprocess optimization using design-of-experiments methodology. Biotechnol. Prog., 24: 1191-1203.

Mendenhall, W., R.J. Beaver and B.M. Beaver, 2009. Introduction to Probability and Statistics. 13th Edn., Brooks/Cole, USA.

Michelson, S. and T. Schofield, 1996. The Biostatistics Cookbook: The Most User-Friendly Guide for Bio/Medical Scientist. Springer, New York, USA., ISBN-13: 9780792341055, Pages: 176.

Mills, K.L., J.J. Filiben, D.Y. Cho, E. Schwartz and D. Genin, 2010. Study of proposed internet congestion control mechanisms. National Institute of Standards and Technology Special Publication No. 500-282. http://www.nist.gov/itl/antd/upload/P1-SP-500-282-Cover-Pages.pdf

Moreira, G.A., G.A. Micheloud, A.J. Beccaria and H.C. Goicoechea, 2007. Optimization of the *Bacillus thuringiensis* var. *kurstaki* HD-δ-endotoxins production by using experimental mixture design and artificial neural networks. Biochem. Eng. J., 35: 48-55.

Nair, A.J., 2005. Basics of Biotechnology. Laxmi Publications (P) Ltd., India, ISBN-13: 9788170086123, Pages: 302.

Nair, A.J., 2008. Principles of Biotechnology. Laxmi Publications (P) Ltd., India, ISBN-13: 9788131800621, Pages: 886.

Najafpour, G., 2006. Biochemical Engineering and Biotechnology. Elsevier, USA., ISBN-13: 9780444528452, Pages: 421.

Nucci, E.R., A.J.G. Cruz and R.C. Giordano, 2010. Monitoring bioreactors using principal component analysis: Production of penicillin G acylase as a case study. Bioproc. Biosyst. Eng., 33: 557-564.

Onsekizoglu, P., K.S. Bahceci and J. Acar, 2010. The use of factorial design for modeling membrane distillation. J. Membr. Sci., 349: 225-230.

Otto, M., 2007. Chemometrics-Statistics and Computer Application in Analytical Chemistry. 2nd Edn., Wiley-VCH, Weinheim, Germany, Pages: 328..

Park, C., J.S. Lim, Y. Lee, B. Lee, S.W. Kim, J. Lee and S. Kim, 2007. Optimization and morphology for decolorization of reactive black 5 by *Funalia trogii*. Enzyme. Microb. Technol., 40: 1758-1764.

Prakasham, R.S., T. Sathish, P. Brahmaiah, C. Subba Rao, R. Sreenivas Rao and P.J. Hobbs, 2009. Biohydrogen production from renewable agri-waste blend: Optimization using mixer design. Int. J. Hydrogen Energ., 34: 6143-6148.

Rajalahti, T. and O.M. Kvalheim, 2011. Multivariate data analysis in pharmaceutics: A tutorial review. Int. J. Pharm., 417: 280-290.

Rao, K.V., 2007. Distribution Free Statistical Tests of Inference. In: Biostatistics, A manual of statistical methods for use in health, nutrition and Anthropology, Rao, K.V., (Ed.). Jaypee Brothers Medical Publishers (P) Ltd., New Delhi, India, pp: 631-657..

Ryan, T.P., 2007. Modern Experimental Design. John Wiley and Sons, New York, USA., Pages: 593.

Santos, V.C., F.A. Hasmann, A. Converti and A. Jr. Pessoa, 2011. Liquid-liquid extraction by mixed micellar systems: A new approach for clavulanic acid recovery from fermented broth. Biochem. Eng. J., 56: 75-83.

Sathish, T., G.S. Lakshmi, Ch.S. Rao, P. Brahmaiah and R.S. Prakasham, 2008. Mixture design as first step for improved glutaminase production in solid-state fermentation by isolated Bacillus. Lett. Appl. Microbiol., 47: 256-262.

Selvarasu, S., Y. Kim do, I.A. Karimi and D.Y. Lee, 2010. Combined data preprocessing and multivariate statistical analysis characterizes fed-batch culture of mouse hybridoma cells for rational medium design. J. Biotechnol., 150: 94-100.

Sivakumar, T., R. Manavalan, C. Muralidharan and K. Valliappan, 2007. Multi-criteria decision making approach and experimental design as chemometric tools to optimize HPLC separation of domperidone and pantoprazole. J. Pharmaceut. Biomed. Anal., 43: 1842-1848.

Sower, V.E., 2011. Essentials of Quality With Cases and Experimental Exercises. John Wiley and Sons, New York, USA., Pages: 416.

Sun, L., C. Wang, C. Ma and L. Shi, 2010. Optimization of renewal regime for improvement of polysaccharides production from *Porphyridium cruentum* by uniform design. Bioproc. Biosyst. Eng., 33: 309-315.

Takayama, K., M. Fujikawa, Y. Obata and M. Morishita, 2003. Neural network based optimization of drug formulations. Adv. Drug. Delivery Rev., 55: 1217-1231.

Taneja, H.C., 2009. Statistical Methods for Engineering and Sciences. I.K. International Publishing House Pvt, Ltd., East Bangalore, India, ISBN: 9789380026664, Pages: 368.

Tang, Y.J., X.L. Xu and J.J. Zhong, 2010. A novel biotransformation process of 40-demethylepipodophyllotoxin to 4-demethylepipodophyllic acid by Bacillus fusiformis CICC 20463, Part II: process optimization. Bioproc. Biosyst. Eng., 33: 237-246.

Taoka, Y., N. Nagano, Y. Okita, H. Izumida, S. Sugimoto and M. Hayashi, 2011. Effect of Tween 80 on the growth, lipid accumulation and fatty acid composition of *Thraustochytrium aureum* ATCC 34304. J. Biosci. Bioeng., 111: 420-424.

Wee, Y.J., L.V.A. Reddy, K.C. Chung and H.W. Ryu, 2009. Optimization of chitosanase production from *Bacillus* sp. RKY3 using statistical experimental designs. J. Chem. Technol. Biotechnol., 84: 1356-1363.

Wei, G., X. Yang, T. Gan, W. Zhou, J. Lin and D. Wei, 2009. High cell density fermentation of *Gluconobacter oxydans* DSM 2003 for glycolic acid production. J. Ind. Microbiol. Biotechnol., 36: 1029-1034.

Wolski, E., E. Rigo, M. Di Luccio, J.V. Oliveira, D. de Oliveira and H. Treichel, 2009. Production and partial characterization of lipases from a newly isolated *Penicillium* sp. Using experimental design. Lett. Appl. Microbiol., 49: 60-66.

Xu, C.P., J. Sinha, J.T. Bae, S.W. Kim and J.W. Yun, 2006. Optimization of physical parameters for exo-biopolymer production in submerged mycelial cultures of two entomopathogenic fungi *Paecilomyces japonica* and *Paecilomyces tenuip*. Lett. Appl. Microbiol., 42: 501-506.

Xu, L.J, Y.S. Liu, L.G. Zhou and J.Y. Wu, 2010. Optimization of a liquid medium for beauvericin production in fusarium redolens Dzf2 mycelial culture. Biotechnol. Bioprocess Eng., 15: 460-466.

Xue, Ch., X.Q. Zhao, W.J. Yuan and F.W. Bai, 2008. Improving ethanol tolerance of a self-flocculating yeast by optimization of medium composition. World J. Microbiol. Biotechnol., 24: 2257-2261.

Yang, W.W., N.R. Mwakatage, R. Goodrich-Schneider, K. Krishnamurthy and T.M. Rababah, 2011. Mitigation of major peanut allergens by pulsed ultraviolet light. Food Bioprocess Technol., 10.1007/s11947-011-0615-6

Zhi, W., J. Song, F. Ouyang and J. Bi, 2005. Application of response surface methodology to the modeling of α-amylase purification byaqueoustwo-phase systems. J. Biotechnol., 118: 157-165.

Zhou, Y., S. Lakshminarayanan and R. Srinivasan, 2011. Optimization of image processing parameters for large sets of in-process video microscopy images acquired from batch crystallization processes: Integration of uniform design and simplex search. Chemometr. Intell. Lab. Syst., 107: 290-302.

Vol.56, n.5: pp. 859-866, September-October 2013
ISSN 1516-8913 Printed in Brazil

BRAZILIAN ARCHIVES OF
BIOLOGY AND TECHNOLOGY
AN INTERNATIONAL JOURNAL

Semliki Forest Virus as a Vector: Pros and Cons for Its Use in Biopharmaceuticals Production

Eutimio Gustavo Fernández Núñez[1,2*], Soraia Attie Calil Jorge[3], Renato Mancini Astray[3], Alexandre Gonçalves de Rezende[3], Bruno Labate Vale da Costa[4], Daniella Cristina Ventini Monteiro[1,3], Carlos Augusto Pereira[1,3] and Aldo Tonso[1]

[1]Laboratório de Células Animais; Departamento de Engenharia Química; Escola Politécnica; Universidade de São Paulo; São Paulo - SP - Brasil. [2]Departamento de Ciências Biológicas; Faculdade de Ciência e Letras; Universidade Estadual Paulista "Julho de Mesquita Filho"; Assis - SP - Brasil. [3]Laboratório de Imunologia Viral; Instituto Butantan; São Paulo - SP - Brasil. [4]Laboratório de Biotecnologia Industrial; Núcleo de Bionanomanufatura; Instituto de Pesquisas Tecnológicas do Estado de São Paulo; São Paulo - SP - Brasil

ABSTRACT

The number of biopharmaceuticals for medical and veterinarian use produced in mammalian cells is increasing year after year. All of them are obtained by stable recombinant cell lines. However, it is recognized that transient gene expression produces high level expression in a short time. In that sense, viral vectors have been extensively used for producing recombinant proteins on lab-scale. Among them, Semliki Forest virus is commonly employed for this purpose. This review discusses the main aspects related to the use of Semliki Forest virus technology as well as its advantages and drawbacks which limit currently its utilization in biopharmaceutical industry on large-scale.

Key words: BHK-21, Large-scale bioprocesses, Mammalian cells, Recombinant proteins, SFV, Transient expression

INTRODUCTION

Mammalian cells have become the major host for recombinant proteins used as biopharmaceuticals with medical and veterinarian applications (Baldi et al. 2007; Conceição et al. 2007). The main factor related to this extensive application is the need of post-translational modifications in order to guarantee the full bioactivity of these macromolecules. Such changes are only accurately performed by the mammalians cells (Walsh 2010).

Currently, there are two established strategies in biopharmaceutical industry and academy to produce heterologous proteins: the use of stable cell lines, or transient gene expression (Kerrigan et al. 2011). The first one is achieved through the insertion of the recombinant gene(s) into the host genome. This approach is useful to produce recombinant protein for extended cultivation times. However, the identification and characterization processes of these cell lines are expensive and prolonged (De Jesus and Wurm 2011). On the other hand, when rapid assessment of many proteins, or several variants of a single protein is required, transient gene expression is the strategy of choice. Furthermore, short upstream processes (1-14 days) are related with transient gene expression (De Jesus and Wurm 2011).

In transient gene expression, non-viral (plasmid vectors) and viral expression vectors have been designed for transferring the genes to mammalian cells. The reasons, which define the expression

*Author for correspondence: eutimiocu@yahoo.com

vector selection for this purpose are: the recombinant protein application, the host cell, bioprocess time, productivity and safety (Baldi et al. 2007). The purity and recovery of plasmid DNA encoding for interest protein are limiting aspects when non-viral expression vectors are chosen (Geisse and Henke 2005). In general, the major concern for using virus as an expression vector is their infective nature, which involves biological risks (Sakamoto et al. 1999). However, the utilization of replication-deficient viral vectors such as Semliki Forest virus (SFV) and Sindbis virus vectors avoids this problem while allowing rapid and high-level gene delivery (Lundstrom et al. 2001a). This review defines the main advantages and drawbacks of SFV utilization for biopharmaceutical production in the mammalian cells and the present and near future challenges for a wide application of this viral vector on large-scale.

TRANSIENT GENE EXPRESSION IN MAMMALIAN CELLS FOR RECOMBINANT PROTEIN PRODUCTION ON LARGE-SCALE

The transient gene expression used on large-scale for recombinant protein production is a relatively new technology. In the past, the volumetric productivities reached by transient gene expression were not competitive with those from the stable cell lines (Hacker et al. 2009). However, recently, productivity up to 1 g/l with HEK-293 cells transfected with plasmid DNA in 14 days bioprocess has been reported (Backliwal et al. 2008). This report encourages new transient gene expressions in order to establish these processes at higher volumetric scales (100-1,000 l range). Beyond, the technical problems related to this gene expression way in the mammalian cells, there are two limiting events for its consolidation in biopharmaceutical industry:

1. At the present time, there is no therapeutic protein using transient gene expression in mammalian cells that has got regulatory approval.
2. There is a perception in the industry that large-scale transient gene expression is not reproducible.

Both elements could be overcome by targeting a protein with high value, which does not require a large amount of recombinant protein to meet the market demands and by developing robust processes on small-scale using scalable devices, respectively (Hacker et al. 2009). The experience with baculovirus-insect cell expression system for commercial manufacture of various veterinary and human vaccines could be also used to solve the current limitations in mammalian cells systems (Cox 2012).

So far, the non-viral vector methods have been the methods of choice for transient gene expression (Matasci et al. 2008). The recombinant gene is usually cloned in a plasmid DNA and transfected into the single-cell suspension culture. Only three DNA delivery methods for introducing plasmids in mammalian cells have been shown to be promising for large-scale operations: calcium phosphate DNA co-precipitation, polyethyleneimine or liposome DNA complexes and electroporation. These DNA transfer systems have demonstrated transfection efficiencies of more than 70%. After DNA delivery, cells are maintained in the culture for protein production during a limited time span, usually 5-10 days (Wurm and Bernard 1999).

Transient gene expression by viral vectors is carried out introducing the recombinant gene of interest in viruses. The transfer of exogenous DNA or RNA into animal cells, in general, as part of viral particle is named as transduction. The advantage of viral transduction over transfection with naked plasmid DNA includes the high efficiency of gene transfer because a natural delivery process is used. The tendency of many viruses to block the host cell protein synthesis and favor the expression of viral genes is also important for heterologous genes expression, which can increase bioprocess productivity. Besides, different viruses can achieve different transformation objectives: short-term infections with high-level transient expression, long-term expression by maintaining the genome as a latent episomal replicon, or stable integration of DNA into the host cell genome (Twyman 2005). The disadvantages of virus as gene transfer vectors include more complex cloning strategies compared to plasmid vectors, the biosafety problems related to bioprocesses with virus and health risks after recombinant protein administration associated to possible presence of viral vector (Twyman 2005; Lee et al. 2005). Many efforts have been addressed to overcome these problems in viral vectors (Lundstrom et al. 2001b; Chen et al. 2011).

Among the viral vectors for recombinant protein expression in the mammalian cells are vaccinia

virus (Pradeau-Aubreton et al. 2010), adenovirus (Pham et al. 2006), alphaviruses (Venezuelan Equine Encephalitis virus and Sindbis virus and the SFV) (Quetglas et al. 2010). Despite of the fact that the Baculovirus expression system is a well established methodology in insect cells for producing eukaryotic proteins (Koroleva et al. 2010; Trowitzsch et al. 2010; Gomez-Casado 2011), the use of vectors based on this virus (BacMam) has also demonstrated efficiency in the mammalian cells (Kost et al. 2005).

SEMLIKI FOREST VIRUS (SFV)

SFV is a single positive-strand RNA virus with an envelope structure. The first part (5'end) of genome encodes the nonstructural proteins, while the second part (3'end) encodes the structural proteins (Dudek and Knipe 2006). Its genome has been introduced into two plasmid vectors as cDNA copies. The expression vector contains the SFV nonstructural genes (nsP1-4), the strong subgenomic SFV 26S promoter and a multilinker cloning region to introduce the foreign genes for recombinant protein expression. The SFV structural proteins are provided from the helper vector, including the envelope and capsid proteins (Liljeström and Garoff 1991). Co-transfection of *in vitro* transcribed recombinant and helper RNA can generate around 10^9-10^{10} recombinant viral particles/ml. These particles have the capacity to infect a wide range of mammalian and other animal cell lines (Lundstrom 2003a). The electroporation is the method of choice for SFV RNAs co-transfection but lipid-mediated transfection can be applied alternatively with relatively good results (Lundstrom 2010).

Because of the presence of RNA packing signal only in the recombinant RNA, no helper RNA will be packaged, which generates replication-deficient particles, increasing vector's biosafety features. To decrease the infection risks, a mutation was inserted in the region encoding the viral spike proteins, inhibiting host entry. Therefore, viral vector could be no-infectious during the storage period and could only be activated *in vitro* by cleavage with α-chymotrypsin (Berglund et al. 1993; Benmaamar et al. 2009). After host cells infection, rapid and high-level transgene expression is obtained. Different proteins have been successfully expressed from the SFV vector. Yields of 10^9 heterologous protein molecules per cell, representing around 25% of the total cellular protein yields have been obtained by this viral vector (Lundstrom 2003a).

The SFV vectors have become increasingly attractive because of their characteristics of rapid expression of high amounts of recombinant protein. After infection, the RNA replication in the host cell cytoplasm results in measurable transgene expression as early as 2 h after the infection. In spite of the great potential for widespread use of SFV for recombinant protein production, two major drawbacks are related to this viral vector: the strong cytotoxic effect on host cells and the short-term expression pattern. In addition, SFV infection of cell culture has been demonstrated to induce apoptosis. Solving, or mitigating these problems would expand even more the applications range of this alphavirus vector (Lundstrom 2002; Hassaine et al. 2006).

RECOMBINANT PROTEIN PRODUCTION BY SEMLIKI FOREST VIRUS VECTOR ON LAB-SCALE

On lab-scale, the SFV vector has been widely used for obtaining sufficient amounts of recombinant proteins for cellular, or molecular assays, pharmacological tests and structural studies (Hoffmann et al. 2001; Werten et al. 2002; Cabaniols et al. 2009). Most of them are functional membrane proteins, receptors (Shukla et al. 2006; Eifler et al. 2007), enzymes (Bikker et al. 1997) and viral proteins (Benmaamar et al. 2009). High volumetric protein expression levels and yields have been obtained by the modified SFV in the mammalian cells, up to 10 mg l^{-1} and 100-300 pmol mg^{-1} of total proteins, for G protein-coupled receptors (Shukla et al. 2007; Sevastsyanovich et al. 2009). The yield enhancement by the use of SFV vector comparing to stable cell lines and other transient transfections could be 20 fold higher (Shukla et al. 2007).

Currently, the studies for improving the SFV as high efficient protein producer vector are, or should be addressed to its genetic modification in order to extend the expression time in the host cells and optimizing the culture parameters during the infection and expression processes such as the host cell lines, temperature, pH, infection and post-infection times and multiplicity of infection (ratio of virus to target cell). The efforts in genetic modifications of the SFV are focused on mutations

in alphavirus replicase to render this vector less cytopathic (Casales et al. 2010). Host cell lines more used for protein transient expressions with this alphavirus are Baby Hamster Kidney (BHK-21), Chinese Hamster Ovary (CHO-K1) and Human Embryonic Kidney (HEK293) in both adherent and suspension cultures (Lundstrom 2003a; Lundstrom 2010). For a single protein expression, the selection of the cell line could be performed through a comparison among available cell lines keeping constant the remaining parameters of cell culture in small volume systems (Blasey et al. 1997; Hassaine et al. 2006).

Deterministic and empiric models definition as well as optimization of the bioprocess parameters on small-scale have not been detailed enough for this expression system. Works in this field could improve the protein expression using the SFV. Probably, the low number of paper on this subject is justified because most of the time, SFV system has been used on lab-scale without seeking to develop subsequently a large-scale bioprocess. For example, a study on temperature demonstrated that the cultures grown at 33°C showed an increase of 10-20 fold expression for luciferase and the expression time could be prolonged (up to 50 h) when compared to 37°C cultures (Schlaeger and Lundstrom 1998). For variables such as the pH and multiplicity of infection, the investigated ranges in literature are 6.4-7.8 and 30-400, respectively. The protein expression has shown to be very sensitive to small pH changes over the course of bioprocess and directly related to the multiplicity of infection (Blasey 1997; Blasey 2000). Nevertheless, a modification of pharmacological profile for some recombinant receptors was observed when the cells were infected with increased concentration of virus (Lundstrom 2003b). This could be a consequence of a saturation of right protein synthesis capacity in host cells. Thus, in future, more detailed studies considering the bioprocess variables should be performed on small-scale. This could be possible if the SFV is definitively established on large-scale processes.

CELL CULTURE STRATEGIES FOR OBTAINING RECOMBINANT PROTEINS BY THROUGH SEMLIKI FOREST VIRUS SYSTEM

Among the alpha virus, only SFV has been used for large-scale recombinant protein production, which showed its popularity because the principles of this kind of vectors are the same. As a rule the cell culture used for transduction should be in exponential growth phase to generate maximal expression levels. To scale-up the Semiliki Forest virus technology, it is absolutely essential to establish efficient infection and expression conditions in suspension cultures of the mammalian cells. In that sense, for reducing the cell costs and to facilitate the purification of recombinant proteins, CHO, HEK293 and BHK lines were adapted in suspension growth in serum-free medium without the decrease in expression level (Lundstrom 2003b). For high volume cultures, compromises need to be made between the optimal virus concentration and feasible virus production. The main disadvantage of applying the SFV system for the large-scale production of the protein is the high cost of virus stock production related to *in vitro* transcription process (Lundstrom 2010) (Fig. 1). In order to reduce the cost for virus preparation, alpha virus packaged cell lines have been developed (Polo et al. 1999; Blasey et al. 2000). This approach could simultaneously increase the production of viral particles.

There are a few studies related to SFV utilization on large-scale protein production by the utilization of bioreactors, spinner (1l) and agitated tank (11.5l) for producing the enzymes (bacterial β-galactosidase and human cyclooxygenase-2) and 5-HT3 receptor (Blasey et al. 1997; Blasey et al. 2000) The culture strategies to perform these bioprocesses were fed-batch and external medium exchange (Fig. 2).

In the fed-batch process, the SFV was inoculated in 10-20% bioreactor volume and BHK cells were kept in contact with the virus for 90 min, and then fresh culture medium was added to complete the bioreactor volume. The bioprocess after the infection step lasted 20 h. High level protein expression (16 mg l^{-1}) was generated in a short time (Blasey et al. 1997). On the other hand, in external medium exchange process, 90% of exhausted culture medium used for the BHK batch cell culture was changed by fresh medium by external cross-flow filtration with a hollow fiber microfilter. Then the BHK cells were infected with the modified SFV for 24 h (Fig. 2).

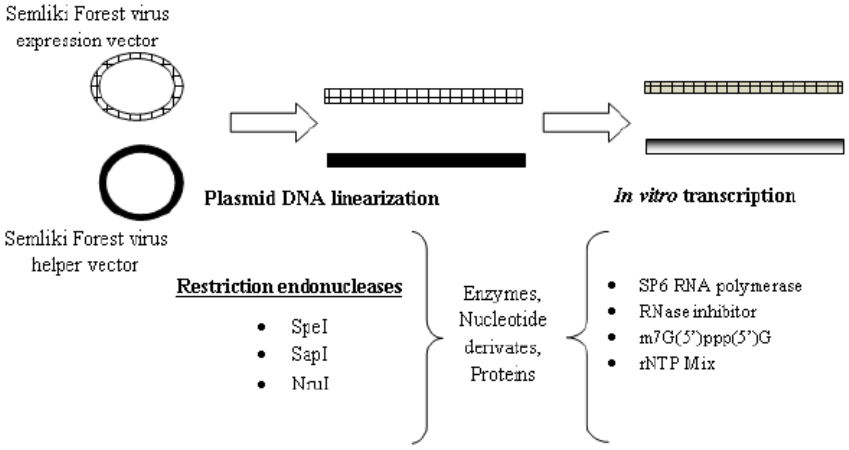

Figure 1 - *In vitro* transcription process for Semliki Forest virus vector and its more costly reagents.

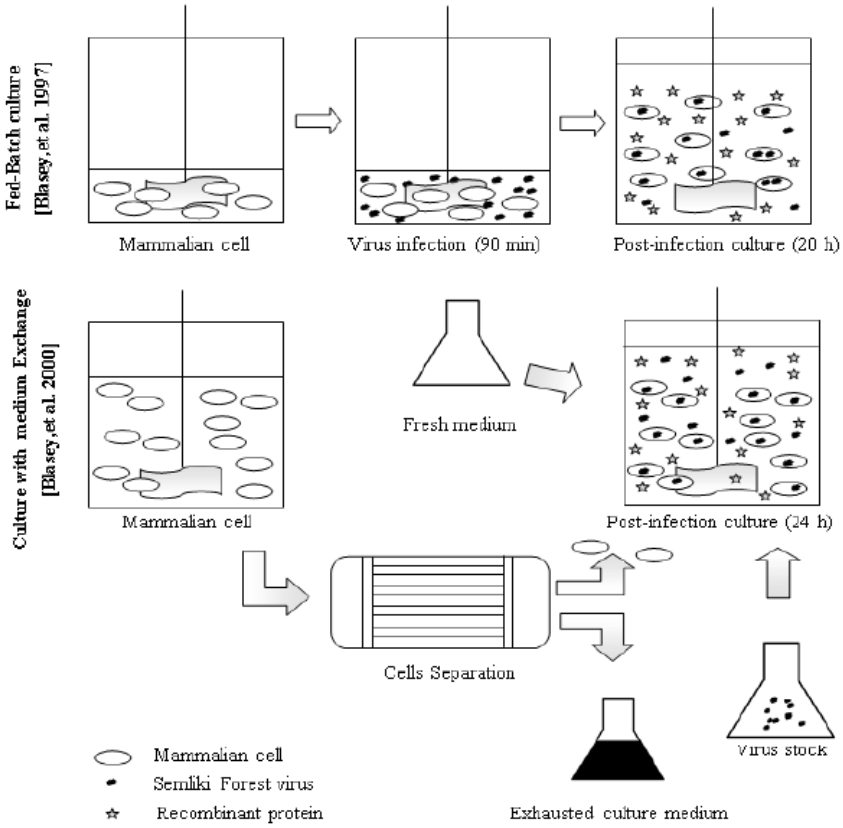

Figure 2 - Culture strategies for transduction and protein expression with Semliki Forest virus on large-scale.

This strategy allowed the expression of 15 mg of 5-HT3 receptors per 11.5 l batch (Blasey et al. 2000). The volumetric productivities for both the processes were higher than those usually obtained for bioprocess with stably transfected mammalian cells (> 0.05 mg l^{-1} for human membrane protein) (Chaudhary et al. 2011). Despite these good performances of this viral vector in the expression

of associated and integral membrane proteins (used in the pharmacological studies), besides the costs of RNA *in vitro* transcription, one of the main challenges related to the SFV vector applications in biopharmaceuticals production is the understanding of metabolic patterns during the infections in order to define the suitable culture medium and bioprocess strategies for improving the volumetric productivity. Then, the SFV vector could achieve equivalent performance with stable cell lines (>1 g l^{-1}).

Another problem, which limits the use of this transient expression vector in high volume bioreactors is virus transduction into the cell because of high cost and low efficiency. In this regard flow electroporation could be an interesting option (Parham et al. 1998). On the other hand, from the analytical point of view, the difficulties related to the establishment of accurate techniques for viral particles quantification (Calgua et al. 2011) could delay the standardization of biopharmaceutics manufacturing based on the SFV vector.

CONCLUSIONS

The SFV, as also the rest of viral vectors for protein transient expression, has been underutilized on large-scale, despite of its high expression level on small-scale. Four most critical aspects should be considered in order to establish definitively this vector as a suitable alternative for biopharmaceutical in high volume bioreactors: reduced cost for the production of virus, suitable culture medium and feed strategies over the course of post-infection stage and transduction process, as well as the precise method for viral particles quantification.

ACKNOWLEDGMENTS

The authors would like to thank Fundação de Amparo à Pesquisa do Estado de São Paulo for post-doctoral fellowship (2010/52521-6) and Conselho Nacional de Desenvolvimento Científico e Tecnológico (CNPq) for scientific grant. First author gratefully acknowledges Relma Tavares de Oliveira Fernández and PhD. Rodolfo Valdés, for the inspiration to write this paper. Carlos A Pereira is recipient of a senior 1A CNPq fellowship.

REFERENCES

Backliwal G, Hildinger M, Chenuet S, Wulhfard S, De Jesus M, Wurm FM. Rational vector design and multi-pathway modulation of HEK 293E cells yield recombinant antibody titers exceeding 1 g/l by transient transfection under serum-free conditions. *Nucleic Acids Res.* 2008; 36(15): e96.

Baldi L, Hacker DL, Adam M, Wurm FM. Recombinant protein production by large-scale transient gene expression in mammalian cells: state of the art and future perspectives. *Biotechnol Lett.* 2007; 29(5): 677-684.

Benmaamar R, Astray RM, Wagner R, Pereira CA. High-level expression of rabies virus glycoprotein with the RNA-based Semliki Forest Virus expression vector. *J Biotechnol.* 2009; 139(4): 283-290.

Berglund P, Sjöberg M, Garoff H, Atkins GJ, Sheahan BJ, Liljeström P. Semliki Forest virus expression system: production of conditionally infectious recombinant particles. *Biotechnology.* 1993; 11(8): 916-920.

Bikker H, Baas F, de Vijlder J-JM. Molecular analysis of mutated thyroid peroxidase detected in patients with total iodide organification defects. *J Clin Endocrinol Metab.* 1997; 82(2): 649-653.

Blasey HD, Brethon B, Hovius R, Vogel HH, Tairi AP, Lundström K, et al. Large scale transient 5-HT3 receptor production with the Semliki Forest Virus Expression System. *Cytotechnology.* 2000; 32(3): 199-208.

Blasey HD, Lundström K, Tate S, Bernard AR. Recombinant protein production using the Semliki Forest Virus expression system. *Cytotechnology.* 1997; 24(1): 65-72.

Cabaniols JP, Mathis L, Delenda C. Targeted gene modifications in drug discovery and development. *Curr Opin Pharmacol.* 2009; 9(5): 657-663.

Calgua B, Barardi CR, Bofill-Mas S, Rodriguez-Manzano J, Girones R. Detection and quantitation of infectious human adenoviruses and JC polyomaviruses in water by immunofluorescence assay. *J Virol Methods.* 2011: 171(1): 1-7.

Casales E, Aranda A, Quetglas JI, Ruiz-Guillen M, Rodriguez-Madoz JR, Prieto J, et al. A novel system for the production of high levels of functional human therapeutic proteins in stable cells with a Semliki Forest virus noncytopathic vector. *N Biotechnol.* 2010; 27(2): 138-148.

Chaudhary S, Pak JE, Pedersen BP, Bang LJ, Zhang LB, Ngaw SM, et al. Efficient expression screening of human membrane proteins in transiently transfected Human Embryonic Kidney 293S cells. *Methods.* 2011; 55(4): 273-280.

Chen CY, Lin CY, Chen GY, Hu YC Baculovirus as a gene delivery vector: recent understandings of molecular alterations in transduced cells and latest applications. *Biotechnol Adv.* 2011; 29: 618-631.

Conceição MM, Tonso A, Freitas CB, Pereira CA. Viral antigen production in cell cultures on microcarriers Bovine parainfluenza 3 virus and MDBK cells. *Vaccine*. 2007; 25(45): 7785-7795.

Cox MMJ. Recombinant protein vaccines produced in insect cells. *Vaccine* 2012; 30(10): 1759-1766.

De Jesus M, Wurm FM. Manufacturing recombinant proteins in kg-ton quantities using animal cells in bioreactors. *Eur J Pharm Biopharm*. 2011; 78(2): 184-188.

Dudek T, Knipe DM. Replication-defective viruses as vaccines and vaccine vectors. *Virology*. 2006; 344(1): 230-239.

Eifler N, Duckely M, Sumanovski LT, Egan TM, Oksche A, Konopka JB, et al. Functional expression of mammalian receptors and membrane channels in different cells. *J Struct Biol*. 2007; 159(2): 179-193.

Geisse S, Henke M. Large-scale transient transfection of mammalian cells: a newly emerging attractive option for recombinant protein production. *J Struct Funct Genomics*. 2005; 6(2-3): 165-170.

Gomez-Casado E, Gomez-Sebastian S, Núñez MC, Lasa-Covarrubias R, Martínez-Pulgarín S, Escribano JM. Insect larvae biofactories as a platform for influenza vaccine production. *Protein Expr Purif*. 2011; 79(1): 35-43.

Hacker DL, De Jesus M, Wurm FM. 25 years of recombinant proteins from reactor-grown cells - where do we go from here? *Biotechnol Adv*. 2009; 27(6): 1023-1027.

Hassaine G, Wagner R, Kempf J, Cherouati N, Hassaine N, Prual C, et al. Semliki Forest virus vectors for overexpression of 101 G protein-coupled receptors in mammalian host cells. *Protein Expr Purif*. 2006; 45(2): 343-351.

Hoffmann M, Verzijl D, Lundstrom K, Simmen U, Alewijnse AE, Timmerman H, et al. Recombinant Semliki Forest virus for over-expression and pharmacological characterisation of the histamine H(2) receptor in mammalian cells. *Eur J Pharmacol*. 2001; 427(2): 105-114.

Kerrigan JJ, Xie Q, Ames RS, Lu Q. Production of protein complexes via co-expression. *Protein Expres Purif*. 2011; 75(1): 1-14.

Koroleva NN, Spirin PV, Timokhova AV, Rubtzov PM, Kochetkov SN, Prasolov VS, et al. Baculovirus vectors for efficient gene delivery and expression in mammalian cells. *Mol Biol*. 2010; 44(3): 479-487.

Kost TA, Condreay JP, Jarvis DL. Baculovirus as versatile vectors for protein expression in insect and mammalian cells. *Nat Biotechnol*. 2005; 23(5): 567-575.

Lee JS, Hadjipanayis AG, Parker MD. Viral vectors for use in the development of biodefense vaccines. *Adv Drug Deliver Rev*. 2005; 57(9): 1293-1314.

Liljeström P, Garoff H. A new generation of animal cell expression vectors based on the Semliki Forest virus replicon. *Nat Biotechnol*. 1991; 9(12): 1356-1361.

Lundstrom K, Schweitzer C, Rotmann D, Hermann D, Schneider EM, Ehrengruber MU. Semliki Forest virus vectors: efficient vehicles for in vitro and in vivo gene delivery. *FEBS Letters*. 2001a; 504(3): 99-103.

Lundstrom K, Rotmann D, Hermann D, Schlaeger EJ. Safety aspects related to recombinant protein expression from Semliki Forest virus vectors. *Cytotechnology*. 2001b; 35(3): 213-221.

Lundstrom K. Expression of Mammalian Membrane Proteins in Mammalian Cells Using Semliki Forest Virus Vectors. In: Mus-Veteau I, editor. Heterologous Expression of Membrane Proteins, Methods in molecular Biology. New York: Humana Press; 2010. p. 149-164.

Lundstrom K. Semliki Forest virus vectors for rapid and high-level expression of integral membrane proteins. *Biochim Biophys Acta*. 2003a; 1610(1): 90-96.

Lundstrom K. Semliki Forest Virus Vectors for Large-Scale Production of Recombinant Proteins. In: Machida CA, editor. Viral vectors for gene therapy. Methods and Protocols, New Jersey: Humana Press; 2003b.p. 525-544.

Lundstrom K. Semliki forest virus-based expression for versatile use in receptor research. *J Recept Signal Tr*. 2002; 22 (1-4): 229-240.

Matasci M, Hacker DL, Baldi L, Wurm, FM. Recombinant therapeutic protein production in cultivated mammalian cells: current status and future prospects. *Drug Discov Today Technol*. 2008; 5(2-3): 37-42.

Parham JH, Iannone MA, Overton LK, Hutchins JT. Optimization of transient gene expression in mammalian cells and potential for scale-up using flow electroporation. *Cytotechnology*. 1998; 28(1-3): 147-155.

Pham PL, Kamen A, Durocher Y. Large-scale transfection of mammalian cells for the fast production of recombinant protein. *Mol Biotechnol*. 2006; 34(2): 225-237.

Polo JM, Belli BA, Driver DA, Frolov I, Sherril S, Hariharan MJ, et al. Stable alphavirus packaging cell lines for Sindbis virus and Semliki Forest virus-derived vectors. *Proc Natl Acad Sci USA*. 1999; 96(8): 4598-4603.

Pradeau-Aubreton K, Ruff M, Garnier JM, Schultz P, Drillien R. Vectors for recombinational cloning and gene expression in mammalian cells using modified vaccinia virus Ankara. *Anal Biochem*. 2010; 404(1): 103-105.

Quetglas JI, Ruiz-Guillen M, Aranda A, Casales E, Bezunartea J, Smerdou C. Alphavirus vectors for cancer therapy. *Virus Res*. 2010; 153(2): 179-196.

Sakamoto S, Ide T, Tokiyosi S, Nakao J, Hamada F, Yamamoto M, et al. Studies on the structures and antigenic properties of rabies virus glycoprotein analogues produced in yeast cells. *Vaccine*. 1999; 17(3): 205-218.

Schlaeger EJ, Lundstrom K. Effect of temperature on recombinant protein expression in Semliki Forest virus infected mammalian cell lines growing in serum- free suspension cultures. *Cytotechnology.* 1998; 28(1-3): 205-211.

Sevastsyanovich Y, Alfasi S, Cole J Recombinant protein production: a comparative view on host physiology. *N Biotechnol.* 2009; 25 (4): 175-180.

Shukla AK, Haase W, Reinhart C, Michel H. Biochemical and pharmacological characterization of the human bradykinin subtype 2 receptor produced in mammalian cells using the Semliki Forest virus system. *Biol Chem.* 2006; 387(5): 569-576.

Shukla AK, Haase W, Reinhart C, Michel H. Heterologous expression and comparative characterization of the human neuromedin U subtype II receptor using the methylotrophic yeast Pichia pastoris and mammalian cells. *Int J Biochem Cell Biol.* 2007; 39(5): 931-942.

Trowitzsch S, Bieniossek C, Nie Y, Garzoni F, Berger I. New baculovirus expression tools for recombinant protein complex production. *J Struct Biol.* 2010; 172(1): 45-54.

Twyman RM. Gene transfer to animal cells. New York: Garland BIOS Scientific Publishers; 2005.

Walsh G. Post-translational modifications of protein biopharmaceuticals. *Drug Discov Today.* 2010; 15(17-18): 773-780.

Werten PJ, Rémigy HW, de Groot BL, Fotiadis D, Philippsen A, Stahlberg H, et al. Progress in the analysis of membrane protein structure and function. *FEBS Letters.* 2002; 529(1): 65-72.

Wurm F, Bernard A. Large-scale transient expression in mammalian cells for recombinant protein production. *Curr Opin Biotechnol.* 1999; 10(2): 156-159.

Received: June 13, 2012;
Accepted: July 05, 2013.

Cytotechnology
DOI 10.1007/s10616-013-9612-0

ORIGINAL RESEARCH

Influence of aeration–homogenization system in stirred tank bioreactors, dissolved oxygen concentration and pH control mode on BHK-21 cell growth and metabolism

Eutimio Gustavo Fernández Núñez · Jaci Leme · Letícia de Almeida Parizotto · Wagner Antonio Chagas · Alexandre Gonçalves de Rezende · Bruno Labate Vale da Costa · Daniela Cristina Ventini Monteiro · Vera Lucia Lopes Boldorini · Soraia Attie Calil Jorge · Renato Mancini Astray · Carlos Augusto Pereira · Celso Pereira Caricati · Aldo Tonso

Received: 2 March 2013 / Accepted: 27 June 2013
© Springer Science+Business Media Dordrecht 2013

Abstract This work focused on determining the effect of dissolved oxygen concentration (DO) on growth and metabolism of BHK-21 cell line (host cell for recombinant proteins manufacturing and viral vaccines) cultured in two stirred tank bioreactors with different aeration-homogenization systems, as well as pH control mode. BHK-21 cell line adapted to single-cell suspension was cultured in Celligen without aeration cage (rotating gas-sparger) and Bioflo 110, at 10, 30 and 50 % air saturation (impeller for gas dispersion from sparger-ring). The pH was controlled at 7.2 as far as it was possible with gas mixtures. In other runs, at 30 and 50 % (DO) in Bioflo 110, the cells grew at pH controlled with CO_2 and $NaHCO_3$ solution. Glucose, lactate, glutamine, and ammonium were quantified by enzymatic methods. Cell concentration, size and specific oxygen consumption were also determined. When $NaHCO_3$ solution was not used, the optimal DOs were 10 and 50 % air saturation for Celligen and Bioflo 110, respectively. In this condition maximum cell concentrations were higher than 4×10^6 cell/mL. An increase in maximum cell concentration of 36 % was observed in batch carried out at 30 % air saturation in a classical stirred tank bioreactor (Bioflo 110) with base solution addition. The optimal parameters defined in this work allow for bioprocess developing of viral vaccines, transient protein expression and viral vector for gene therapy based on BHK-21 cell line in two stirred tank bioreactors with different agitation–aeration systems.

Keywords BHK-21 · Stirred tank bioreactor · Dissolved oxygen · Mammalian cell culture · BHK-21 cell metabolism

E. G. F. Núñez (✉) · L. de Almeida Parizotto · B. L. V. da Costa · C. A. Pereira · A. Tonso
Laboratório de Células Animais, Departamento de Engenharia Química, Escola Politécnica, Universidade de São Paulo, Av. Prof. Luciano Gualberto, Trav. 3, 380, Butantã, P.O. Box 61548, São Paulo, SP 05508-900, Brazil
e-mail: eutimiocu@yahoo.com

J. Leme · W. A. Chagas · C. P. Caricati
Laboratório Especial de Pesquisa e Desenvolvimento em Imunológicos Veterinários, Instituto Butantan, Av. Vital Brasil, 1500, Butantã, São Paulo, SP 05503-900, Brazil

A. G. de Rezende · D. C. V. Monteiro · V. L. L. Boldorini · S. A. C. Jorge · R. M. Astray · C. A. Pereira
Laboratório de Imunologia Viral, Instituto Butantan, Av. Vital Brasil, 1500, Butantã, São Paulo, SP 05503-900, Brazil

Introduction

Mammalian cells culture has been widely used for recombinant proteins and viral vaccines production, as well as gene therapy (Park et al. 2010; Vester et al. 2010; Merten 2006). Among cell lines with extensive utilization for these purposes are Chinese hamster

Published online: 12 July 2013

ovary (CHO), NS0 mouse myeloma, Baby hamster kidney (BHK), Human embryonic kidney 293 (HEK-293) and few human-derived cell lines (Krampe and Al-Rubeai 2010). Specifically, BHK cells have found applications primarily in veterinarian viral vaccines (foot-and-mouth disease and rabies viruses), and recently in human recombinant therapeutic proteins such as Factor VIII (Bödeker et al. 1994; Kallel et al. 2003; Auniņš 2010). Microcarrier support (pseudo-suspension) and suspension cell culture systems have been explored for this cell line when the scale-up of bioprocess is desired, because of monolayer culture limitations on large-scale (Kallel et al. 2003; Perrin et al. 1995; Butler 2005; Astley et al. 2007). Nevertheless, microcarriers increase process cost and require extra optimization steps during development like microcarrier type and concentration. To overcome these drawbacks, cell lines, including BHK, have been adapted to grow as single cells in suspension. Thus, higher cell densities and concomitant volumetric productivities could be achieved as well as the scalability of the manufacturing process becomes easier (Silva et al. 2008).

Several bioreactors configurations have been assessed for mammalian cell culture. For suspension culture, homogeneous bioreactors similar to those for bacterial and yeast cultures can be used (Kelley et al. 2008). Stirred tank, air-lift and bubble column bioreactors have already been operated successfully with suspension cultures of mammalian cells (Sambanis and Hu 2008; Doelle et al. 2009; Handa-Corrigan et al. 1989). The selection of bioreactors to produce a particular biopharmaceutical from this type of animal cells has to meet special demands such as gentle aeration and agitation in order to avoid cell damage, in parallel some process parameters like pH, temperature and dissolved oxygen must be well controlled (Doelle et al. 2009). Concentrations of toxic metabolites (lactate and ammonia) need to be at low levels (Doelle et al. 2009; Cruz et al. 2000a). The main goal in this task is to obtain high cell and/or product concentration.

The aims of this work was to determine the influence of aeration-homogenization system in stirred tank bioreactors at different dissolved oxygen concentrations as well as pH control mode on BHK-21 cell growth and metabolism. The results could be useful for optimizing viral vaccines production and transient heterologous protein expression.

Materials and methods

Cell line and culture medium

BHK-21 (C-13) cells (Sigma-Aldrich ECACC Cell Lines, Lyon, France) adapted to single cell suspension culture were kindly supplied by Dr. Renaud Wagner from Ecole Superieure Biotechnologie de Strasbourg (France). The culture medium used had the following composition by volume: Iscove's Modified Dulbecco Medium with glutamine and Phenol red (IMDM, catalog number 12200-036, Gibco, Grand Island, NY, USA) 45.5 %, High glucose Dulbecco's Modified Eagle Medium (DMEM, catalog number 12100-046, Gibco, NY, USA) 45.5 %, heat inactivated fetal bovine serum (Catalog number 10082-147, Gibco) 5 %, 10 % m/v Pluronic F-68 (Sigma-Aldrich, St. Louis, MO, USA) aqueous solution 2 %, and 4 mM glutamine (Sigma-Aldrich) aqueous solution 2 %.

Inoculum preparation

One milliliter of BHK-21 cells (2×10^6 cell/mL) was thawed and placed in a 75 cm^2 tissue culture flask (vertical position) with 30 mL of culture medium for growing. Four days later, the cell suspension was used to inoculate (0.12×10^6 cell/mL) consecutively other tissue culture flasks with 25 and 75 cm^2, enough culture medium was added to reach final cellular suspensions of 10 and 30 mL, respectively. Inoculum for bioreactors was generated from 100 to 250 mL spinner flasks (Bellco Glass Inc., Vineland, NJ, USA), with operation volumes of 50 and 100 mL, respectively; the stirring speed was maintained at 30 rpm (Sci-Era quad drive stirrer system with a stirrer (Bellco Biotechnology, Vineland, NJ, USA). Spinners were previously inoculated (0.25×10^6 cell/mL) from 75 cm^2 tissue culture flask in the exponential phase. After 72 h, the inoculums for bioreactors were ready, the cell concentration and viability in spinners were $4.27 \times 10^6 \pm 0.85 \times 10^6$ cell/mL and 100 %, respectively. All the procedures described in this section were perfomed in an incubator (Thermoforma 3110, Marietta, OH, USA) at 37 °C and 5 % of carbon dioxide atmosphere.

Bioreactor cultures

Batch experiments in bioreactors were carried out in a 5 L Celligen (New Brunswick Scientific, Edison, NJ)

without aeration cage and 2 L Bioflo 110 (New Brunswick Scientific, Edison, NJ) at 37 °C, 80 rpm, with 2 and 1 L working volumes, respectively. The initial cell concentration was 0.25×10^6 cell/mL. For each bioreactor, dissolved oxygen was studied at 10, 30 and 50 % air saturation throughout the batch and the pH was controlled at 7.2 until possible using a gas mixture (carbon dioxide, air, oxygen and nitrogen). Two additional experiments were performed in Bioflo 110 at 30 and 50 % air saturation with controlling pH at 7.2 during the whole batch time, adding $NaHCO_3$ solution (8 % m/v) when necessary. Temperature, pH and dissolved oxygen over the course of batch cultures were online acquired by an in house LabVIEW program (National Instruments, Austin, TX ,USA). Other bioreactor operation parameters and aeration-homogenization details are shown in Table 1.

Cell counting and sizing

The cells were counted using improved Neubauer counting chamber (Precicolor, HBG, Giessen-Lützellinden, Germany) with proper sample dilution with Phosphate Buffer Saline. Viable cells were quantified in parallel using the trypan blue exclusion method (Augusto et al. 2010).

In some samples cell concentration and size were determined by Scepter handheld automated cell counter (Millipore, Billerica, MA, USA).

Nutrient and metabolite analysis

Five milliliter samples at different times during batches were taken. They were centrifuged at 750*g* for 4 min (Sorvall Biofuge Primo R Centrifuge, Thermo Electron Corp., Langenselbold, Germany). Subsequently, supernants were filtered through 0.22 µm filter (Millex-GV filter unit, Sao Paulo, Brazil) and frozen at −20 °C until analysis of nutrients and metabolites.

Glucose, lactate, glutamine and glutamate concentrations from supernant samples were measured using enzyme-coupled reaction and electrochemical detection, in YSI 2700 Select Bioanalyzer (YSI Life Sciences, Yellow Springs, OH, USA).

Ammonium quantification was performed by means of enzymatic–colorimetric method at 340 nm (EnzyChrom™ Ammonia/Ammonium Assay Kit (ENH3-100), BioAssay Systems, Hayward, CA, USA). Briefly, NADH was converted to NAD^+ in the presence of NH_3, ketoglutarate and glutamate dehydrogenase. The decrease in optical density is directly proportionate to ammonium and ammonia concentration in the samples.

Estimation of maximum specific growth rate, metabolite synthesis and nutrient consumption factors

Maximum specific growth rate, μ_{max}, was calculated by plotting natural logarithm of viable cell concentration versus time during exponential phase (Augusto et al. 2010).

Metabolite (lactate, glutamate and ammonium) to cell yield $\left(Y_{\frac{M}{x}}\right)$ for a given period was determined as Eq. 1:

$$Y_{M/x} = \frac{\Delta M}{\Delta X_v} = \frac{M(t_2) - M(t_1)}{X_v(t_2) - X_v(t_1)} \quad (1)$$

where $M(t_x)$ and X_v (t_x) are metabolite and cell concentration for a specific moment of the cell culture.

Nutrient (glucose and glutamine) consumption to cell yield $\left(Y_{\frac{N}{x}}\right)$ for a given period was calculated as Eq. 2:

$$Y_{N/x} = \frac{\Delta N}{\Delta X_v} = \frac{N(t_1) - N(t_2)}{X_v(t_2) - X_v(t_1)} \quad (2)$$

Table 1 Some operation parameters and aeration–homogenization devices for each stirred tank bioreactor

Bioreactor	Volumetric gas flow (mL/min)	VVM (min^{-1})*	Aeration–homogenization device	K_La (h^{-1})**
Celligen	400	0.2	Rotating gas-sparger	2.37
Bioflo 110	200		Classical (impeller for gas dispersion)	4.54

* VVM Volume of gas per liquid volume per minute

** K_La Volumetric oxygen transfer coefficient was determined experimentally by means of dynamic oxygen-electrode method (Scargiali et al. 2010)

where $N(t_x)$ is nutrient concentration for a specific moment of the cell culture.

Nutrient to metabolite conversion yield coefficients $\left(Y_{\frac{M}{N}}\right)$ (glutamine–ammonium and glucose–lactate pairs), for a given time interval, were calculated as Eq. 3:

$$Y_{M/N} = \frac{\Delta M}{\Delta N} = \frac{M(t_2) - M(t_2)}{N(t_1) - N(t_2)} \quad (3)$$

Cell specific oxygen consumption rate

The cell specific oxygen uptake rate (qO_2, nmol O_2 $cell^{-1}$ min^{-1}) was determined by dynamic method without modifications. It was quantified from the depletion in the dissolved oxygen concentration after stopping the gas flow. In this condition the mass balance for the dissolved oxygen can be simplified as Eq. 4. The qO_2 is obtained as the rate of oxygen uptake ratio (OUR_d) and cell concentration (X_v). OUR_d is calculated from the slope of the plot of dissolved oxygen concentration versus time after stopping gas flow (Eq. 4) (Garcia-Ochoa et al. 2010). The procedure was repeated at several moments during the batch experiment. Specific oxygen consumption rate were calculated assuming air saturation concentration of 0.21 mM for oxygen at 37 °C (Cruz et al. 2000a).

$$\left(\frac{dC}{dt}\right)_d = -q_{O_2} \cdot X_v = -OUR_d \quad (4)$$

where $\left(\frac{dC}{dt}\right)_d$ is the accumulation of oxygen in the liquid phase.

Results

Influence of aeration–homogenization system in stirred tank bioreactors, dissolved oxygen concentration (batches performed without base addition to control pH)

The optimal dissolved oxygen concentration for batch experiments without $NaHCO_3$ solution (8 % m/v) addition was different for each bioreactor under study. The highest maximum cell concentrations were 4.34×10^6 cell/mL and 4.59×10^6 cell/mL for Bioflo 110 (50 % DO) and Celligen (10 % DO), respectively (Table 2). As a rule the best batch cultures (maximum cell concentration as a criterion) with this kind of partial pH control were associated to longer times of culture with pH values oscillating around 7.2. The pH decrease for Bioflo 110 (50 % DO) and Celligen (10 % DO) appeared at 2.75 and 2.32 days, in that order (Fig. 1). Simultaneously, the ammonium and lactate synthesis factors were lower than those related to other batches performed at different DO in this pH control condition (Table 2). The glutamine and glucose metabolism at optimal DO conditions were more efficient. Specifically, for glucose, values of lactate-glucose conversion factors were the lowest and distant of 2 (theoretical value for total conversion to lactate) (Table 2).

The μ_{max} values were in the 1.30–1.93 day^{-1} and 1.49–1.81 day^{-1} ranges for Bioflo 110 and Celligen, respectively (Table 2). The end of exponential phase in all experiments was around 2 days after bioreactor inoculation (Fig. 2). In almost all experiments, the viability was inferior to 90 % after 4 days from the inoculum, the exception was the batch performed in Celligen at 10 % DO (cell viability = 92.9 %) (Fig. 2d). This batch matched with the lowest ammonium synthesis (Table 2).

Influence of pH control mode

When pH was controlled during the whole batch, similar (50 % DO) and improved (30 % DO) values of maximum cell concentrations with respect to those for batches without base solution addition were observed (Table 2; Fig. 2). Concurrently, the glucose was totally exhausted (Fig. 2).

Glutamine consumption to cell yields for the batch performed at 30 % DO with base addition was lower than the same batch without $NaHCO_3$ solution (8 % m/v) addition at the end of the exponential phase (36 %) and maximum cell concentration (39 %), meanwhile the same values for this parameter were observed at 50 % DO with both pH control modes (Table 2). Besides, the yield of lactate and ammonium per cell were also inferior at 30 % DO with base addition with respect to similar batches without base addition. Opposite performance was observed at 50 % DO (Table 2).

General findings

Discrepancies between cell counting by hemocytometer and scepter handheld automated cell counter were

Table 2 Nutrient consumption, metabolite synthesis, conversion nutrient to metabolite factors and other characteristic parameters for each batch experiment

Bioreactor	DO (%)	$NaHCO_3$ addition	X_{max}–H (10^6cell/mL)	X_{max}–S (10^6cell/mL)	μ_{max} (day^{-1})	Reference time (day)	$Y_{\frac{Gln}{x}}$ (pg/cell)	$Y_{\frac{Glc}{x}}$ (pg/cell)	$Y_{\frac{Glu}{x}}$ (pg/cell)	$Y_{\frac{NH_4}{x}}$ (pg/cell)	$Y_{\frac{Lac}{x}}$ (pg/cell)	$Y_{\frac{Glc}{Gln}}$ (mol/mol)	$Y_{\frac{NH_4}{Gln}}$ (mol/mol)	$Y_{\frac{Lac}{Glc}}$ (mol/mol)
Bioflo 110	10	Without	1.85	1.73	1.30	1.78^{EEP}	197	1317	10	14	1094	0.05	0.59	1.68
						2.23^{MCC}	238	1287	14	34	1049	0.06	1.17	1.65
	30	Without	3.63	2.95	1.93	2.23^{EEP}	139	655	12	14	536	0.09	0.85	1.65
						2.82^{MCC}	130	696	11	13	565	0.09	0.84	1.64
		With	4.94	3.94	1.52	2.24^{EEP}	102	533	3	8	378	0.03	0.60	1.44
						2.78^{MCC}	93	681	3	9	440	0.03	0.78	1.31
	50	Without	4.34	3.73	1.55	2.16^{EEP}	147	539	7	8	372	0.05	0.42	1.40
						2.83^{MCC}	115	581	7	8	368	0.06	0.58	1.28
		With	4.24	3.68	1.68	2.30^{EEP}	141	654	6	4	559	0.05	0.25	1.73
						2.88^{MCC}	116	988	7	6	752	0.06	0.44	1.54
Celligen	10	Without	4.59	3.51	1.81	1.98^{EEP}	111	692	7	0.2	492	0.06	0.01	1.44
						2.95^{MCC}	100	864	6	5.0	604	0.06	0.04	1.42
	30	Without	3.07	2.97	1.69	2.10^{EEP}	181	1045	27	5.5	919	0.15	0.25	1.78
						2.80^{MCC}	146	1059	19	4.4	914	0.13	0.25	1.75
	50	Without	3.16	3.35	1.49	2.01^{EEP}	204	1090	22	22	902	0.11	0.88	1.67
						2.67^{MCC}	223	1619	25	26	1335	0.11	0.94	1.67

All factors were calculated using as initial moment, the time when the first sample of batch experiments was taken. Reference times, end of exponential phase (EEP) and maximum cell concentration (MCM), were used to define the end of time interval to calculate factors. Gln, Glc, Glu, NH_4 and Lac represent glutamine, glucose, glutamate, ammonium and lactate, respectively. X_{max}–H and X_{max}–S represent maximum viable cell concentration determined by hemocytometer and total cell concentration by Millipore® Scepter handheld automated cell counter, respectively

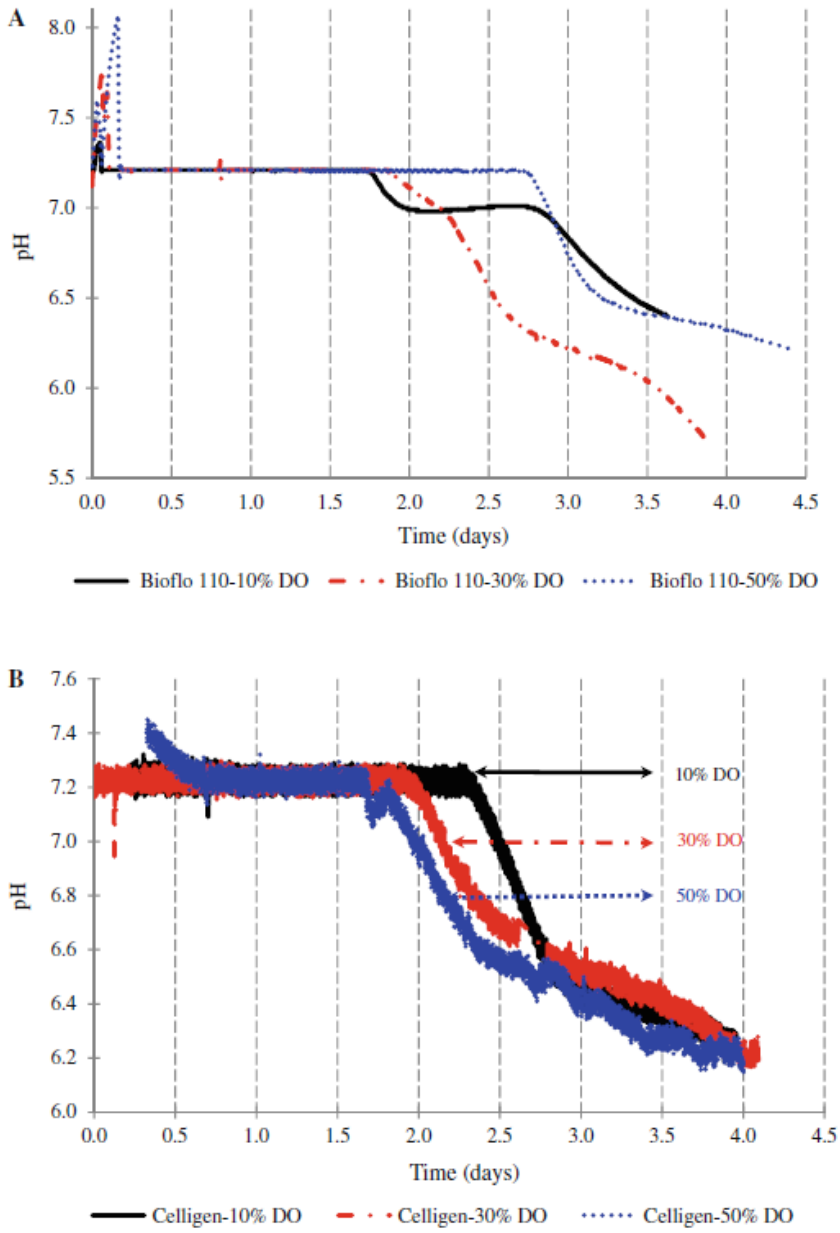

Fig. 1 pH profiles for the experiments performed in Celligen and Bioflo 110 bioreactors without addition of base solution to control pH. **a** Batches in Bioflo 110. **b** Batches in Celligen

detected. This was most evident for cell concentration higher than 3.5×10^6 cell/mL (Table 2). Probably, the changes of culture medium at high cell concentration interfere in impedance-based particle detection used by the scepter counter.

The oxygen cell consumption was higher in batches performed without base addition in Celligen. However, in both experimental conditions, a decrease in the cell specific oxygen consumption rate throughout the experiment was confirmed (Fig. 3). At the end of the batches, the qO_2 values were similar (1.14–4.75 10^{-7} nmol O_2 $cell^{-1}$ min^{-1}). A similar inverse relationship between cell size and culture time was also observed. As a conclusion, for this parameter, highest maximum cell concentrations were associated to smallest cell size at the end of batch culture. When maximum cell

Fig. 2 Profiles of viable cell concentration, cell viability, nutrients (glutamine and D-glucose) and metabolites (glutamate, ammonium and L-Lactate).
a Bioflo 110–10 % DO.
b Bioflo 110–30 % DO.
c Bioflo 110–50 % DO.
d Celligen-10 % DO.
e Celligen-30 % DO.
f Celligen-50 % DO.
g Bioflo 110–30 % DO (with $NaHCO_3$ addition).
h Bioflo 110–50 % DO (with $NaHCO_3$ addition)

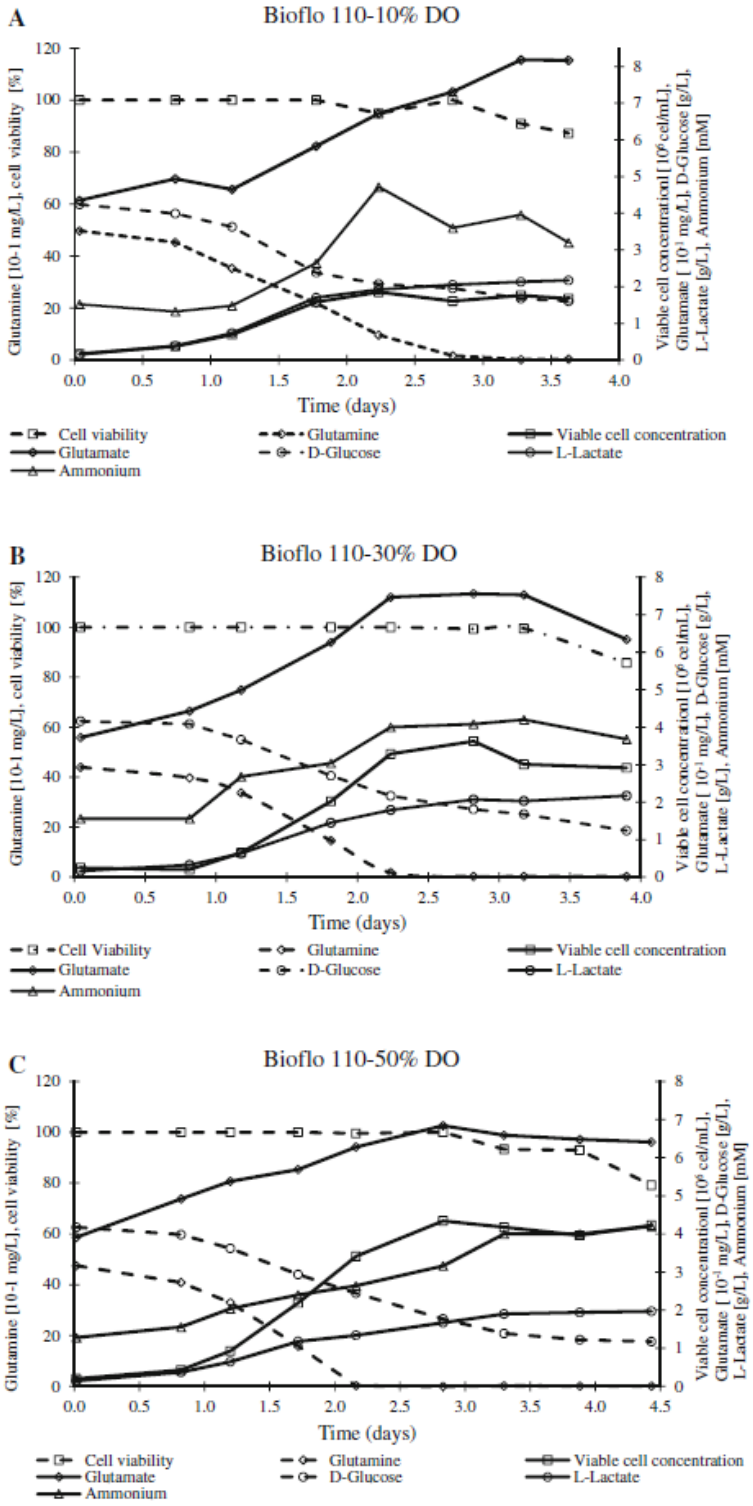

Fig. 2 continued

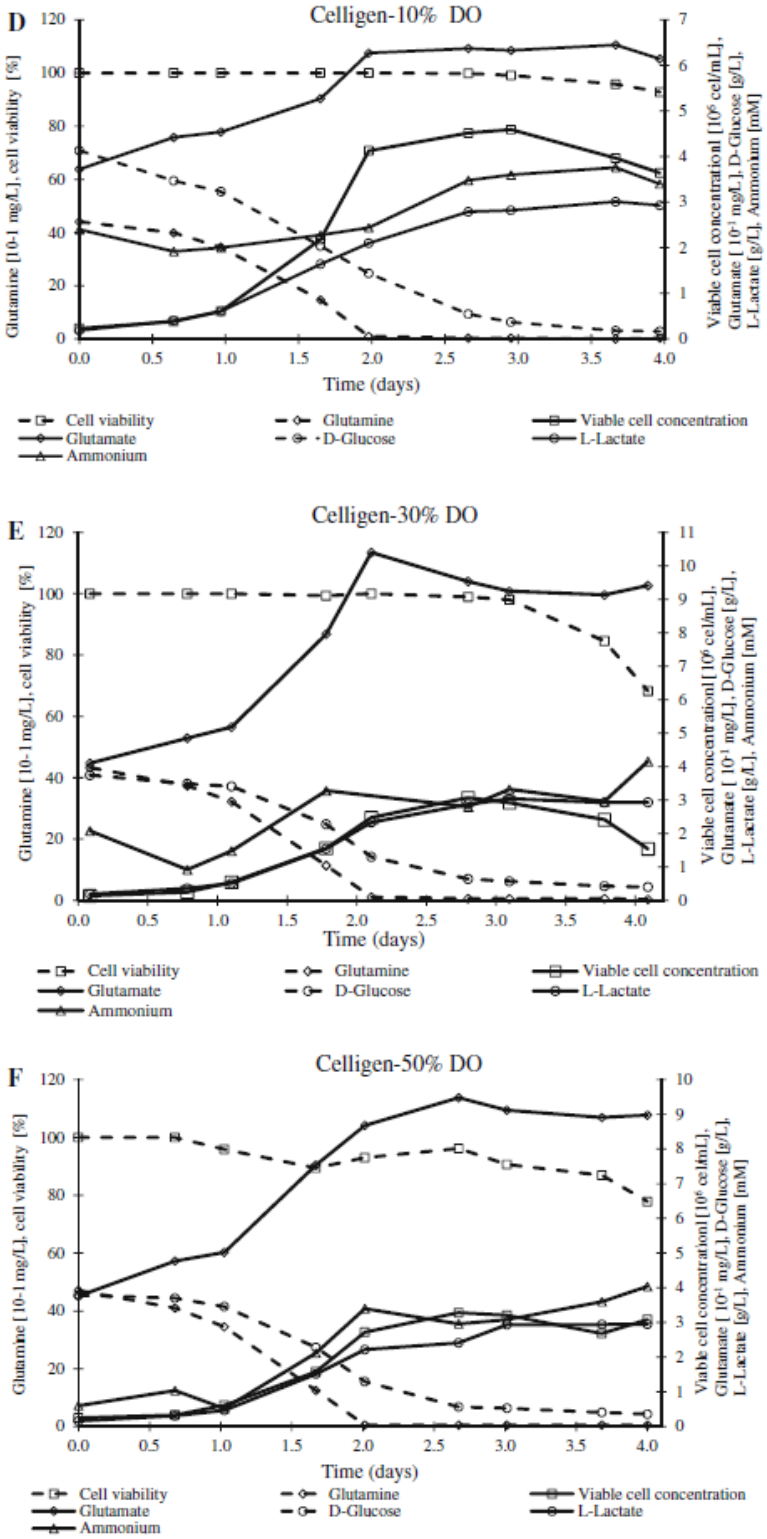

Fig. 2 continued

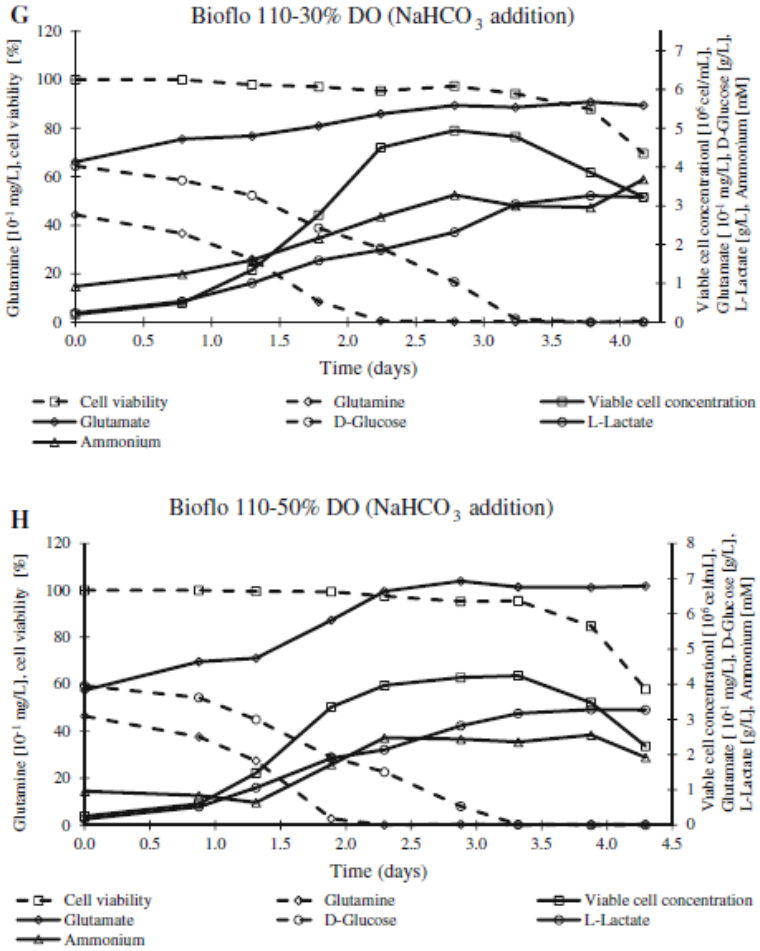

concentrations were higher than 4×10^6 cell/mL, the cell sizes were smaller than 11 µm (Fig. 4).

Discussion

Despite the high number of publications about BHK-21 culture in bioreactors and metabolism (Kallel et al. 2003; Perrin et al. 1995; Teixeira et al. 2005; Cruz et al. 2000b), combined studies about different bioreactors assessment at different dissolved oxygen concentrations are not often addressed. Similarly, the impact of pH control mode (with or without base addition) is not usually set.

In the present work a classical stirred tank bioreactor (Bioflo 110) was compared to a modified cell lift impeller bioreactor (Celligen) (Mirro and Voll 2009). The modifications consisted of removing the aeration cage (useful for cell culture with microcarriers) and the working volume level was lower in relation to the discharge ports. Thus, the agitation device was a rotating gas-sparger. To avoid cell damage caused by shear forces resulting from mechanical agitation and aeration, it was included in culture medium composition, Pluronic F-68 (0.2 % m/v) was included in culture medium composition, its protecting effect was reinforced with fetal bovine serum addition (Molina-Grima et al. 1997).

The maximum cell concentrations ($1.85-4.94 \times 10^6$ cell/mL, Table 2) for both bioreactors under study, operating in different conditions, were higher or similar to other reported values for this parameter in BHK-21 or recombinant BHK-21 cells suspension cultures using fetal bovine serum or serum-free or

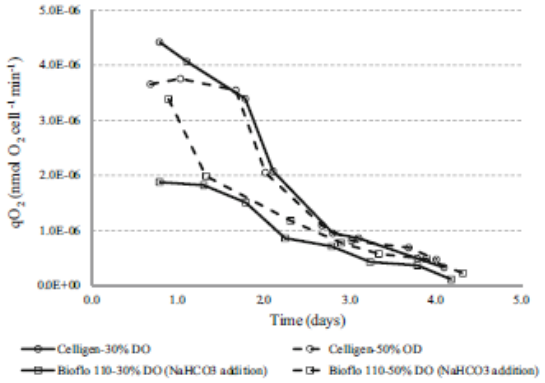

Fig. 3 Cell specific oxygen consumption rate profile for batches performed in different bioreactors with or without $NaHCO_3$ addition

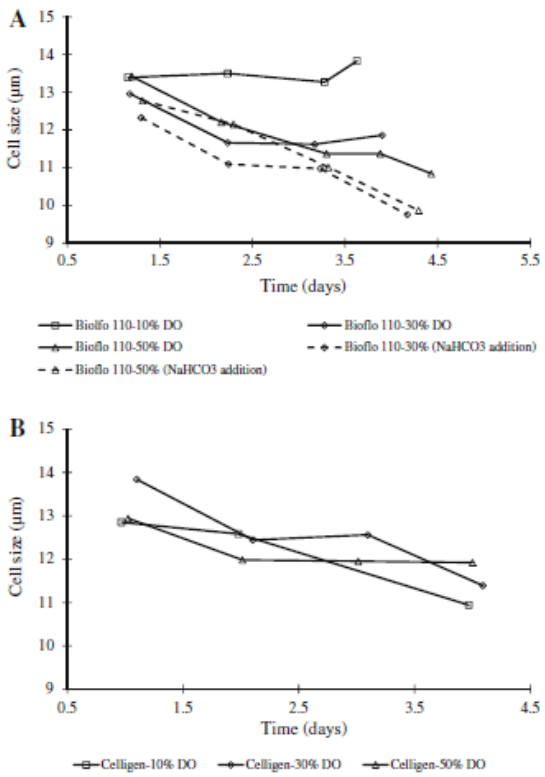

Fig. 4 Cell size profiles defined by Millipore® Scepter handheld automated cell counter. **a** Bioflo. **b** Celligen

protein-free media in batch mode ($1-3.2 \times 10^6$ cell/mL) (Handa-Corrigan et al. 1989; Cruz et al. 2002; Moreira et al. 1995; Ishaque et al. 2007). In general, the studies related with increase of cell concentration in BHK-21 cell lines are focused on the optimization of the glutamine and glucose metabolism (Cruz et al. 2000a; Cruz et al. 2000b; Butler and Jenkins 1989). Rarely, the influence of cell physical environment and the concentration of other important molecule for both metabolic pathways, oxygen, are explored for this purpose. In the present work, low glucose and glutamine consumption to cell yield, as well as low lactate-glucose and ammonium-glutamine yield coefficients were observed in both bioreactors when highest maximum cell concentrations were reached (Table 2). This suggests that 10 and 50 % DO for Celligen and Bioflo 110 (without base addition) are proper conditions for more efficient glucose and glutamine metabolism of BHK-21 cell with a culture medium with 4 g/L of glucose and 3.72 mM of glutamine. The earlier drop of initial pH (7.2) (Fig. 1) in those experiments with low values of maximum cell concentration could be explained by the high production of lactate and ammonium, metabolites responsible for pH decrease and growth inhibition (Cruz et al. 2000a). However, carbon dioxide (CO_2) accumulation effect (inducing pH decrease) in culture media should not be neglected. The differences between optimal DO for each bioreactor could be justified by different efficient conditions for CO_2 stripping out. It has been reported that aeration systems designed for effective oxygen transfer will not necessarily be efficient for CO_2 removal (Birch 2010). Probably, gas mixtures to keep constant low DO (10 %) are suitable to CO_2 stripping from culture broth and favoring BHK-21 metabolism and respiration in a stirred tank bioreactor with a rotating gas-sparger (Celligen with modifications).

The effective pH control throughout the whole batch prevents the intracellular acidification and as a consequence, normal cell physiology is guaranteed. Thus the negative effects of lactate and ammonium ions is reduced, because of the reduction of their intrinsic toxicity and osmolarity effects. Therefore, the improvement of maximum cell concentration and glutamine consumption to cell yield at 30 % DO in the Bioflo 110 as well as the total glucose total consumption (30 and 50 % DO) when base solution was added is justified by this pH control mode in bioreactor (Table 2; Fig. 2b, e). However, an increase in the maximum cell concentration was not observed at 50 % DO. Probably, the bioconversion yield ($Y_{\frac{Gln}{x}}$, $Y_{\frac{Glc}{x}}$) without or with base addition was similar because gas

mixture compositions at this DO are able to maintain pH constant until the minimum limit value for glutamine consumption to cell yield for BHK-21 cell line at 50 % DO. Thus, it was demonstrated that base addition to control pH at 7.2 was not necessary to improved maximum cell concentration at 50 % DO in the Bioflo 110 bioreactor (Figs. 1a, 2c, h).

Based on the direct relationship between the end of the exponential phase and glutamine depletion, glutamine could be considered the limiting substrate. However, the increase of this amino acid concentration in culture medium is not a suitable alternative in order to increase maximum cell concentration because high ammonium synthesis could be induced at glutamine concentration above 4 mM (Butler and Jenkins 1989). Ammonium levels for this culture medium (3.72 mM of glutamine) were already high enough to promote apoptosis in BHK cells (>2 mM) (Teixeira et al. 2005). In addition, ammonium is released by cells due to the amino acids (Schneider et al. 1996), and not only due to glutamine metabolism; the values of $Y_{NH_4/Gln}$ are much lower than 2 (theoretical value for a complete oxidation of glutamine through the tricarboxylic acid cycle) (Table 2). This result suggests that glucose is the principal energetic source for BHK cells in both bioreactors in the 10–50 % DO range, in particular for Celligen 10 % DO (Table 2). On the other hand, batch with low maximum cell concentrations in Celligen (30 and 50 % DO) were associated to high $Y_{Glu/Gln}$ values. This could be justified by the enhanced action of glutaminase (responsible for enzymatic glutamine degradation into glutamate and ammonium in bioreaction broth) contained in fetal bovine serum (Ozturk and Palsson 1990), at 30 and 50 % DO in the rotating gas-sparger bioreactor (Table 2).

Considering that lactate was only produced by aerobic glycolysis (lactate formation is also possible from glutamine (Schneider et al. 1996)), more than 64 % $\left(Y_{Lac/Glc} = 1.28\right)$ of glucose was metabolized following this metabolic route for all experiments (Table 2); the rest was metabolized through tricarboxylic acid cycle. Under normal condition, mammalian cells in bioreactors consume large amounts of glucose; nearly 90 % of this monosaccharide is converted to lactate (Mulukutla et al. 2010). For DO concentration which ensures highest cell concentration in Celligen without aeration cage (10 % air saturation), upto 71 % of glucose was converted to lactate. With the same criterion, for the best conditions in stirred tank bioreactor assessed in this work (DO at 30 % air saturation and pH control with base solution addition), the lactate–glucose conversion percentage was at most of 66 %. Thus, the use of glucose in optimal conditions for both bioreactors was similar to other reported values for BHK-21 culture at high glucose concentrations ($Y_{Lac/Glc}$, in 1.5–1.6 mol/mol range) (Cruz et al. 1999) and suitable for mammalian cell culture (much less than 90 %) (Mulukutla et al. 2010).

The maximum lactate concentration at the end of the exponential phase among performed batches was 2.33 g/L (26 mM), for Celligen at 30 % air saturation (Fig. 2). Therefore, the BHK-21 cell culture in conditions considered in this work should not be inhibited by lactate, because it has been reported that inhibitory lactate concentrations for BHK-21 cells were around 28 mM in suspension cultures (Cruz et al. 2000a).

The proximity of conversion factors for two critical moments of the batch (Table 2), the end of the exponential phase and the maximum cell concentration, was confirmed. In general, the time difference is around 12 h. This also suggests a substrate (glutamine) inhibition of growth as was previously mentioned (Radlett et al. 1971).

The maximum specific growth rate for mammalian cells varies in the range of 0.55–1.39 day^{-1} (Dietmair et al. 2012). In both Celligen and Bioflo BHK-21 cultures, the maximum specific growth rates were higher or next to the superior limit of the usual range for this variable (Table 2). This is an important parameter for maximizing production of viruses when they are more active in cycling cells. It has been demonstrated by several authors that enhanced cell growth rates should lead to an increased viral production rate (Merten 2004). Thus, BHK-21 cell line, culture medium and bioreactor configurations used in this study are suitable for viral vaccine manufacturing, transient protein expression and gene therapy vector production.

Regarding, cell specific oxygen uptake rates, their profiles and values for evaluated conditions in both bioreactors were similar to others as previously reported (Cruz et al. 2000a; Cruz et al. 1999) for the BHK-21 cell line at high initial glucose concentration (4 g/L). The decrease of cell specific oxygen uptake

rates over the course of bioconversion could be justified by changes in medium composition and cell growth phase (Garcia-Ochoa et al. 2010; Jorjani and Ozturk 1999). The lactate concentration increase has a direct influence on cell specific oxygen uptake rate decrease (Cruz et al. 2000a). Higher initial cell specific oxygen uptake rates in Celligen is an evidence of more efficient glucose metabolism in this bioreactor compared to the Bioflo 110 bioreactor at the beginning of batches (Fig. 3).

Low cell size was an indicative of the high cell concentration in both bioreactor (Figs. 2, 4). One of the causes of this relationship could be the osmolarity increase. Higher osmolarity results in a decrease of cell volume due to the enhanced efflux of water (Seewöster and Lehmann 1997). It has been reported that accumulation of lactate leads to high osmolarity (Li et al. 2010). As high lactate concentrations were directly correlated with high cell concentrations (Fig. 2), this metabolite could be the main component for the increase in osmolarity.

Conclusion

Taking into consideration the highest maximum BHK-21 cell concentration as choice criterion, best dissolved oxygen concentrations for assessed stirred tank bioreactors were 10 (rotating gas-sparger) and 50 % (with impeller for gas dispersion) air saturation. As a consequence, the impact of aeration–homogenization system on BHK-21 cell growth and metabolism was quantified. These findings are valid when no $NaHCO_3$ solution (8 % m/v) is added to control pH. Addition of base solution in conjunction with CO_2 in aeration mixtures could be significant, but it depends on dissolved oxygen concentration. In this work, maximum BHK-21 cell concentration at 30 % air saturation in classical stirred tank was improved in 36 % when the pH was controlled during the whole bioreaction time with respect to a similar experiment perfomed without base addition. Nevertheless, no differences were detected for 50 % air saturation for the same bioreactor. The optimal parameters defined in this work allow for bioprocess development for manufacturing of viral vaccines, transient protein expression and viral vector production for gene therapy purposes based on the use BHK-21 cells grown in suspension in two types of bioreactors operating in batch mode.

Acknowledgments The authors would like to thank Fundação de Amparo à Pesquisa do Estado de São Paulo (FAPESP) for post-doctoral fellowship (2010/52521-6), Fundação para o Desenvolvimento Tecnológico da Engenharia (FDTE) and Conselho Nacional de Desenvolvimento Científico e Tecnológico (CNPq: 483009/2010-5) for scientific grants. First author gratefully acknowledges his wife and daughter, Relma and Giovanna for the inspiration to write this paper.

References

Astley K, Naciri M, Racher A, Al-Rubeai M (2007) The role of $p21^{cipl}$ in adaptation of CHO cells to suspension and protein-free culture. J Biotechnol 130:282–290

Augusto EFP, Moraes AM, Piccoli RAM, Barral MF, Suazo CAT, Tonso A, Pereira CA (2010) Nomenclature and guideline to express the amount of a membrane protein synthesized in animal cells in view of bioprocess optimization and production monitoring. Biologicals 38:105–112

Aunipš JG (2010) Viral vaccine production in cell culture. In: Flickinger MC (ed) Encyclopedia of industrial biotechnology: bioprocess, bioseparation, and cell technology. Wiley, New York, pp 1–35

Birch JR (2010) Suspension culture, animal cells. In: Flickinger MC (ed) Encyclopedia of industrial biotechnology: bioprocess, bioseparation, and cell technology. Wiley, Hoboken, pp 1–28

Bödeker BGD, Newcomb R, Yuan P, Braufman A, Kelsey W (1994) Production of recombinant factor VIII from perfusion cultures: I. Large-scale fermentation. In: Spier RE, Griffiths JB, Berthold W (eds) Animal cell technology: Products of today, prospects for tomorrow. Butterworth-Heinemann, Oxford, UK, pp. 580–583

Butler M (2005) Animal cell cultures: recent achievements and perspectives in the production of biopharmaceuticals. Appl Microbiol Biotechnol 68:283–291

Butler M, Jenkins H (1989) Nutritional aspects of the growth of animal cells in culture. J Biotechnol 12:97–110

Cruz HJ, Ferreira AS, Freitas CM, Moreira JL, Carrondo MJT (1999) Metabolic responses to different glucose and glutamine levels in baby hamster kidney cell culture. Appl Microbiol Biotechnol 51:579–585

Cruz HJ, Freitas CM, Alves PM, Moreira JL, Carrondo MJT (2000a) Effects of ammonia and lactate on growth, metabolism, and productivity of BHK cells. Enzyme Microb Tech 27:43–52

Cruz HJ, Moreira JL, Carrondo MJT (2000b) Metabolically optimised BHK cell fed-batch cultures. J Biotechnol 80:109–118

Cruz HJ, Conradt HS, Dunker R, Peixoto CM, Cunha AE, Thomaz M, Burger C, Dias EM, Clemente J, Moreira JL, Rieke E, Carrondo MJT (2002) Process development of a recombinant antibody/interleukin-2 fusion protein expressed in protein-free medium by BHK cells. J Biotechnol 96:169–183

Dietmair S, Nielsen LK, Timmins NE (2012) Mammalian cells as biopharmaceutical production hosts in the age of omics. Biotechnol J 7:75–89

Doelle HW, Fiechter A, van Griensven M, Kasper C, Pörtner R, Schlegel G, Shimizu S, Stahl F, Suck K, Yamada H, Zorn H (2009) Biotechnology 6. Special applications. Ullmann's encyclopedia of industrial chemistry. Wiley, New York, pp 73–112

Garcia-Ochoa F, Gomez E, Santos VE, Merchuk JC (2010) Oxygen uptake rate in microbial processes: an overview. Biochem Eng J 49:289–307

Handa-Corrigan A, Emery AN, Spier RE (1989) Effect of gas–liquid interfaces on the growth of suspended mammalian cells: mechanisms of cell damage by bubbles. Enzyme Microb Tech 11:230–235

Ishaque A, Thrift J, Murphy JE, Konstantinov K (2007) Overexpression of Hsp70 in BHK-21 cells engineered to produce recombinant factor VIII promotes resistance to apoptosis and enhances secretion. Biotechnol Bioeng 97:144–155

Jorjani P, Ozturk SS (1999) Effects of cell density and temperature on oxygen consumption rate for different mammalian cell lines. Biotechnol Bioen 64:349–356

Kallel H, Rourou S, Majoul S, Loukil H (2003) A novel process for the production of a veterinary rabies vaccine in BHK-21 cells grown on microcarriers in a 20-l bioreactor. App Microbiol Biotechnol 61:441–446

Kelley BD, Chiou TW, Rosenberg M, Wang DIC (2008) Industrial animal cell culture. In: Rehm HJ, Reed G (eds) Biotechnology set, 2nd edn. Wiley, Weinheim, pp 23–38

Krampe B, Al-Rubeai M (2010) Cell death in mammalian cell culture: molecular mechanisms and cell line engineering strategies. Cytotechnology 62:175–188

Li F, Vijayasankaran N, Shen AY, Kiss R, Amanullah A (2010) Cell culture processes for monoclonal antibody production. MAbs 2:466–477

Merten O-W (2004) State-of-the-art of the production of retroviral vectors. J Gene Med 6:S105–S124

Merten O-W (2006) Introduction to animal cell culture technology—past, present and future. Cytotechnology 50:1–7

Mirro R, Voll K (2009) Which impeller is right for your cell line? A guide to impeller selection for stirred-tank bioreactors. BioProcess Int 7:52–57

Molina-Grima E, Chisti Y, Moo-Young M (1997) Characterization of shear rates in airlift bioreactors for animal cell culture. J Biotechnol 54:195–210

Moreira JL, Alves PM, Feliciano AS, Aunins JG, Carrondo MJT (1995) Serum-free and serum-containing media for growth of suspended BHK aggregates in stirred vessels. Enzyme Microb Tech 17:437–444

Mulukutla BC, Khan S, Lange A, Hu WS (2010) Glucose metabolism in mammalian cell culture: new insights for tweaking vintage pathways. Trends Biotechnol 28:476–484

Ozturk SS, Palsson BO (1990) Chemical decomposition of glutamine in cell culture media: effect of media type, pH, and serum concentration. Biotechnol Prog 6:121–128

Park JH, Park HH, Park TH (2010) Cellular engineering for the high-level production of recombinant proteins in mammalian cell systems. Korean J Chem Eng 27:1042–1048

Perrin P, Madhusudana S, Gontier-Jallet C, Petres S, Tordo N, Merten O-W (1995) An experimental rabies vaccine produced with a new BHK-21 suspension cell culture process: use of serum-free medium and perfusion-reactor system. Vaccine 13:1244–1250

Radlett PJ, Telling RC, Stone J, Whiteside JP (1971) Improvements in the growth of BHK-21 cells in submerged culture. Appl Microbiol 22:534–537

Sambanis A, Hu WS (2008) Cell culture bioreactors. In: Rehm HJ, Reed G (eds) Biotechnology set, 2nd edn. Wiley, Weinheim, pp 105–125

Scargiali F, Busciglio A, Grisafi F, Brucato A (2010) Simplified dynamic pressure method for kLa measurement in aerated bioreactors. Biochem Eng J 49:165–172

Schneider M, Marison IW, von Stockar U (1996) The importance of ammonia in mammalian cell culture. J Biotechnol 46:161–185

Seewöster T, Lehmann J (1997) Cell size distribution as a parameter for the predetermination of exponential growth during repeated batch cultivation of CHO cells. Biotechnol Bioeng 55:793–797

Silva AC, Delgado I, Sousa MFQ, Carrondo MJT, Alves PM (2008) Scalable culture systems using different cell lines for the production of Peste des Petits ruminants vaccine. Vaccine 26:3305–3311

Teixeira A, Cunha AE, Clemente JJ, Moreira JL, Cruz HJ, Alves PM, Carrondo MJT, Oliveira R (2005) Modelling and optimization of a recombinant BHK-21 cultivation process using hybrid grey-box systems. J Biotechnol 118:290–303

Vester D, Rapp E, Kluge S, Genzel Y, Reichl U (2010) Virus–host cell interactions in vaccine production cell lines infected with different human influenza A virus variants: a proteomic approach. J Proteomics 73:1656–1669

AIChE

A Multivariate Calibration Procedure for UV/VIS Spectrometric Monitoring of BHK-21 Cell Metabolism and Growth

Jaci Leme[†]
Laboratório Especial de Pesquisa e Desenvolvimento em Imunológicos Veterinários, Instituto Butantan. Av. Vital Brasil, 1500, Butantã, 05503-900, São Paulo, SP–Brazil

Eutimio Gustavo Fernández Núñez[†]
Dept. de Engenharia Química, Laboratório de Células Animais, Escola Politécnica, Universidade de São Paulo. Av. Prof. Luciano Gualberto, trav. 3, 380, Butantã, 05508-900, São Paulo, SP–Brazil

Dept. de Ciências Biológicas, Universidade Estadual Paulista "Júlio de Mesquita Filho" Campus-Assis, Avenida Dom Antonio 2100, Bairro Parque Universitário, 19806-900, Assis, SP – Brasil

Letícia de Almeida Parizotto
Dept. de Engenharia Química, Laboratório de Células Animais, Escola Politécnica, Universidade de São Paulo. Av. Prof. Luciano Gualberto, trav. 3, 380, Butantã, 05508-900, São Paulo, SP–Brazil

Wagner Antonio Chagas, Erica Salla dos Santos, and Aline Tojeira Prestia Caricati
Laboratório Especial de Pesquisa e Desenvolvimento em Imunológicos Veterinários, Instituto Butantan. Av. Vital Brasil, 1500, Butantã, 05503-900, São Paulo, SP–Brazil

Alexandre Gonçalves de Rezende
Laboratório de Imunologia Viral, Instituto Butantan. Av. Vital Brasil, 1500, Butantã, 05503-900, São Paulo, SP–Brazil

Bruno Labate Vale da Costa
Dept. de Engenharia Química, Laboratório de Células Animais, Escola Politécnica, Universidade de São Paulo. Av. Prof. Luciano Gualberto, trav. 3, 380, Butantã, 05508-900, São Paulo, SP–Brazil

Laboratório de Biotecnologia Industrial, Núcleo de Bionanomanufatura, Instituto de Pesquisas Tecnológicas do Estado de São Paulo, Av. Prof. Almeida Prado 532 Cid. Universitária - Butantã, 05508-901, São Paulo, SP–Brazil

Daniela Cristina Ventini Monteiro, Vera Lucia Lopes Boldorini, Soraia Attie Calil Jorge, and Renato Mancini Astray
Laboratório de Imunologia Viral, Instituto Butantan. Av. Vital Brasil, 1500, Butantã, 05503-900, São Paulo, SP–Brazil

Carlos Augusto Pereira
Dept. de Engenharia Química, Laboratório de Células Animais, Escola Politécnica, Universidade de São Paulo. Av. Prof. Luciano Gualberto, trav. 3, 380, Butantã, 05508-900, São Paulo, SP–Brazil

Laboratório de Imunologia Viral, Instituto Butantan. Av. Vital Brasil, 1500, Butantã, 05503-900, São Paulo, SP–Brazil

Celso Pereira Caricati
Laboratório Especial de Pesquisa e Desenvolvimento em Imunológicos Veterinários, Instituto Butantan. Av. Vital Brasil, 1500, Butantã, 05503-900, São Paulo, SP–Brazil

Aldo Tonso
Dept. de Engenharia Química, Laboratório de Células Animais, Escola Politécnica, Universidade de São Paulo. Av. Prof. Luciano Gualberto, trav. 3, 380, Butantã, 05508-900, São Paulo, SP–Brazil

DOI 10.1002/btpr.1847
Published online December 19, 2013 in Wiley Online Library (wileyonlinelibrary.com)

Monitoring mammalian cell culture with UV–vis spectroscopy has not been widely explored. The aim of this work was to calibrate Partial Least Squares (PLS) models from off-line UV–vis spectral data in order to predict some nutrients and metabolites, as well as viable cell concentrations for mammalian cell bioprocess using phenol red in culture medium. The BHK-21 cell line was used as a mammalian cell model. Spectra of samples taken from batches performed at different dissolved oxygen concentrations (10, 30, 50, and 70% air saturation), in two bioreactor configurations and with two strategies to control pH

[†]Both authors contributed equally to this work.
Correspondence concerning this article should be addressed to E. G. Fernández Núñez at eutimiocu@yahoo.com.

© 2013 American Institute of Chemical Engineers

were used to calibrate and validate PLS models. Glutamine, glutamate, glucose, and lactate concentrations were suitably predicted by means of this strategy. Especially for glutamine and glucose concentrations, the prediction error averages were lower than 0.50 ± 0.10 mM and 2.21 ± 0.16 mM, respectively. These values are comparable with those previously reported using near infrared and Raman spectroscopy in conjunction with PLS. However, viable cell concentration models need to be improved. The present work allows for UV–vis at-line sensor development, decrease cost related to nutrients and metabolite quantifications and establishment of fed-batch feeding schemes. © 2013 American Institute of Chemical Engineers *Biotechnol. Prog.*, 30:241–248, 2014
Keywords: UV–vis spectroscopy, partial least squares, BHK-21, cell culture monitoring

Introduction

Since 2004, when Food and Drug Administration launched the Process Analytical Technology (PAT), biopharmaceutical companies were encouraged to adopt modern bioprocess monitoring techniques based on on-line or at-line analysis of key variables. This initiative is useful for early detection of faults, as a consequence, to maximize the probability of high quality products at the end of the process.[1] The concepts associated to PAT can be also applied during the initial stages of bioprocess development at the lab scale, both in academic and industrial contexts, to characterize and validate them.[2]

Multivariate data analysis is considered to be a helpful tool within PAT because of its potential for expanding understanding and reducing development bioprocess time.[3] Multivariate techniques, such as Principal Component Analysis and Partial Least Squares (PLS), reduce the high number of dimensions of the collected data over the course of batches. Thus, they enable the identification of correlations between relevant variables.[4]

At present, few process-related variables (pH, temperature, dissolved oxygen concentration, biovolume, and cell density) can be monitored using in situ probes.[5,6] Hence, to access to the real-time evolution of cell metabolism, the development of new PAT methods for metabolic parameters are needed. The combinations of spectroscopic methods and multivariate data analysis in animal cell cultures have been used to simultaneously provide on-line, at-line and off-line information about several bioprocess variables, including culture medium composition (nutrients and metabolites) and living cells number.[1,7–9] Among spectroscopic techniques, near infrared spectra has been widely exploited with this purpose.[1,10] Specifically, in mammalian cell culture, nuclear magnetic resonance, fluorescence and Raman spectroscopies have been also used for monitoring nutrients, metabolites and viable cell concentration.[11,12] The lack of use of ultraviolet-visible spectroscopy in mammalian cell bioprocess could be justify by the poor information of UV–vis spectra due to the broad and unspecific bands obtained, the inability to detect higher energy electronic levels in molecules, as well as the spectral interferences of a second, dispersed phase (cells and gas bubbles) because of light scattering effects.[10]

Most of the biopharmaceuticals are complex recombinant proteins, for this reason, mammalian cells are the hosts of choice because they ensure the correct post-translational modifications to confer function and safety.[13] This kind of animal cells has been also frequently used for viral vaccine production.[14] Among mammalian cells, the BHK-21 cell line has found applications in veterinarian viral vaccines and heterologous protein production, even in the transient mode.[15,16]

Many media formulations for mammalian cell culture often contain an optional pH indicator, phenol red. This dye provides a useful, visual but qualitative mode for monitoring metabolism within a culture device.[17]

The aim of this work was to calibrate a PLS model for glutamine, glutamate, glucose, lactate, and viable cell concentration based on off-line ultraviolet-visible spectra for BHK-21 suspension cell culture in bioreactors. This study could represent an important step for developing non-invasive on-line metabolic monitoring devices for BHK-21 cell bioreactors.

Material and Methods

Cell line and culture medium

BHK-21 (C-13) cells (Sigma-Aldrich ECACC Cell Lines, Lyon, France) adapted to single cell suspension culture were kindly supplied by Dr. Renaud Wagner from Ecole Superieure Biotechnologie de Strasbourg, France. The culture medium for this cell line had the following composition by volume: Iscove's Modified Dulbecco Medium with glutamine and Phenol red (IMDM, catalog number 12200-036, Gibco, NY) 45.5%, High glucose Dulbecco's Modified Eagle Medium (DMEM, catalog number 12100-046, Gibco, NY) 45.5%, heat inactivated fetal bovine serum (Catalog number 10082-147, Gibco, Grand Island, NY) 5%, 10% m/v Pluronic F-68 (Sigma-Aldrich, St. Louis, MO) aqueous solution 2%, and 4 mM glutamine (Sigma-Aldrich, Tokyo, MO) aqueous solution 2%.

Inoculum preparation

One milliliter of BHK-21 cells (2×10^6 cell/mL) was thawed and placed in a 75 cm^2 tissue culture flask (vertical position) with 30 mL of culture medium for growing. Four days afterwards, the cell suspension was used to inoculate (0.12×10^6 cell/mL) consecutively other tissue culture flasks with 25 and 75 cm^2; enough culture medium was added to reach final cellular suspensions of 10 and 30 mL, respectively. Inoculum for bioreactors was generated from 100 and 250 mL spinner flasks (Bellco Glass, Vineland, NJ), with working volumes of 50 and 100 mL, respectively; the stirring speed was maintained at 30 rpm (Sci-Era quard drive stirrer system with a stirrer, Bellco Biotechnology, Vineland, NJ). Spinners were previously seeded (0.25×10^6 cell/mL) from 75 cm^2 tissue culture flask in the exponential phase. After 72 h, the inoculums for bioreactors were ready; the cell concentration and viability in spinners were 4.27×10^6 cell/mL $\pm 0.85 \times 10^6$ cell/mL and 100%, respectively. All the procedures described in this section were performed into an incubator (Thermoforma 3110, Marietta, OH) at 37°C and 5% of carbon dioxide atmosphere.

Bioreactor cultures

Batch experiments in bioreactors were carried out in a 5 L Celligen (New Brunswick Scientific, Edison, NJ) without

aeration cage and 2 L Bioflo 110 (New Brunswick Scientific, Edison, NJ) at 37°C, agitation at 80 rpm. Bioreactors operated with 2 and 1 L working volumes, respectively, with initial cell concentration of 0.25×10^6 cell/mL.

Using a variable gas mixture (carbon dioxide, air, oxygen, and nitrogen), different controlled dissolved oxygen concentrations were assessed: for Celligen (400 mL/min volumetric gas flow), 10, 30, and 50% of air saturation was used and for the experiments performed in the Bioflo 110 (200 mL/min volumetric gas flow), 10, 30, 50, and 70% were used. The pH for both bioreactors was also controlled at 7.2 just with CO_2 until it was possible, according to buffering capacity of $NaHCO_3$-CO_2 system.

Additional experiments were performed in duplicate in Bioflo 110 at 30 and 50% air saturation controlling pH at 7.2 during whole batch time, adding gas CO_2 or $NaHCO_3$ solution (8% m/v) when necessary. Temperature, pH and dissolved oxygen over the course of batch cultures were acquired online using a homemade LabVIEW program (National Instruments, Austin, TX).

Cell counting

The cells were counted using Neubauer improved counting chamber (Precicolor HBG, Germany) with proper sample dilution with Phosphate Buffer Saline. Cell viability was quantified in parallel using the trypan blue dye exclusion method.[18]

Nutrient and metabolite analysis

Five milliliter samples at different times during batches were taken (8 or 9 samples for each batch). They were centrifuged at 750*g* for 4 min at 4°C (Sorvall Biofuge Primo R Centrifuge, Thermo Electron Corp. Germany). Subsequently, supernatants were filtered through 0.22 μm filter (Millex-GV filter unit, Sao Paulo, Brazil) and frozen at −20°C until spectral, nutrients and metabolites analysis.

Glucose, lactate, glutamine, and glutamate (g/L) concentrations from supernatant samples were measured using enzyme-coupled reaction and electrochemical detection, in YSI 2700 select bioanalyzer (YSI Life Sciences, Yellow Springs, OH).

UV–vis spectrum analyses

Samples were thawed and equilibrated at room temperature. Then, they were dissolved 10-fold in deionized water. Dissolved samples were pipetted in disposable polymethylmethacrylate UV–vis cuvettes (1.5 mL, Kartell, Noviglio, Italy). Deionized water was used as blank. UV–vis spectra of samples from 280 to 800 nm (1 nm width pass) were performed in Biomate 3 spectrophotometer (Thermo Fisher Scientific, Waltham, MA). Absorbance data were recorded via hyperterminal of an external computer. Subsequently, data were exported to Micosoft Office Excel 2007 (Microsoft Corporation, Redmond) for graphing and further processing.

PLS modeling

Seventy (5 batches, 43 experimental points) and seventy six (3 batches, 26 experimental points) percent of the collected samples were used to calibrate a PLS models for batches performed without and with $NaHCO_3$ solution addition, respectively. The remaining data were used for model validation; experiments carried out at 50 % air saturation in both bioreactors were used to validate PLS models adjusted for batches without base solution addition, whereas one of the batches performed at 50% air saturation with $NaHCO_3$ solution addition was used for model validation in bioconversion with base solution addition to control pH.

The X matrix included sample absorbances within the spectral range under study. On the other hand, Y matrix was composed by the glucose, lactate, glutamine, glutamate, and viable cell concentrations. PLS modeling was performed in SIMCA 13 demo version software (Umetrics, Umea, Sweden). The validation of PLS models was done by means of statistical significance evaluation of intercept and slope in simple linear models for predicted and actual values of parameters under consideration. The software used with this purpose was Statgraphics Plus 5.0 (Statistical Graphics Corporation, VA). The graphs were set in Microsoft Excel 2007.

Results

The UV–vis spectra for supernatant samples of BHK cell cultures were characterized for three peaks with maximum absorbance around 286, 422, and 560 nm (Figures 1–3). The 286 nm peak did not show a clear relation with batch time. However, as a rule 422 nm peak increased as time increased, contrary performance for 560 nm peak was observed. However, from 600 nm no changes in absorbance were observed.

In the final moments of the batches with $NaHCO_3$ solution addition to control pH, the decrease of absorbance at 560 nm was not as marked as those for batches without pH control at the end of experiment (generally, after the second day of cell cultures; Figures 1–3).

The spectral data was well correlated with glutamine, glutamate, glucose, and lactate concentrations, together with the natural logarithm of viable cell concentration for both pH control modes. Six and four PLS components were necessary to model satisfactory batches performed without and with base solution, respectively. Values of R^2 (percent of variation of the training set –Y with PLS- explained by the model) and Q^2 (percent o f the variation of the training set – Y with PLS – predicted by the model according to cross validation), both with and without base solution addition, were >0.5 (Table 1).

The validation of PLS models were confirmed by the statistical significance of simple linear model between observed and predicted values ($P < 0.05$, data not shown) and the intercept (0) and slope (1) values of these linear models (Table 2). Statistically similar values ($P > 0.05$) for intercept and slope to 0 and 1, respectively, it is an evidence that the present chemometric method do not have signal interference and predicted values for parameters under consideration are similar to actual values.

The accuracy of PLS models was assessed by means of prediction error, the errors for glutamine and glutamate concentrations were <0.5 mM. The error range for glucose and lactate was in the 1.51–3.08 mM range. Viable cell concentration error for batches with pH control during the whole batch was two-fold higher than those related to batches without $NaHCO_3$ addition (Table 3). In general, similar predictions for glutamine, glutamate, glucose and lactate were observed for a batch performed without $NaHCO_3$ addition

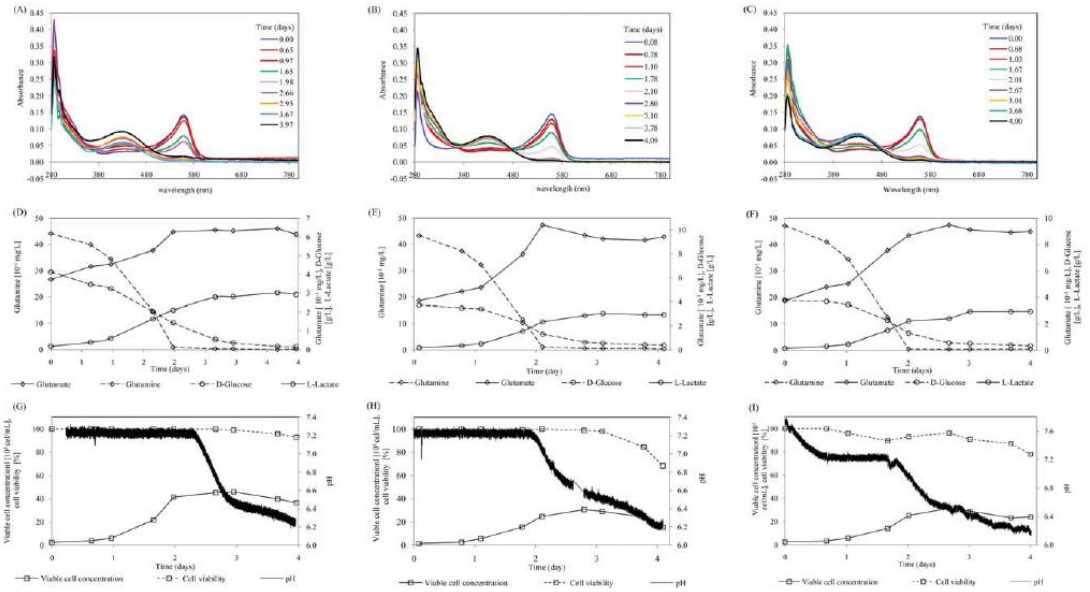

Figure 1. UV–vis Spectral (A–C), nutrients and metabolites (D–F), and pH profile and growth data (G–I) of samples from batches performed without base solution addition (pH control) at 10, 30, and 50% dissolved oxygen in Celligen bioreactor, respectively.

(Figure 4) respect to a batch with total time pH control (Figure 5; Table 3).

Discussion

Determinations of some substances or even biomedia characterization with specific analytical techniques are usually expensive, both on-line and off-line quantifications. The global direct methods for these purposes were developed to overcome this trouble; they are a combination of a hard part, for sensing and a soft part, for data treatment.[19] The UV–vis spectroscopy is one of the hard candidates that has been successfully tested for in situ determination, notwithstanding its use has been mainly used in wastewater characterization.[19,20]

UV–vis radiation has much more energy than infrared radiations, the most utilized electromagnetic spectrum range in bioprocess substances and biomass monitoring.[21] The UV–vis radiation absorption by a substance causes the excitation and transition of the outer electrons of the atomic or molecular orbitals. Therefore, rotational and vibrational levels of molecular orbitals are overlapped on the electronic levels, generating absorption spectra with broad bands. Besides, UV–vis spectra of aqueous samples are affected by presence of a second, dispersed phase (such as: bubbles or cells in bioreactors), because of light scattering effects.

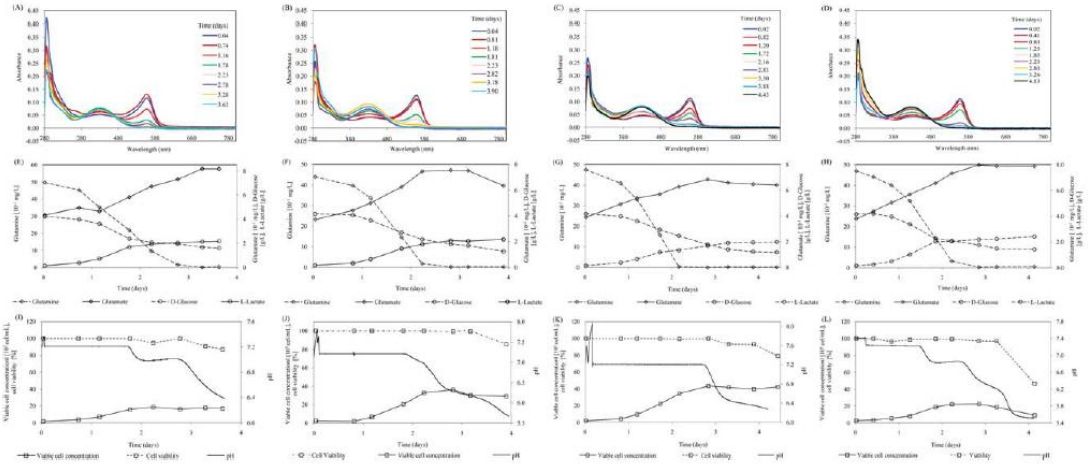

Figure 2. UV–vis Spectral (A–D), nutrients and metabolites (E–H), and pH profile and growth data (I–L) of samples from batches performed without base solution addition (pH control) at 10, 30, 50, and 70% dissolved oxygen in Bioflo 110 bioreactor, respectively.

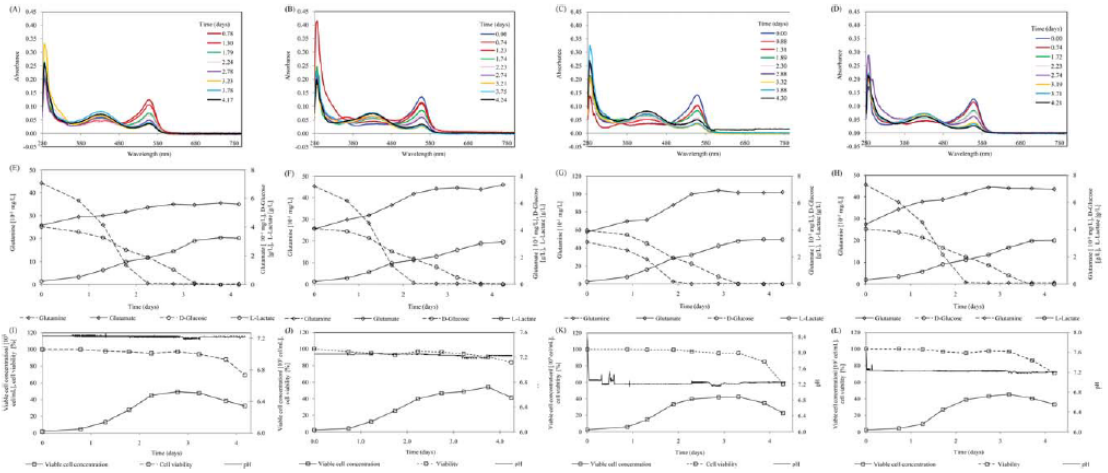

Figure 3. UV–vis Spectral (A–D), nutrients and metabolites (E–H), and pH profile and growth data (I–L) of samples from batches performed with $NaHCO_3$ addition (pH control) at 30 (repetition 1 and 2) and 50% (repetition 1 and 2) dissolved oxygen in Bioflo 110 bioreactor, respectively.

Table 1. Summary of Plot Cumulative R^2 and Q^2 for Monitored Parameters in Training Step for Batches Carried Out Without and With $NaHCO_3$ Addition

	Batches Without $NaHCO_3$ Addition			Batches with $NaHCO_3$ Addition		
Parameter	Number of PLS Components	R^2	Q^2	Number of PLS Components	R^2	Q^2
Glutamine concentration (mg/L)	6	0.928	0.883	4	0.865	0.761
Glutamate concentration (mg/L)		0.760	0.671		0.742	0.574
Glucose concentration (g/L)		0.957	0.926		0.973	0.880
Lactate concentration (g/L)		0.966	0.944		0.970	0.874
Ln [viable cell concentration (cell/mL)]		0.872	0.777		0.861	0.789

Table 2. Summary of Linear Models Parameter Significances in Validation Step for Observed vs Predicted Parameters

	Batches Without $NaHCO_3$ Addition Null Hypothesis		Batches with $NaHCO_3$ Addition Null Hypothesis	
Parameter	Intercept = 0	Slope = 1	Intercept = 0	Slope = 1
Glutamine concentration (mg/L)	0.513	0.645	0.979	0.571
Glutamate concentration (mg/L)	0.837	0.756	0.894	0.626
Glucose concentration (g/L)	0.243	0.922	0.613	0.077
Lactate concentration (g/L)	0.562	0.529	0.057	0.099
Ln [viable cell concentration (cell/mL)]	0.584	0.749	0.485	0.506

These spectra can provide poor information, but the utilization of multivariate data analysis has enabled to extract valuable information from them.[10] Up to date, in microorganism fermentation processes and animal cell cultures, UV–vis monitoring has not found wide application.[22] In this work, sample spectra were determined with cell removal for avoiding light scattering effects. In addition, two bioreactors with different aeration-homogenization systems were included in order to test the ability of UV–vis -PLS models for predicting culture broth components and viable cell concentration in dissimilar culture conditions without base solution addition to control pH. Other set of experiments with $NaHCO_3$ addition to control pH was also performed for calibrating another set of PLS models. The use of $NaHCO_3$ solution can modify the off-line UV–vis spectra of phenol red. For this reason, modeling was performed individually for each set of experiments. Both pH control modes were assessed because the BHK-21 cell line can be cultured in bioreactors using these two strategies in the batch mode.[23] Probably, this article could be one of the first works using this technique in mammalian cell culture.

The off-line spectral data from BHK-21 cell culture samples in bioreactor confirmed the three critical wavelengths associated to phenol red indicator, previously reported, 430, 475, and 560 nm.[24] The phenol red has two different isomers depending on the acidity of its host solution. With pH diminishing, the peaks at 430 and 560 nm, increase and decrease, respectively. The 475 nm wavelength is an isosbestic wavelength (Absorbance is independent of pH). Previously, it was developed a pH sensor using UV–vis spectroscopy, taking advantage of the relationship between UV–vis phenol red indicator spectrum and pH.[24] In this work, spectral changes were detected, even when pH was the same inside the bioreactor (first four samples from batches performed without $NaHCO_3$ solution (8 % m/v) addition (Figures 1 and 2) or for all samples from batches carried out with this reagent

Table 3. Summary of Prediction Error Averages for Each Parameter

Parameter	Prediction Error Average	
	Batches Without $NaHCO_3$ Addition	Batches With $NaHCO_3$ Addition
Glutamine concentration (mM)	0.31 ± 0.08	0.50 ± 0.10
Glutamate concentration (mM)	0.05 ± 0.01	0.05 ± 0.01
Glucose concentration (mM)	2.21 ± 0.46	1.51 ± 0.43
Lactate concentration (mM)	3.08 ± 0.49	1.89 ± 0.40
Ln [viable cell concentration (cell/mL)]	0.33 ± 0.07	0.52 ± 0.09
Viable cell concentration (cell/mL)	$5.96\ 10^5 \pm 7.06\ 10^5$	$1.23\ 10^6 \pm 2.31\ 10^5$

The represented values are the average ± standard error.

(Figure 3)]. Probably, this could be explained by sample dilution (10-fold) or due to the fact of being off-line determination, where gas composition in liquid phase is not the same respect to sample into the bioreactor, causing pH changes. The principle on which is based the proposed UV–vis approach is the relationship between metabolism of glutamine and glucose and Phenol red spectrum modifications. Both nutrients, after metabolism, can generate compounds (lactate and ammonium) which decrease the culture medium pH.[25,26] As a consequence, these nutrients and metabolites could be correlated to viable cell concentration for a cell culture in the batch mode, as it was recently performed.[27] The other significant peak (286 nm) in spectra of BHK-21 culture supernatant samples is likely associated to extracellular proteins and single aromatic amino acids. The absorbance of aromatic amino acids residues: Tryptophan, Tyrosine, and Phenylalanine, from 250 to 300 nm, are used to quantify the aromatic content of proteins[28] and therefore, they would be useful in estimation of total protein content in culture supernatant samples. However, a defined pattern of this spectral peak was not found. For these reasons, the wavelengths with high statistical importance on response variables in PLS (data not shown) were those associated with the Phenol red indicator.

The PLS models developed in this work were created using as input variables matrices, the sample absorbances from 280 to 800 nm, whereas the output variables matrices were the nutrient, metabolites and viable cell concentration quantified off-line. This vectorial method, PLS, is useful to find suitable correlations between both matrices. Six and four principal components (pairs of vectors, scores and loadings, in which are discomposed the original matrices) were necessary for properly modeling the response variables in batch culture performed without and with base solution addition, respectively (Table 1). Better correlations for glutamine, glucose, and lactate were detected from the training data used to calibrate PLS models. This can be justified by the relationship among pH and lactate and ammonium concentration in culture broth, as a consequence of glutamine and glucose metabolism.

In validation set data, the prediction errors for the glutamine and glucose models (Table 3) were improved or similar to the values reported for a PLS model based on near infrared spectral data in mammalian or insect culture media as well as those for mammalian cell cultures using Raman spectroscopy.[9,11,29]

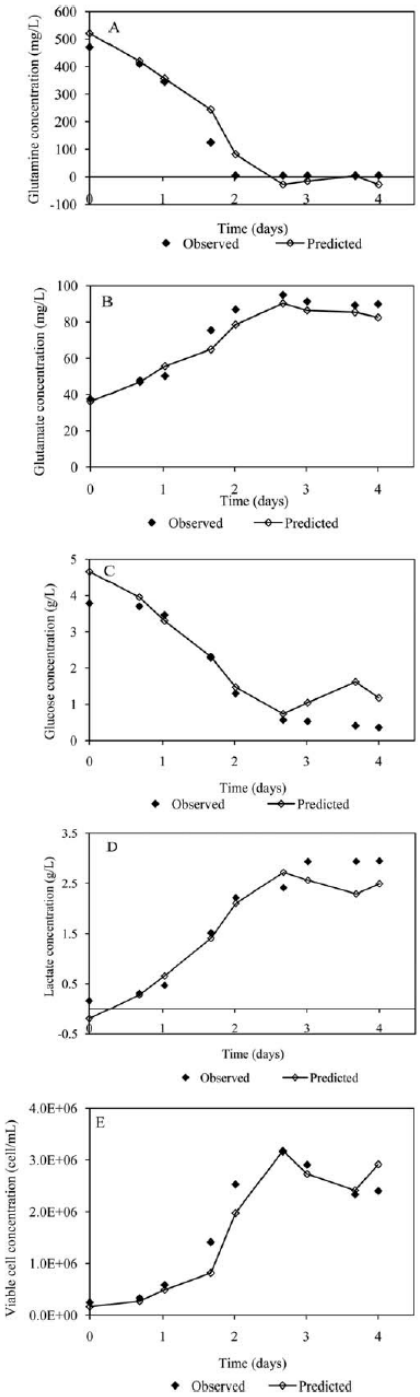

Figure 4. Predicted and actual values for different parameters from a batch at 50% OD without $NaHCO_3$ addition, in Celligen. A: Glutamine. B: Glutamate. C: Glucose. D: Lactate. E: Viable cell concentration.

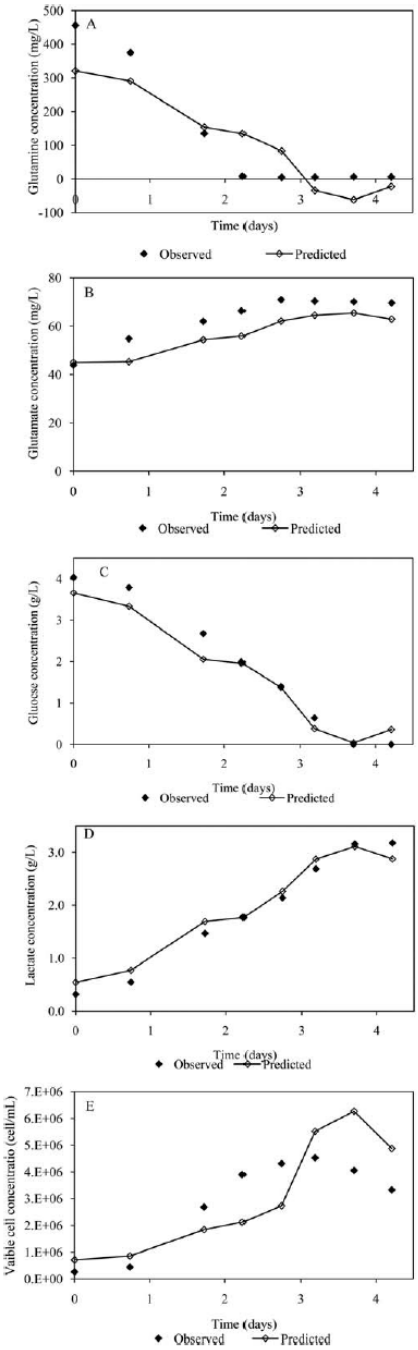

Figure 5. Predicted and actual values for different parameters from a batch at 50% OD with $NaHCO_3$ addition, in Bioflo 110. A: Glutamine. B: Glutamate. C: Glucose. D: Lactate. E: Viable cell concentration.

The nutrients and metabolites considered in this study were suitably predicted for two set of data, but in batches with $NaHCO_3$ addition, predictions should be improved, specifically for glutamine and glutamate (Figures 4 and 5). The increase of training data set could solve this problem. Analogous performance, with respect to viable cell concentration prediction was observed (Table 3, Figures 4 and 5). Regarding errors of this parameter, in the batch carried out with partial pH control (better prediction), where most of the cell concentrations were well predicted, the error in some samples was higher than 15%, the expected error for an experienced individual with cell counting using hemocytometer method.[30] Probably, the nutrients consumption and metabolites synthesis patterns are different for each dissolved oxygen concentration, then it would be necessary to calibrate a specific viable cell concentration for a particular dissolved oxygen concentration.

From the results of this work, fed-batch feeding schemes could be established. Additionally, an at-line UV–vis sensor could be also developed based on the current availability of UV-grade optical fibers, sensitive and cheaper array detectors, together with PLS technique.[10] The utilization of PLS technique associated to UV–vis spectra from samples of mammalian cell cultures using phenol red as pH indicator in culture medium could be an alternative to biomedia characterization using other more powerful spectral techniques like near infrared, fluorescence and more recently Raman spectroscopy.[11]

Conclusions

UV–vis off-line spectroscopy in combination with PLS model was able to estimate critical components of the culture medium of BHK-21 cell culture independent of dissolved oxygen concentration used, bioreactor and the strategy to control pH. This work opens possibilities for at-line sensor development for mammalian cell using phenol red in culture medium and decrease cost related to nutrients and metabolite quantifications. PLS model calibration must be performed for individual mammalian cell line.

Acknowledgments

The authors would like to thank Fundação de Amparo à Pesquisa do Estado de São Paulo (FAPESP) for post-doctoral fellowship (2010/52521-6), Fundação para o Desenvolvimento Tecnológico da Engenharia (FDTE), and Conselho Nacional de Desenvolvimento Científico e Tecnológico (CNPq: 483009/2010-5) for scientific grants. Corresponding author gratefully acknowledges his wife and daughter, Relma and Giovanna for the inspiration to write this article.

Literature Cited

1. Teixeira AP, Oliveira R, Alves PM, Carrondo MJT. Advances in on-line monitoring and control of mammalian cell cultures: Supporting the PAT initiative. *Biotechnol Adv*. 2009;27:726–732.
2. Huber R, Ritter D, Hering T, Hillmer AK, Kensy F, Müller C, Wang L, Büchs J. Robo-Lector – a novel platform for automated high-throughput cultivations in microtiter plates with high information content. *Microb Cell Fact*. 2009;8:1–15.
3. Gunther JC, Conner JS, Seborg DE. Process monitoring and quality variable prediction utilizing PLS in industrial fed-batch cell culture. *J. Process Contr*. 2009;19:914–921.
4. Cimander C, Mandenius CF. Online monitoring of a bioprocess based on a multi-analyser system and multivariate statistical process modeling. *J Chem Technol Biotechnol*. 2002;77:1157–1168.
5. Rudolph G, Lindner P, Gierse A, Bluma A, Martinez G, Hitzmann B, Scheper T. On-line monitoring of microcarrier based fibroblast cultivations with in situ microscopy. *Biotechnol Bioeng*. 2008;99:136–145.

6. Logan D, Carvell J. A Biomass monitor for disposable bioreactors. *Bioprocess Int*. 2011;9:48–54.
7. Petiot E, Bernard-Moulin P, Magadoux T, Gény C, Pinton H, Marc A. In situ quantification of microcarrier animal cell cultures using near-infrared spectroscopy. *Process Biochem*. 2010; 45:1427–1431.
8. Landgrebe D, Haake C, Höpfner T, Beutel S, Hitzmann B, Scheper T, Rhiel M, Reardon KF. On-line infrared spectroscopy for bioprocess monitoring. *Appl Microbiol Biotechnol*. 2010;88: 11–22.
9. Riley MR, Rhiel M, Zhou X, Arnold MA, Murhammer DW. Simultaneous measurement of glucose and glutamine in insect cell culture media by near infrared spectroscopy. *Biotechnol Bioeng*. 1997;55:11–15.
10. Lourenço ND, Lopes JA, Almeida CF, Sarraguça MC, Pinheiro HM. Bioreactor monitoring with spectroscopy and chemometrics: A review. *Anal Bioanal Chem.* 2012;404:1211–1237.
11. Abu-Absi NR, Kenty BM, Cuellar ME, Borys MC, Sakhamuri S, Strachan DJ, Hausladen MC, Li ZJ. Real time monitoring of multiple parameters in mammalian cell culture bioreactors using an in-line Raman spectroscopy probe. *Biotechnol Bioeng*. 2011; 108:1215–1221.
12. Rathore AS, Bhushan N, Hadpe S. Chemometrics applications in biotech processes: A review. *Biotechnol Prog*. 2011;27: 307–315.
13. Dietmair S, Nielsen LK, Timmins NE. Engineering a mammalian super producer. *J Chem Technol Biotechnol*. 2011;86: 905–914.
14. Croughan MS, Hu WS. From microcarriers to hydrodynamics: Introducing engineering science into animal cell culture. *Biotechnol Bioeng*. 2006;95:220–225.
15. Aunins JG. Viral Vaccine Production in Cell Culture. In: Flickinger MC, editor. *Encyclopedia of Industrial Biotechnology: Bioprocess, Bioseparation, and Cell Technology*. New York: Wiley; 2010:1–35.
16. Lundstrom K, Schweitzer C, Rotmann D, Hermann D, Schneider EM, Ehrengruber MU. Semliki Forest virus vectors: e¤cient vehicles for in vitro and in vivo gene delivery. *FEBS Lett*. 2001;504:99–103.
17. Sandell L, Sakai D. Mammalian Cell Culture. In: Gallagher SR, Wiley EA, editors. *Current Protocols Essential Laboratory Techniques*. Wiley; 2011: 4.3.1–4.3.32. http://onlinelibrary.wiley.com/doi/10.1002/9780470089941.et0403s5/abstract, doi: 10.1002/9780470089941. et0403s5.
18. Freshney RI. *Culture of Animal Cells: A Manual of Basic Technique and Specialized Applications*, 6th ed. Hoboken: Wiley; 2010.
19. Pons MN, Le Bonté S, Potier O. Spectral analysis and fingerprinting for biomedia characterization. *J Biotechnol*. 2004;113: 211–230.
20. Langergraber G, Fleischmann N, Hofstaedter F. A multivariate calibration procedure for UV/VIS spectrometric quantification of organic matter and nitrate in wastewater. *Water Sci Technol*. 2003;47:63–71.
21. Cervera AE, Petersen N, Lantz AE, Larsen A, Gernaey KV. Application of near-infrared spectroscopy for monitoring and control of cell culture and fermentation. *Biotechnol Prog*. 2009; 25:1561–1581.
22. Liauw M A, Baylor LC, Rourke PEO. Chapter 4: UV - visible Spectroscopy for On-line Analysis. In: Bakeev KA, editor. *Process Analytical Technology: Spectroscopic Tools and Implementation Strategies for the Chemical and Pharmaceutical Industries*, 2nd ed. United Kingdom: Wiley; 2010:81–106.
23. Fernández-Núñez EG, Leme J, Parizotto LA, Chagas WA, Rezende AG, Costa BLV, Monteiro DCV, Boldorini VLL, Jorge SAC, Astray RM, Pereira CA, Caricati C P, Tonso A. Influence of aeration–homogenization system in stirred tank bioreactors, dissolved oxygen concentration and pH control mode on BHK-21 cell growth and metabolism. *Cytotechnology*. In press; doi: 10.1007/s10616-013-9612-0.
24. Xu X, Smith S, Urban J, Cui Z. An in line non-invasive optical system to monitor pH in cell and tissue culture. *Med. Eng. Phys*. 2006;28:468–474.
25. Cruz HJ, Ferreira AS, Freitas CM, Moreira JL, Carrondo MJT. Metabolic responses to different glucose and glutamine levels in baby hamster kidney cell culture. *Appl Microbiol Biotechnol*. 1999;51:579–585.
26. Cruz HJ, Freitas CM, Alves PM, Moreira JL, Carrondo MJT. Effects of ammonia and lactate on growth, metabolism, and productivity of BHK cells. *Enzyme Microb Technol*. 2000;27: 43–52.
27. Craven S, Shirsat N, Whelan J, Glennon B. Process model comparison and transferability across bioreactor scales and modes of operation for a mammalian cell bioprocess. *Biotechnol Prog*. 2013;29:186–196.
28. Kamerzell TJ, EsfandiaryR, Joshi SB, Middaugh CR, Volkin DB. Protein-excipient interactions: Mechanisms and biophysical characterization applied to protein formulation development. *Adv Drug Deliv Rev*. 2011;63:1118–1159.
29. Rhiel, M, Cohen, MB, Murhammer, DW, Arnold, MA. Nondestructive near-infrared spectroscopic measurement of multiple analytes in undiluted samples of serum-based cell culture media. *Biotechnol Bioeng*. 2002;77:73–82.
30. Hoffman TL. Chapter 3: Counting cells. In: Celis JE. *Cell Biology. A Laboratory Handbook*, 3rd ed. Volume 1, Burlington: Elsevier; 2006:21–24.

Manuscript received Jul. 9, 2013, and revision received Dec. 10, 2013.